N72-30248

DYNAMIC LOAD SIMULATOR

FINAL REPORT

Program Period:

24 June 1971 to 24 May 1972

Prepared for

NATIONAL AERONAUTICS AND SPACE ADMINISTRATION
MANNED SPACECRAFT CENTER
HOUSTON, TEXAS, 77058

Contract Number NAS-9-12016

AVSD-0076-72-RR

23 June 1972

Prepared by

AVCO GOVERNMENT PRODUCTS GROUP
Systems Division
201 Lowell Street
Wilmington, Massachusetts, 01887

DYNAMIC LOAD SIMULATOR

FINAL REPORT

Program Period:

24 June 1971 to 24 May 1972

Prepared for

NATIONAL AERONAUTICS AND SPACE ADMINISTRATION
MANNED SPACECRAFT CENTER
HOUSTON, TEXAS, 77058

Contract Number NAS-9-12016

AVSD-0076-72-RR

23 June 1972

Prepared by

K. P. Joncas, Project Engineer
Dynamic Load Simulator

Approved by

S. Birnbach, Project Manager
Dynamic Load Simulator

AVCO GOVERNMENT PRODUCTS GROUP
Systems Division
201 Lowell Street
Wilmington, Massachusetts, 01887

ACKNOWLEDGMENTS

A number of individuals have contributed substantially to this program.

The contributions of the following Avco Systems Division personnel whose contributions were most significant are hereby acknowledged. Calvin Cook and William E. Brown for data acquisition and processing; Dr. Marc Weinberger for model development; Carleton Russell, Jr. for computer optimization; Leonard Smith for model circuit design; and Lloyd Bruce for variable R circuit design.

The continued interest and helpful suggestions of Kent Castle of the NASA Manned Spacecraft Center are also hereby acknowledged.

TABLE OF CONTENTS

TABLE OF CONTENTS (Concluded)

LIST OF FIGURES

LIST OF FIGURES (Continued)

LIST OF FIGURES (Continued)

LIST OF FIGURES (Continued)

LIST OF FIGURES (Continued)

LIST OF FIGURES (Continued)

LIST OF FIGURES (Continued)

LIST OF FIGURES (Continued)

LIST OF FIGURES (Concluded)

LIST OF TABLES

LIST OF TABLES (Concluded)

LIST OF APPENDIXES

1. INTRODUCTION

This document is the final report of the Dynamic Load Simulator program (Phase II). This was an eleven-month program (24 June 1971 to 24 May 1972) conducted by Avco Corporation's Systems Division (Avco/SD) for the National Aeronautics and Space Administration (NASA) under Contract Number NAS-9-12016. The basic objective of the program was the design and development of an engineering model of a load simulator capable of duplicating the dynamic and steady-state response of electrical loads on the power lines. The simulator will be used to:

1. Demonstrate the feasibility and usefulness of such devices.

2. Provide a test bed for evaluating and improving the techniques employed.

1.1 BACKGROUND

The design and development of electrical power distribution/conditioning systems is highly dependent on the characteristics of the power sources and the loads. Their influence becomes progressively more significant as the operational functions of the total integrated system become more critical, such as exemplified in complex spacecraft systems. During the past and present manned spacecraft programs (from Project Mercury through Apollo), in order to meet projected schedules it was necessary to evaluate system performance using load simulators which, at best, could only duplicate the steady-state load conditions. Subsequent vehicle testing and flight experience has consistently uncovered system operational problems caused by the transient (or dynamic) characteristics of the various loads reflected back into the system. Identification of the problem at this point in the program resulted in costly workaround and/or corrective action. Recognizing this, a two-phase program was undertaken to investigate concepts for providing more realistic loads, and to develop prototype hardware and software capable of implementing and evaluating these concepts.

The Phase I study program was undertaken to investigate various concepts and techniques for identifying and simulating both the steady-state and dynamic characteristics of electrical loads for use during integrated system test and evaluation. These investigations showed that it is feasible to design and develop interrogation and simulation equipment to perform the desired functions.

The current program was undertaken to develop hardware capable of providing this simulation. During these activities, actual spacecraft loads were interrogated by stimulating the loads with their normal input voltage and measuring the resulting input voltage and current time histories.

Using an existing computer program with some modification, general network models consisting of resistance (R), inductance (L), and capacitance (C) elements were optimized by an iterative process of selecting element values and comparing the time-domain response of the model with those obtained from the real equipment during the interrogation.

A general-purpose simulator was developed with the capability of realizing a variety of R, L, and C network topologies where the element values were discretely variable. The different models, corresponding to real spacecraft equipment, are set up manually for each case by suitable switching and patching.

Also developed during the current program was a variable resistance (variable R) device with the capability of reproducing a resistance-time curve upon application of a suitable, externally provided control signal. In practice, the current/voltage-time history of an article of hardware is obtained during the interrogation process and this data is then processed and stored. In operation, this signal is retrieved from storage and applied as the control input to the variable R. The output resistance of the variable R, connected to the power source normally used to operate the real equipment, is then made to vary as a function of this control. Thus, the power input current is caused to vary just as the input current to the real equipment.

The dynamic load simulator model is capable of simulating electrical loads with the following input power characteristics:

Voltage	100 to 130 V, 60 or 400 Hz, 1-phase 20 VDC to 60 VDC
Current	up to 8 amperes
Power	up to 250 watts

The variable R is capable of simulating loads with these power characteristics, but is limited to positive, non-zero-crossing voltages only.

The dynamic load simulator system concept is described in Figure 1-1 which shows the flow of activities from initial data acquisition, through data processing, and, finally, simulator operation.

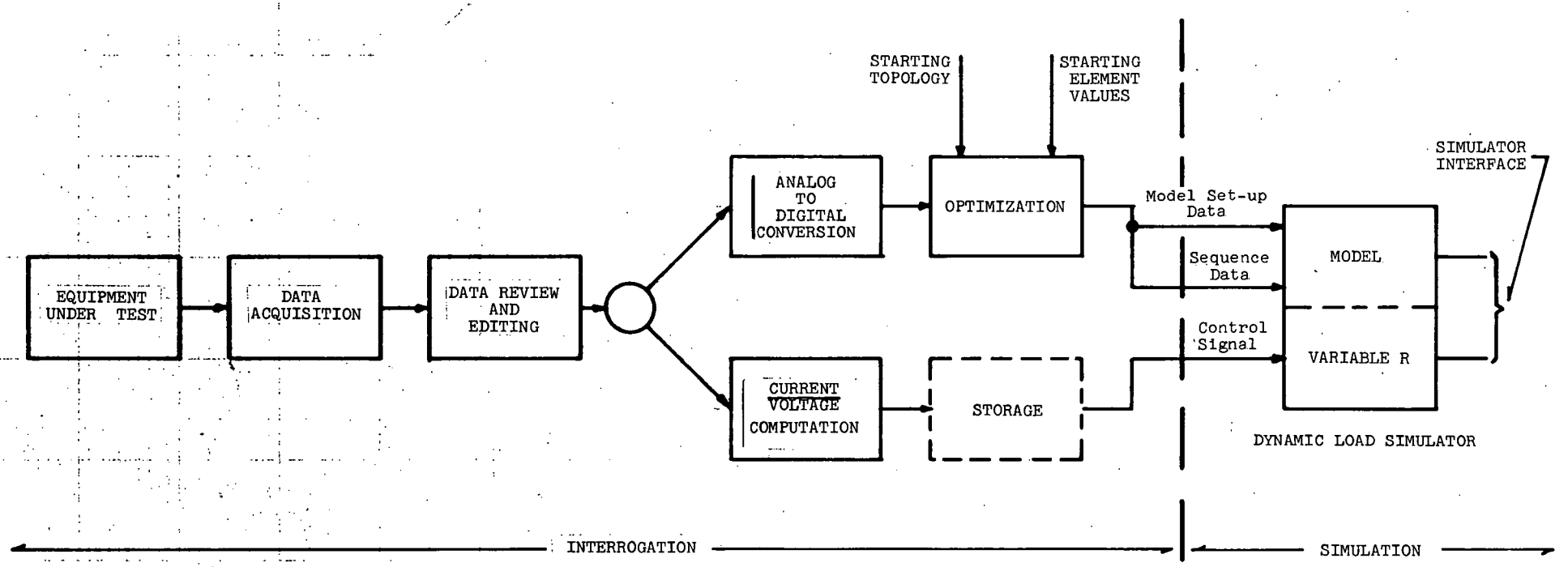

FIGURE 1-1 Interrogation/Simulation--Simplified Flow Diagram

1.2 DEFINITIONS

The terms interrogation and simulation are used extensively throughout this report. A definition of these terms follows:

Interrogation:--The quantitative determination of those parameters of a device that describe its dynamic and steady-state electrical response on the power lines to a specified application of voltage.

Simulation:--The duplication on the power lines of the dynamic and steady-state response of an electrical load.

1.3 REPORT ORGANIZATION

The final report is organized as follows:

1. INTRODUCTION

   Provides background information, defines key terms, indicates the way the report is organized, and lists pertinent contractual publications.

2. CONCLUSIONS AND RECOMMENDATIONS

   Presents conclusions drawn from the study and recommendations for future action.

3. PROGRAM ACCOMPLISHMENTS

   Describes accomplishments of the program in the areas of interrogation and simulation.

4. INTERROGATION

   Describes interrogation activities--from interrogation of spacecraft electrical equipment at NASA MSC, through data acquisition and processing, to subsequent modelling and optimization.

5. SIMULATION

   Discusses the design of the dynamic load simulator, and implementation of that design in an engineering model.

6. SIMULATOR EVALUATION

   Describes evaluation of the simulator's ability to satisfy program goals.

1.4 PUBLICATIONS

Avco Systems Division documents published under this contract (in addition to this final report and an operating and maintenance manual) are listed on Table 1-I. All are monthly progress reports. For summaries of these documents, see Appendix A.

TABLE 1-I

MONTHLY PROGRESS REPORTS, DYNAMIC LOAD SIMULATOR

1. Dynamic Load Simulator, First Monthly Progress Report, for the Period 24 June 1971 to 31 July 1971, Avco Systems Division, AVSD-0365-71-CR, 5 August 1971.

2. Dynamic Load Simulator, Second Monthly Progress Report, for the Period 1 August 1971 to 31 August 1971, Avco Systems Division, AVSD-0404-71-CR, 7 September 1971.

3. Dynamic Load Simulator, Third Monthly Progress Report, for the Period 1 September 1971 to 30 September 1971, Avco Systems Division, AVSD-0443-71-CR, 6 October 1971.

4. Dynamic Load Simulator, Fourth Monthly Progress Report, for the Period 1 October 1971 to 5 November 1971, Avco Systems Division, AVSD-0491-71-CR, 9 November 1971.

5. Dynamic Load Simulator, Fifth Monthly Progress Report, for the Period 6 November 1971 to 30 November 1971, Avco Systems Division, AVSD-0518-71-CR, 8 December 1971.

6. Dynamic Load Simulator, Sixth Monthly Progress Report, for the Period 1 December 1971 to 31 December 1971, Avco Systems Division, AVSD-0004-72-CR, 5 January 1972.

7. Dynamic Load Simulator, Seventh Monthly Progress Report, for the Period 1 January 1972 to 31 January 1972, Avco Systems Division, AVSD-0046-72-CR, 9 February 1972.

8. Dynamic Load Simulator, Eighth Monthly Progress Report, for the Period 1 February 1972 to 29 February 1972, Avco Systems Division, AVSD-0092-72-CR, 6 March 1972.

2. CONCLUSIONS AND RECOMMENDATIONS

2.1 CONCLUSIONS

The dynamic load simulation hardware developed during this program provides two different and independent means of simulating the dynamic and steady-state response of electrical loads on the power lines.

The hardware has been evaluated on the basis of its ability to simulate specific items of spacecraft equipment whose response characteristics were determined by interrogation. As shown in Section 6, both the model and variable R device showed good correspondence with the actual equipment response.

Although the model element inventory was influenced by the specific needs of the models developed for the five items of equipment simulated, the inventory covers a wide range of element values. Also, the model topology is general and, in both the Phase I work and the work just completed, this topology has been shown to have the versatility necessary for modelling a variety of equipments.

The variable R device has been shown to provide excellent simulation of equipment response when driven by a control signal derived from the interrogation data. Since the variable R resistance is controlled by an analog of the desired response, very complex and non-linear responses may be achieved.

The hardware, housed in a convenient operating console, along with a detailed operating and maintenance manual provides means for further evaluation and improvement of the techniques employed.

2.2 RECOMMENDATIONS

The program just completed has demonstrated the feasibility of the dynamic load simulation concept and has provided hardware for evaluation and improvement of the techniques employed.

It is recommended that the next step in the evolvement of this technology be the application of the dynamic load simulation principles to a specific system test and evaluation program. It is further recommended that the design be improved to provide for a degree of automation in the man/machine interfaces and that particular future emphasis be placed on the production design of the equipment to permit its manufacture at reduced cost.

3. PROGRAM ACCOMPLISHMENTS

The Phase 1 study, conducted under NASA contract NAS-9-10429, established the feasibility of dynamic electrical load simulators. The final report of that study[1] has served as the basis for the design and development effort on this program.

To develop hardware capable of simulating the dynamic and steady-state response of electrical loads on the power lines, and to demonstrate and evaluate its performance, the following program was undertaken.

1. Interrogation:--Using Avco data acquisition equipment, Avco interrogated nine items of spacecraft hardware of NASA's Manned Spacecraft Center (MSC).

2. Data Processing:--Using Avco data processing equipment, Avco converted the analog data obtained in 1., above, into a digital format compatible with model optimization needs, and developed a control tape for use in operating the variable R device.

3. Selection of Equipment for Model Synthesis:--On the basis of the data obtained and processed, a selection was made of equipments to be modelled.

4. Model Synthesis and Optimization:--Circuit models were developed capable of suitably simulating the response of the equipment interrogated in 1., above. The computer program identified in the Phase 1 report was used to select model values that optimally reproduce the equipment response characteristics.

5. Simulator Design, Development, and Fabrication:--A simulator capable of simulating the response of the selected equipments was designed, developed, and fabricated.

---

1. A Study of Dynamic Load Simulators for Electrical Systems Test Facility, Final Report, Program Period: 29 December 1969 to 30 June 1970; AVSD-0364-70-RR, 17 August 1970.

6. Simulator Evaluation and Installation:--The simulator response was compared with both the computer-model-predicted response and the actual equipment response to assess the accuracy of the simulation. The simulator was then delivered to MSC and installed and checked out by Avco personnel.

7. Documentation:--A maintenance handbook to furnish information necessary for proper use and maintenance of the equipment was provided. It explains the circuit functions, describes the operating procedures, provides safety precautions, specifies power requirements, and presents maintenance data.

A flow diagram of this program is shown in Figure 3-1.

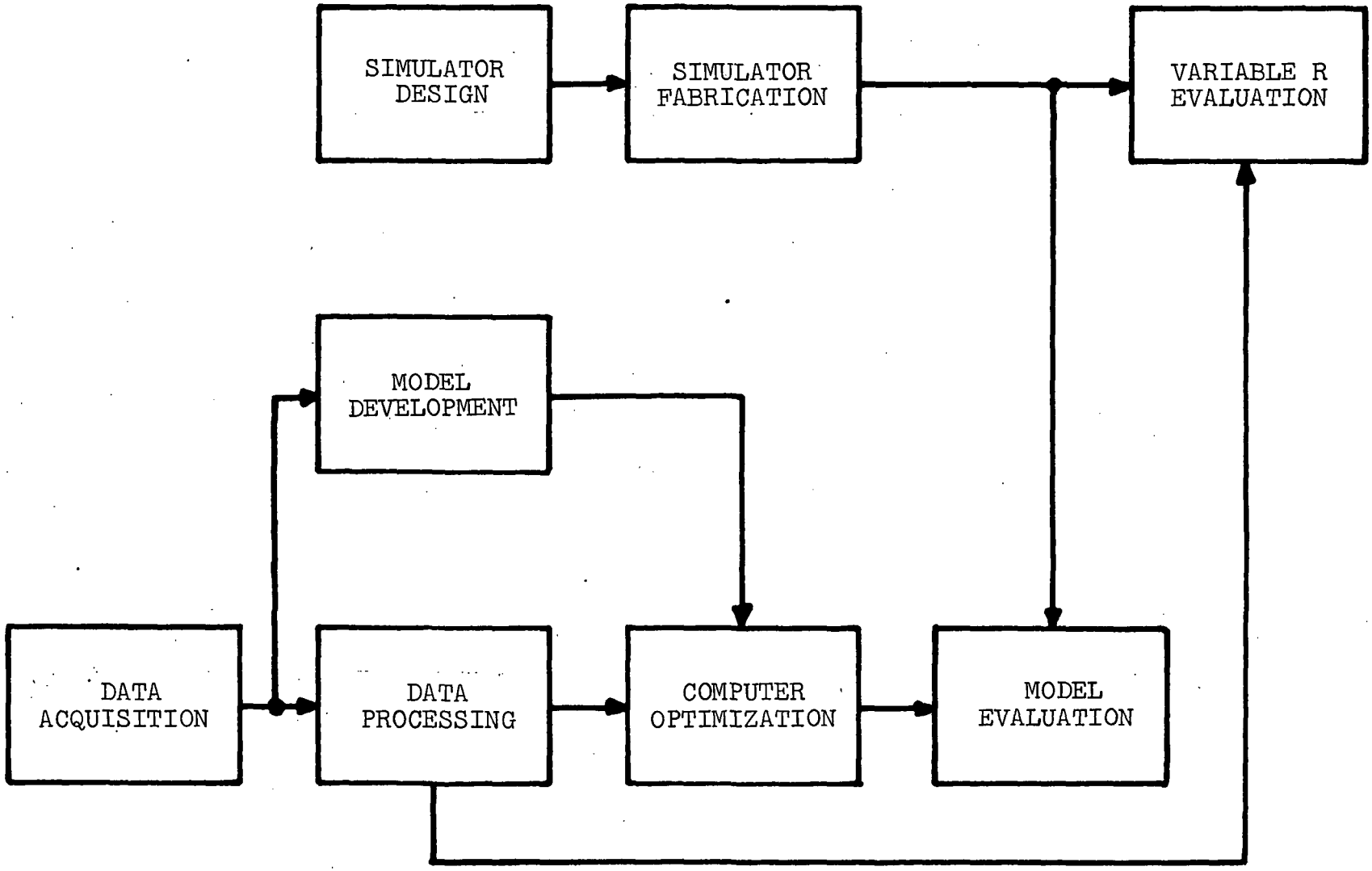

FIGURE 3-1 Dynamic Load Simulator Program Flow Diagram

4. INTERROGATION

In all, nine items of spacecraft electrical equipment were made available at NASA MSC for interrogation. The following discussions identify the equipment and describe the data acquisition and processing activities, and the subsequent modelling and optimization efforts. On the basis of the equipment responses, five of the nine equipments were subsequently selected for modelling and seven equipments were selected for demonstrating the variable R.

4.1 DATA ACQUISITION

Avco personnel visited MSC to interrogate the spacecraft equipment provided by NASA. The equipment interrogated is identified in Table 4-I. Each equipment is identified by a number corresponding to the test run number assigned during the interrogation.

Interrogation consisted of application of the equipment operating voltage and the recording of this voltage and the resultant input current during turn-on, steady-state operation, and turn-off.

Suitable calibration signals were recorded on the same recorder tracks prior to each test to permit accurate interpretation of results. An Inter-Range Instrumentation Group (IRIG) time code, previously recorded on a spare track, provides the means for editing and cueing.

Facsimiles of the current and voltage traces for each of the equipments interrogated are shown in Figures 4-1 through 4-17. A quick-look and an expanded-look trace is provided for each case except the first--for which a quick-look trace is not necessary. The quick-look provides an over-all view of the waveform (long-time duration) while the expanded-look provides a detailed view of the transient portion of the waveform (short-time duration).

A portable acquisition system was used to monitor the MSC equipment at the NASA facility and record the measurements on analog magnetic tape. A simplified block diagram of the data acquisition system is shown in Figure 4-18. A differential amplifier and wide-band voltage-controlled oscillator (VCO) were used to convert each voltage/current data point for input to a wide-band instrumentation tape recorder. Data bandwidths of greater than 0 to 10 KHz were obtained with a nominal calibration accuracy of 2% and noise level of 3%, peak-to-peak, which resulted in a dynamic range of 33 to 1.

The voltage measurements greater than 10 volts required signal conditioning prior to the VCO. The signal conditioning was designed to provide less than 1% loading to the circuit source impedance.

The current measurements were obtained with standard meter shunts selected to provide necessary current carrying capacity and maximum outputs to assure optimum signal-to-noise ratios. Table 4-II identifies the on-site data acquisition equipment.

TABLE 4-I

LIST OF EQUIPMENT PROVIDED BY NASA FOR INTERROGATION

Run Number	Equipment	Power Source
3	Motor Switch	28 VDC
6	Heat Exchanger Valve	115 VAC, 400 Hz
8	Varo Inverter	28 VDC
9	Apollo Inverter	28 VDC
10	Rotron Fan	115 VAC, 400 Hz
11	VHF/AM Transceiver	28 VDC
12	Recovery Beacon	28 VDC
13	UHF/FM Transmitter	28 VDC
16	HF Transceiver	28 VDC

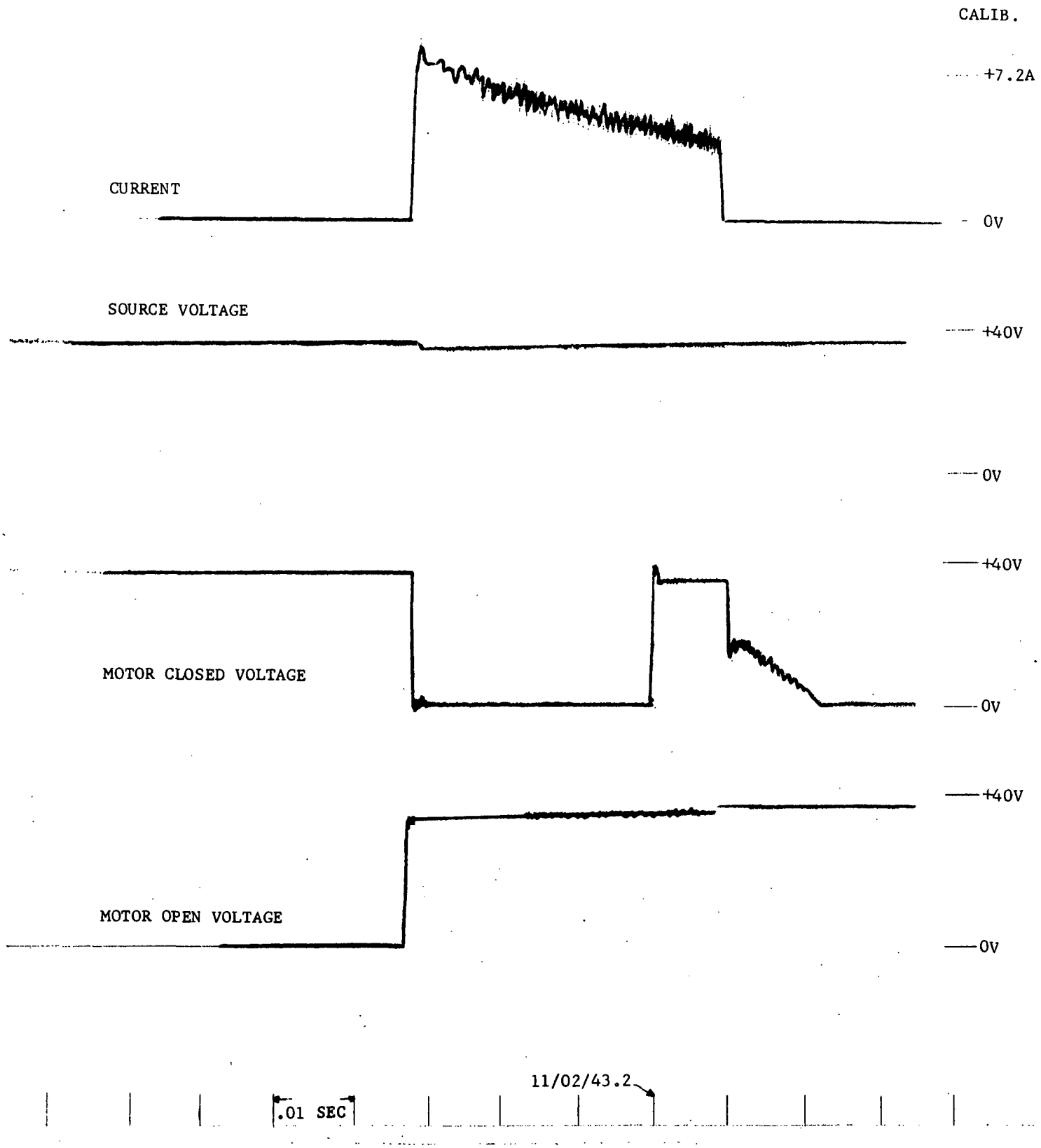

FIGURE 4-1 Voltage and Current Traces, Run 3C--Motor Switch (Expanded)

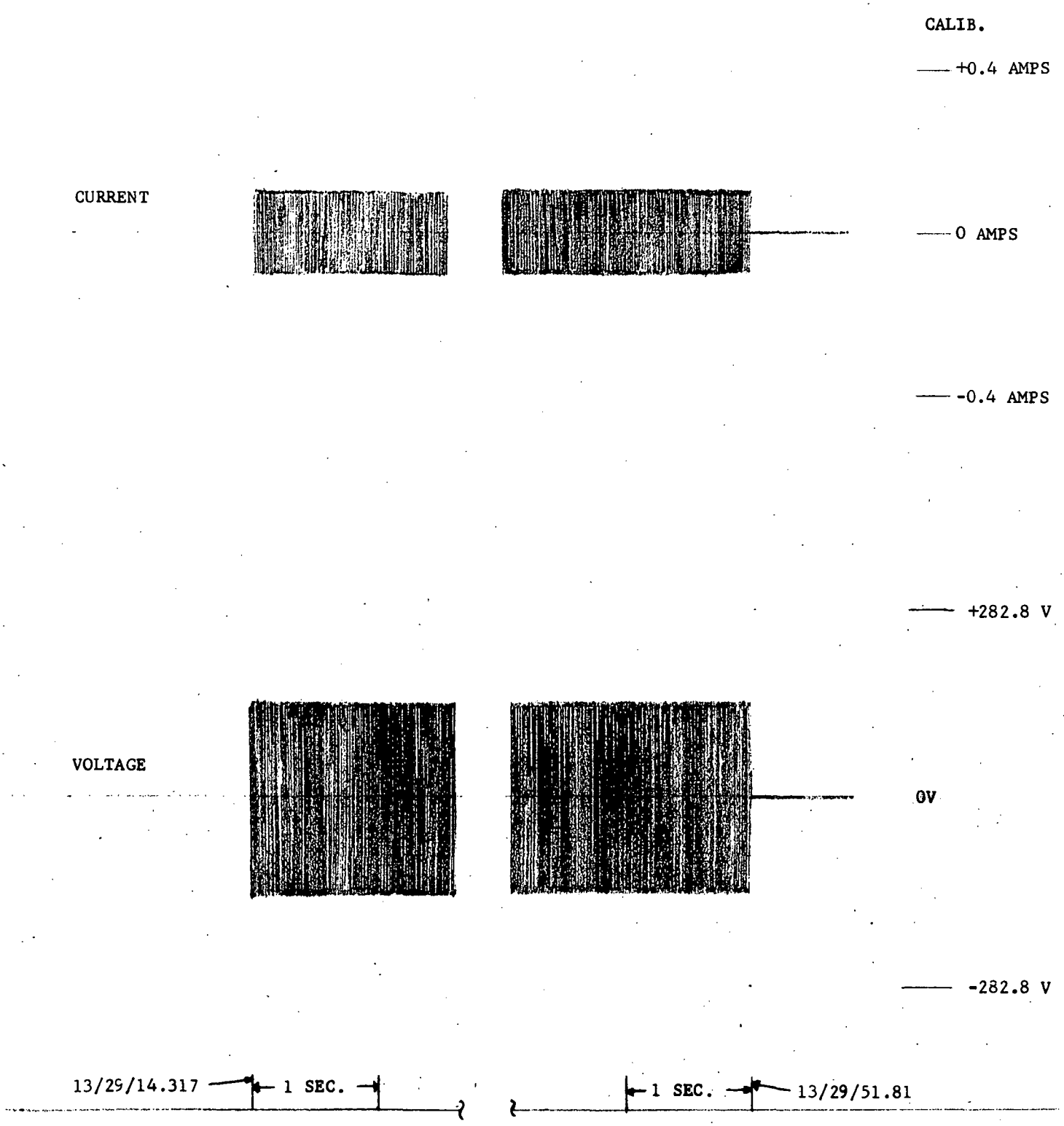

FIGURE 4-2 Voltage and Current Traces, Run 6B--Heat Exchanger Valve

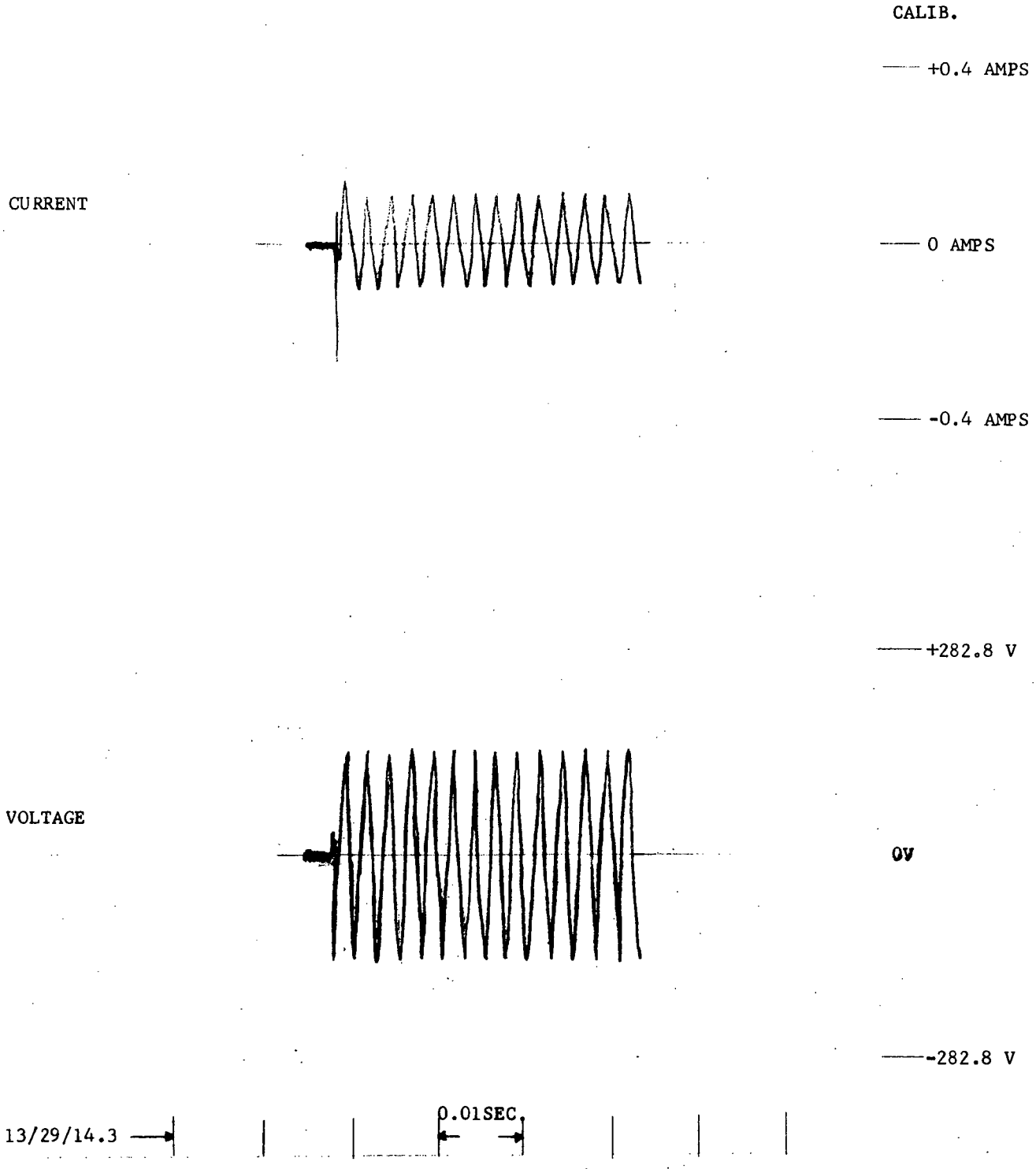

FIGURE 4-3 Voltage and Current Traces, Run 6B--Heat Exchanger Valve (Expanded)

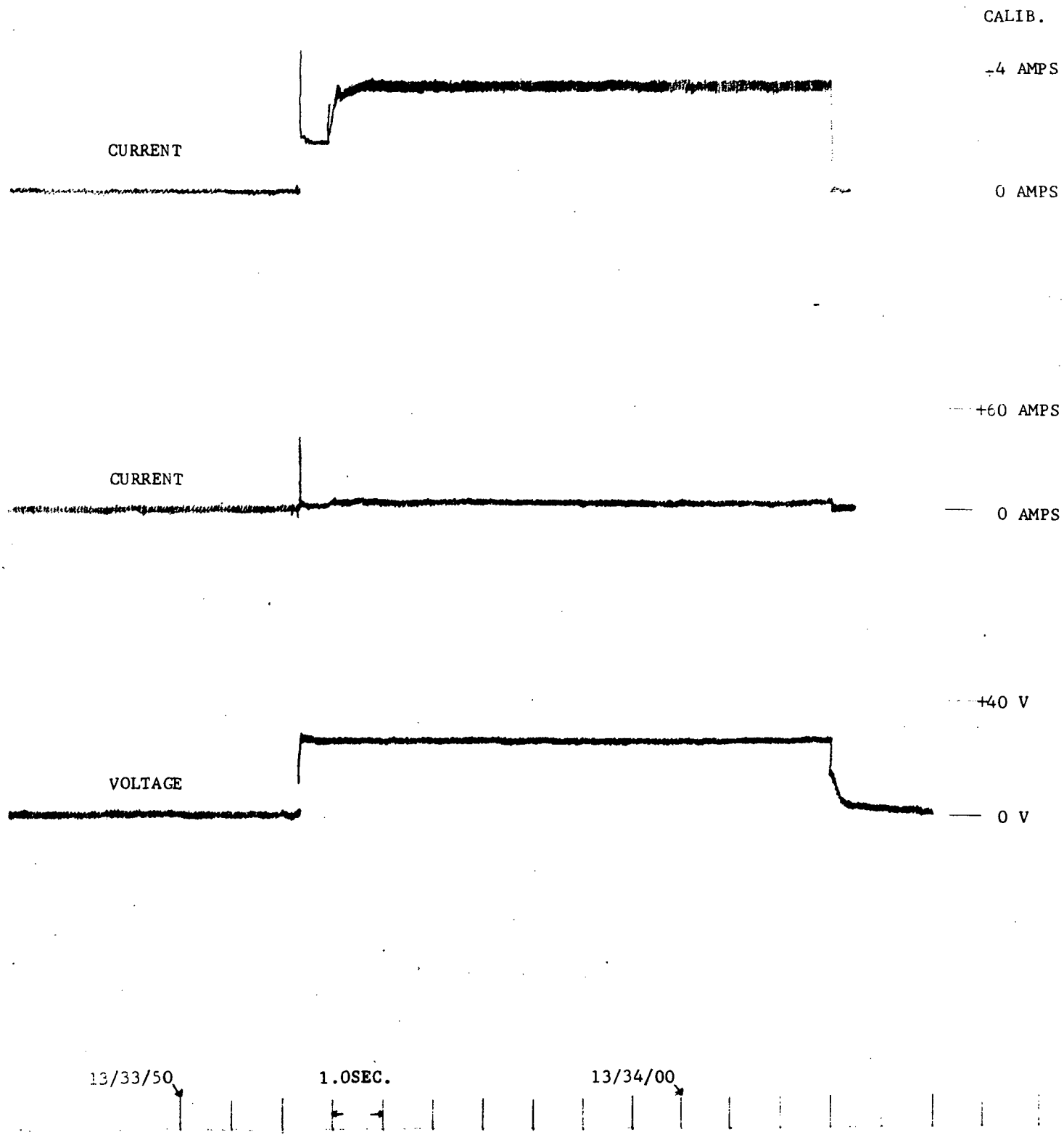

FIGURE 4-4 Voltage and Current Traces, Run 8A--Varo Inverter

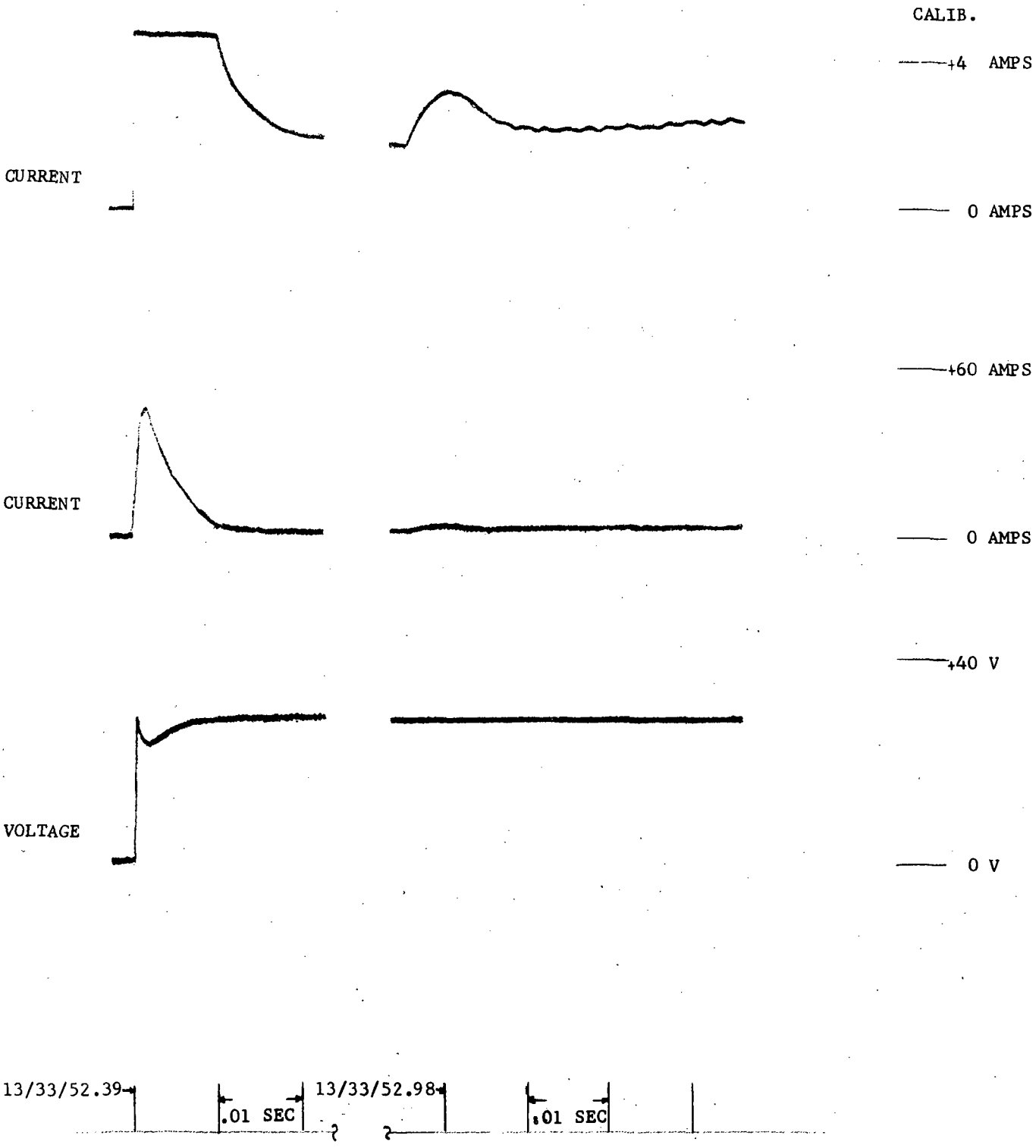

FIGURE 4-5 Voltage and Current Traces, Run 8A--Varo Inverter (Expanded)

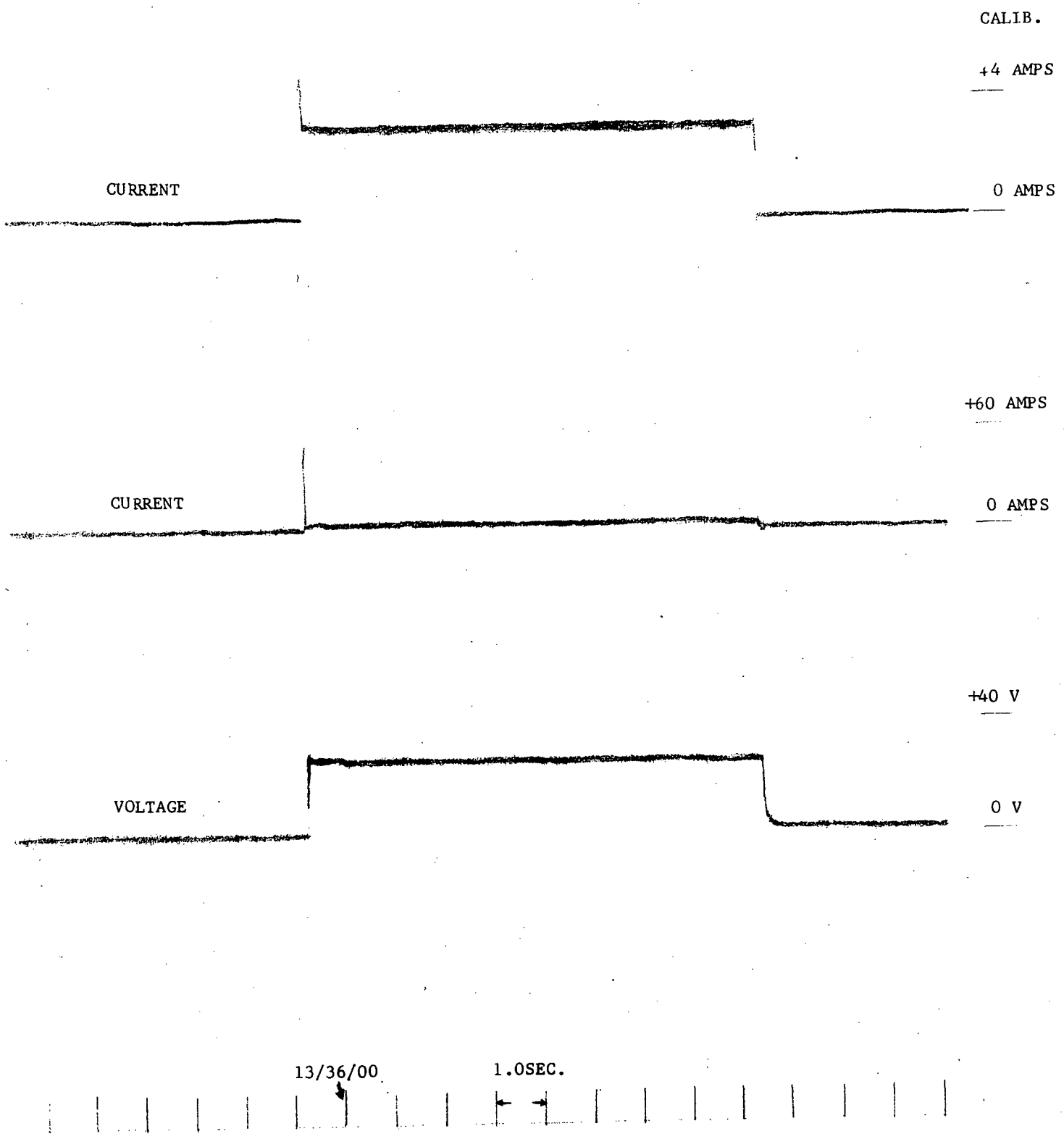

FIGURE 4-6 Voltage and Current Traces, Run 9A--Apollo Inverter

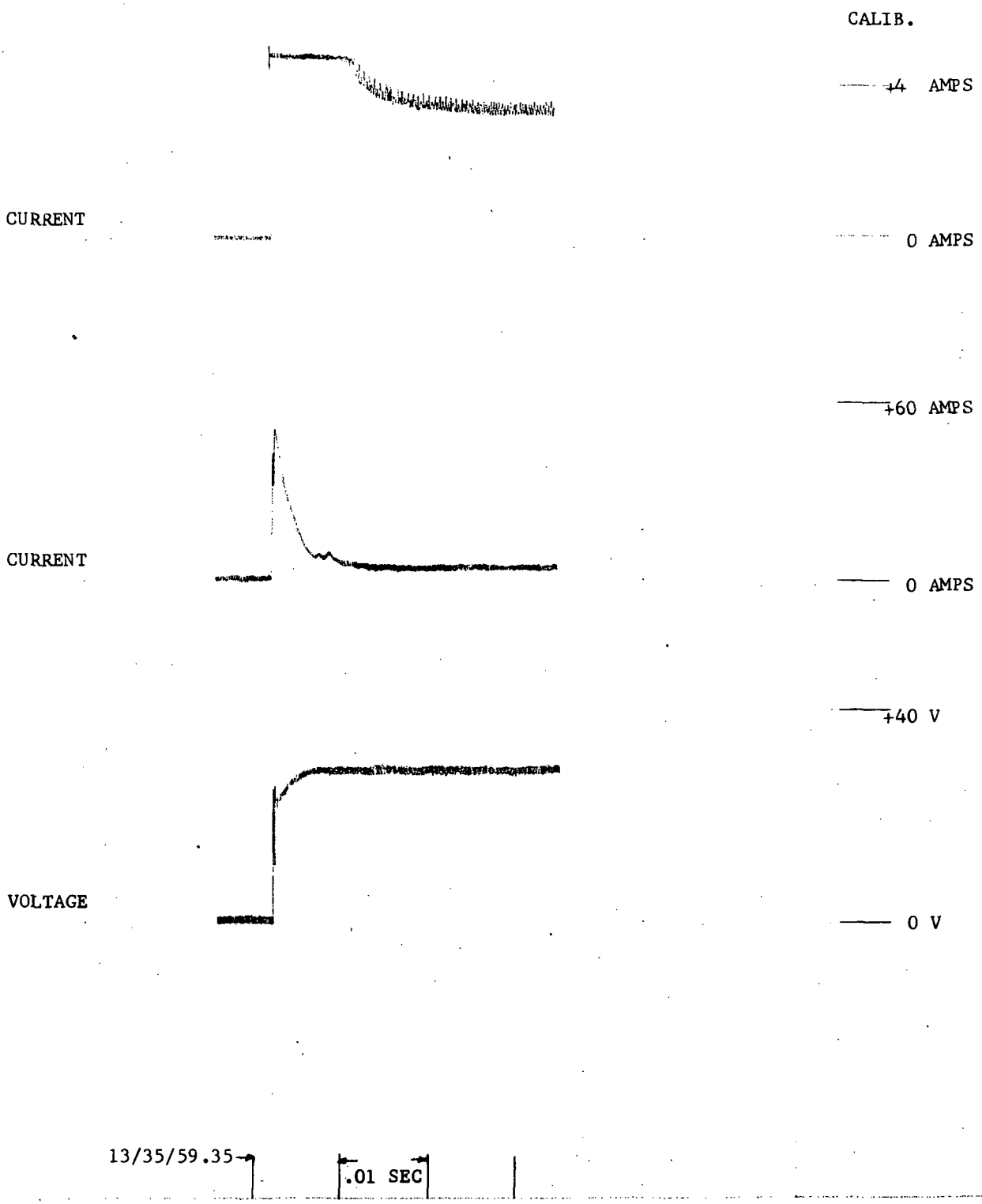

FIGURE 4-7 Voltage and Current Traces, Run 9A--Apollo Inverter (Expanded)

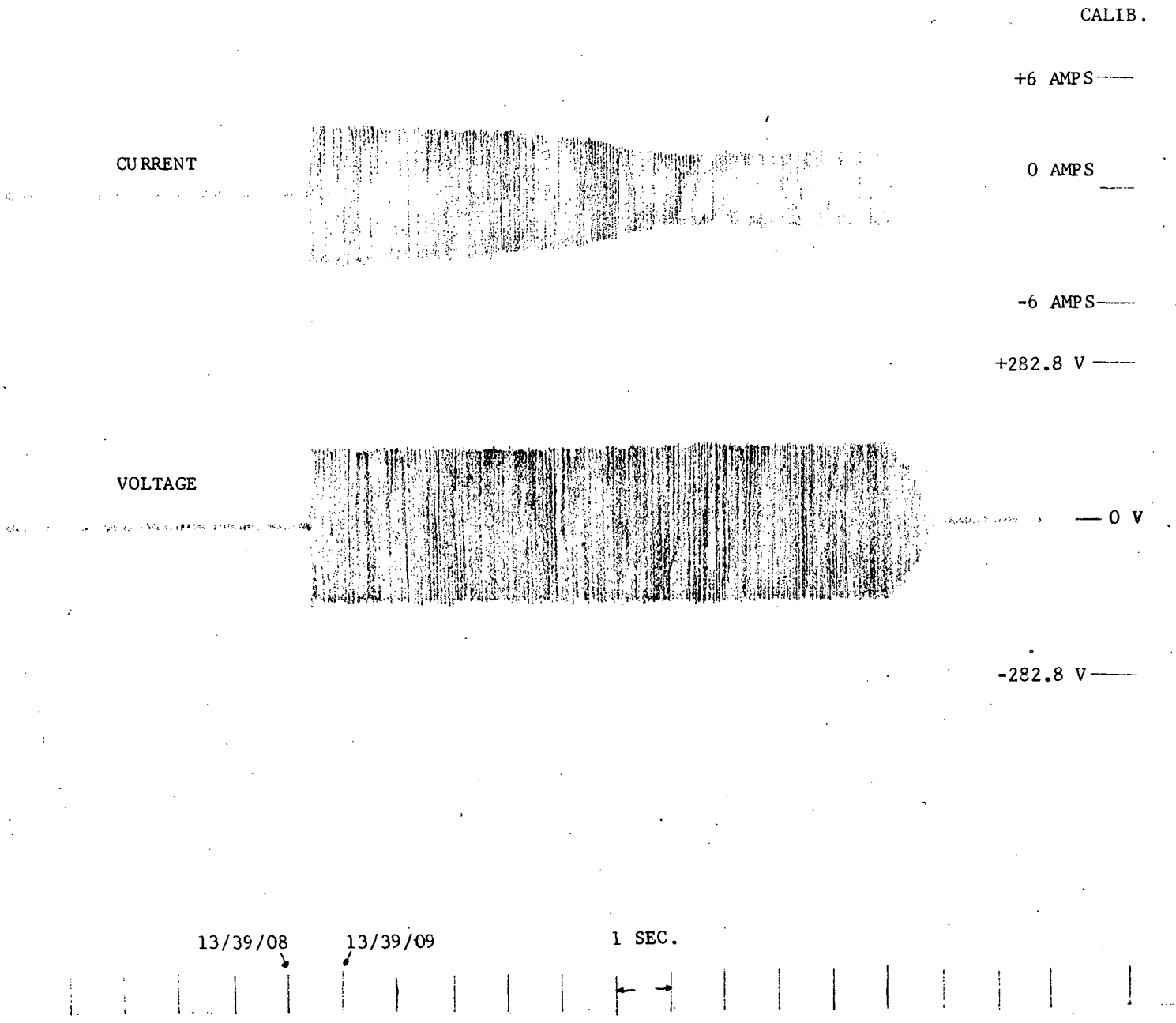

FIGURE 4-8 Voltage and Current Traces, Run 10B--Rotron Fan

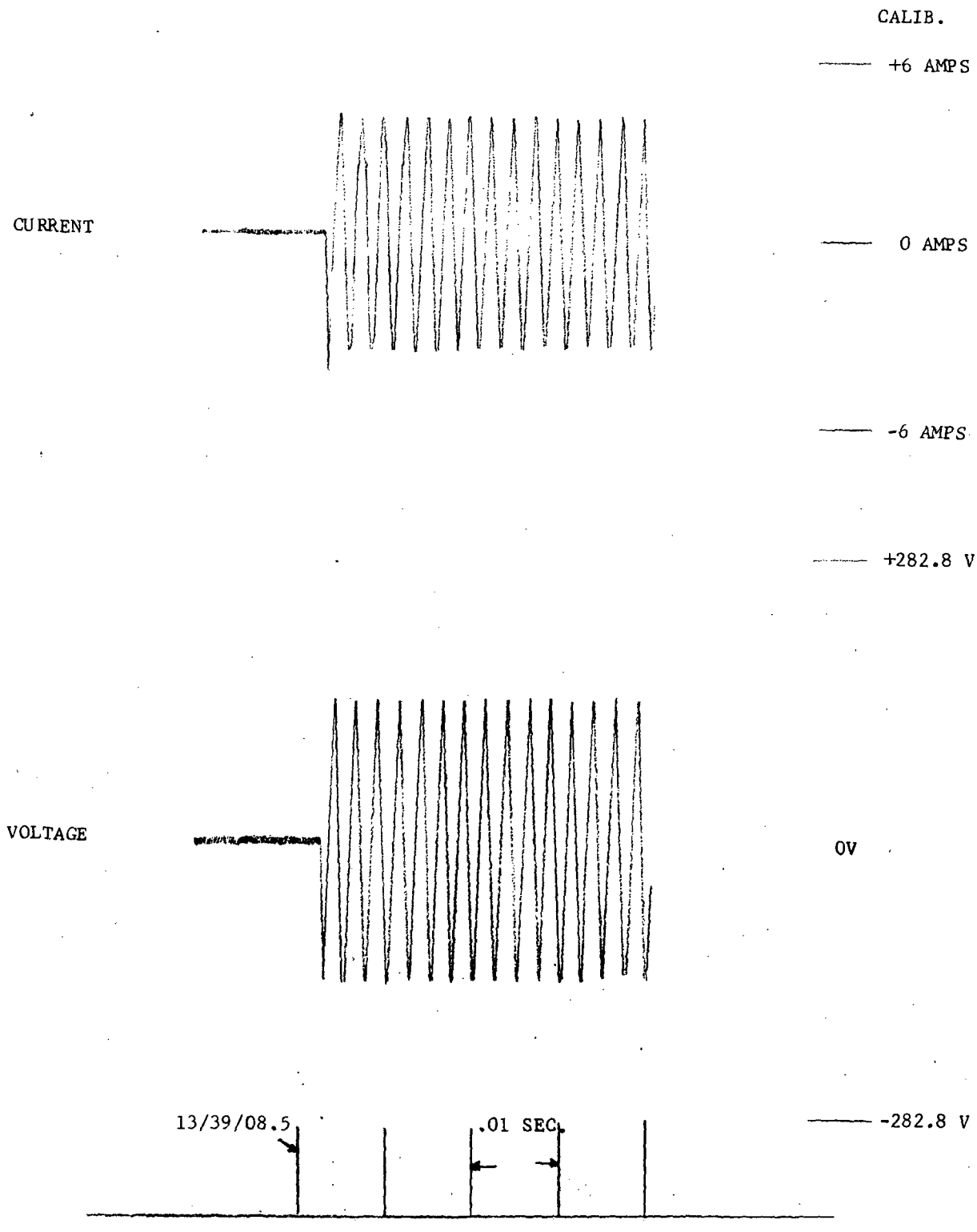

FIGURE 4-9 Voltage and Current Traces, Run 10B--Rotron Fan (Expanded)

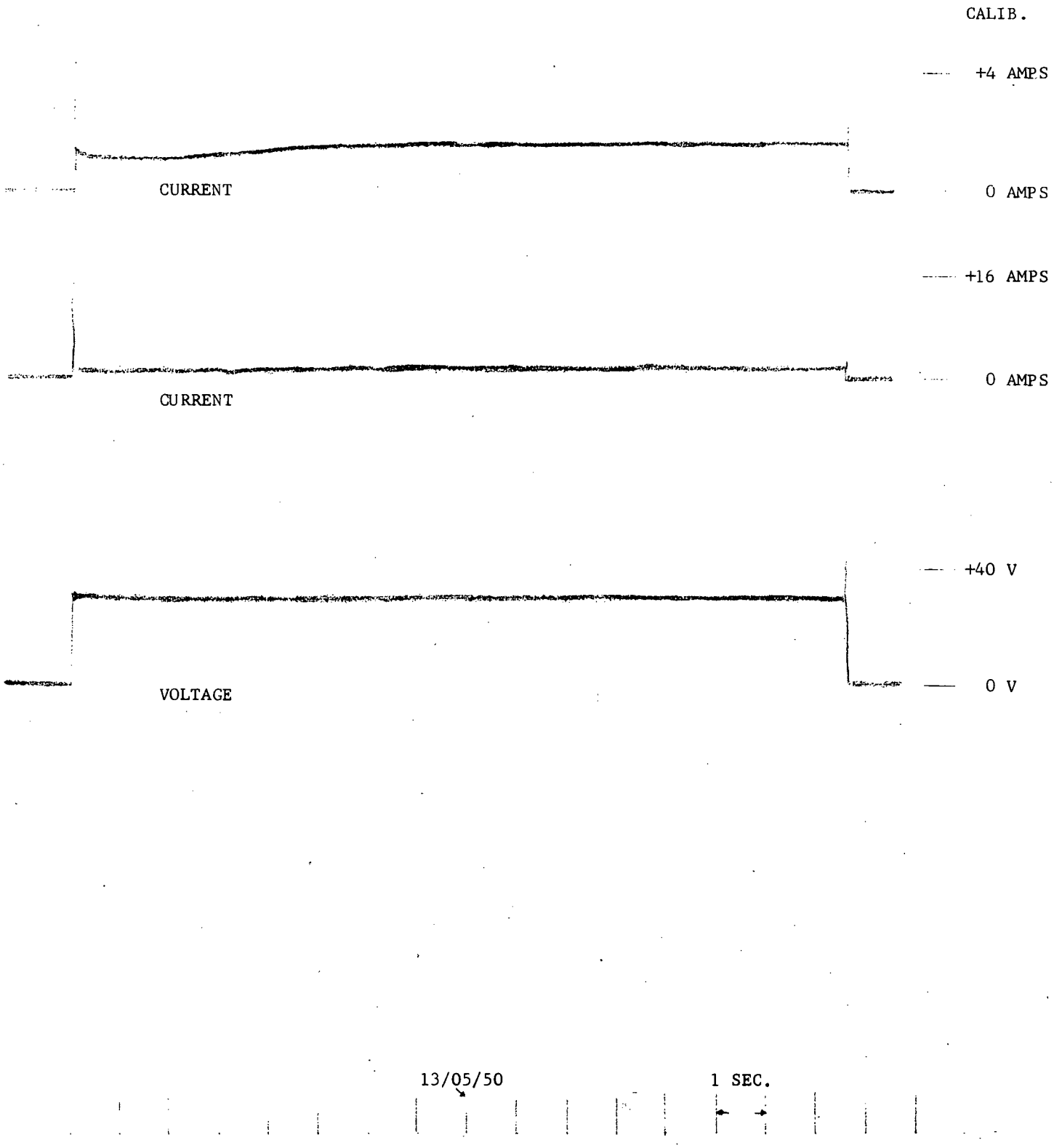

FIGURE 4-10 Voltage and Current Traces, Run 11C--VHF/AM Transceiver

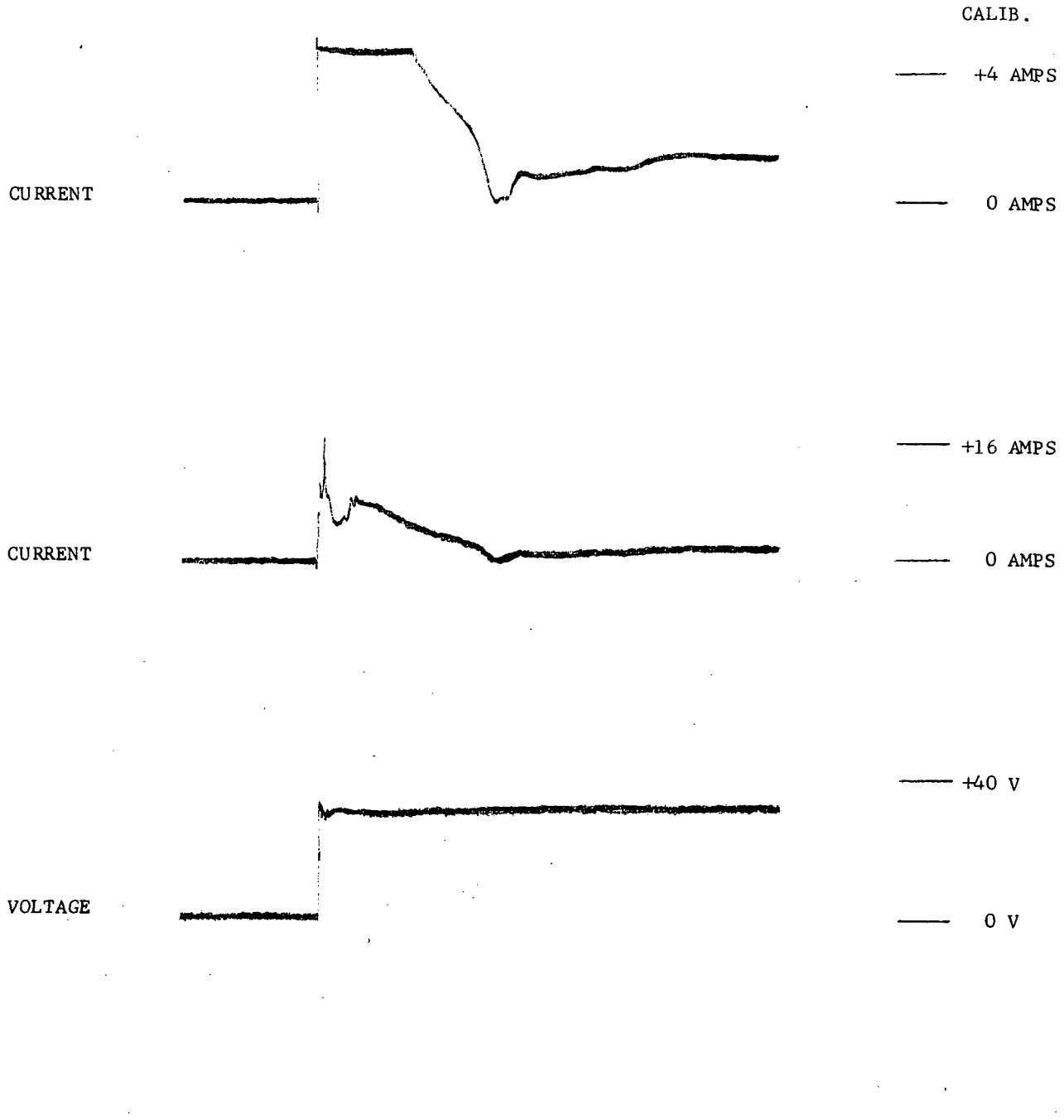

FIGURE 4-11 Voltage and Current Traces, Run 11C--VHF/AM Transceiver (Expanded)

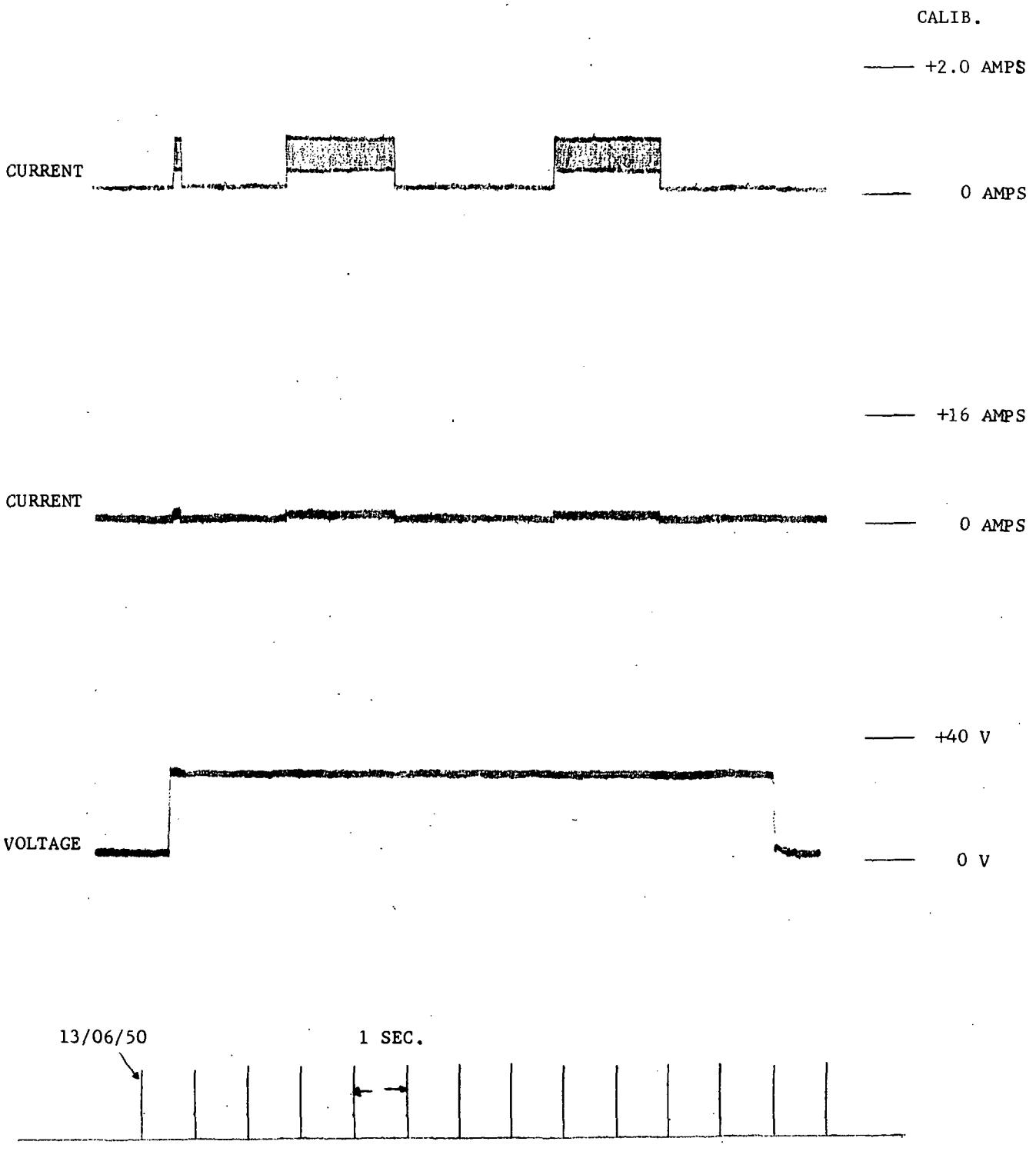

FIGURE 4-12 Voltage and Current Traces, Run 12A--Recovery Beacon

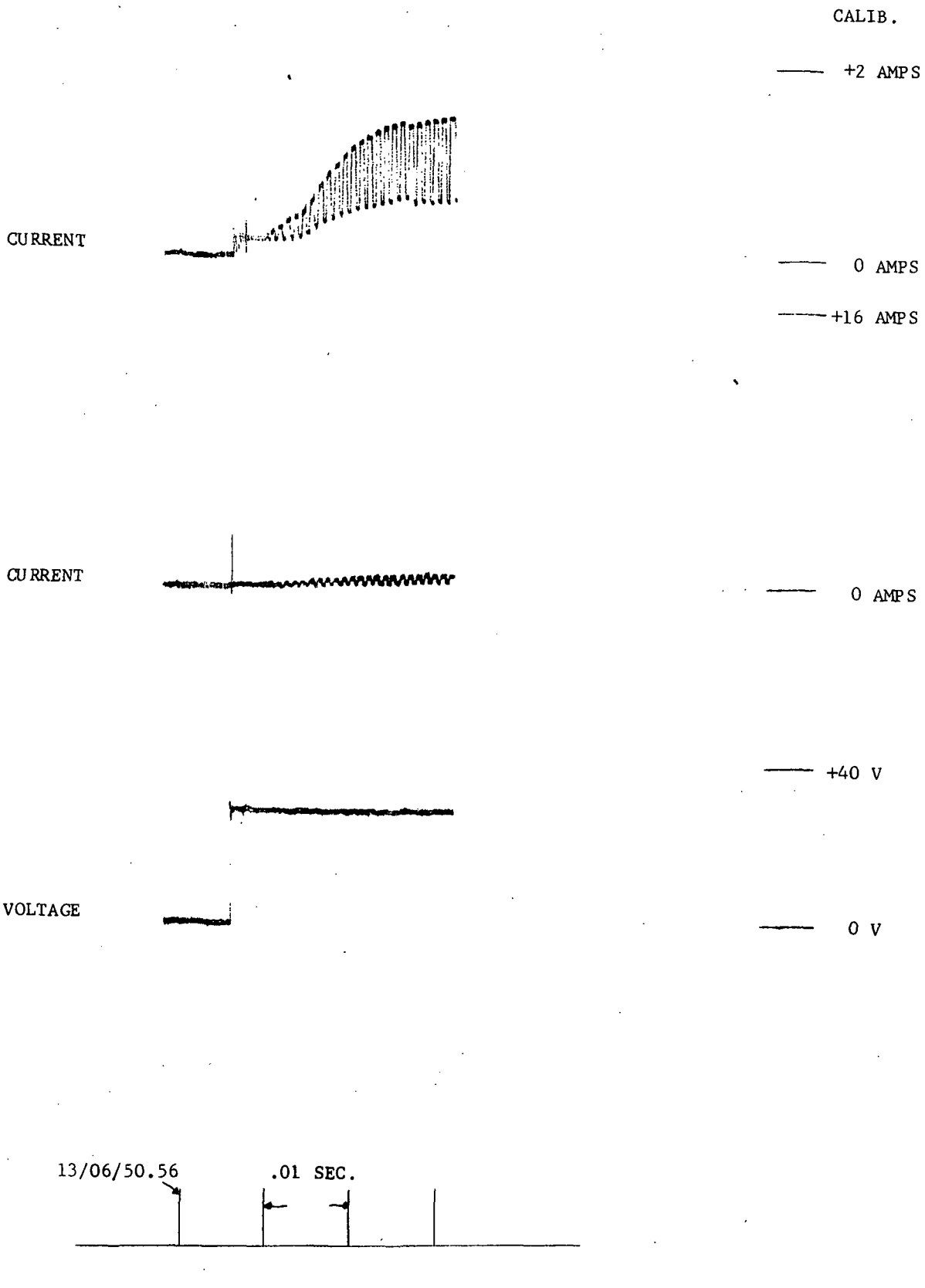

FIGURE 4-13 Voltage and Current Traces, Run 12A--Recovery Beacon (Expanded)

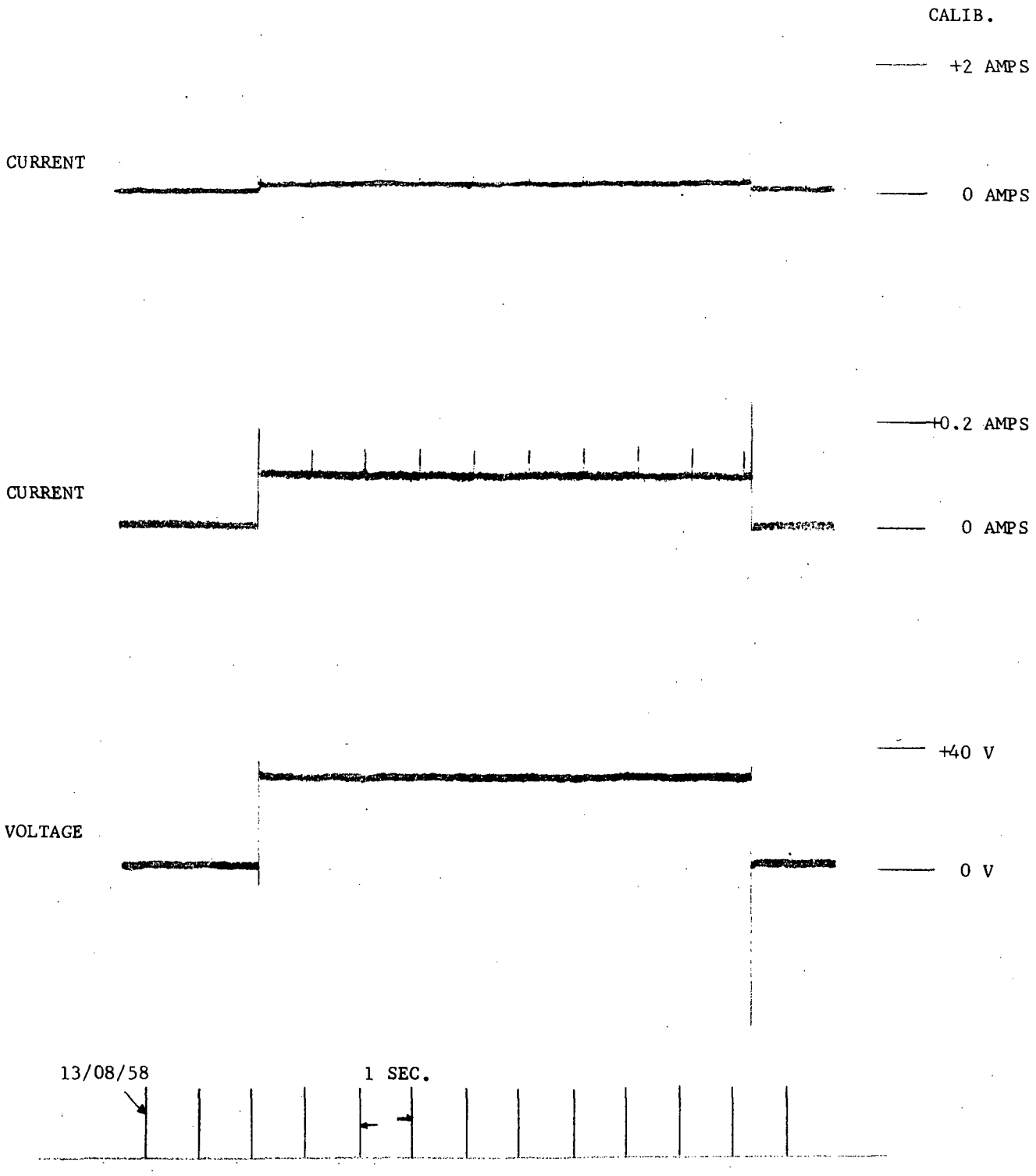

FIGURE 4-14 Voltage and Current Traces, Run 13B--UHF/FM Transmitter

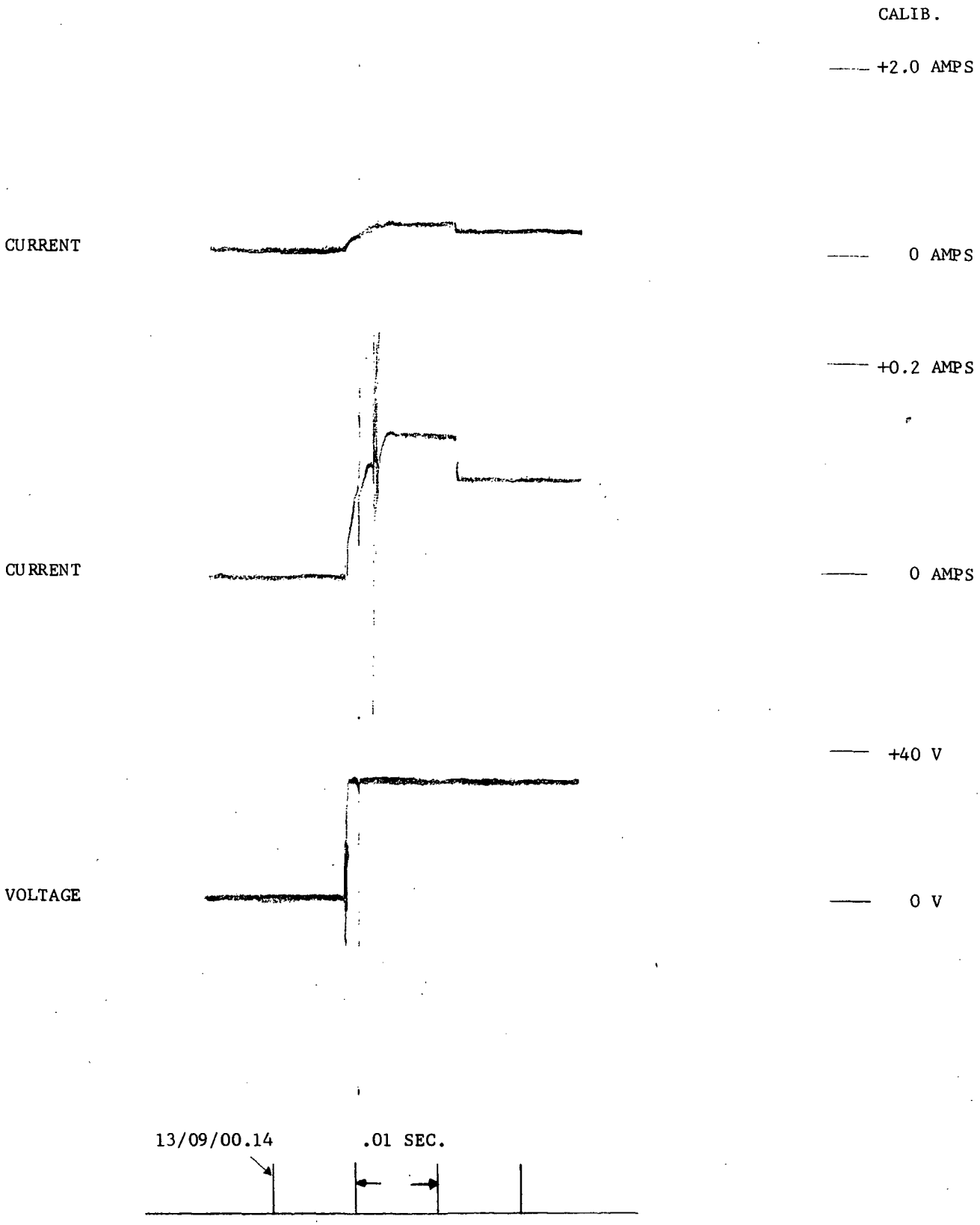

FIGURE 4-15 Voltage and Current Traces, Run 13B--UHF/FM Transmitter (Expanded)

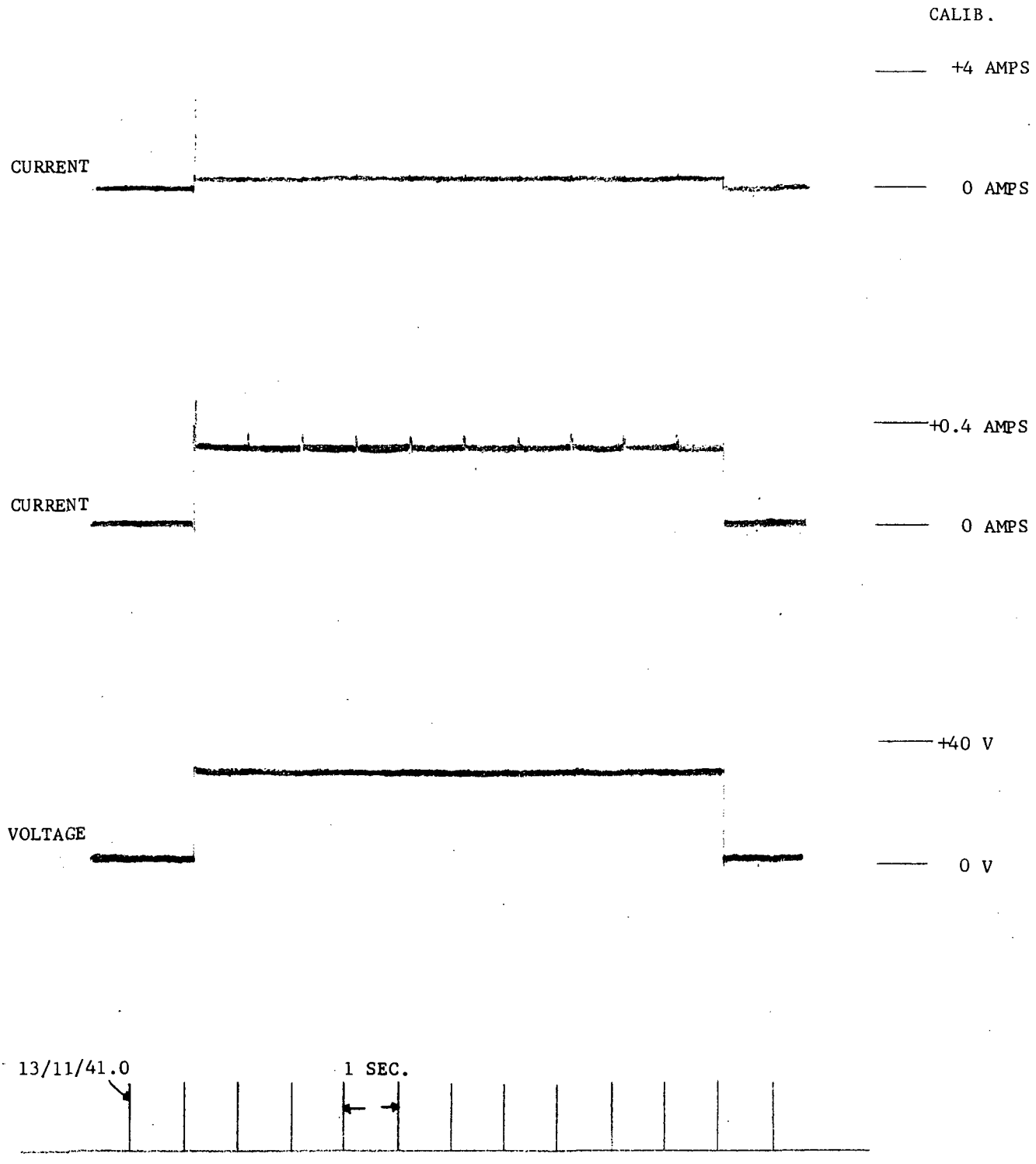

FIGURE 4-16 Voltage and Current Traces, Run 16A--HF Transceiver

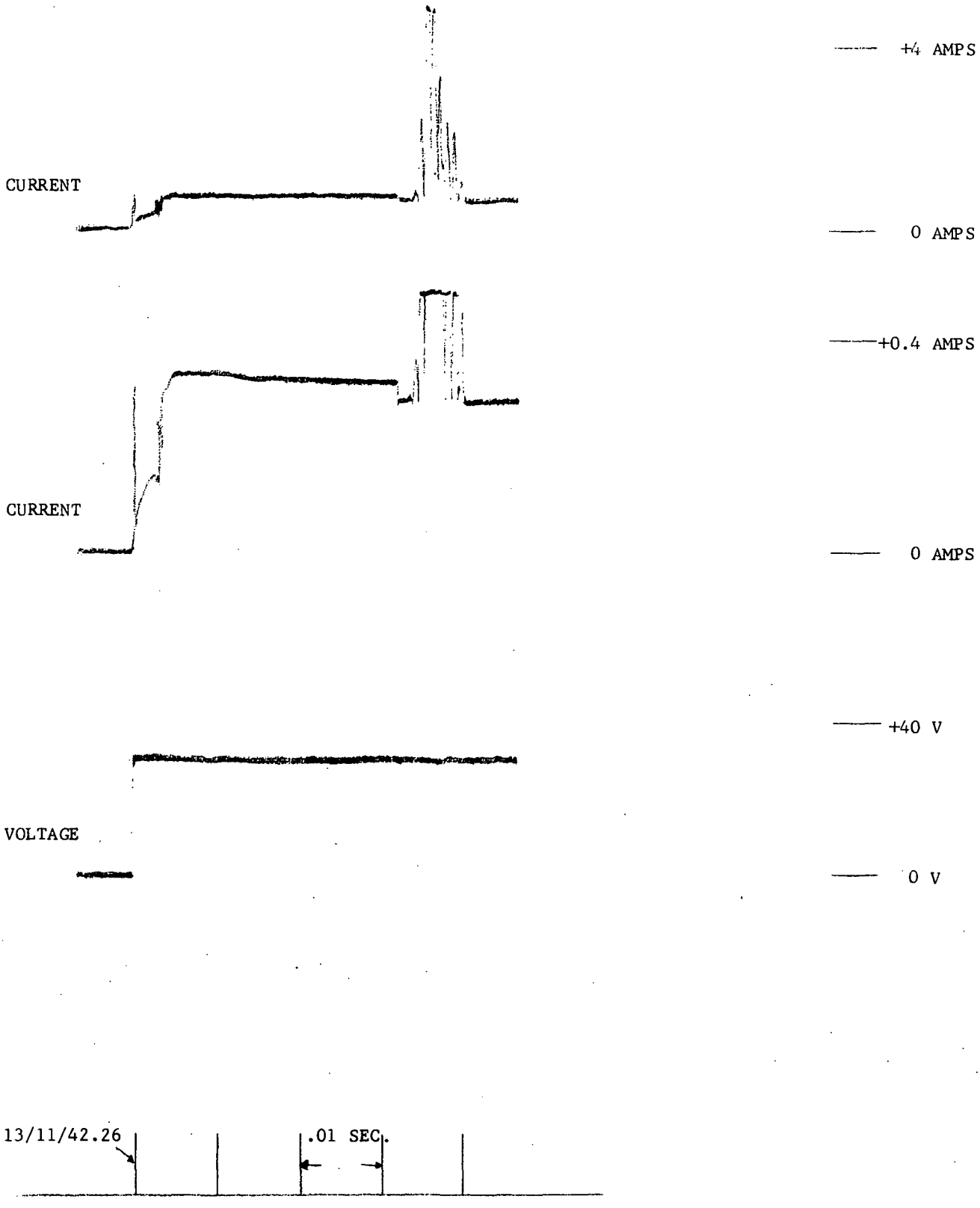

FIGURE 4-17 Voltage and Current Traces, Run 16A--HF Transceiver (Expanded)

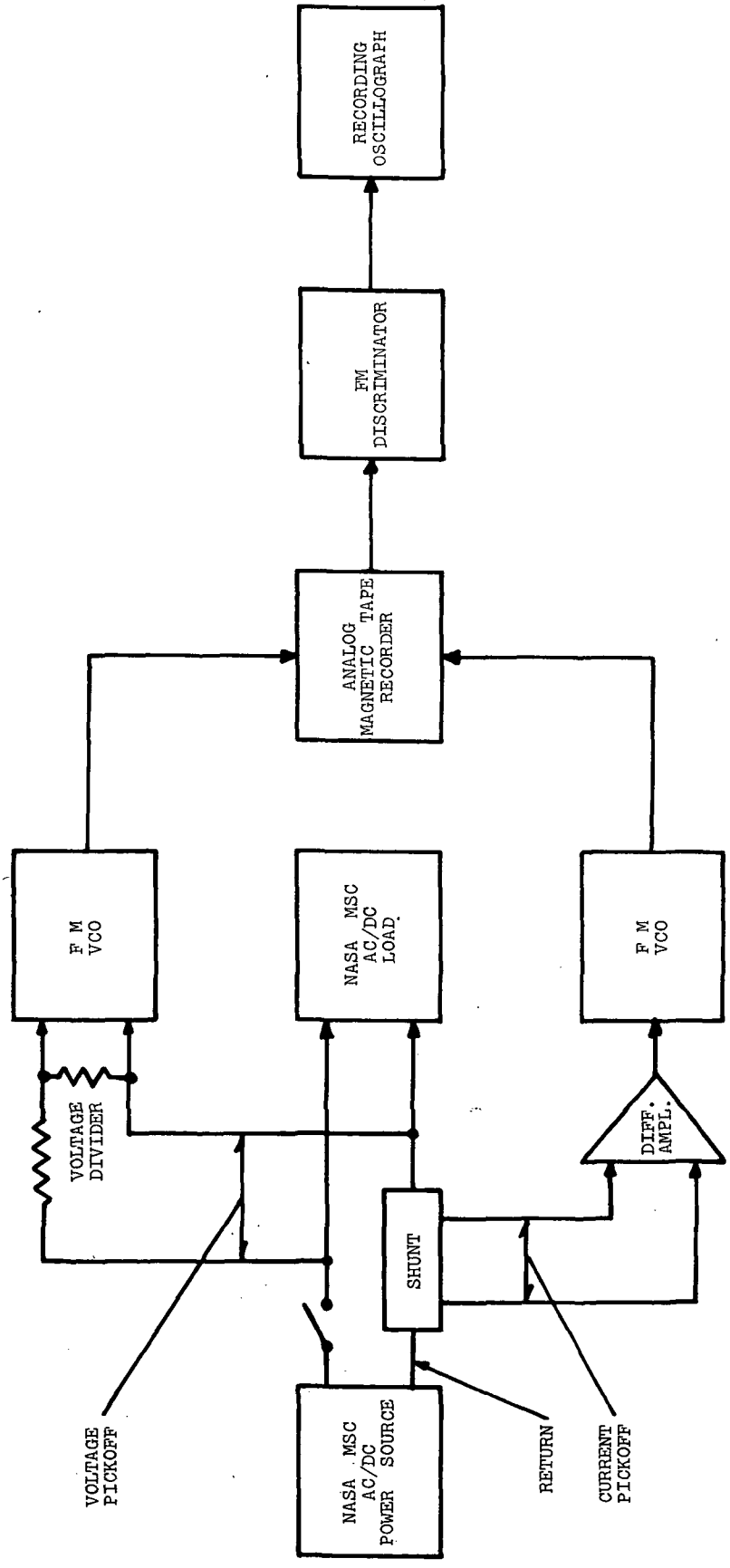

FIGURE 4-18 On-Site Data Acquisition System--Simplified Diagram

TABLE 4-II

ON-SITE DATA ACQUISITION EQUIPMENT LIST

Description	Manufacturer	Model
Analog Tape Recorder	Consolidated Electrodynamics Corporation	VR-3600
FM Discriminator	Electro-Mechanical Research, Inc.	287
Recording Oscillograph	Consolidated Electrodynamics Corporation	5-124
Voltage Controlled Oscillator	Electro-Mechanical Research, Inc.	4570
Differential Amplifier	Hewlett-Packard	2470A
Precision Voltage Source	Electronic Development Corporation	VS-11-R

4.2 DATA PROCESSING

The analog magnetic tapes recorded at MSC were returned to Avco Systems Division's Data Processing Center for processing for input to the model optimization activities and for preparation of a variable R control tape.

4.2.1 Data Processing for Model Optimization Input

The analog magnetic tapes were processed to provide a digital representation of the current/voltage-time history data for use in the model synthesis and optimization computer program. These tapes were reproduced and the signals demodulated to provide voltage representations of the measured current/voltage data. Oscillograph recordings were made to determine the areas of interest, and the start/stop digitizing times were read from the IRIG format B time code. This record was used to define the digital sampling rate required to adequately define the data.

The analog magnetic tape recordings, recorded at 120 inches/second, were reproduced at a tape speed of 15 inches/second thereby providing a time base expansion factor of 8 to 1. The FM-recorded data was demodulated using EMR Model 287 FM Discriminators. The output voltage of the discriminators was fed to the input of the Astrodata Analog-to-Digital (A/D) Conversion System.

A sampling rate of 12,500 samples/second/channel was selected to provide an equivalent real time sample rate of 100,000 samples/second/channel. This rate was selected to provide 10 samples/cycle of the maximum information frequency, i.e., 10 KHz.

For each digitizing run the calibration signals recorded on the analog tape were also digitized to allow the digital representation of the voltage and current values to be calibrated to their corresponding engineering units, i.e., volts and amperes. The A/D system output digital tape was then processed on the IBM System 360/75 computer to provide calibrated current/voltage data interpolated to a common time base.

The existing computer optimization program can accept a maximum of 200 data points. Therefore, each of the transient intervals of interest was divided linearly into this number of samples during the analog-to-digital conversion.

Only the transient intervals were sampled since the steady-state conditions are either end points of transient intervals or easily determined by straight-forward calculation.

The data for the five equipments selected for modelling (see Paragraph 4.3.1) was then provided on punched cards for input to the optimization program.

A block diagram of the data processing system is shown in Figure 4-19. The data processing equipment is identified in Table 4-III.

To better visualize the data, and to confirm that the digitized data is a true representation of the original response data, the data on the punched cards was plotted. These plots are shown in Figures 4-20 through 4-31. They correspond to the traces provided in Figures 4-1 through 4-17.

As a convenience in describing or comparing the data in this report, the response curves shown in these figures (4-20 through 4-31) will be used as the reference traces.

4.2.2 Data Processing for Variable R Control Tape

The variable R control signal is an analog of the conductance-time curve of the equipment to be simulated. This signal is obtained by interrogating the equipment to be simulated and computing the input current/voltage ratio versus time, $G(t) = I(t)/E(t)$, and then scaling this function on the basis of the variable R transfer characteristic. Thus, the control voltage, $V_C = KG(t) = K\left[\underline{I}(t)/E(t)\right]$. See Figure 4-32 for a simplified block diagram of the process for generating a control tape.

The variable R delivered as part of the Model DLS 1000 Simulator is a 250-watt, peak, device. The control voltage/load voltage combination must be chosen consistent with this constraint or the variable R will limit the load current, thus altering the desired response.

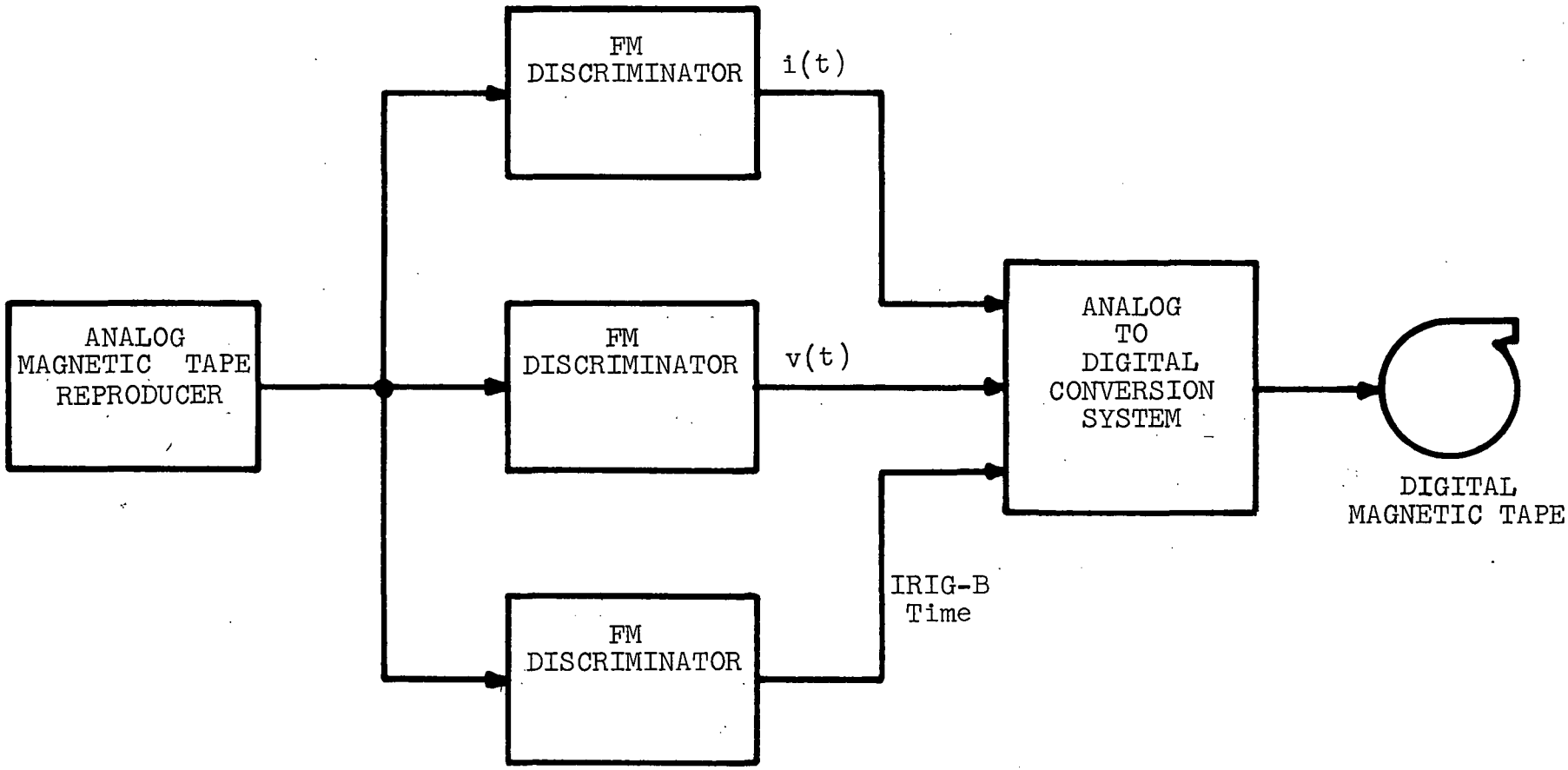

FIGURE 4-19 Processing System for Obtaining Input Data to Optimization Program--Simplified Diagram

TABLE 4-III

DATA PROCESSING EQUIPMENT LIST

Description	Manufacturer	Model
Analog Tape Reproducer	Consolidated Electrodynamics Corporation	VR-3600
FM Discriminator	Electro-Mechanical Research Inc.	287
Analog-to-Digital System	Astrodata, Inc.	1

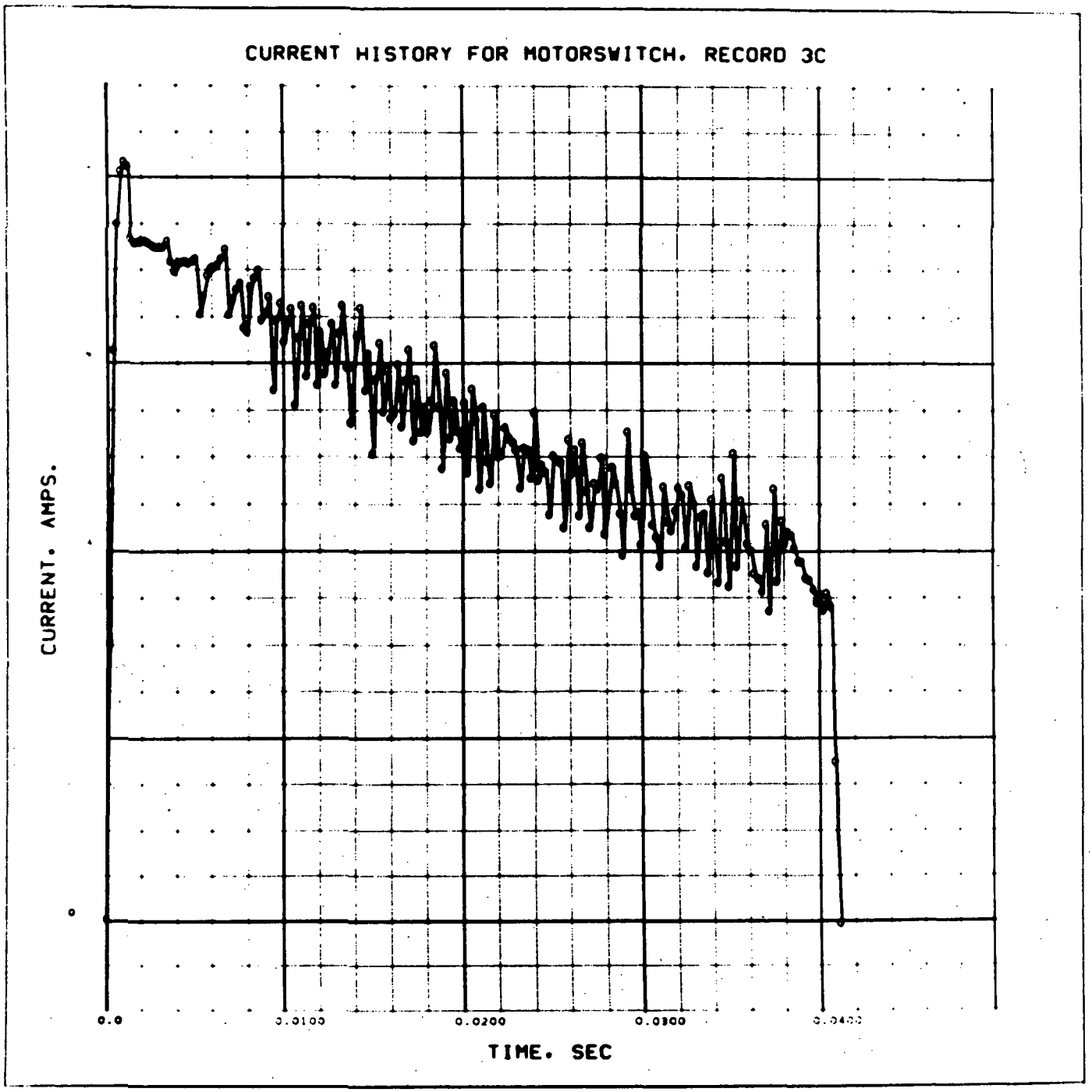

FIGURE 4-20 Current History for Motor Switch, Run 3C

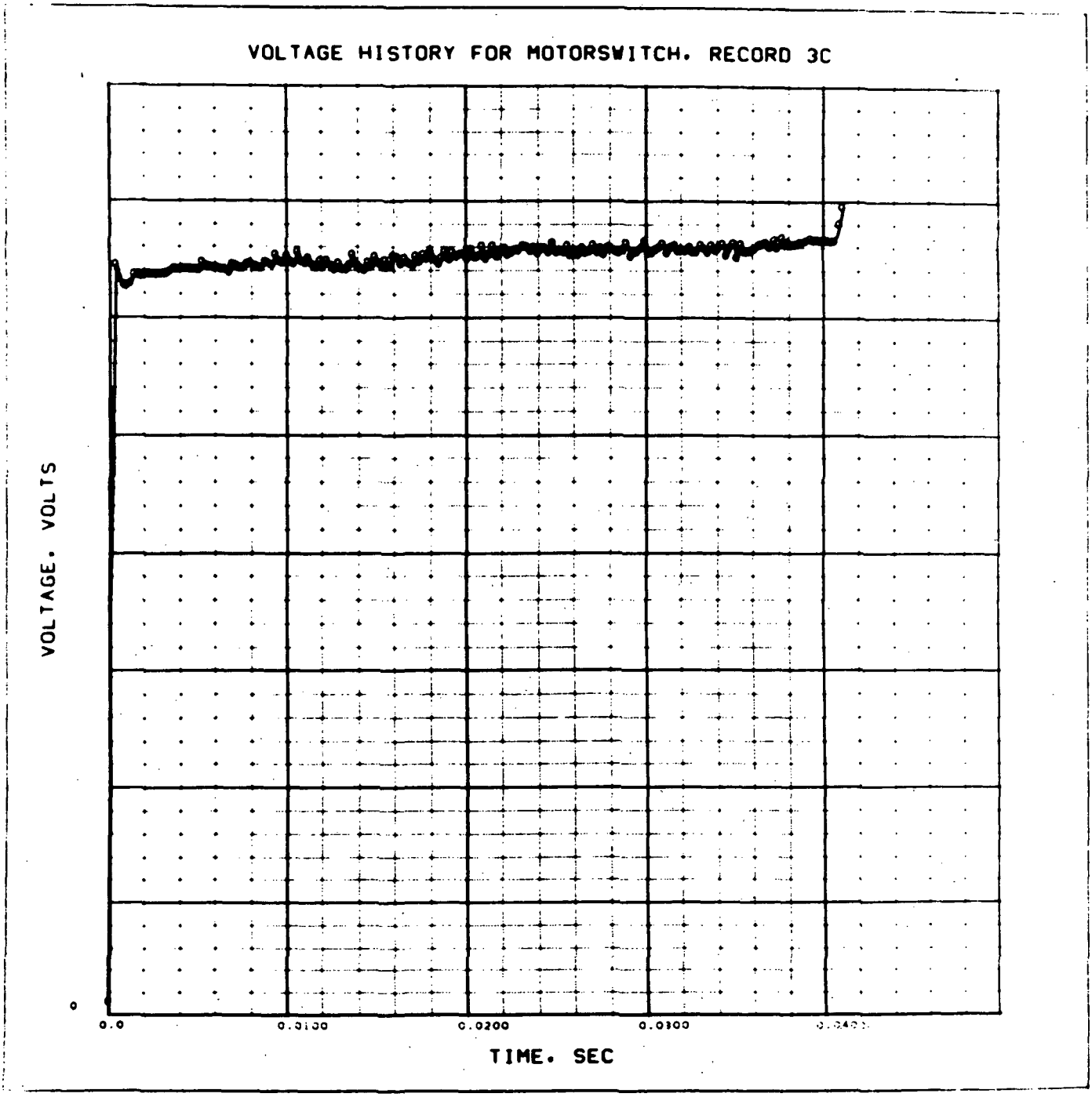

FIGURE 4-21 Voltage History for Motor Switch, Run 3C

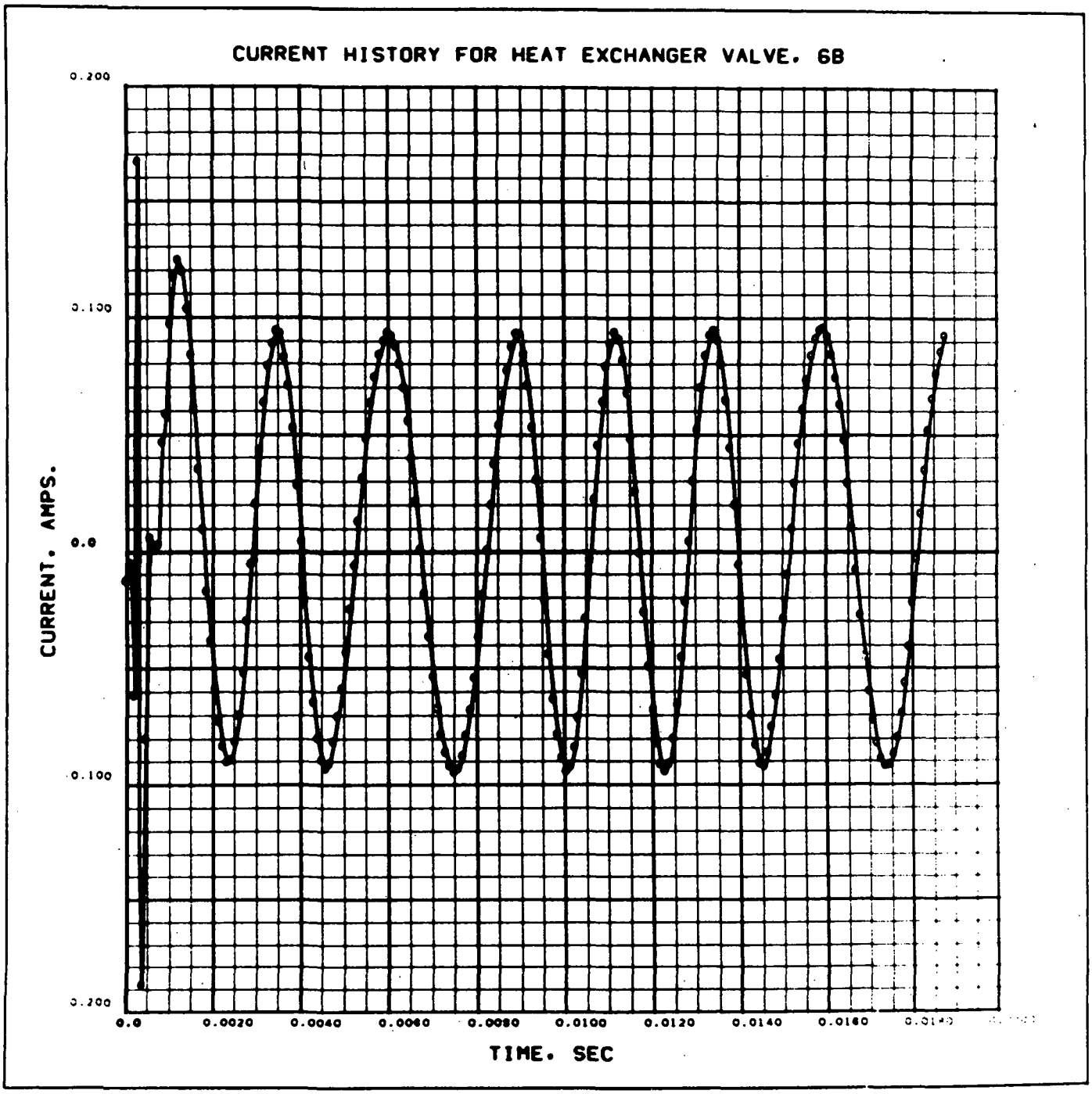

FIGURE 4-22 Current History for Heat Exchanger Valve, Run 6B

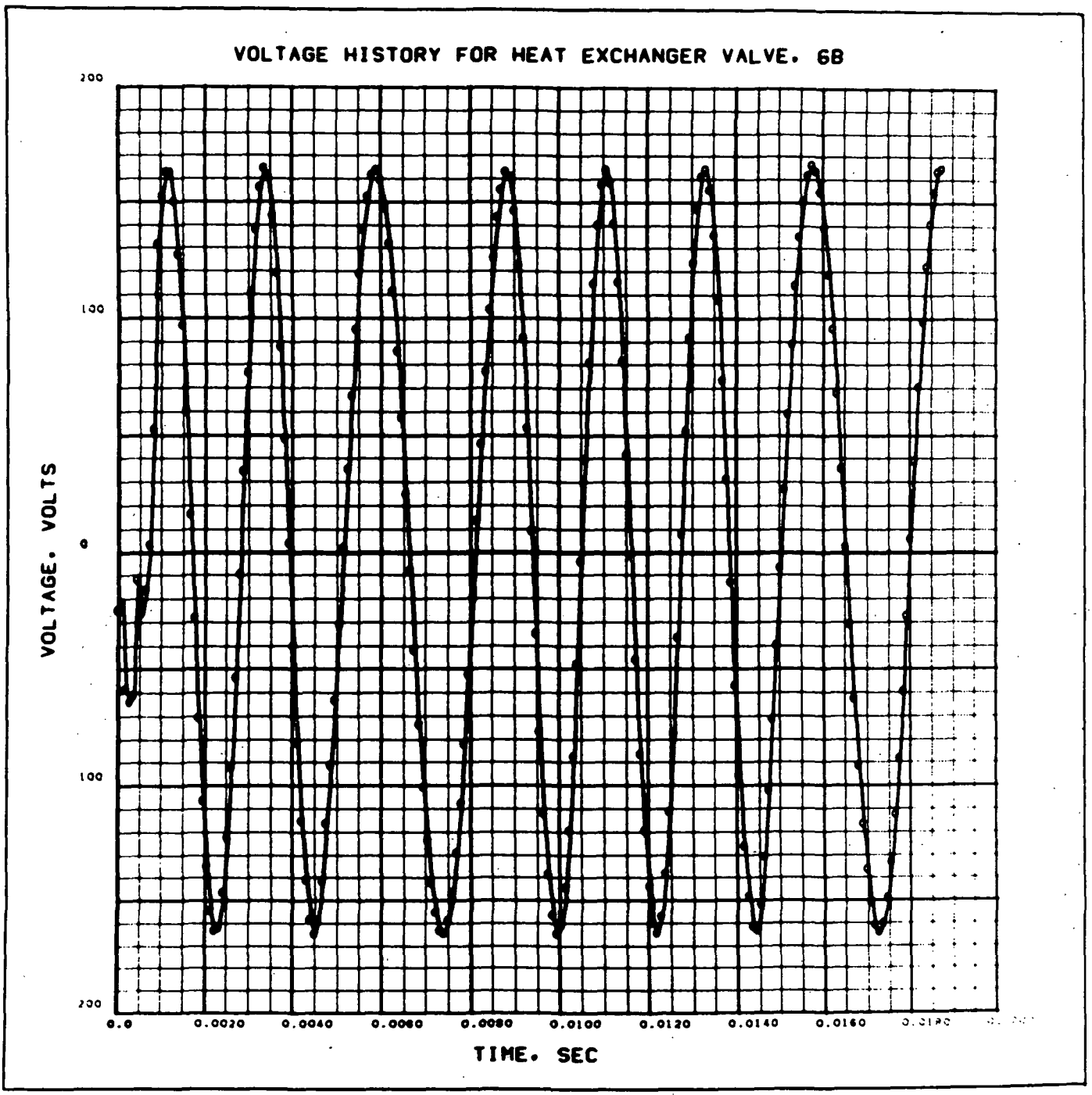

FIGURE 4-23 Voltage History for Heat Exchanger Valve, Run 6B

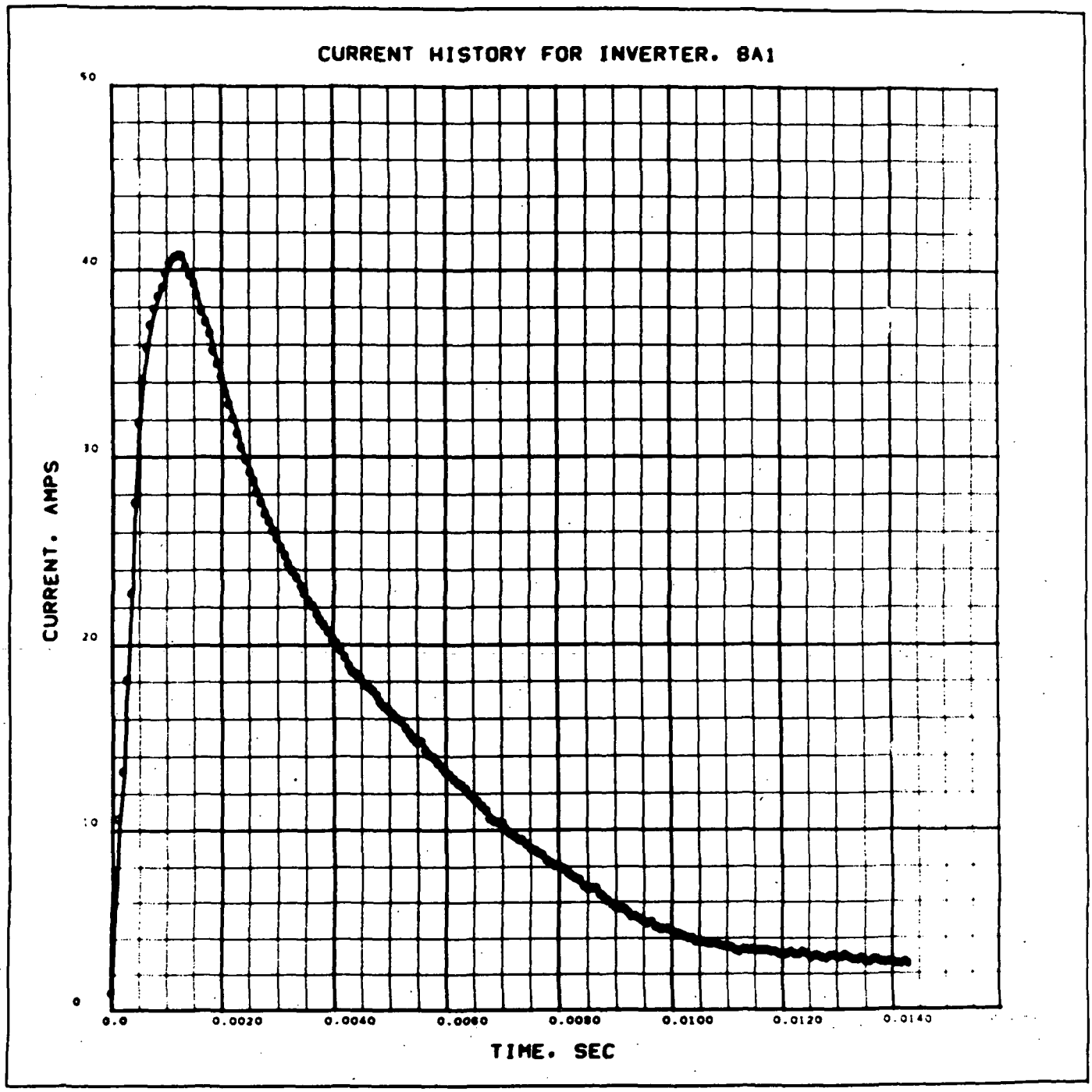

FIGURE 4-24 Current History for Varo Inverter, First Event, Run 8A1

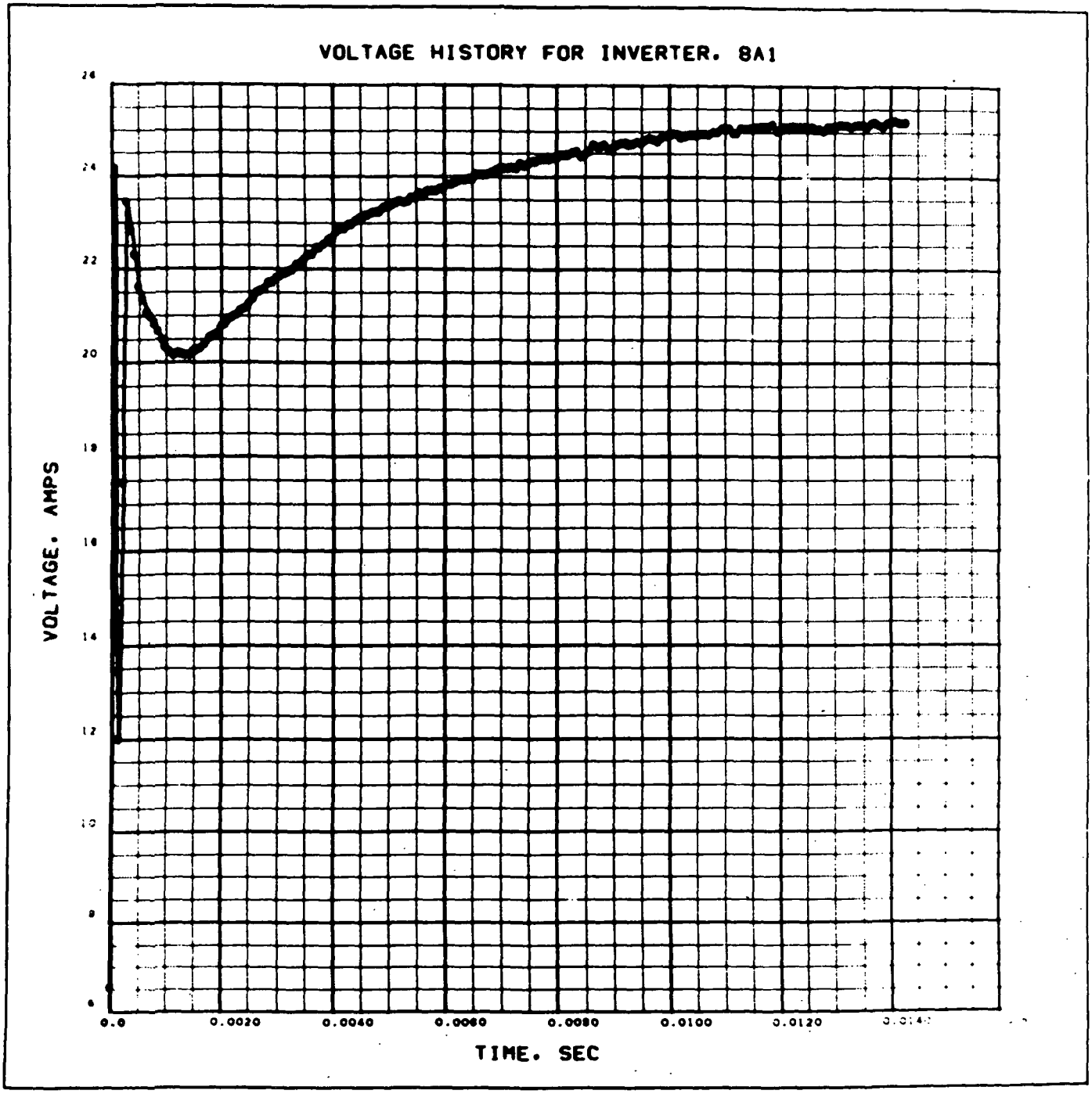

FIGURE 4-25 Voltage History for Varo Inverter, First Event, Run 8A1

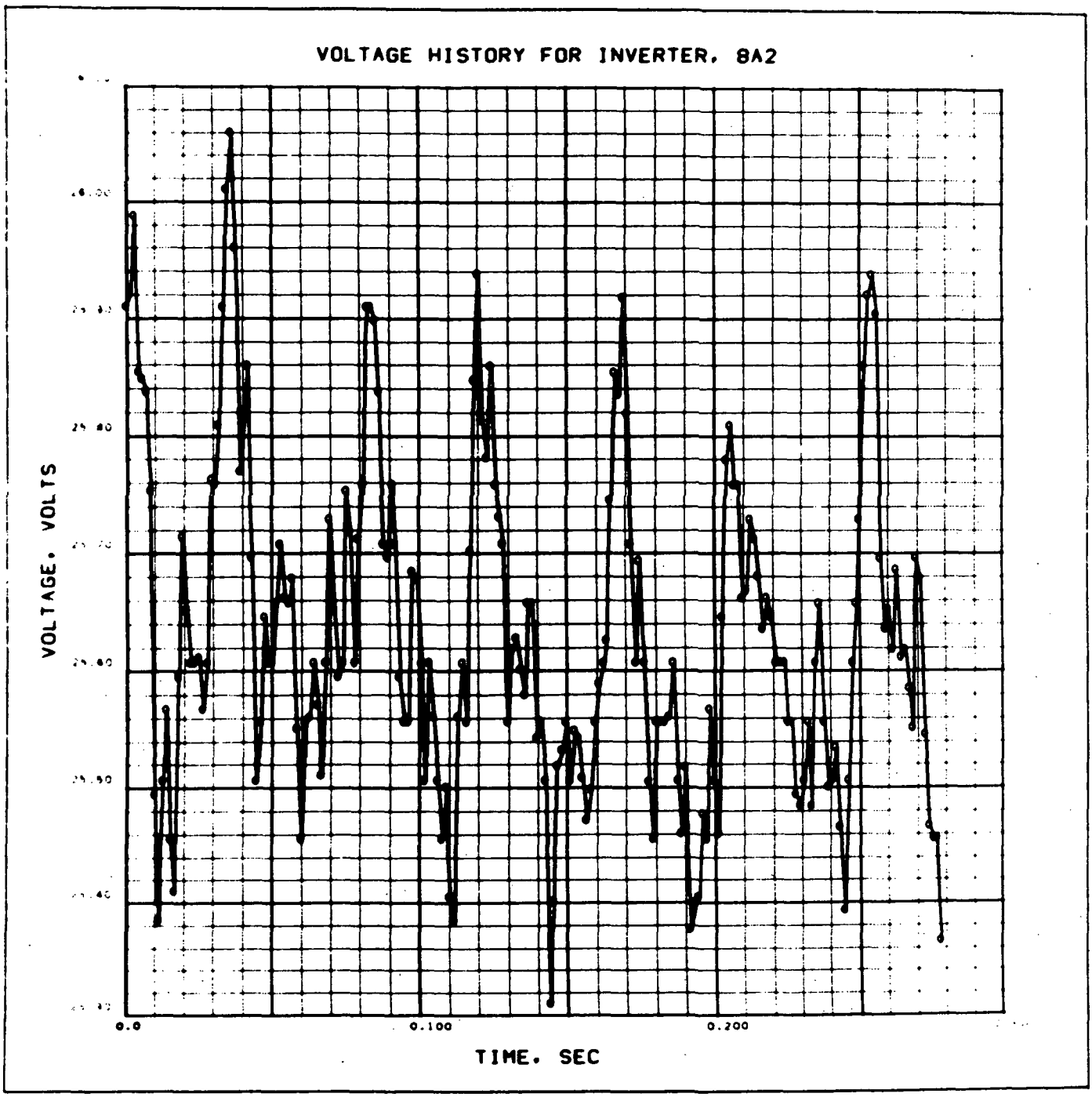

FIGURE 4-26 Current History for Varo Inverter, Second Event, Run 8A2

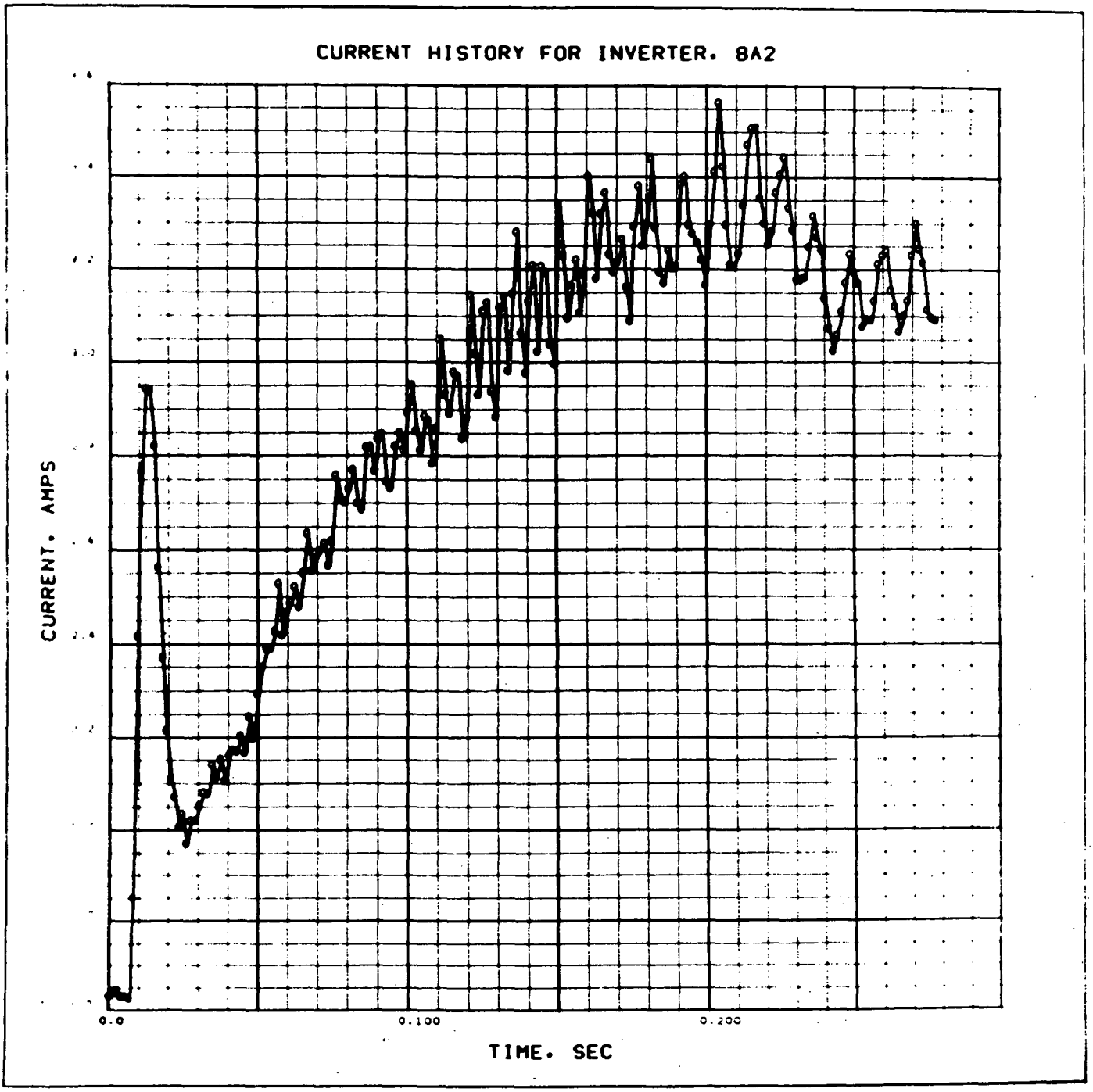

FIGURE 4-27 Voltage History for Varo Inverter, Second Event, Run 8A2

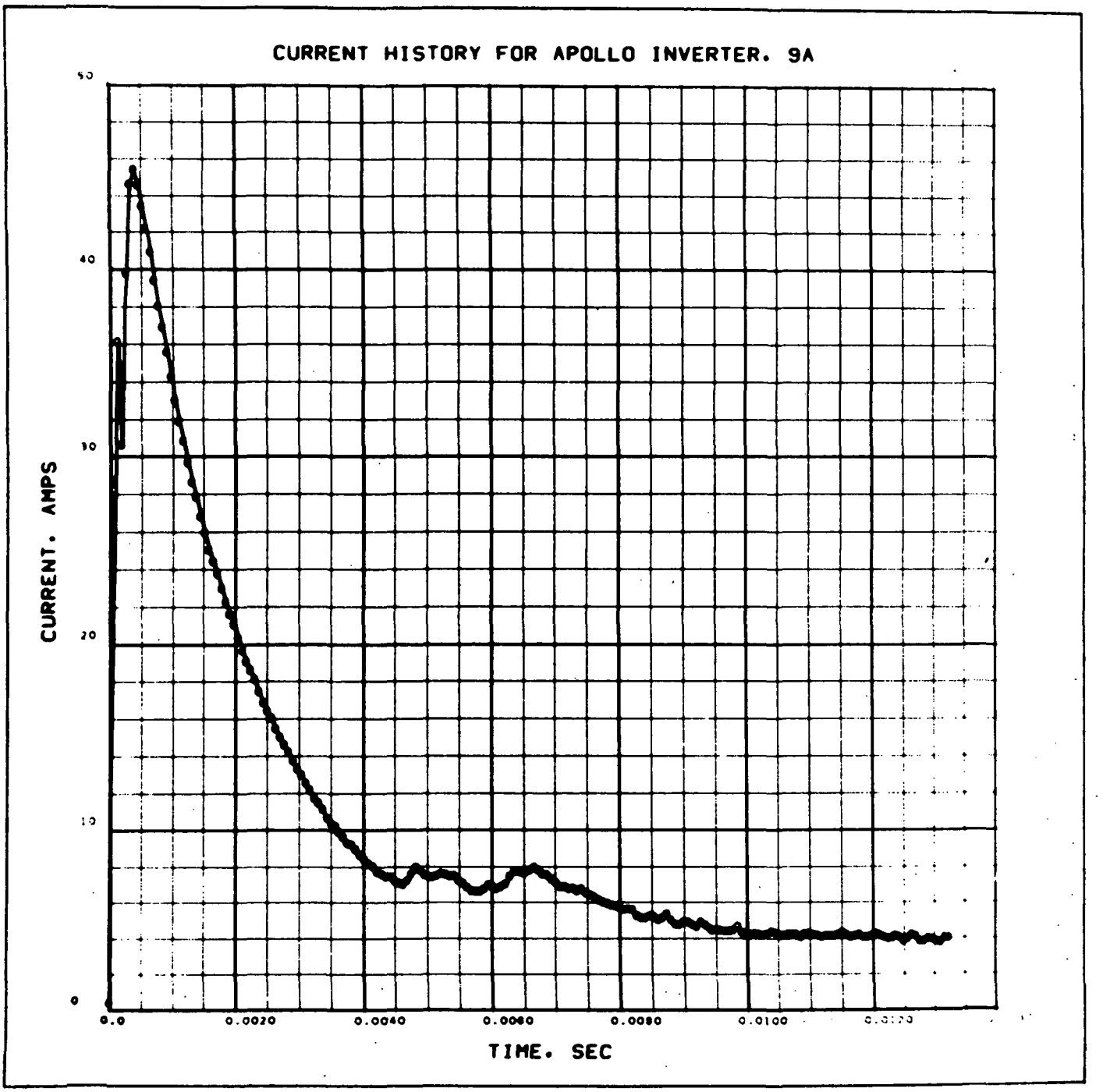

FIGURE 4-28 Current History for Apollo Inverter, Run 9A

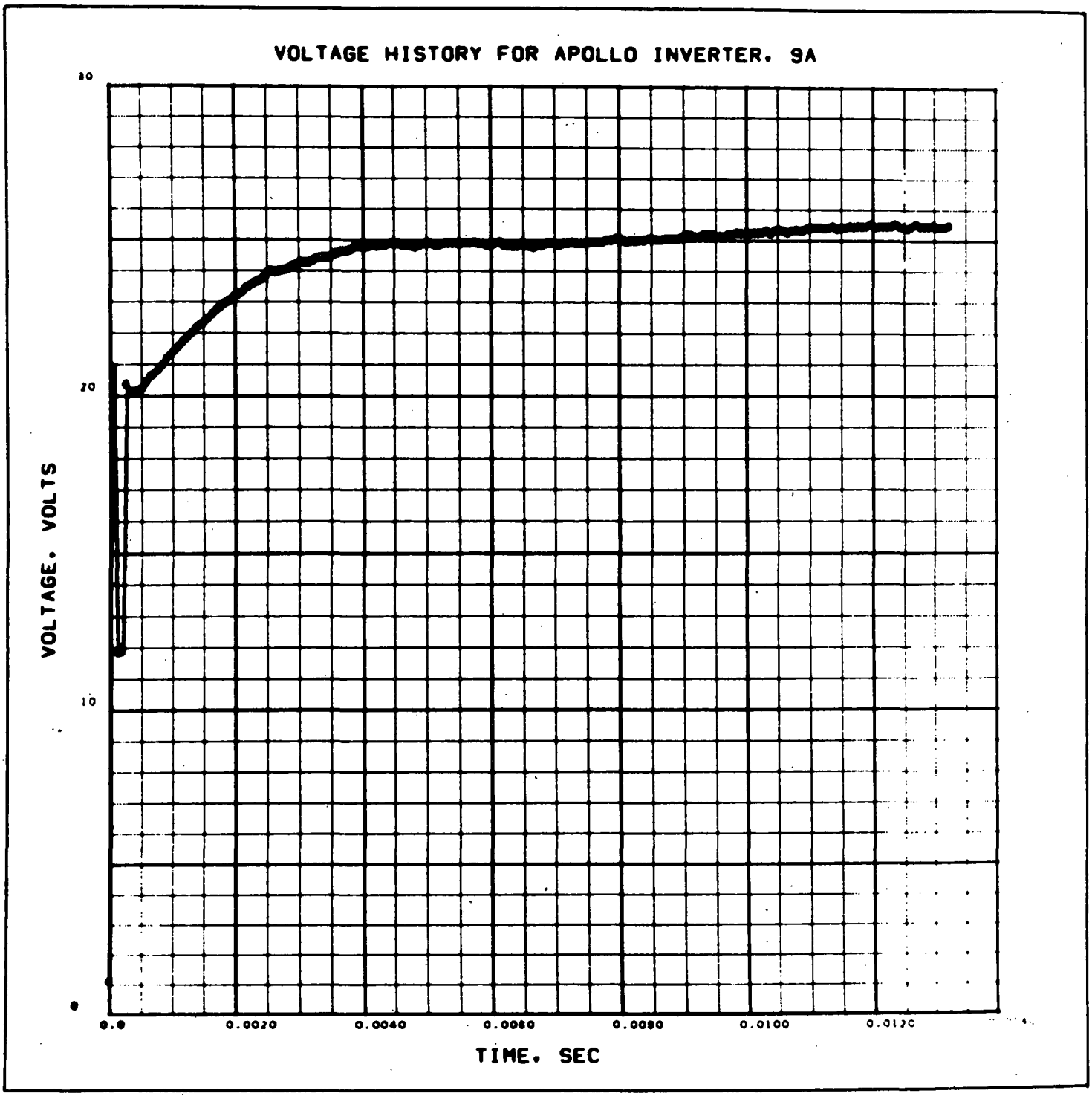

FIGURE 4-29 Voltage History for Apollo Inverter, Run 9A

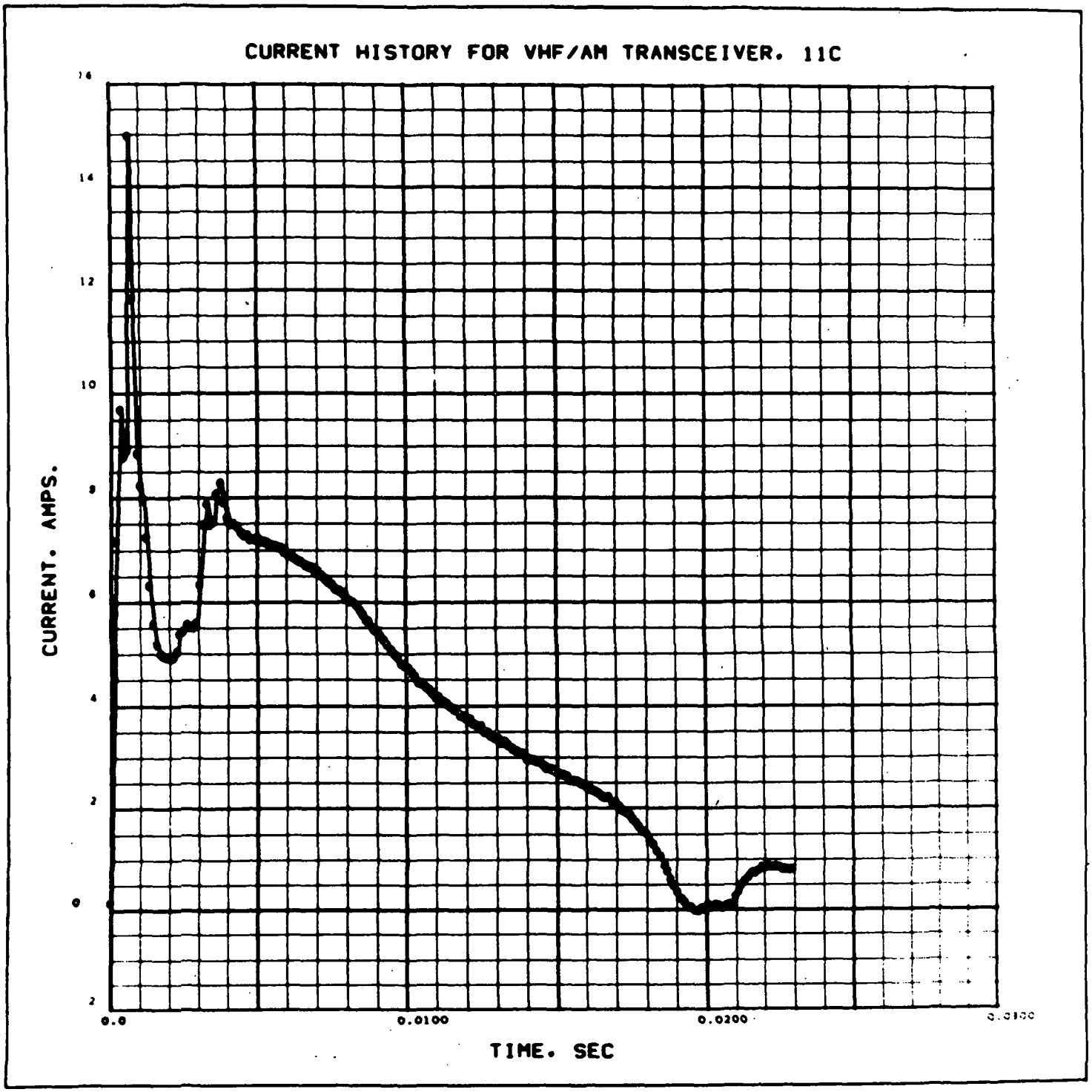

FIGURE 4-30 Current History for VHF/AM Transceiver, Run 11C

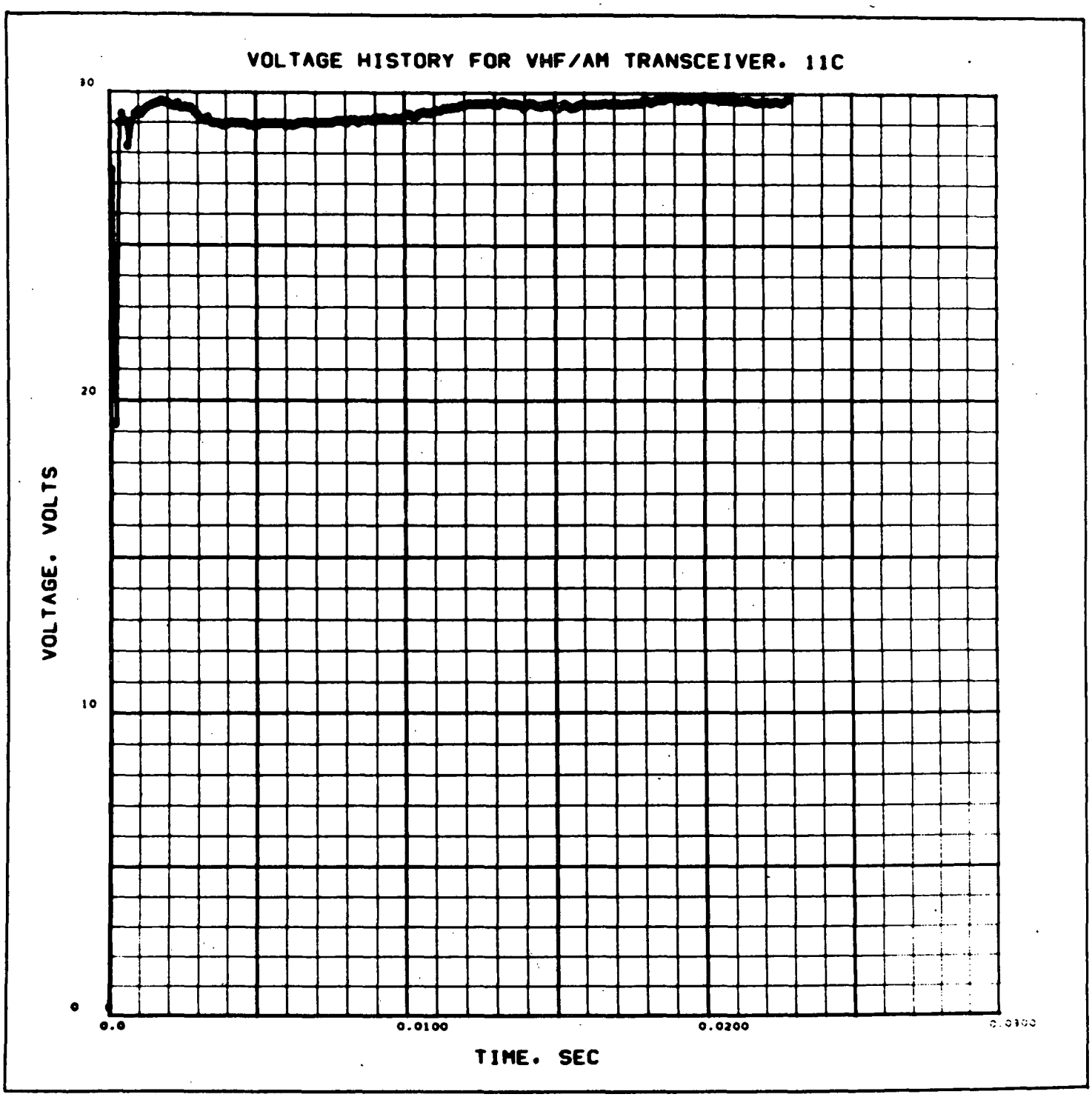

FIGURE 4-31 Voltage History for VHF/AM Transceiver, Run 11C

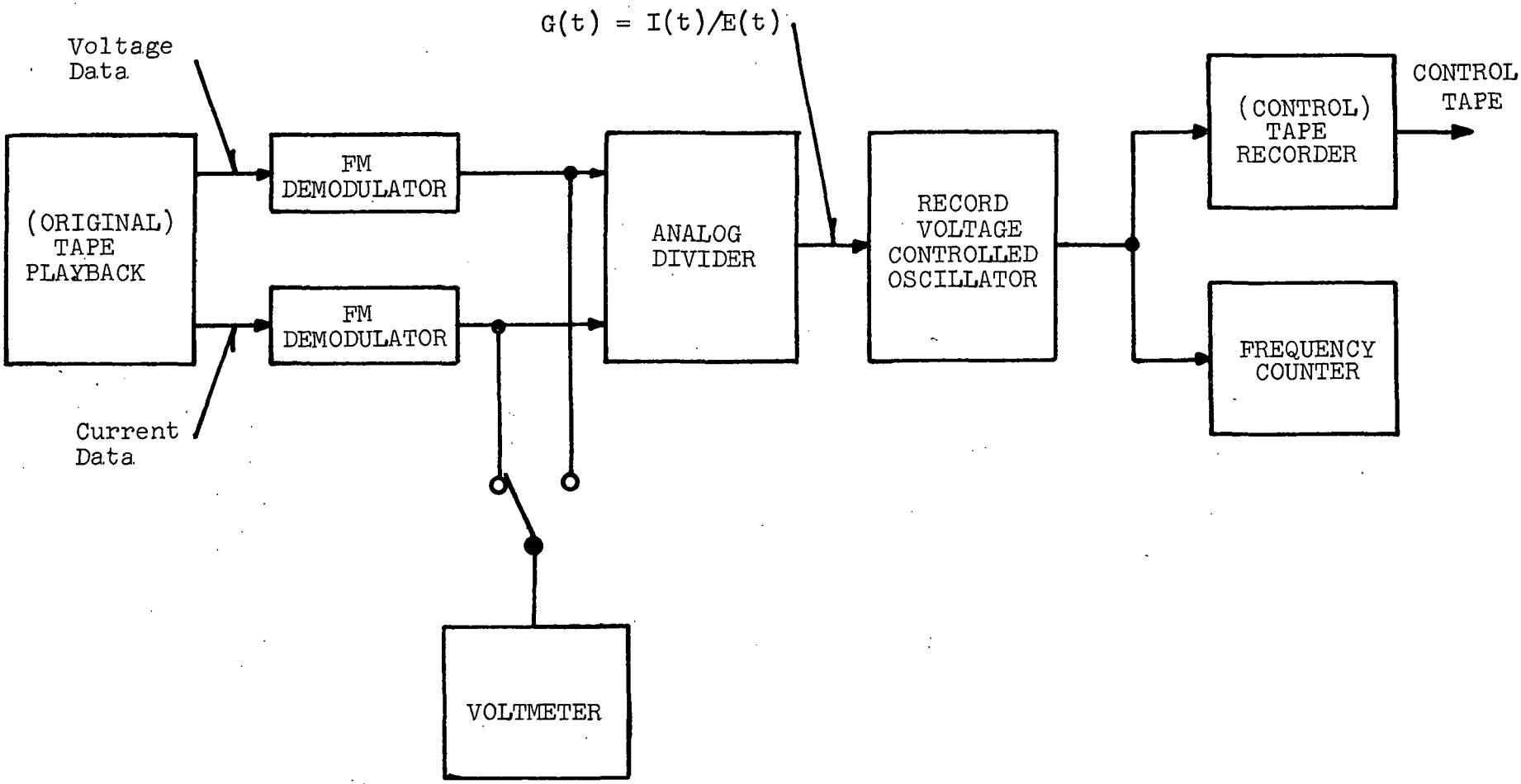

FIGURE 4-32 Simplified Block Diagram of Set-up for Calibrating and Generating Variable R Control Tape

4.3 SELECTION OF EQUIPMENT FOR SIMULATION

4.3.1 Model Simulation

The voltage and current data shown in Figures 4-1 through 4-17 for each of the interrogated equipments was reviewed and a selection was made of five of the nine equipments for model synthesis. In general, the equipment chosen provided the more "interesting" characteristics of the group and required maximum exercise of the model optimization routines and simulation hardware. These equipments are identified in Table 4-IV.

Four equipments were not selected for modelling. They were eliminated for the following reasons.

One of the items of equipment is an AC operated fan (Rotron Fan - Run 10) whose current waveform has a varying envelope. The number of data points required to accurately describe this waveform would exceed the capacity of the optimization program as it is currently configured.

It can be seen from the graph, Figure 4-8, that the dynamics of the envelope are much slower than the oscillator frequency. Therefore, because of the limited number of sampling points that the existing synthesis program can handle within a reasonable computing time, no direct design of the model by computer was considered.

The other three items of equipment not selected (recovery beacon - Run 12, UHF/FM transmitter - Run 13, and HF transceiver - Run 16) have simple periodic current waveforms. The transient behavior of these waveforms is less complex than that of the selected equipment and simulation of these transient intervals could be achieved. However, their periodic behavior would require programmed periodic switching within the network model. Although the model is capable of programmed branch switching, such switching can occur only once per operation.

4.3.2 Variable R Simulation

Each of the interrogated equipments that is operated by a DC source was selected for demonstrating the variable R. Therefore, seven equipments (Runs 3, 8, 9, 11, 12, 13, and 16) were chosen,as follows:

TABLE 4-IV

INTERROGATED EQUIPMENT SELECTED FOR MODELLING

Run Number	Equipment	Power Source
3C	Motor Switch	35 VDC
6B	Heat Exchanger	114 VAC, 400 Hz
8A	Varo Inverter	26 VDC
9A	Apollo Inverter	26 VDC
11C	VHF/AM Transceiver	30 VDC

Run Number	Equipment	Power Source
3C	Motor Switch	35 VDC
8A	Varo Inverter	26 VDC
9A	Apollo Inverter	26 VDC
11C	VHF/AM Transceiver	30 VDC
12A	Recovery Beacon	26 VDC
13B	UHF/AM Transmitter	28 VDC
16A	HF Transceiver	28 VDC

Four of these items were also chosen for modelling (see Paragraph 4.3.1), thus permitting a comparison of model response and variable R response for the same equipment.

4.4 MODEL DEVELOPMENT

Early in the program a general network model was developed capable of providing responses suitable for simulating the equipment interrogated at NASA.

This model consists of three branches containing resistance, capacitance, and inductance elements where each branch is in the configuration shown in Figure 4-33. Each of the model elements is variable and the branch topology may be varied by eliminating any of the elements.

4.4.1 Model Structure

It was required that the model be flexible to permit simulation of as large a variety of equipment as possible, and that it also be constructed with the simplest possible components to reduce its cost and to increase its reliability and repeatability. Therefore, the model consists of passive resistances, inductances (without coupling), and capacitances. These elements can take a discrete set of values, give adequate coverage of given ranges, and be used to construct linear, lumped networks in the form of one-ports (one-terminal pair devices).

On an admittance basis, consider the branch structure shown in Figure 4-33 as a basic building block with four adjustable positive parameters: R_k, L_k, C_k, G_k.

It is understood that this network is meant to include simpler sub-networks, such as shown in Figures 4-34 and 4-35.

These networks are obtained (at least in the mathematical limit sense) by letting G_k, $C_k \longrightarrow \infty$, or R_k, $L_k \longrightarrow 0$.

The current I_k and voltage V are connected by the admittance operator (S = Laplace transform operator)

$$Y_K(S) = \frac{\frac{1}{L_K}\left(S + \frac{G_K}{C_K}\right)}{S^2 + \left(\frac{G_K}{C_K} + \frac{R_K}{L_K}\right)S + \left(\frac{1}{C_K L_K} + \frac{G_K}{C_K} \cdot \frac{R_K}{L_K}\right)}$$

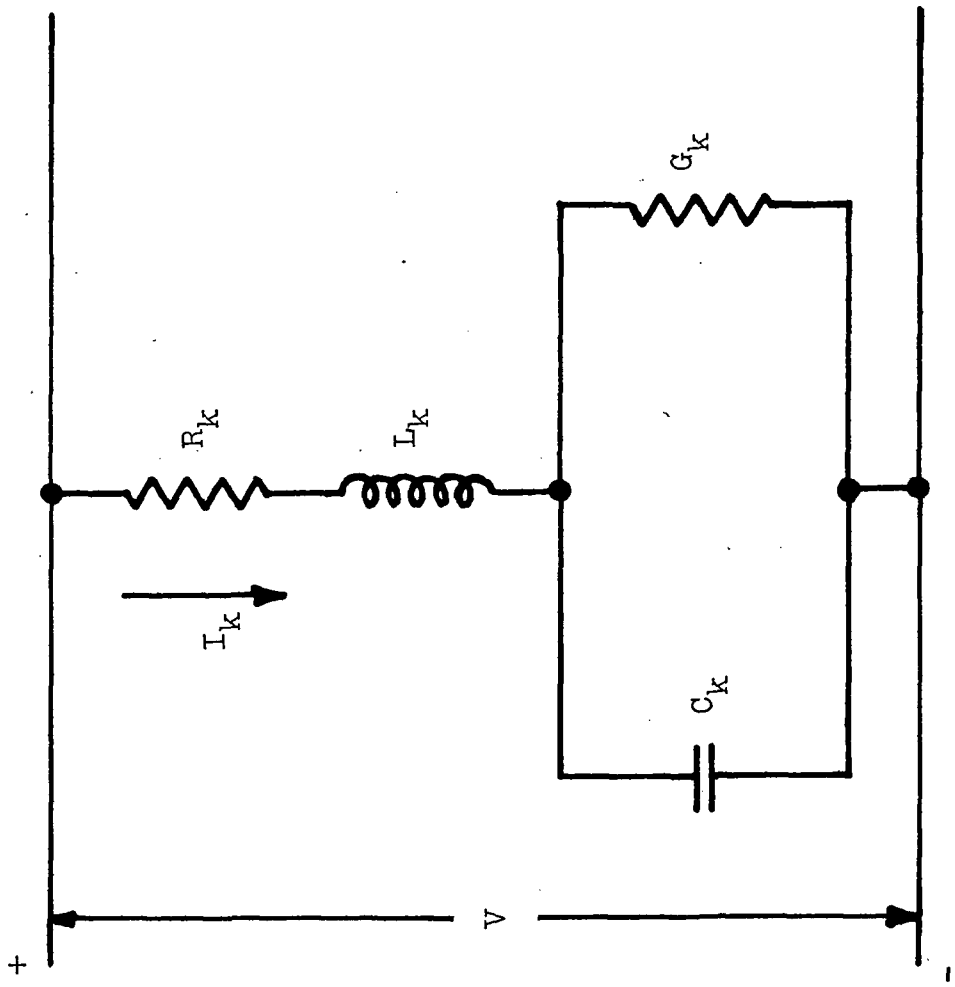

FIGURE 4-33 General Branch Structure

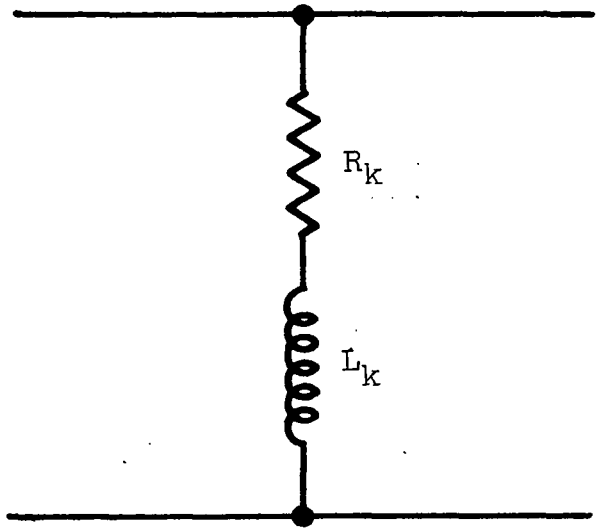

FIGURE 4-34 Branch Sub-Network (Resistance-Inductance)

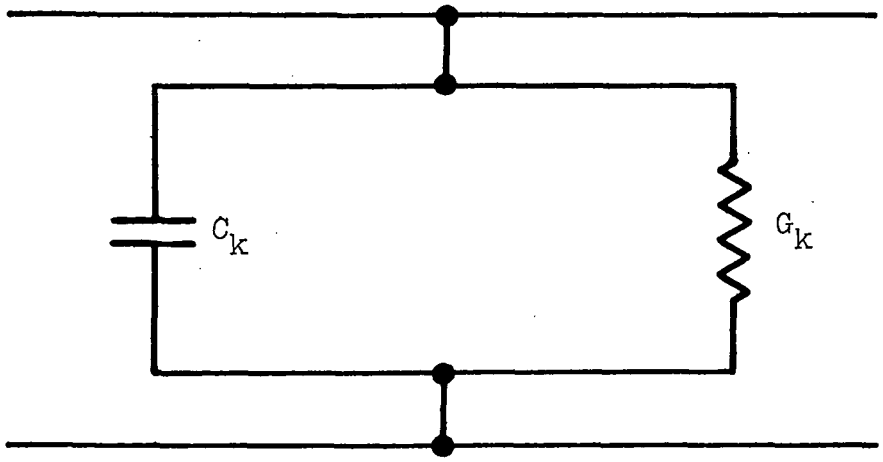

FIGURE 4-35 Branch Sub-Network (Conductance-Capacitance)

This operator provides two real or complex conjugate roots in the system impulse response.

N blocks in parallel result in the admittance

$$Y(S)=\sum_{K=1}^{N} Y_K(S)$$

with 2N poles. Even with the restriction to non-negative element values, good flexibility and adaptivity is maintained.

While it would be desirable for element values R, L, C, G to be continuously variable over their range, one must work with discrete values in a practical realization. Starting with the results found in previous work (Phase 1 Report) and estimating needs based upon the interrogation performed on the real equipment at NASA, the numerical ranges identified in Table 4-V were selected.

With these 20 elements one can build three elementary blocks (branches) as shown earlier ($N \leq 5$) with elements to spare. If fewer branches are needed per device, one simulator can simultaneously simulate up to three different types of equipment. Note that large capacitance values can be involved when purely electrical means are used to simulate mechanical effects, such as inertias (which cause large initial current peaks). Within each decade, for example in the R = 1 ohm to R = 10 ohm resistor range, the discrete values that can be obtained are distributed approximately uniformly on a logarithmic scale to provide uniform sensitivity (Δ R)/R. This minimizes deviations in network response caused by rounding-off to make theoretically optimum values correspond to those available.

Previous work has shown that for many devices a relatively good model can be constructed with 12 parameters and that only little improvement is gained by more complexity (i.e., one has reached the point of diminishing returns). For a larger number of elements, the computation time needed by the search for the optimum becomes large with correspondingly higher cost.

TABLE 4-V

ELEMENT VALUE RANGES AND QUANTITIES

Element	Range	Quantity	Chassis
Resistance	0.1 to 1 ohm	1	R1
	1 to 10 ohms	2	R1
	10 to 100 ohms	3	R1/R2
	100 to 1K ohms	1	R2
	1K to 10K ohms	1	R2
Capacitance	0.1 to 1 microfarad	1	C
	1 to 10 microfarads	1	C
	10 to 100 microfarads	1	C
	100 to 1000 microfarads*	1	C
	1000 to 10,000 microfarads*	1	C
Inducatance	0.01 to 0.1 millihenry	1	L1
	0.1 to 1 millihenry	1	L1
	1 to 10 millihenries	3	L1
	10 to 100 millihenries	1	L2
	100 to 1000 millihenries	1	L2

* For DC application only.

Additional flexibility can be achieved by timed switching, i.e., in certain cases one particular network is used only during a fraction of the entire simulation time, to be replaced by one or more others for the remaining portion. The sketch of Figure 4-36 illustrates this scheme.

(Switching networks may simply mean switching some elements in a given configuration, or else completely changing the topology). In some applications (see the Phase 1 Report) there is good physical justification for switching because the real device works in very distinct modes.

Since the models are linear, good agreement for one pair of signals will, in principle, also provide good agreement for other pairs if the real devices are also linear. Strongly non-linear devices may require several models according to their mode of operation.

4.4.2 Model Optimization Criterions

The selection of a "best" set of component values as well as a "best" topological configuration required definition of some criterion of goodness of fit. Again using the admittance basis, let Y (t) be the admittance impulse response of a candidate network. Then Y (t) is a function of all component values or search parameters R, etc.

$$Y(t) = Y(t; R_k, L_k, C_k, G_k)$$

If i (t), v (t) are the true current and voltage as recorded during the time interval $(t_o, t_o + T)$, the approximating current, $i_a(t)$, is given (for zero initial conditions) by the following:

$$i_a(t) = \int_{t_o}^{t_o+T} \mu(t')\, y(t-t')\, dt'$$

and the current-error is

$$e(t) = i_a(t) - i(t)$$

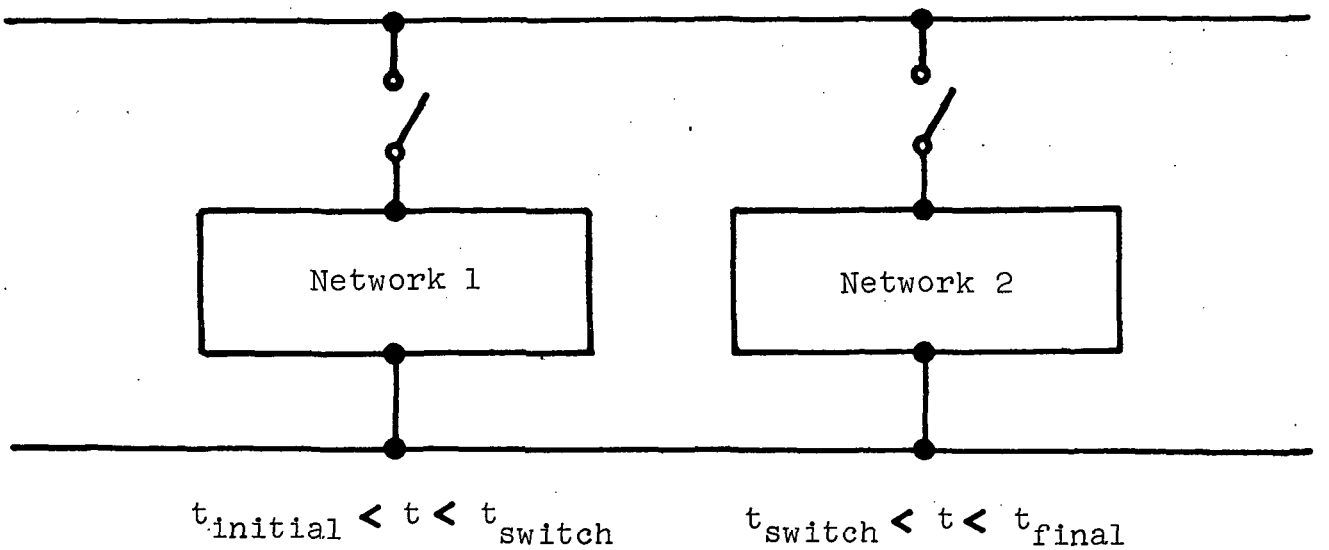

FIGURE 4-36 Simplified Diagram Showing Timed Switching Altering Model Topology Dynamically

The following types of criterions can then be considered.

$$J_1 = \frac{1}{T}\int_{t_0}^{t_0+T} |e|\,dt$$

$$J_2 = \frac{1}{T}\int_{t_0}^{t_0+T} |e\mu|\,dt$$

$$J_3 = \frac{1}{T}\int_{t_0}^{t_0+T} e^2\,dt$$

$$J_4 = \frac{1}{T}\int_{t_0}^{t_0+T} e^2\mu^2\,dt$$

$$J_5 = \frac{1}{T}\int_{t_0}^{t_0+T} \left(\frac{de}{dt}\right)^2 dt$$

$$J_6 = \frac{1}{T}\int_{t_0}^{t_0+T} \left[\frac{d(e\mu)}{dt}\right]^2 dt$$

These correspond, respectively, to mean absolute current error, mean absolute power error, mean square current error, mean square power error, mean square current derivative error, and mean square power derivative error. All these criterions have been used with success in previous work (Phase 1 Report). Note, too, that all of the preceding criterions are of the time-averaging kind that produce smoother criterions. Such criterions are relatively easy to deal with in the optimization algorithms.

Point-type criterions such as

$$J = \max |e(t)| \qquad t_0 \le t \le t_0 + T$$

are often not smooth with respect to the component values (search parameters) and present serious divergence problems in the optimization algorithm. Therefore, the use of point-type criterions was not considered for this program.

Network synthesis theory indicates that a given network response may be exactly or approximately realized by various configurations. Accordingly, one expects an optimization difficulty in that there may be more than one local optimum in many instances. This complicates the search for the absolute optimum and may require using several starting guesses to find the global optimum.

It should also be noted that the use of a timed switching approach amounts to using time-dependent weighting-factors in the earlier expressions for the criterion J_1, etc.

The method used is as direct as possible since synthesis is done in the time-domain where the specifications are prescribed.

The computer optimizations of several of the models revealed a need for emphasizing certain aspects of a response more than others. To accomodate this, certain of the criterions identified above were provided with weighting factors resulting in the criterions listed on Table 4-VI.

The weighting vectors W_i and X_i and the bias terms B_M and B_S are inputs which can be controlled by the user of the code. The measured response of the real equipment is described by the current and voltage histories, L_i and V_i, while the predicted current response of the simulator to the imposed voltage, V_i, is called I_{A_i}.

The first criterion, JM_1, is the weighted-biased root-mean-square (RMS)-criterion for current while the second, JM_2, is the corresponding criterion for power. The third criterion, JD_1, is the weighted-biased RMS criterion for the current derivative, dI/dt while the fourth, JD_2, is the corresponding criterion for the power derivative d(I*V)/dt.

These four criterions allow various individual points to be given more emphasis than other points. In some of the applications in this program, the point representing the peak current was to be emphasized. This form of the criterion allows any combination of points to be weighted. For example, a final point could be emphasized, if an exceptionally good match of the steady-state current were desired. Provisions are also made to allow negative and positive errors to be weighted (biased) separately. This is based on the expectation that it is better for the simulator to draw more current than does the real equipment, if it cannot match the real equipment.

There are reasons for expecting that simulation criterions that include the time rate of change of current or power may be useful in the future. Criterions for these derivatives are included in the original 8 and weighted-biased, RMS criterions for these derivatives are also included in the 4 new criterions.

TABLE 4-VI

WEIGHTED CRITERIONS

Current Magnitude

$$JM_1 = \left\{ \frac{1}{\sum_{i=1}^{N+1}(W_i)} \sum_{i=1}^{N+1} \left\{ \omega_i \, (IA_i - I_i)^2 \, C_{1_i} \right\} \right\}^{1/2}$$

$$C_{1_i} = \begin{cases} 1.0 & \text{IF } (|IA_i| - |I_i|) \text{ is } \geq 0. \\ B_M & \text{IF } (|IA_i| - |I_i|) \text{ is } < 0. \end{cases}$$

Power Magnitude

$$JM_2 = \left\{ \frac{1}{\sum_{i=1}^{N+1}(W_i)} \sum_{i=1}^{N+1} \left\{ \omega_i \left(IA_i * V_i - I_i * V_i \right)^2 C_{2_i} \right\} \right\}^{1/2}$$

$$C_{2_i} = \begin{cases} 1.0 & \text{IF } (|IA_i * V_i| - |I_i * V_i|) \text{ is } \geq 0. \\ B_M & \text{IF } (|IA_i * V_i| - |I_i * V_i|) \text{ is } < 0. \end{cases}$$

Current Derivative

$$JD_1 = \left\{ \frac{1}{\sum_{i=1}^{N}(X_i)} \sum_{i=1}^{N} \left\{ X_i \left(\frac{dIA}{dt_i} - \frac{dI}{dt_i} \right)^2 C_{3_i} \right\} \right\}^{1/2}$$

$$C_{3_i} = \begin{cases} 1.0 & \text{IF } (\left|\frac{dIA}{dt_i}\right| - \left|\frac{dI}{dt_i}\right|) \text{ is } \geq 0. \\ B_S & \text{IF } (\left|\frac{dIA}{dt_i}\right| - \left|\frac{dI}{dt_i}\right|) \text{ is } < 0. \end{cases}$$

Power Derivative

$$JD_2 = \left\{ \frac{1}{\sum_{i=1}^{N}(X_i)} \sum_{i=1}^{N} \left\{ X_i \left(\frac{d(IA * V)}{dt_i} - \frac{d(I * V)}{dt_i} \right) C_{4_i} \right\} \right\}^{1/2}$$

$$C_{4_i} = \begin{cases} 1.0 & \text{IF } (\left|\frac{d(IA * V)}{dt_i}\right| - \left|\frac{d(I * V)}{dt_i}\right|) \geq 0. \\ B_S & \text{IF } (\left|\frac{d(IA * V)}{dt_i}\right| - \left|\frac{d(I * V)}{dt_i}\right|) < 0. \end{cases}$$

4.4.3 Model Synthesis

Using the model structures described in Paragraph 4.4.1 as a basis, preliminary models were identified for each of the selected equipments identified in Paragraph 4.3.1. These models, obtained by engineering judgment based upon the time-domain response of each equipment to be modelled, were then used as the starting point for the computer optimizations described in Paragraph 4.5. These preliminary models are shown in Figures 4-37 through 4-41 along with tables of initial values for the model elements.

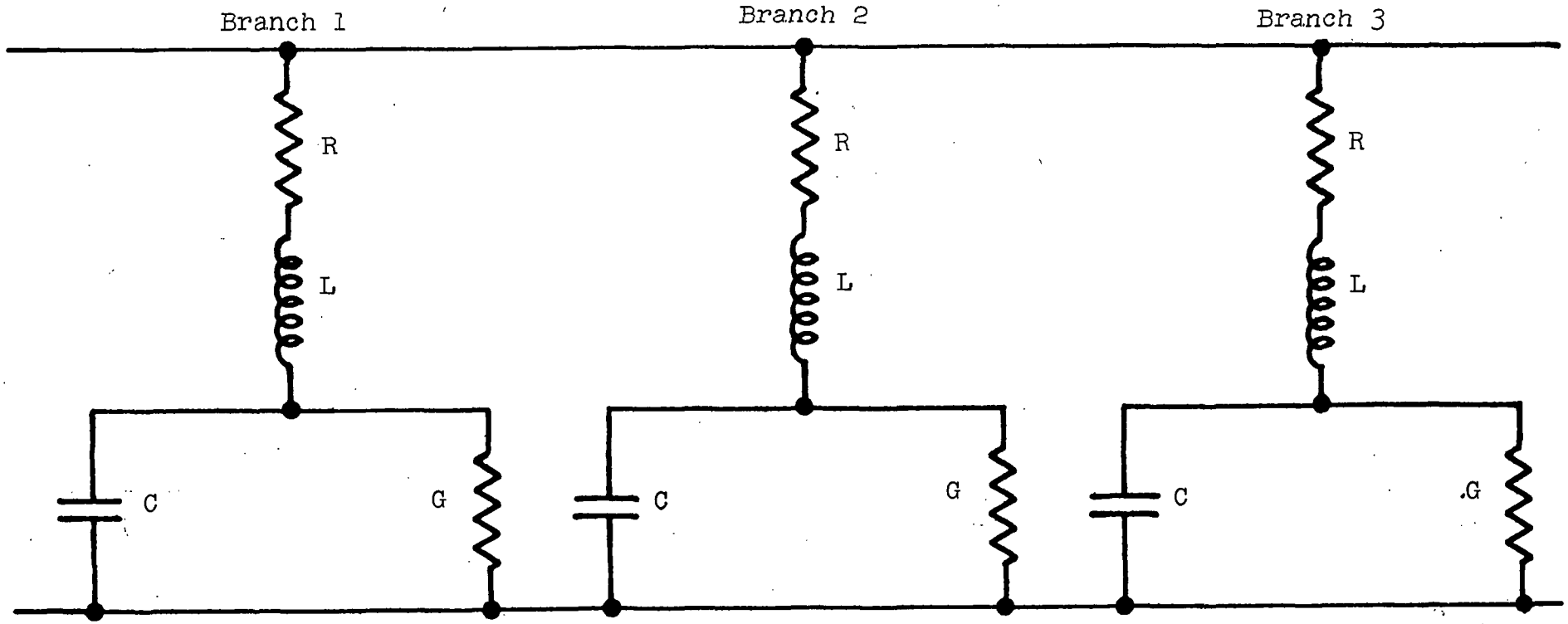

	Branch 1	Branch 2	Branch 3
R (ohms)	3.97	4.197	0.
L (H)	3.66×10^{-3}	2.288×10^{-3}	6.8×10^{-3}
C (f)	9.075×10^{-3}	0.18×10^{-3}	1.66×10^{-6}
G (1/ohms)	0.0882	20×10^{-6}	0
1/G (ohms)	11.34	5×10^{4}	∞

FIGURE 4-37 Initial Estimate Model for Motor Switch, Run 3C

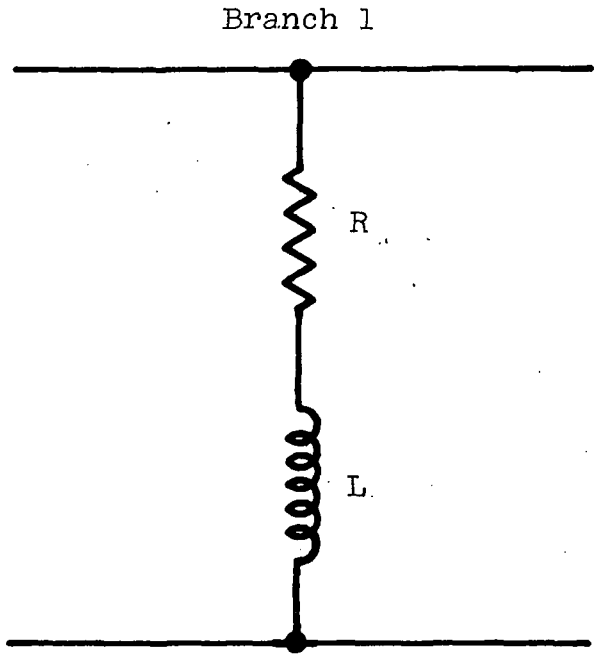

	Branch 1
R (ohms)	1544.
L (H)	0.358

FIGURE 4-38 Initial Estimate Model for Heat Exchanger Valve, Run 6B

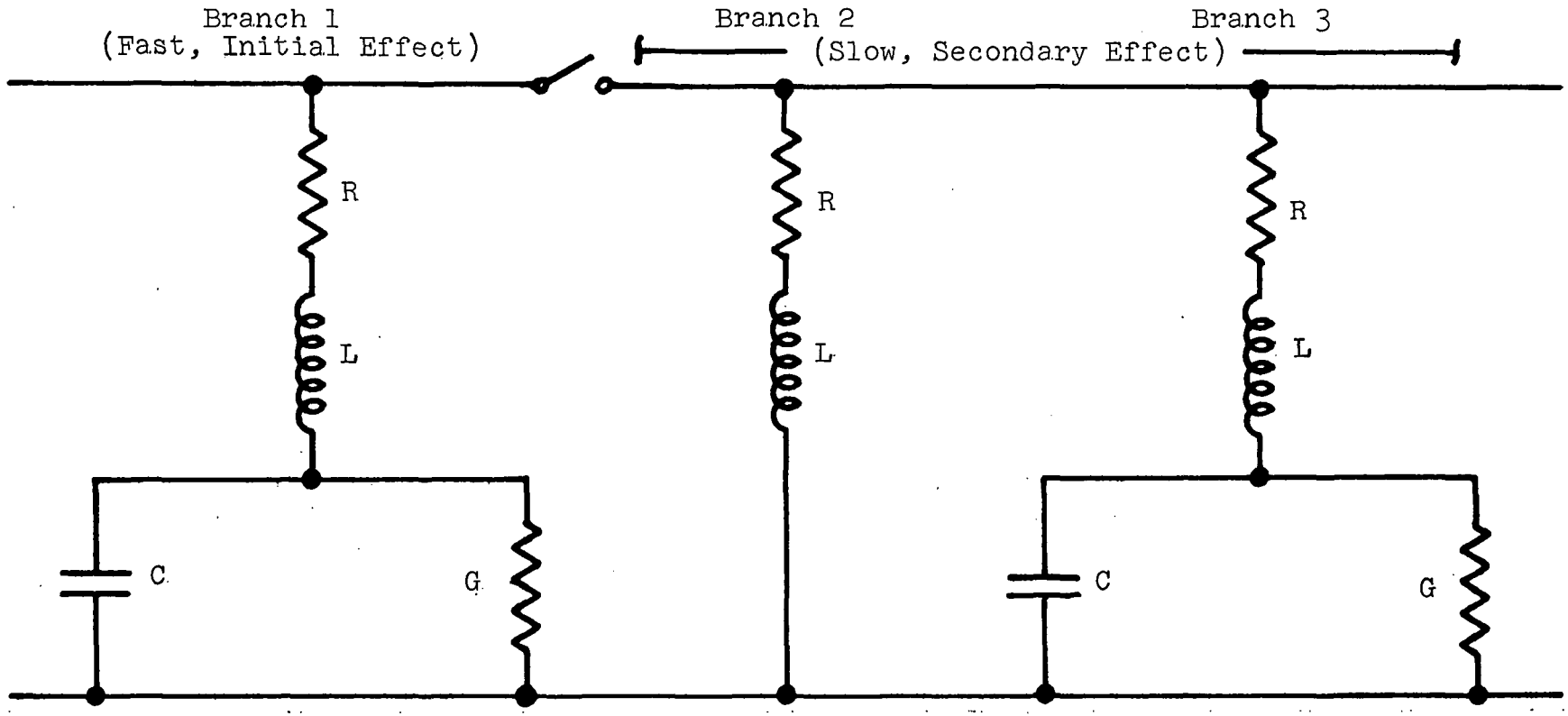

	Branch 1	Branch 2	Branch 3
R (ohms)	0.4834	15.1	15.3
L (H)	0.2336×10^{-3}	1087	50×10^{-3}
C (f)	899×10^{-3}	--	0.3×10^{-3}
G (1/ohms)	0.08658	--	0.0013
1/G (ohms)	11.55	--	7.675×10^{3}

FIGURE 4-39 Initial Estimate Model for Varo Inverter, Run 8A

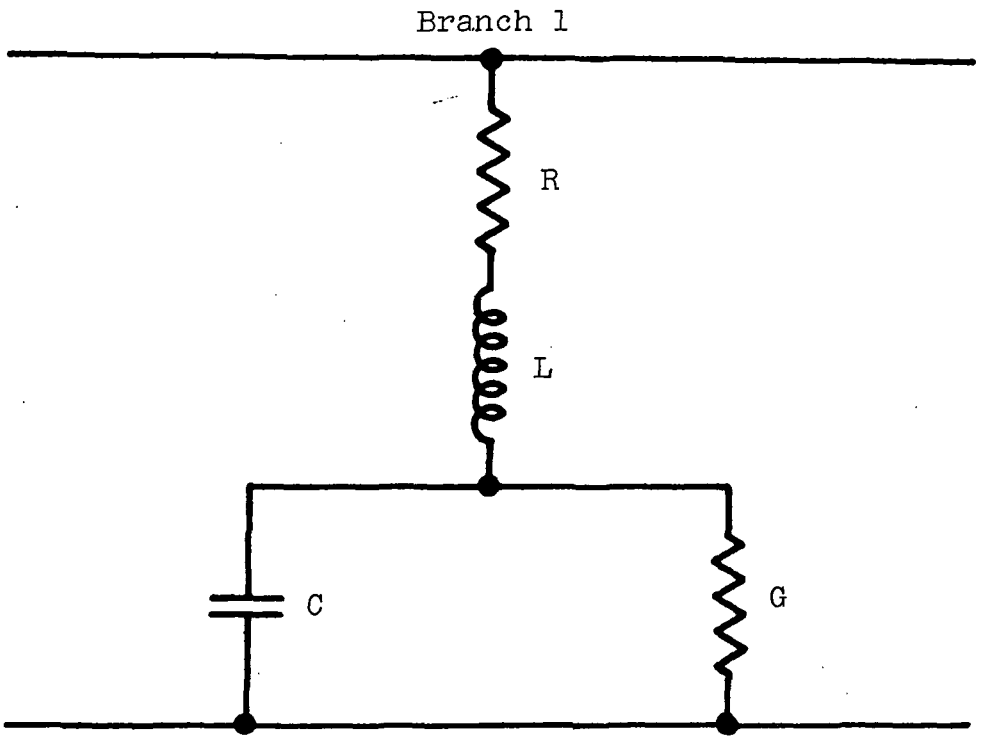

	Branch 1
R (ohms)	0.68
L (H)	0.25×10^{-3}
C (f)	3.4×10^{-3}
G (1/ohms)	0.085
1/G (ohms)	11.8

FIGURE 4-40 Initial Estimate Model for Apollo Inverter, Run 9A

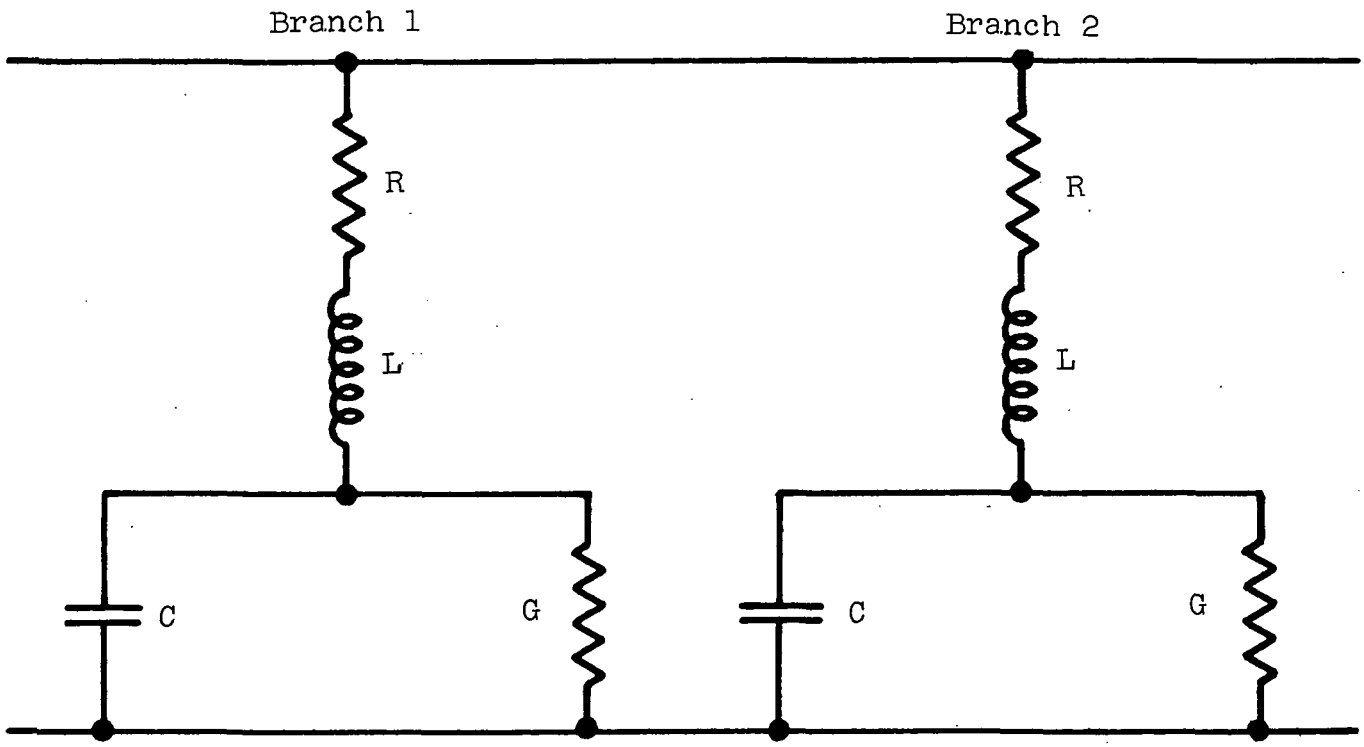

Branch 1		Branch 2
2.78	R (ohms)	1.11
1.47×10^{-3}	L (H)	132×10^{-3}
3.8×10^{-3}	C (f)	166×10^{-6}
0	G (1/ohms)	0.000 033
∞	1/G (ohms)	30 024

FIGURE 4-41 Initial Estimate Model for VHF/AM Transceiver, Run 11C

4.5 COMPUTER OPTIMIZATION

4.5.1 Program Description

As a means of quickly selecting model element values for each problem and of evaluating the resulting responses, a computer operation is indicated.

The feasibility of using existing numerical optimization techniques to select component values for dynamic load simulators was demonstrated in the Phase 1 study. A program developed for the selection of decoy configurations was adapted to select electrical component values for the examples shown in the Phase 1 final report. This program, which operates on Avco's IBM 360/75 digital computer, provided the foundation and structure for the optimization software used during this phase. The major elements of the program are outlined in Figure 4-42. The input requirements are shown in the upper section, and the program itself is divided into analysis and optimization modules.

The inputs to this program consist of an identification of the type of simulation network and starting values (initial guess) for the network parameter. Up to 20 parameters can be evaluated and/or optimized. The data describing the actual measured response of the equipment to be simulated serves as an input to the program. The data acquisition and processing system must supply this data in the form of time-history tables of current and voltage in selected units and in selected punched card formats. The program is formulated for up to 200 time points. The combinations of criterions to be used to judge the adequacy of the simulation are identified by input quantities. Also, any constraints on the calculated criterion values or on the allowable ranges of the design parameters are provided as input.

In those cases where the dynamic response is simulated in segments (by switching between two or more networks) the optimization is performed for each segment independent of the other segments. Inputs are provided to identify the initial conditions for the present segment (resulting from the final conditions of the previous segment).

The analysis module: (1) calculates the transient behavior of the simulator network, and (2) calculates comparisons of the calculated response with the input data that describes the response of the system to be simulated.

The optimization (or synthesis) module contains the logic and calculations required to determine those values of the network parameters that will provide an acceptable or optimum simulation of the original

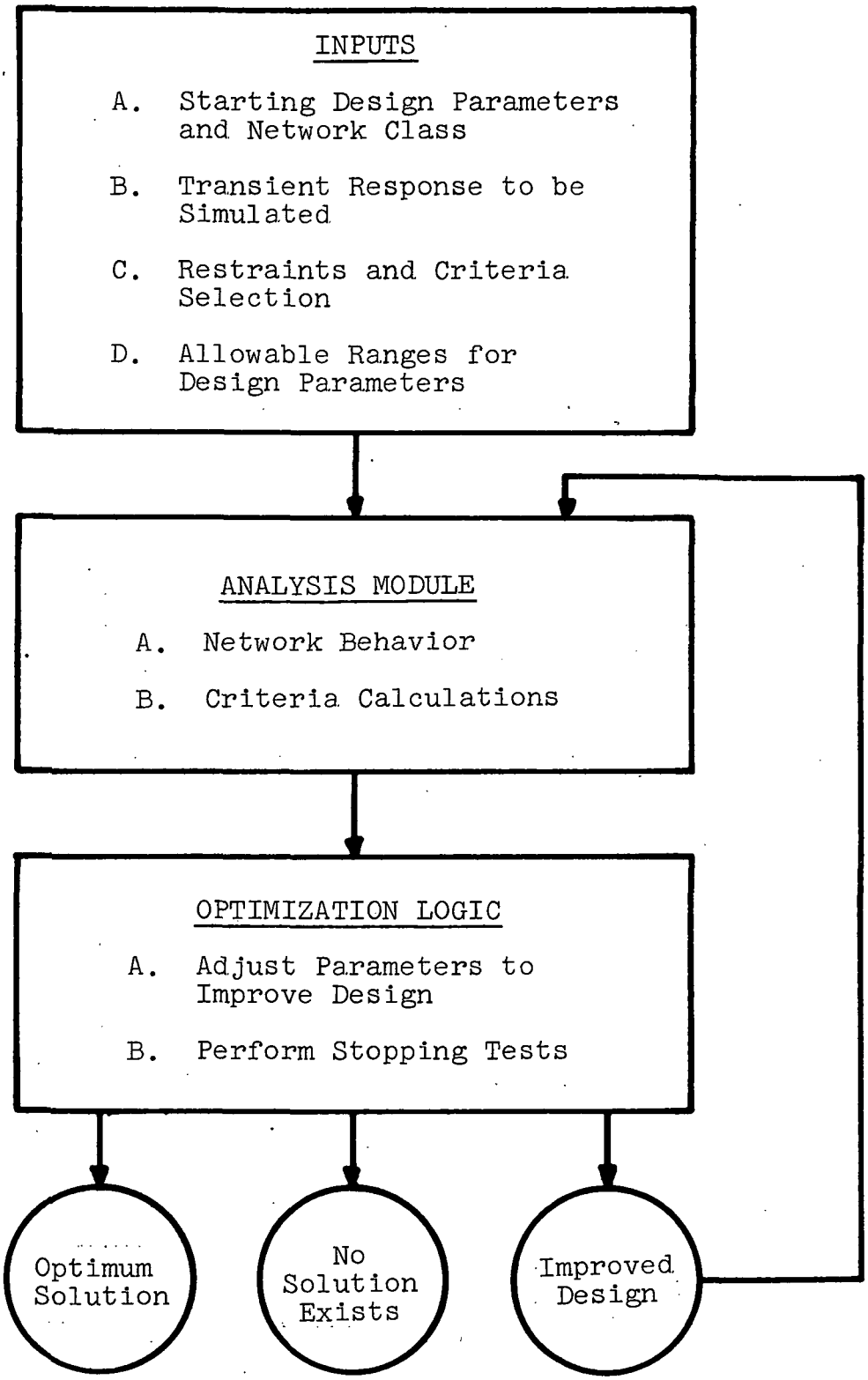

FIGURE 4-42 Program for Obtaining Optimum Model Solution

system. By an iterative process the synthesis module organizes the relationships between the values of the network parameters being tried and the magnitude of the errors (mismatch) which result. From these relationships, new design values that will improve the simulation are selected and fed back into the analysis module.

The process normally converges upon those values of the network parameters that minimize the selected criterions. If the problem is over-constrained so that there is no acceptable solution, the program identifies this result. The Davidon and Rosenbrock optimization techniques described in Appendix B of the Phase 1 final report were retained in this program. The Fibonacci optimizers are not appropriate for this problem due to their limited number of variables and were not retained in the program.

This optimization program is formulated with a model based on continuous values of the design parameters. After running the optimizer, the user can round-off the optimum values to the nearest discrete values available in the simulator. These rounded-off values can be evaluated, if desired, by running the optimizer program in a mode such that it stops after the first pass through the analysis module.

The output of the program summarizes the various trials along the way to a solution, and detailed printouts of the optimization network behavior are provided. This program differs from the one described in the Phase 1 study in that it was improved by providing the capability of working with the element values directly instead of the time constants, and by adding the capability of biasing the criterions (weighted criterions) to suit the particular characteristics of each waveform.

4.5.2 Optimization Results

Using as a starting point the preliminary models of Paragraph 4.4.3, the optimization program described in Paragraph 4.5.1 was run on the Avco 360/75 digital computer to select optimum values for each of the model elements. The response data for the five interrogated equipments selected for modelling was provided in digital punched card form. One of the equipments modelled--the Varo inverter, Run 8A--was treated as two separate problems during the optimization studies. The response data for this equipment shows a high initial current transient followed a period of time later by a low-amplitude current transient. These two intervals were treated separately and are identified as Run 8A1 and Run 8A2, respectively.

For optimization efforts, the last two points of the motor switch (Run 3C) data and the first five points of the Varo inverter second event (Run 8A2) data were deleted. These points are simulated by switching techniques that are unnecessary to include in the optimization study.

It should be noted that the results and discussions that follow are the calculated results determined by the optimization program and are not representative of actual simulator performance. Simulator performance evaluation is treated in Section 6.

For each device, numerical optimization techniques were applied using Avco programs 2918 and 5010 to obtain an unconstrained continuous variable optimum set of element values. Eight element values were optimized for the motor switch (Run 3C) and the "ripple circuit" was held fixed during the optimization. In those cases where the initial value of the parallel resistor implied an open circuit, this was considered a part of the network topology and the value of the parallel resistor was, therefore, not optimized. Although the network for the Varo inverter included four branches, the "ripple-circuit" branch was deleted from the optimization studies consistent with the hardware limitation of three branches.

Two figures-of-merit were used in all of the optimizations. The early optimizations used the average value of the square of the difference between the measured current and the predicted values (Criterion J3). The final optimizations--those described in Paragraph 4.5.2.3--used a weighted version of this criterion (Criterion JM1).

The results are presented for each of the five electrical devices in turn. For each device, the results for the optimum solution, the nearest rounded-off solution, and the optimum rounded-off solution are shown. The results are shown in the form of a predicted simulator current response (connected X's) compared with the measured response (unconnected O's). A plot of the difference between the simulated and measured response is also shown. In all figures the current is in amperes and the time is in seconds. The sign convention for the errors is that a positive error indicates that the simulator is drawing more current than the original device. The errors are in units of amperes.

4.5.2.1 Initial Optimization Results

The element values obtained from the initial optimization study of each of the six responses were unconstrained. That is, they were not limited to those values available in the simulator. A summary of these initial values is provided in Table 4-VII.

TABLE 4-VII

INITIAL OPTIMUM ELEMENT VALUES

Equipment Type	Branch	Element Values				Switch Time
		Resistance	Inductance	Capacitance	1/Conductance	t
		ohms	henries	farads	ohms	secs
Motor Switch Run 3C	1	5.747	1.626×10^{-3}	1.059×10^{-4}	53910.	0.0408
	2	short	6.803×10^{-3}	1.664×10^{-6}	open	
	3	4.316	2.804×10^{-3}	9.079×10^{-3}	10.66	
Heat Exchanger Valve Run 6B	1	1724.	0.2093	5.923×10^{-3}	0.2613	- -
Varo Inverter Run 8A	1	0.4038	2.026×10^{-4}	7.387×10^{-3}	12.53	0.585
	2	15.12	1.086	- -	- -	
	3	13.26	4.166×10^{-2}	4.023×10^{-4}	2.10×10^{17}	
Apollo Inverter Run 9A	1	0.337	5.826×10^{-5}	3.24×10^{-3}	5.429	- -
VHF/AM Transceiver Run 11C	1	1.371	1.098×10^{-3}	1.800×10^{-4}	1.309×10^{5}	- -
	2	3.154	5.709×10^{-3}	3.066×10^{-3}	open	

1. Motor Switch, Run 3C (Initial)

The motor switch simulation was provided by a three-branch network that can be switched off after 0.0408 seconds. One branch was used to provide the "ripple." This branch was held fixed while the other eight element values were optimized to produce a minimum of the average value of the square of the current error.

The simulation resulting from the optimized element values is shown in Figure 4-43. The error plot shown in Figure 4-44 indicates that some of the ripples may be out of phase with the original data; however, it does not appear that this phase relationship would be significant.

2. Heat Exchanger Valve, Run 6B (Initial)

The initial results for the heat exchanger valve, Run 6B, were obtained for a one-branch circuit having four elements. The corresponding current response and current error plots are shown in Figures 4-45 and 4-46, respectively.

3. Varo Inverter, Run 8A (Initial)

The primary network for the simulation of the Varo inverter, Run 8A, consisted of a 4-element branch designed to simulate the initial 40-ampere transient plus two branches added (switched) later to simulate the secondary 3.5-ampere transient. The problem has been uncoupled so that the two parts of the network can be optimized separately.

a. First Event - The current response of the branch designed for the first event is shown in Figure 4-47, and the current error plot is shown in Figure 4-48.

b. Second Event - The current response of the network (2 branches) designed to provide the second event is shown in Figure 4-49, and the corresponding error plot is shown in Figure 4-50.

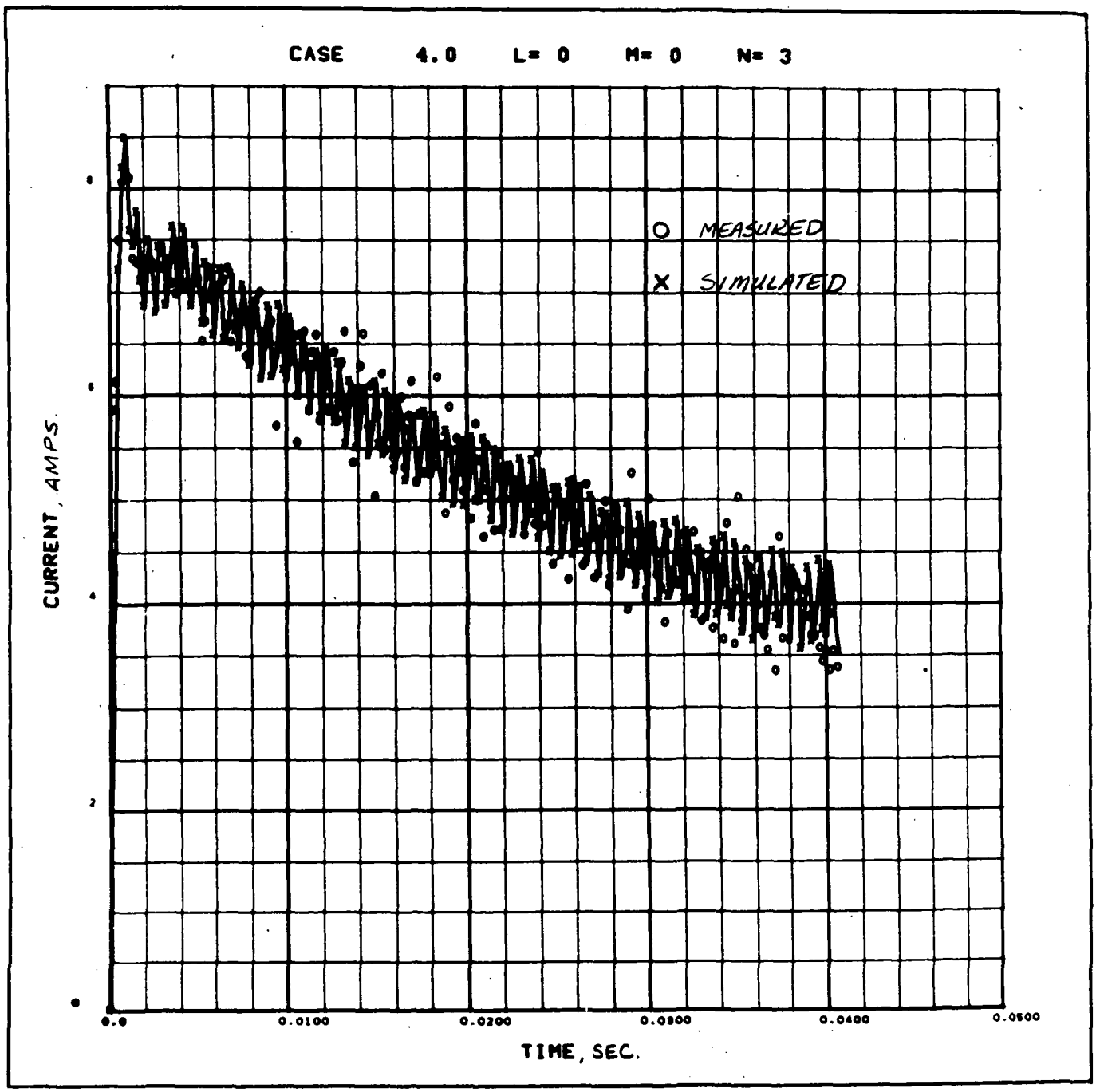

FIGURE 4-43 Simulation of Motor Switch, Run 3C, Using Optimized Element Values

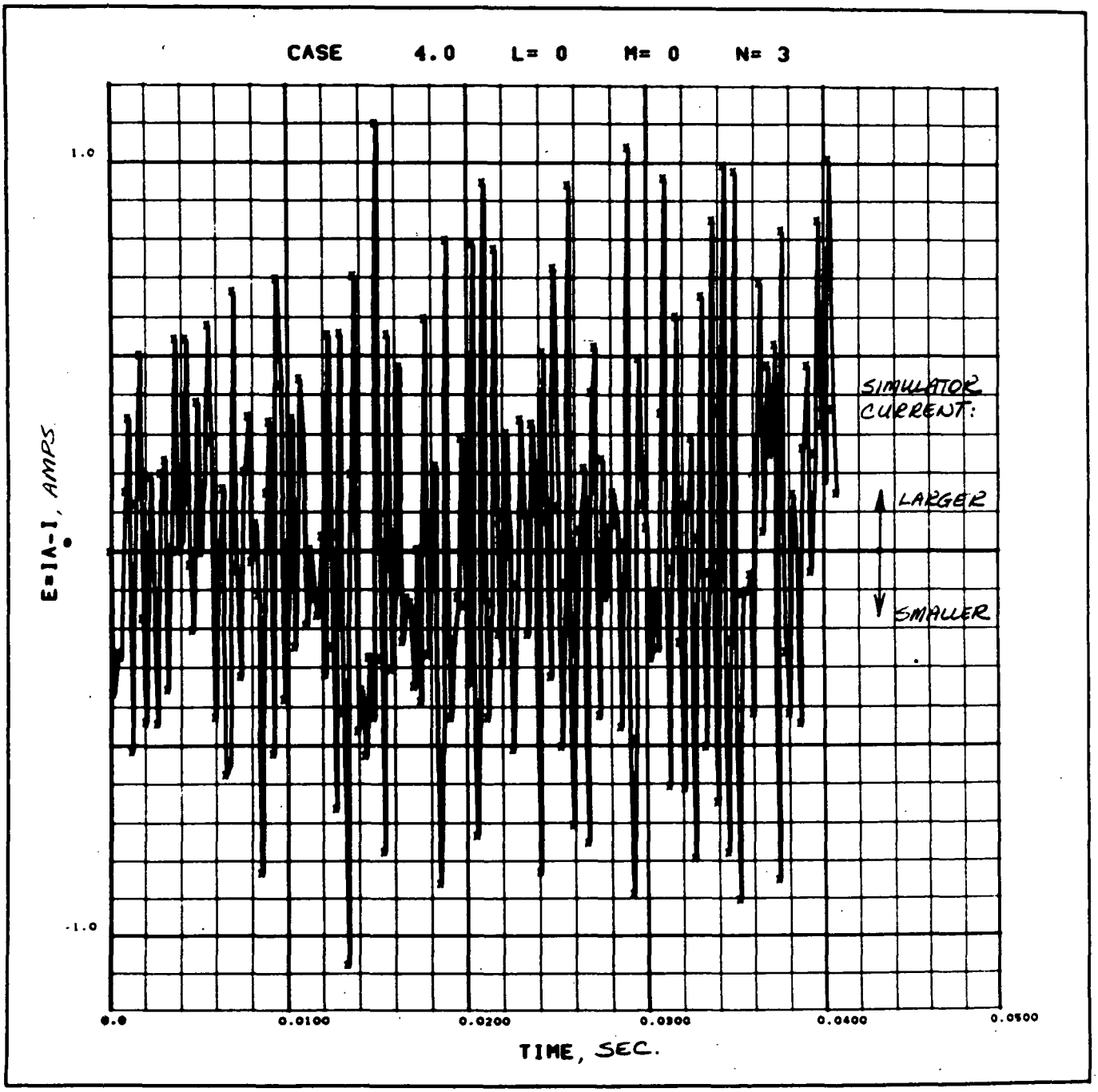

FIGURE 4-44 Current Errors for Motor Switch, Run 3C, Using Optimized Element Values

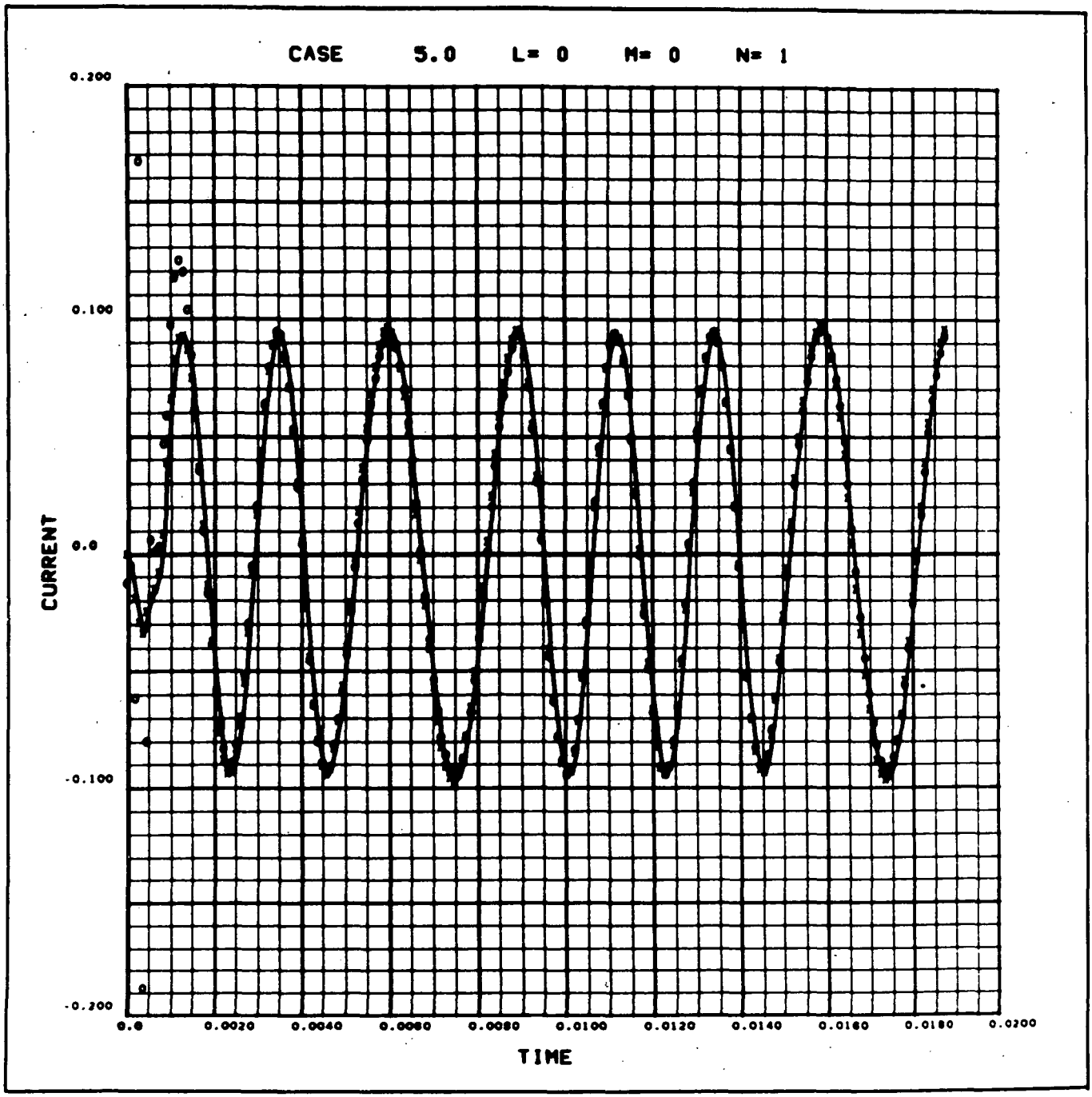

FIGURE 4-45 Simulation of Heat Exchanger Valve, Run 6B, Using Optimized Element Values

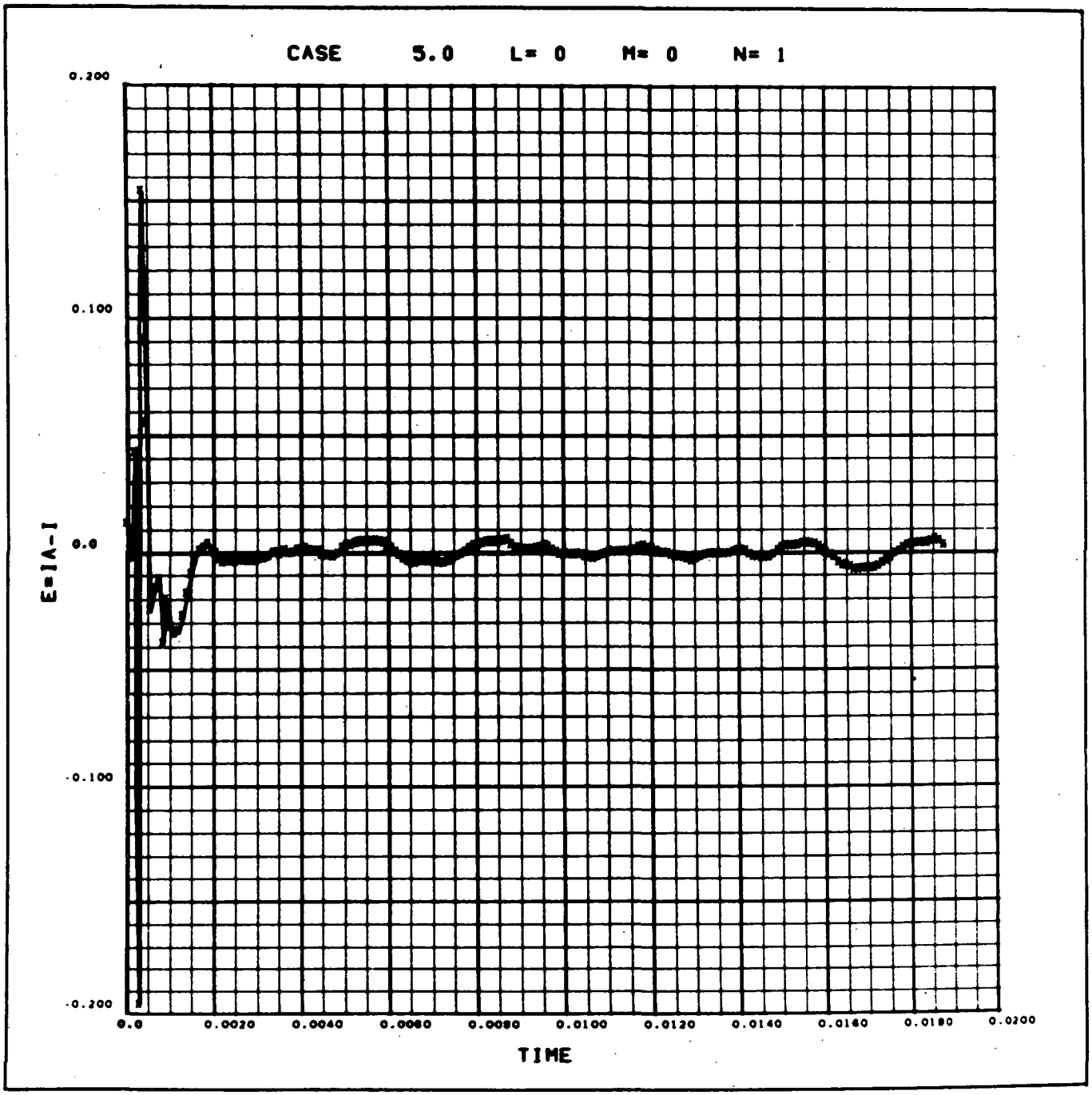

FIGURE 4-46 Current Errors for Heat Exchanger Valve, Run 6B, Using Optimized Element Values

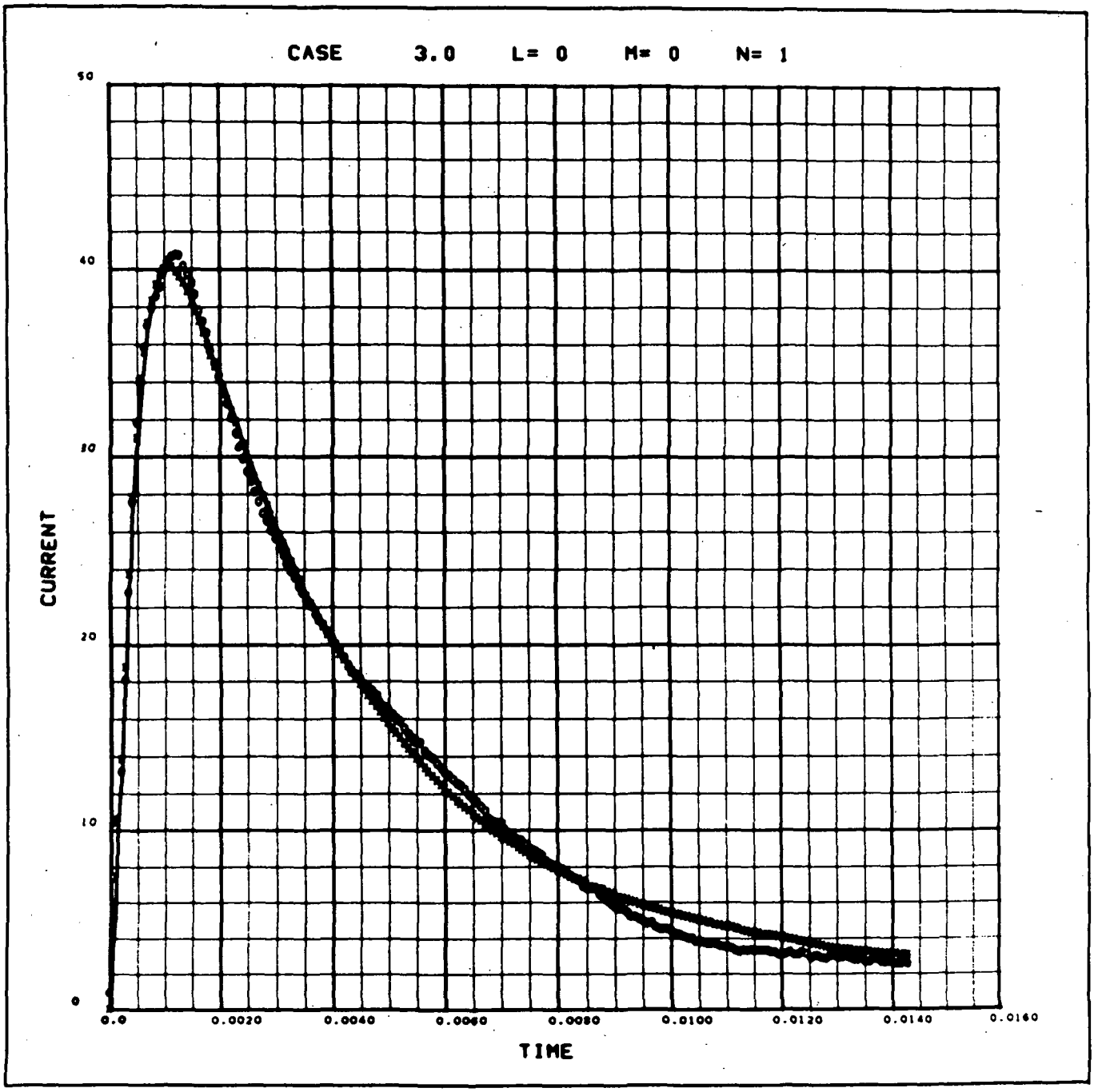

FIGURE 4-47 *Simulation of Varo Inverter, First Event, Run 8A1, Using Optimized Element Values*

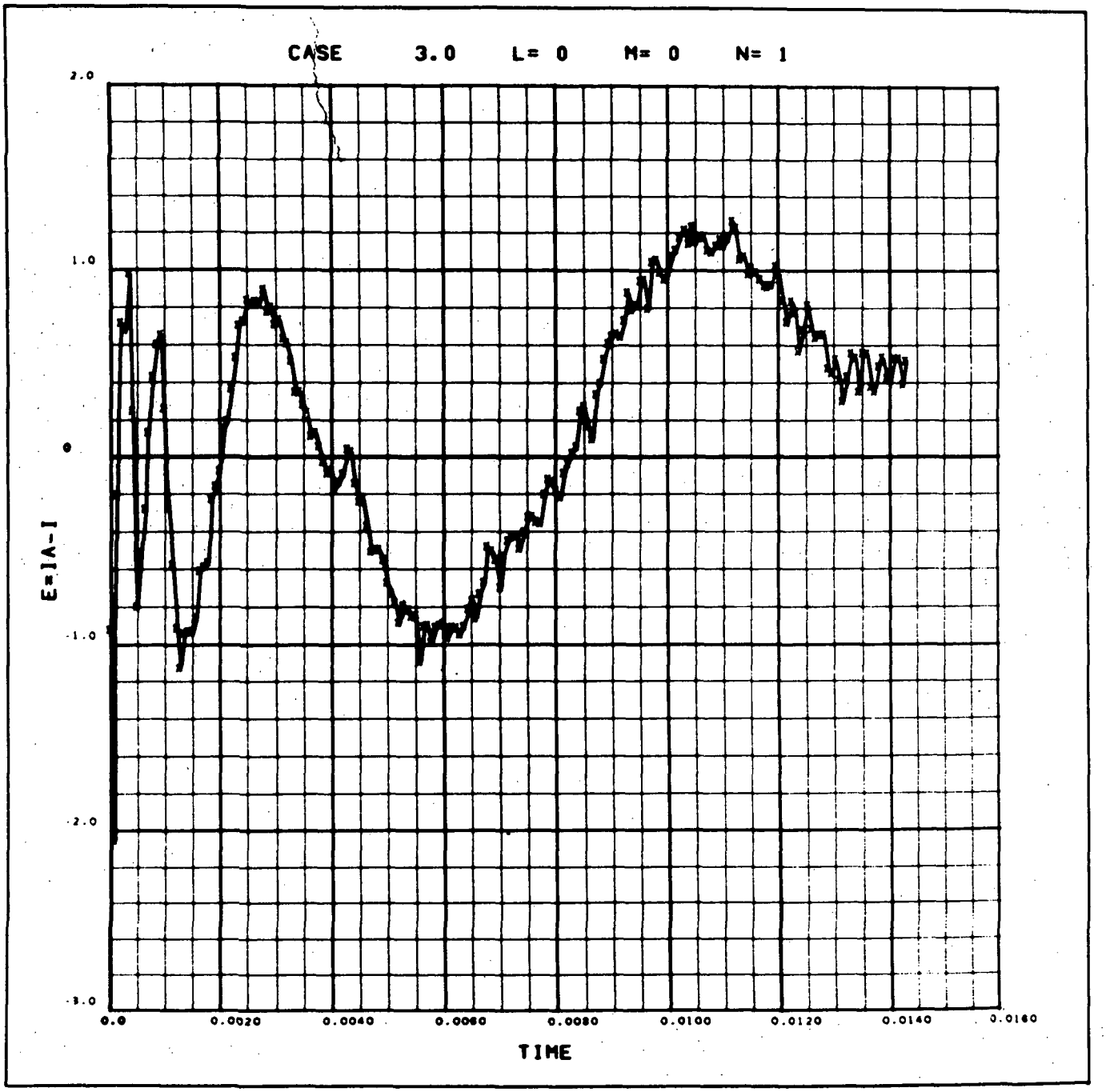

FIGURE 4-48 Current Errors for Varo Inverter, First Event, Run 8A1, Using Optimized Element Values

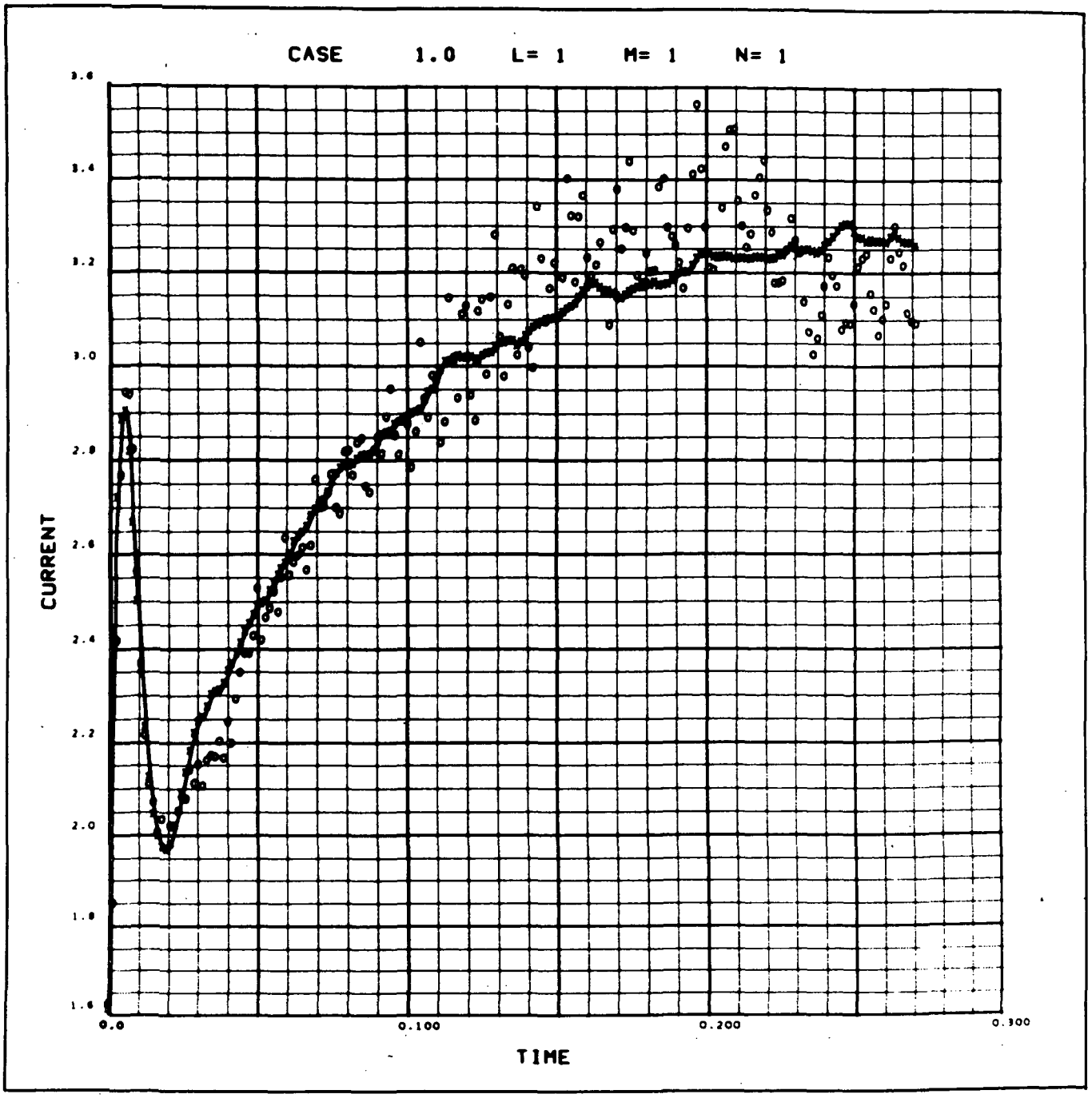

FIGURE 4-49 Simulation of Varo Inverter, Second Event, Run 8A2, Using Optimized Element Values

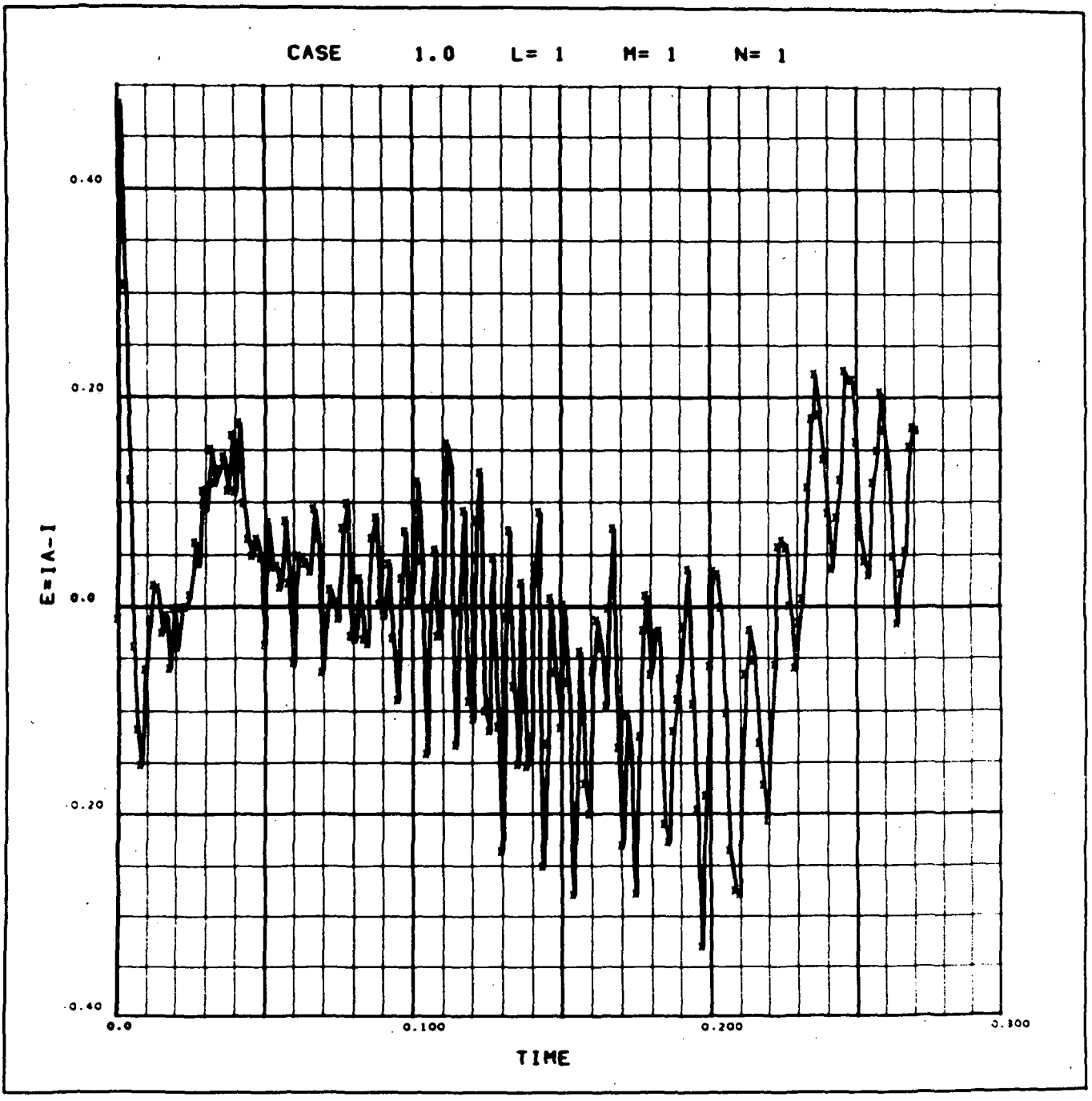

FIGURE 4-50 Current Errors for Varo Inverter, Second Event, Run 8A2, Using Optimized Element Values

4. Apollo Inverter, Run 9A (Initial)

A single four-element branch was used to simulate the Apollo inverter (Run 9A). The current response for this initial model is shown in Figure 4-51 with the corresponding error plot shown in Figure 4-52.

5. VHF/AM Transceiver, Run 11C (Initial)

The network topology used to simulate the VHF/AM transceiver consisted of two branches. One branch had four elements, and the other had three (no parallel resistor). The optimum values produced the simulation shown in Figure 4-53. The error plot is shown in Figure 4-54.

4.5.2.2 Nearest Rounded-Off Value Results

The optimization studies described in Paragraph 4.5.2.1 assumed an unconstrained element value inventory. In order to evaluate the results using a limited inventory, each of the values determined in Paragraph 4.5.2.1 was rounded off (either up or down) to the nearest discrete value available in the simulator. The nominal element values used are identified in Table 4-VIII. The predicted responses are provided in Figures 4-55 through 4-66.

4.5.2.3 Optimum Rounded-Off Value Results

In an attempt to improve on the results obtained by rounding off each element value to the nearest available discrete value, the optimization was repeated. This time each element was rounded off to both the next higher and next lower value and a comparison made of the resulting responses. A selection was then made of the optimum combination. For example, in the case of the motor switch (Run 3C), rounding-off the elements as described in Paragraph 4.5.2.2 resulted in an increase in the response current level. Therefore, in an attempt to improve the response, each of the elements was varied both up and down to the nearest discrete value. The ripple circuit branch was held constant for this exercise since it does not contribute to the average current level. Thus, 7 elements remained to be varied. Since each element can be varied either up or down from the initial value, there are 2^7, or 256, combinations to be tried. All 256 models were evaluated and the one producing the smallest RMS current error was selected.

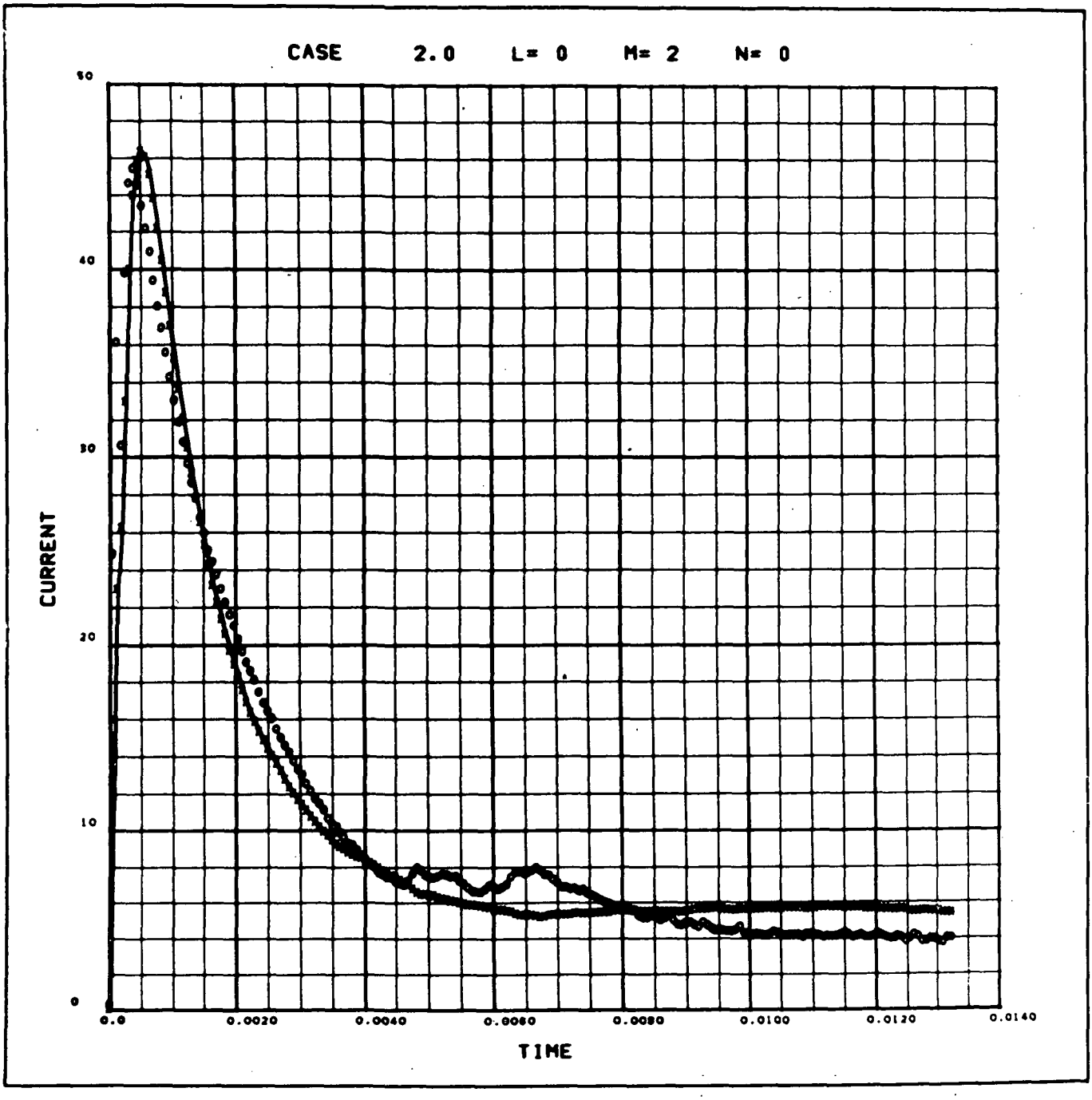

FIGURE 4-51 Simulation of Apollo Inverter, Run 9A, Using Optimized Element Values

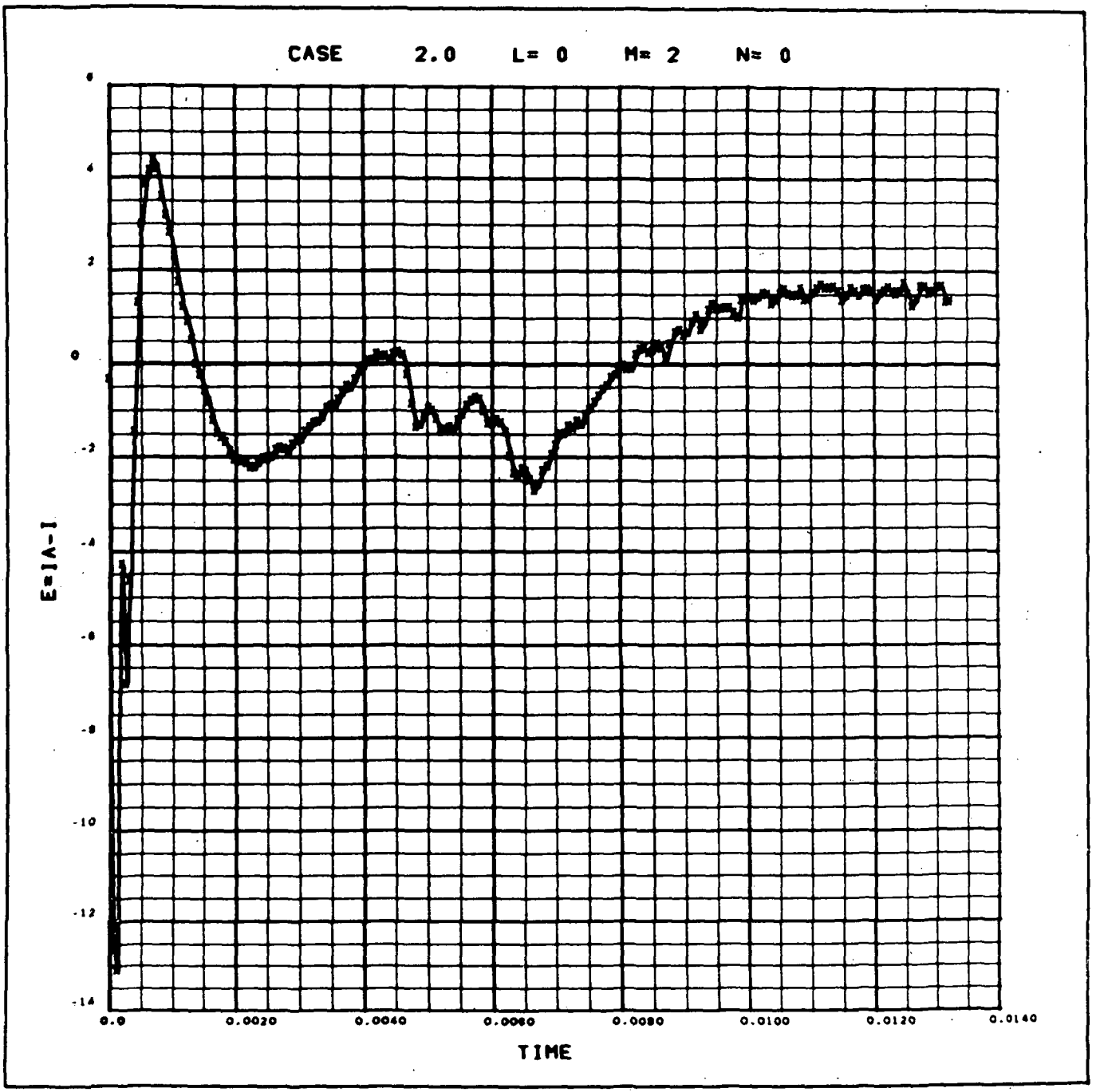

FIGURE 4-52 Current Errors for Apollo Inverter, Run 9A, Using Optimized Element Values

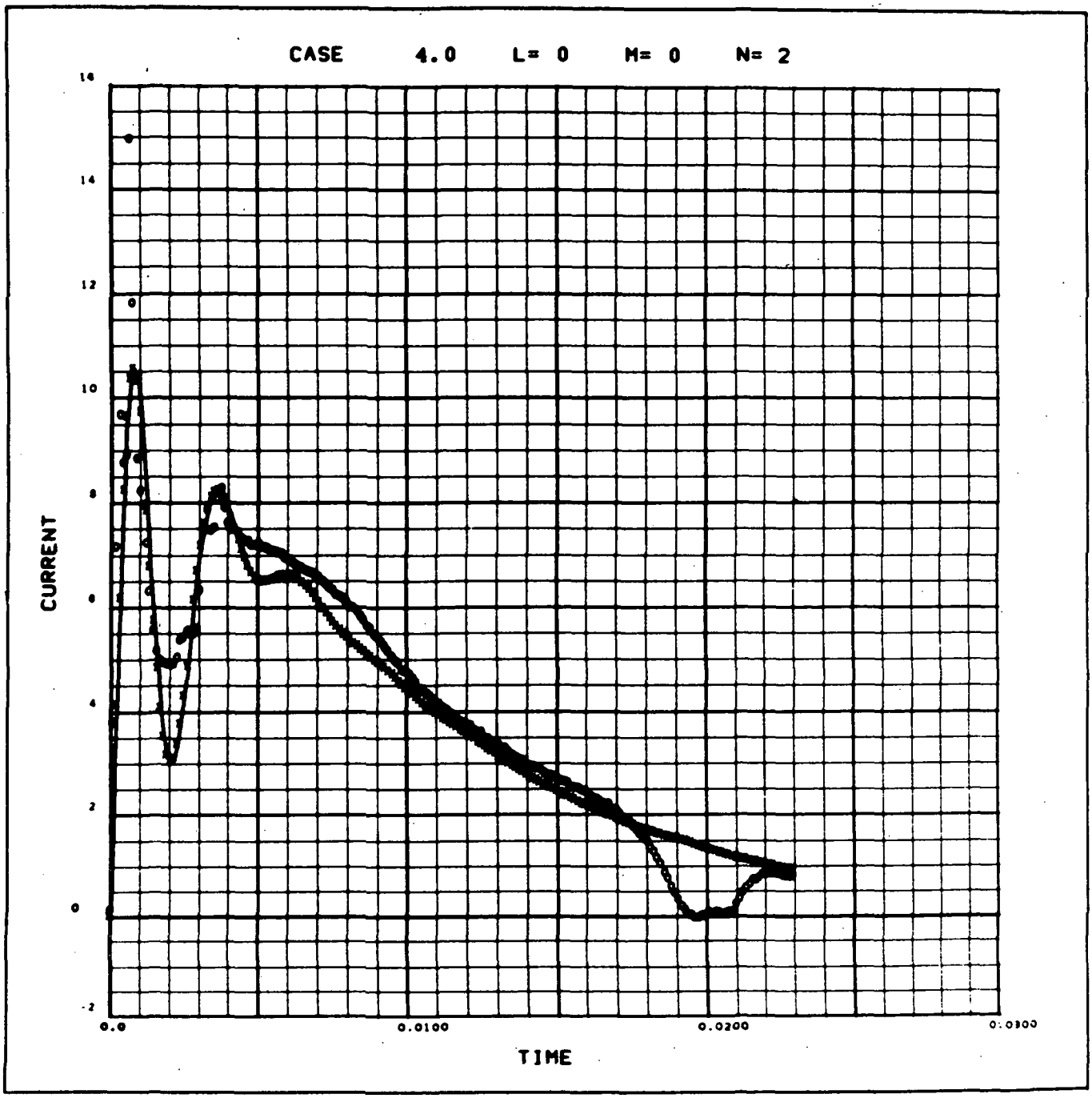

FIGURE 4-53 Simulation of VHF/AM Transceiver, Run 11C, Using Optimized Element Values

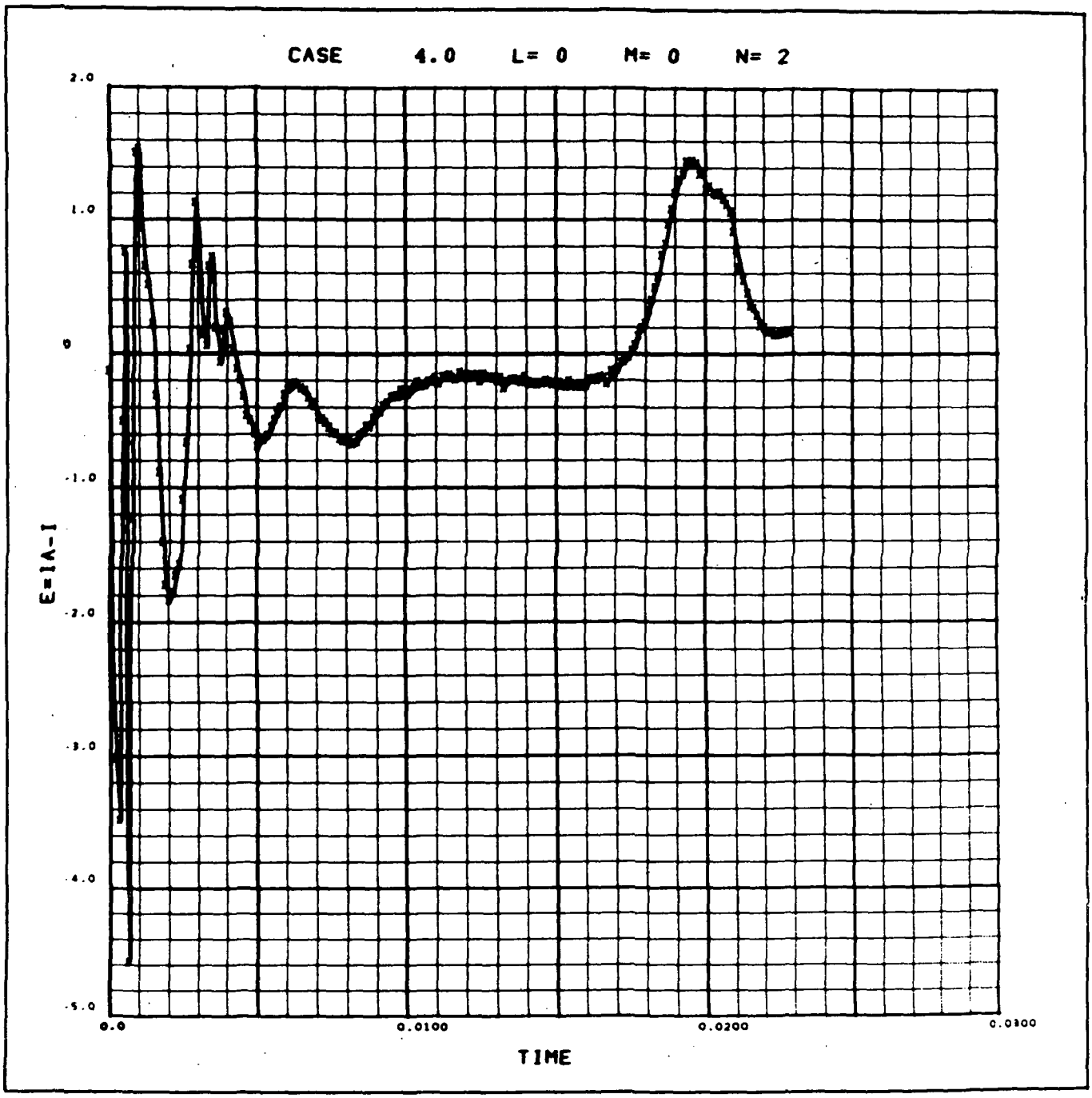

FIGURE 4-54 Current Errors for VHF/AM Transceiver, Run 11C, Using Optimized Element Values

TABLE 4-VIII

NEAREST ROUNDED ELEMENT VALUES

Equipment Type	Branch	Element Values				Switch Time t
		Resistance	Inductance	Capacitance	1/Conductance	
		ohms	henries	farads	ohms	secs
Motor Switch Run 3C	1	6.2	1.5×10^{-3}	1.0×10^{-4}	open	0.0408
	2	short	6.2×10^{-3}	1.5×10^{-2}	open	
	3	4.0	3.0×10^{-3}	1.0×10^{-2}	10.0	
Heat Exchanger Valve Run 6B	1	1500.	0.2	5.0×10^{-3}	0.25	- -
Varo Inverter Run 8A	1	0.4	2.0×10^{-4}	8.0×10^{-3}	12.0	0.585
	2	15.0	1.0	- -	- -	
	3	12.0	0.04	4.0×10^{-4}	open	
Apollo Inverter Run 9A	1	0.3	6.2×10^{-5}	3.0×10^{-3}	5.0	- -
VHF/AM Transceiver Run 11A	1	1.2	1.0×10^{-3}	2.0×10^{-4}	open	- -
	2	3.0	6.2×10^{-3}	3.0×10^{-3}	open	

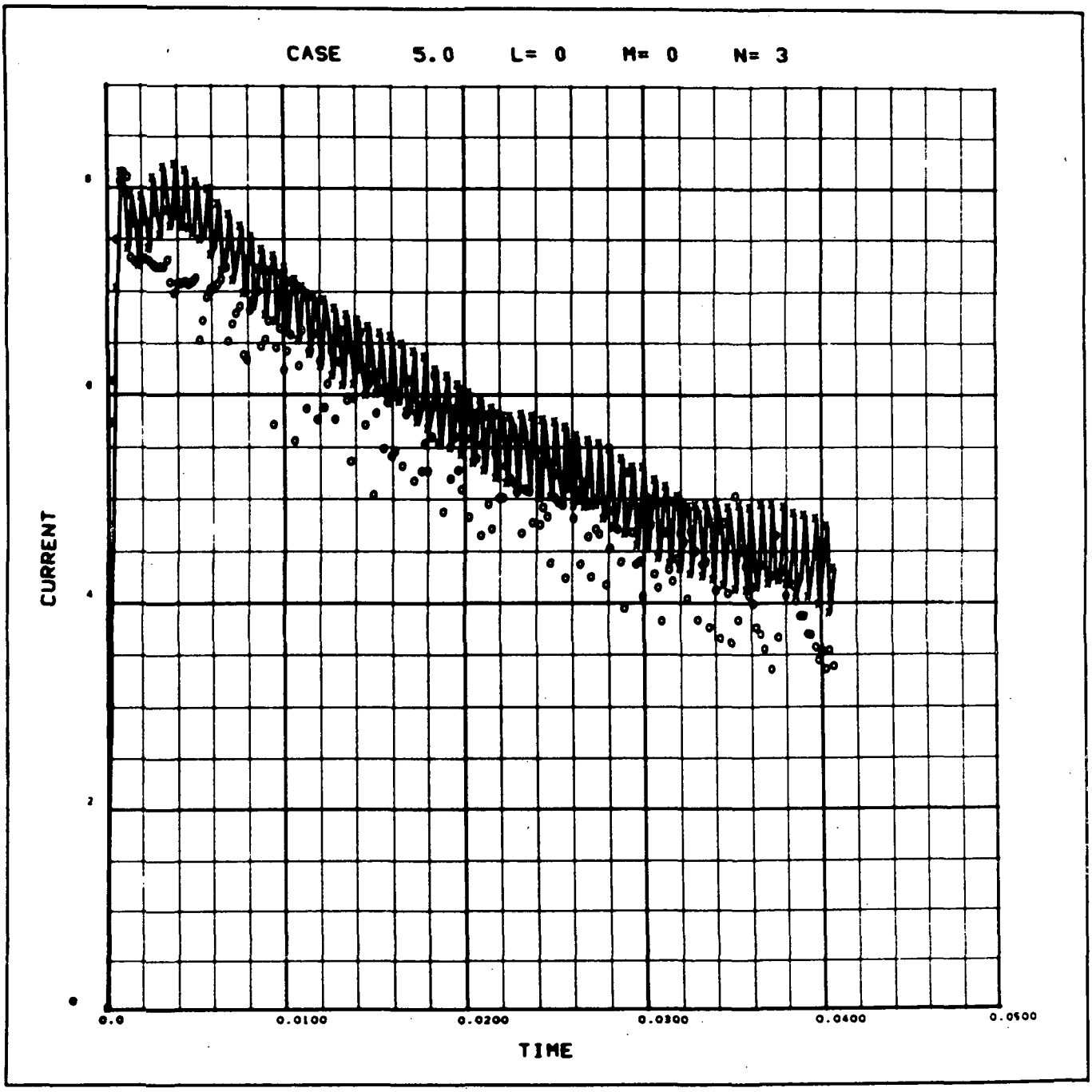

FIGURE 4-55 Simulation of Motor Switch, Run 3C, Using Rounded Element Values

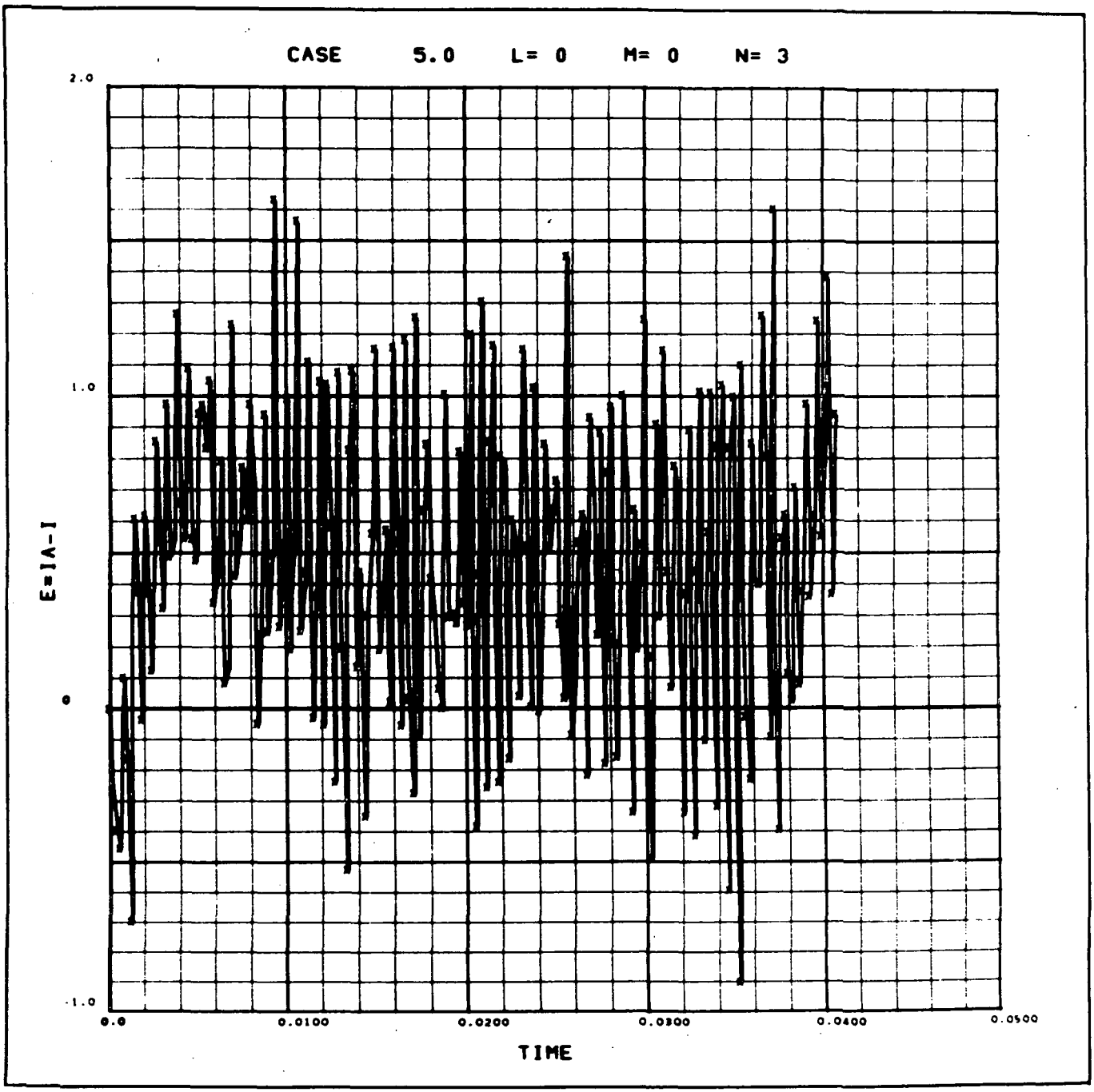

FIGURE 4-56 Current Errors for Motor Switch, Run 3C, Using Rounded Element Values

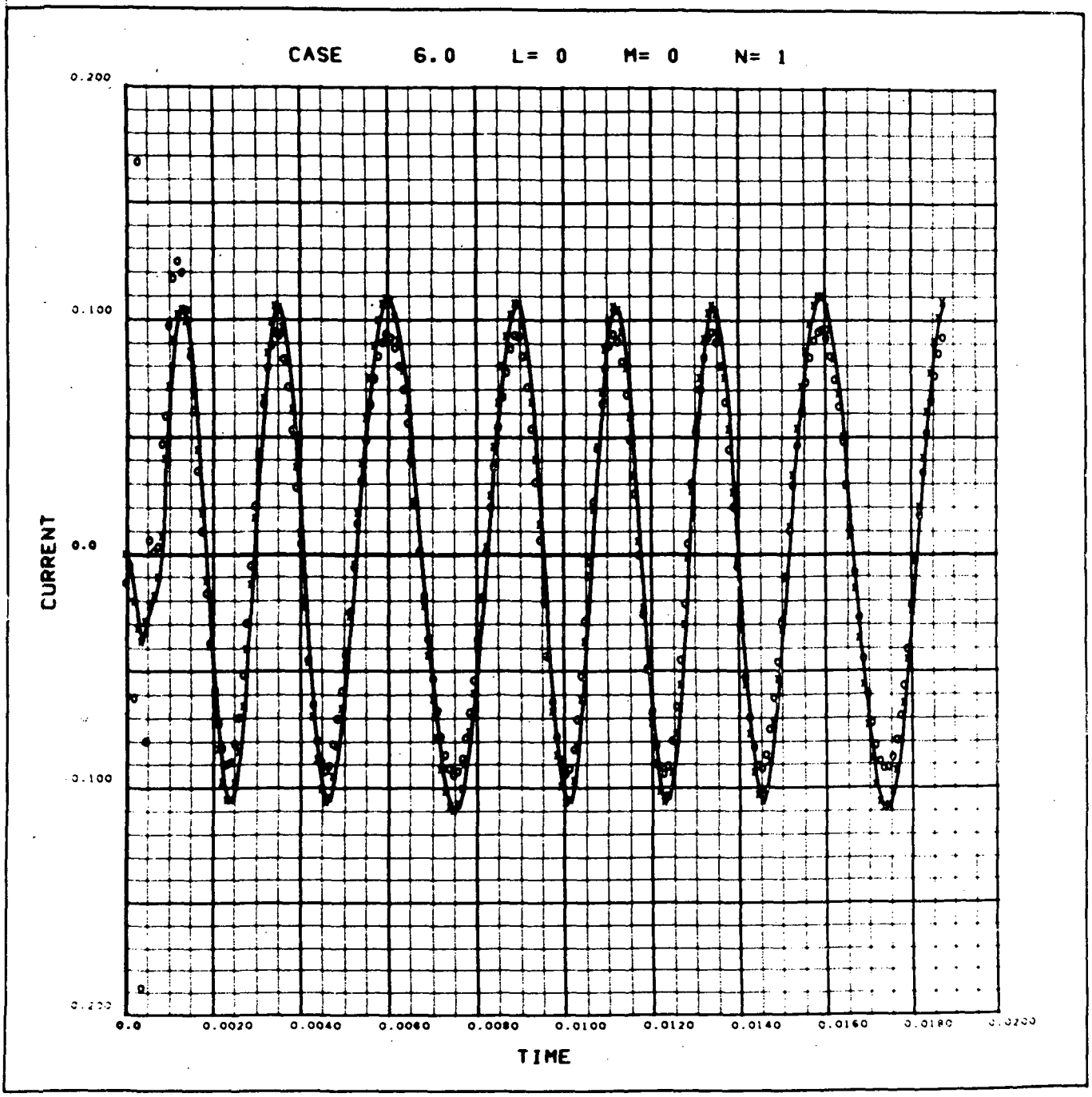

FIGURE 4-57 Simulation of Heat Exchanger Valve, Run 6B, Using Four Rounded Element Values

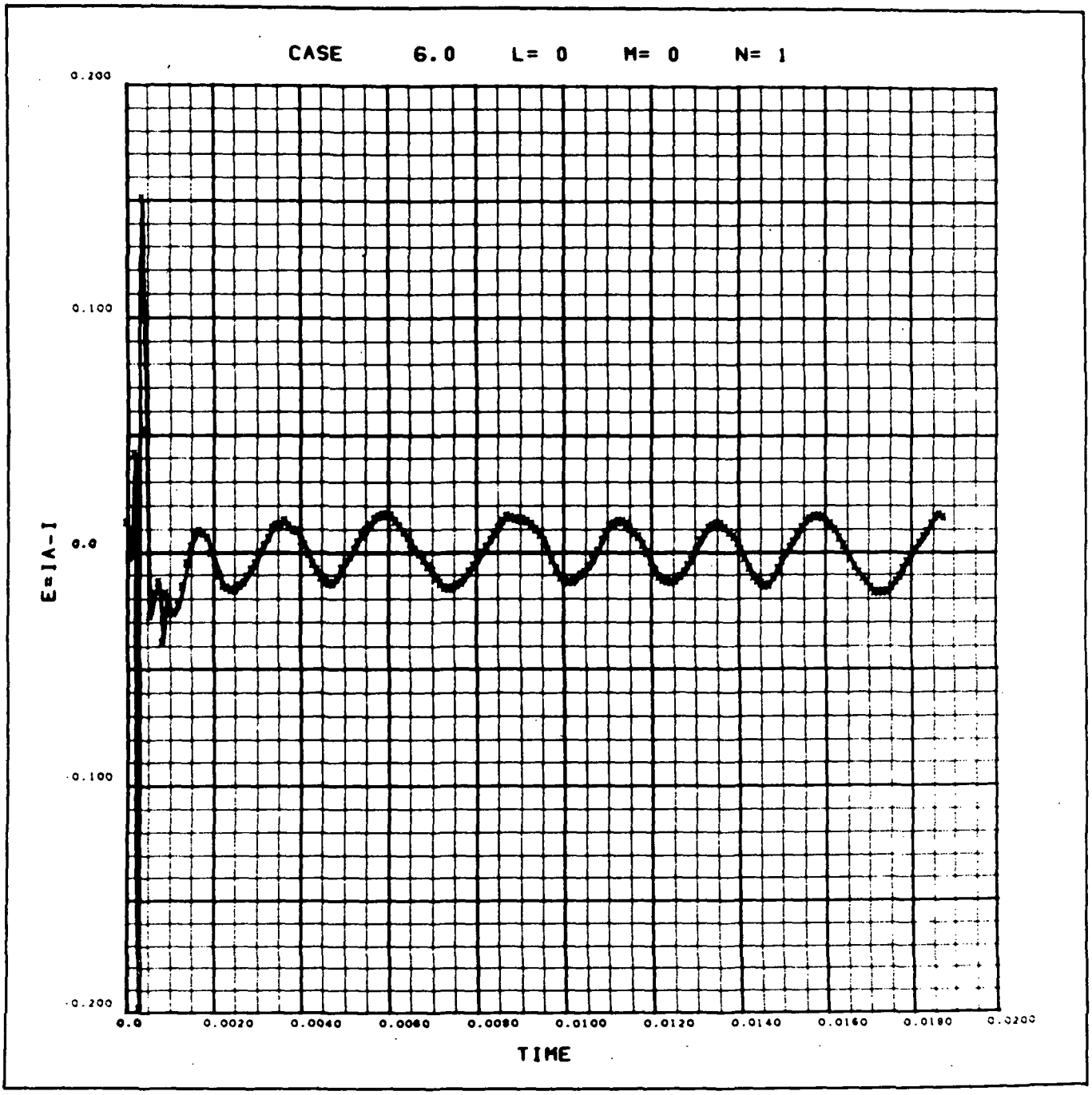

FIGURE 4-58 Current Errors for Heat Exchanger Valve, Run 6B, Using Four Rounded Element Values

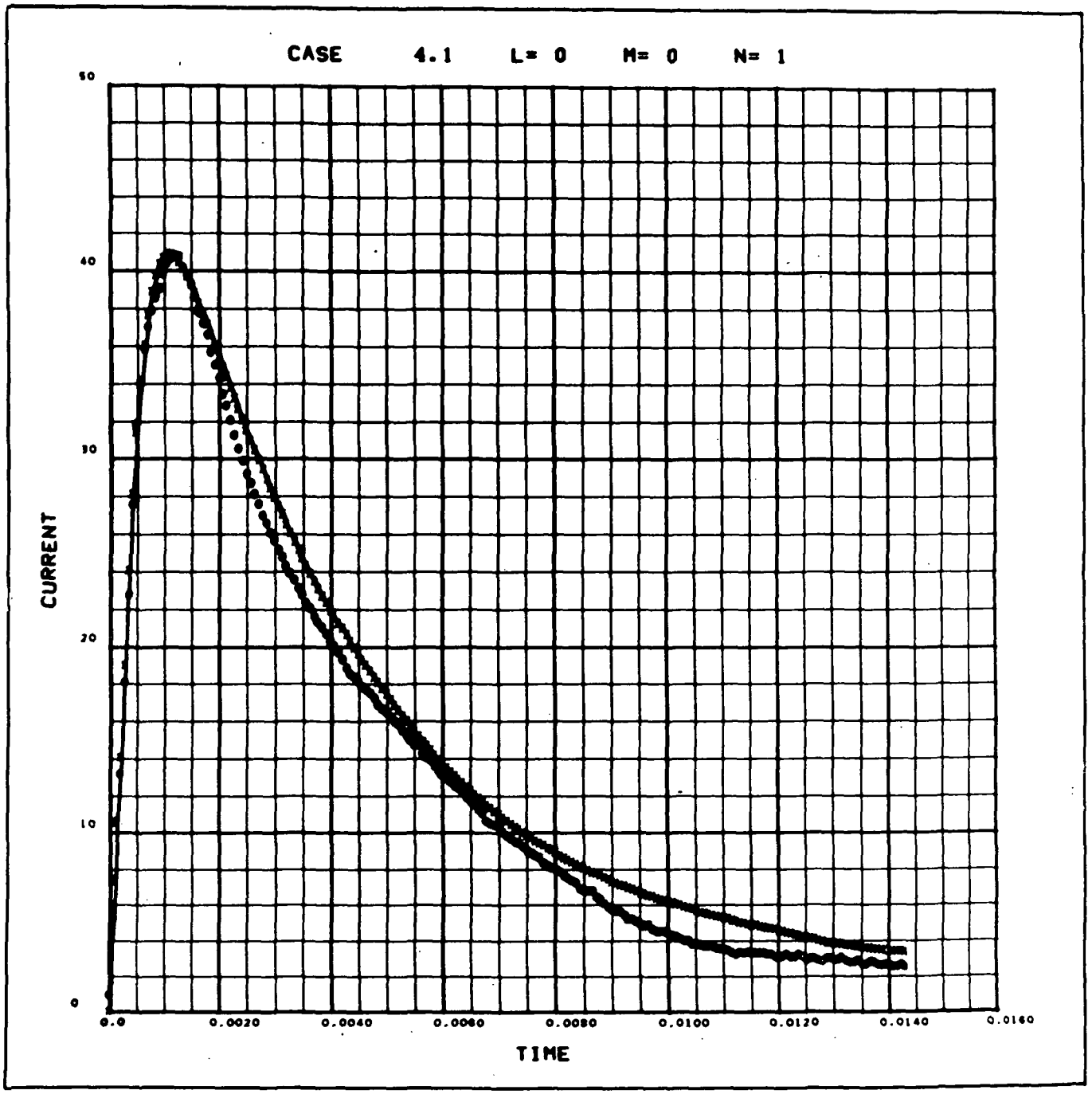

FIGURE 4-59 Simulation of Varo Inverter, First Event, Run 8A1, Using Rounded Element Values

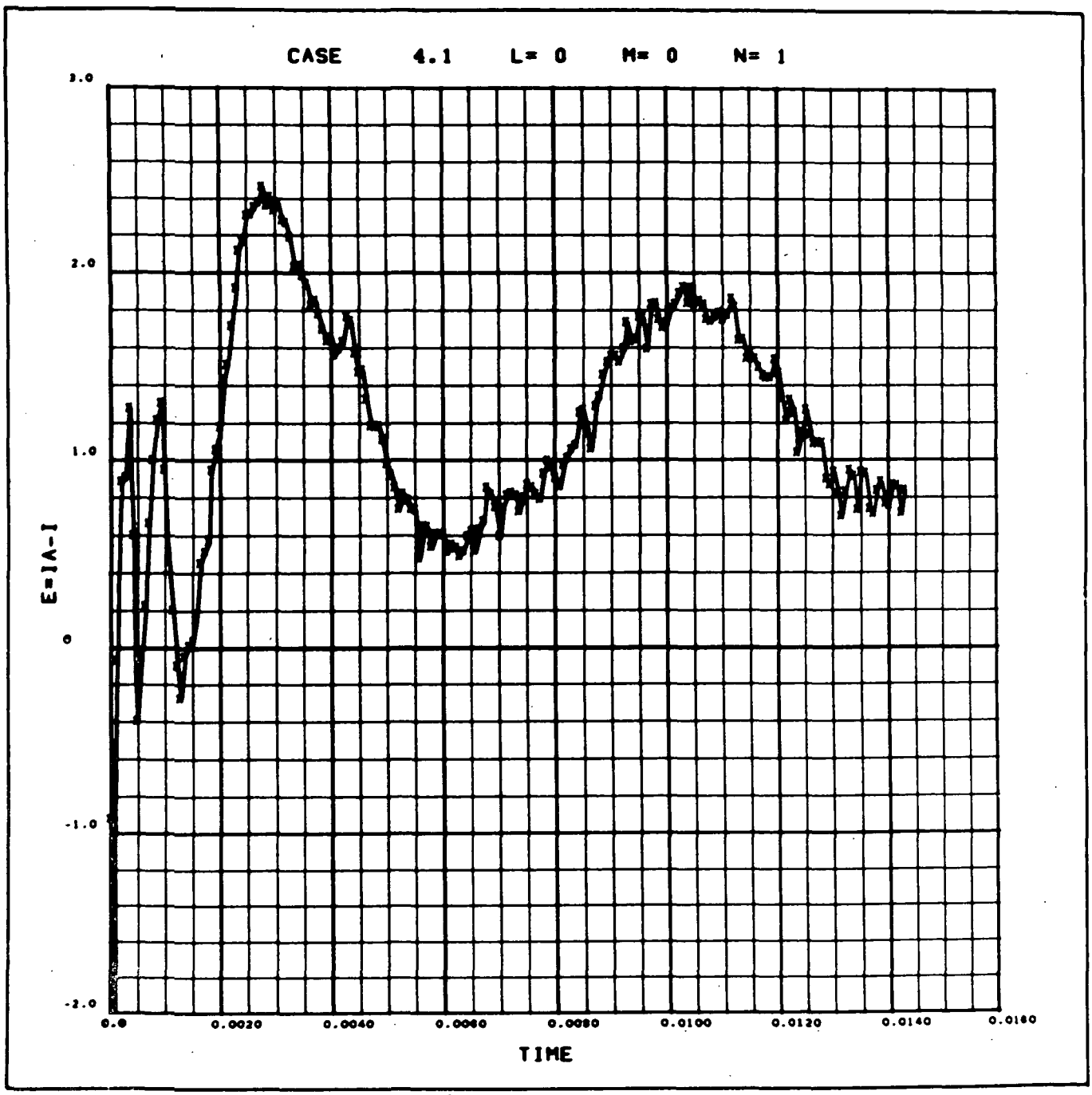

FIGURE 4-60 Current Errors for Varo Inverter, First Event, Run 8A1, Using Rounded Element Values

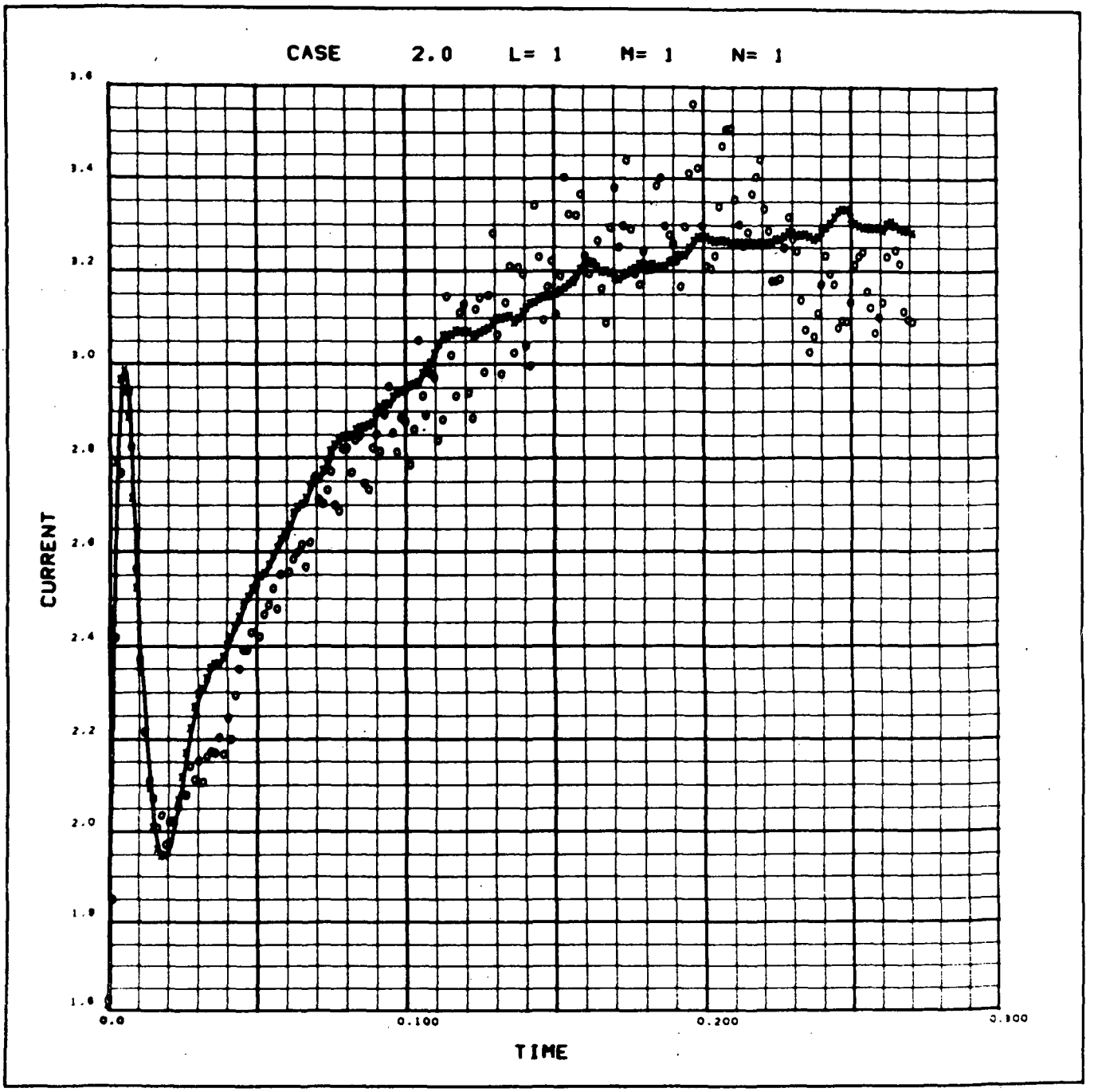

FIGURE 4-61 Simulation of Varo Inverter, Second Event, Run 8A2, Using Rounded Element Values

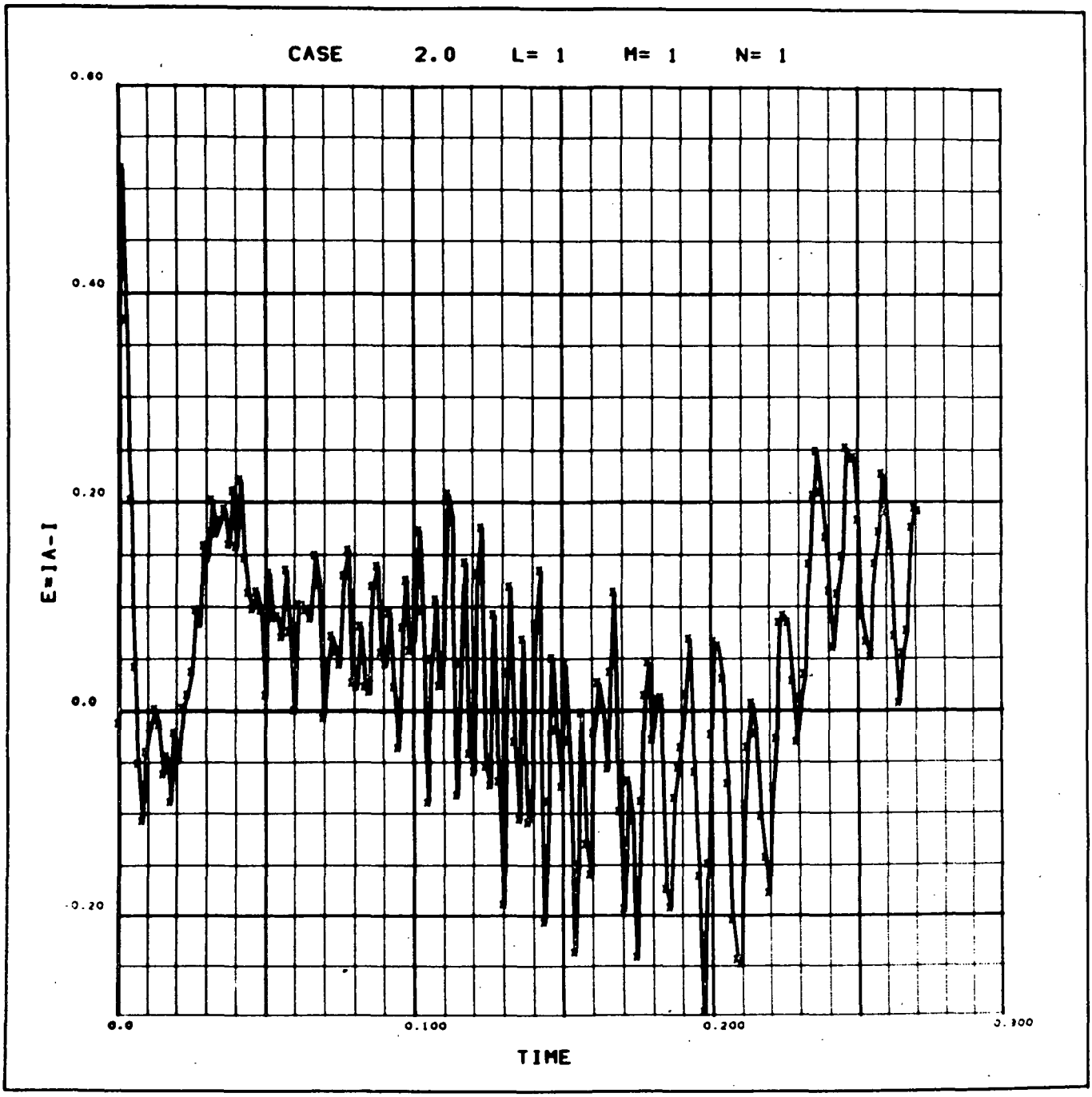

FIGURE 4-62 Current Errors for Varo Inverter, Second Event, Run 8A2, Using Rounded Element Values

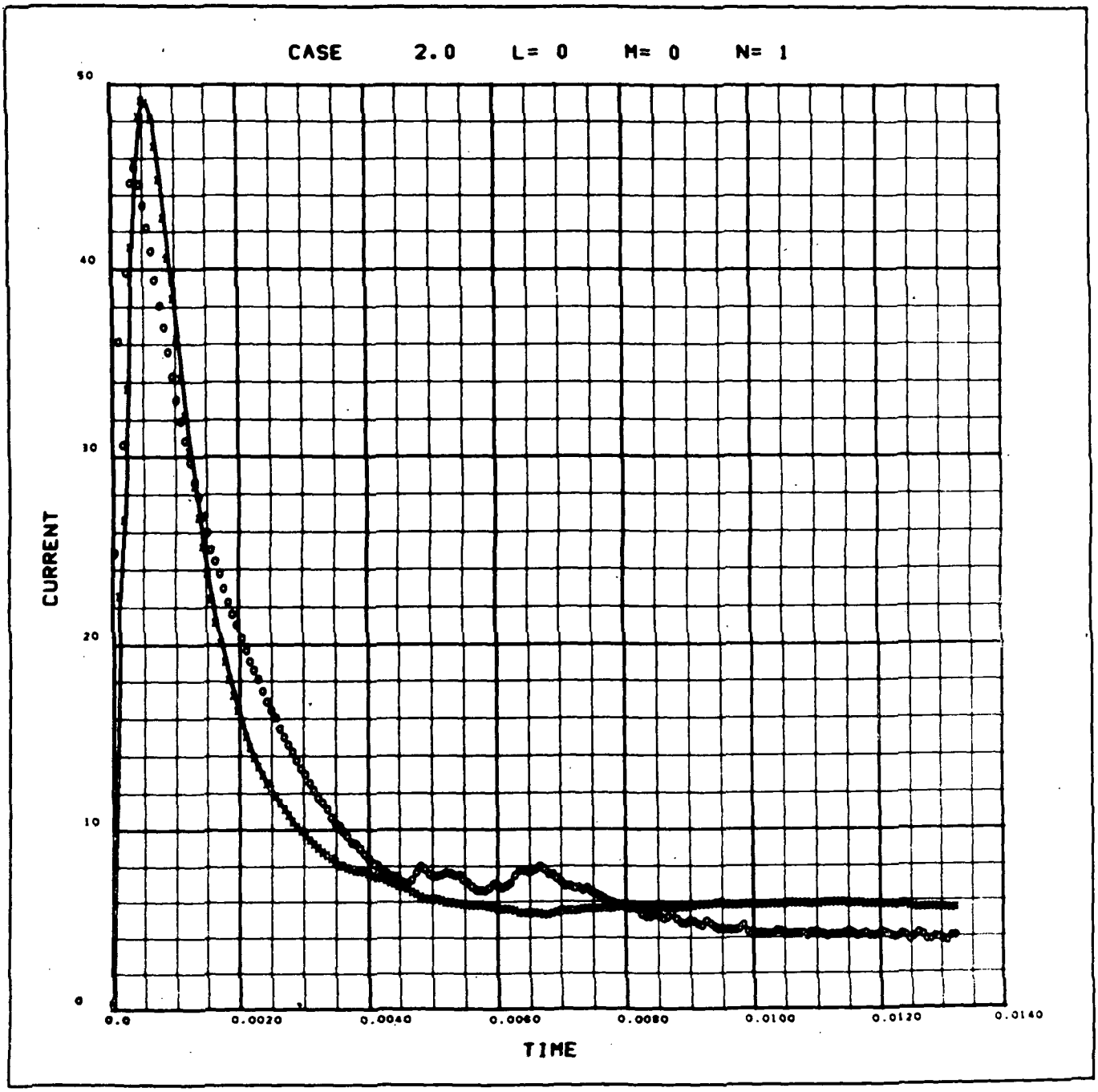

FIGURE 4-63 Simulation of Apollo Inverter, Run 9A, Using Rounded Element Values

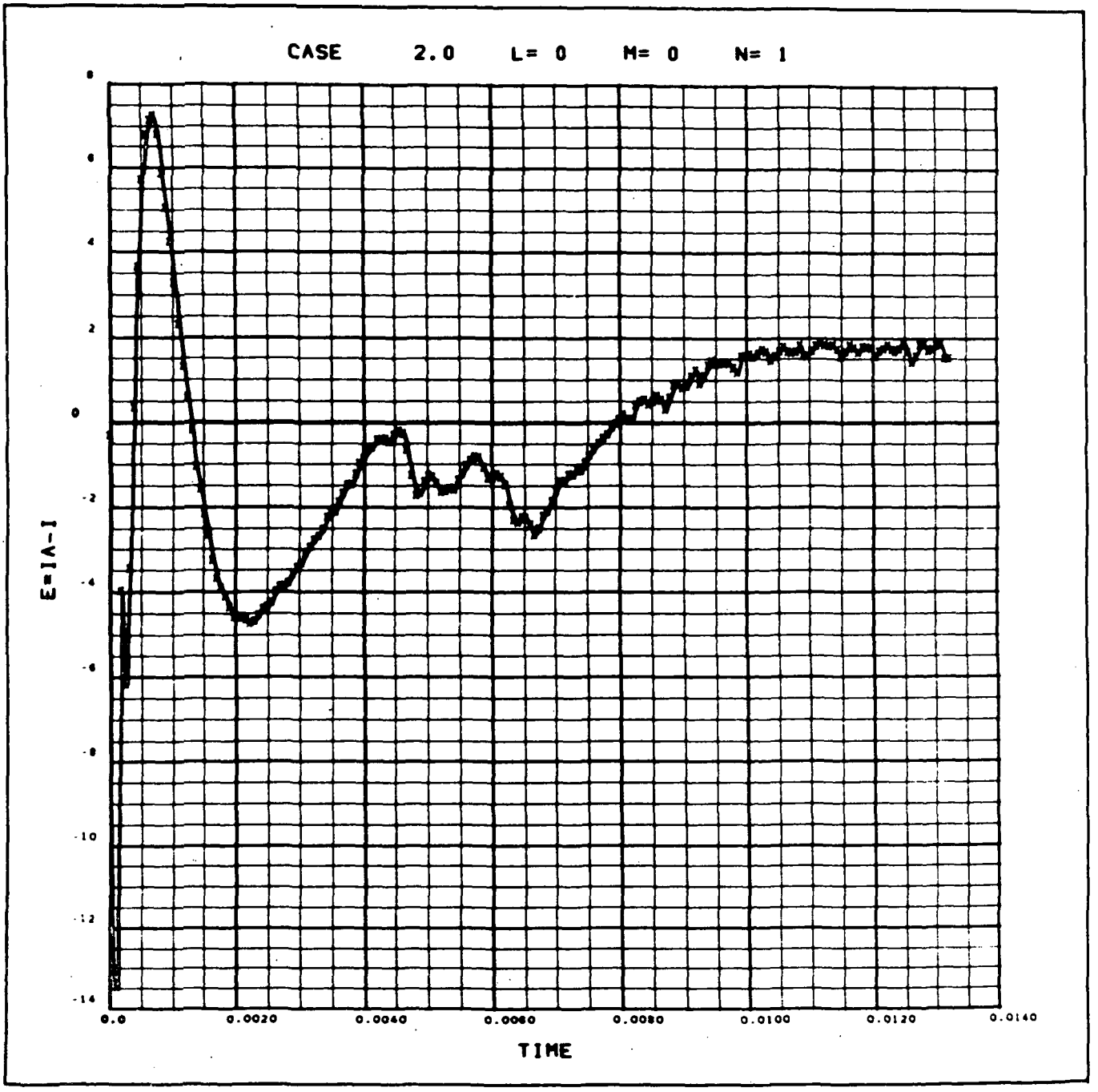

FIGURE 4-64 Current Errors for Apollo Inverter, Run 9A, Using Rounded Element Values

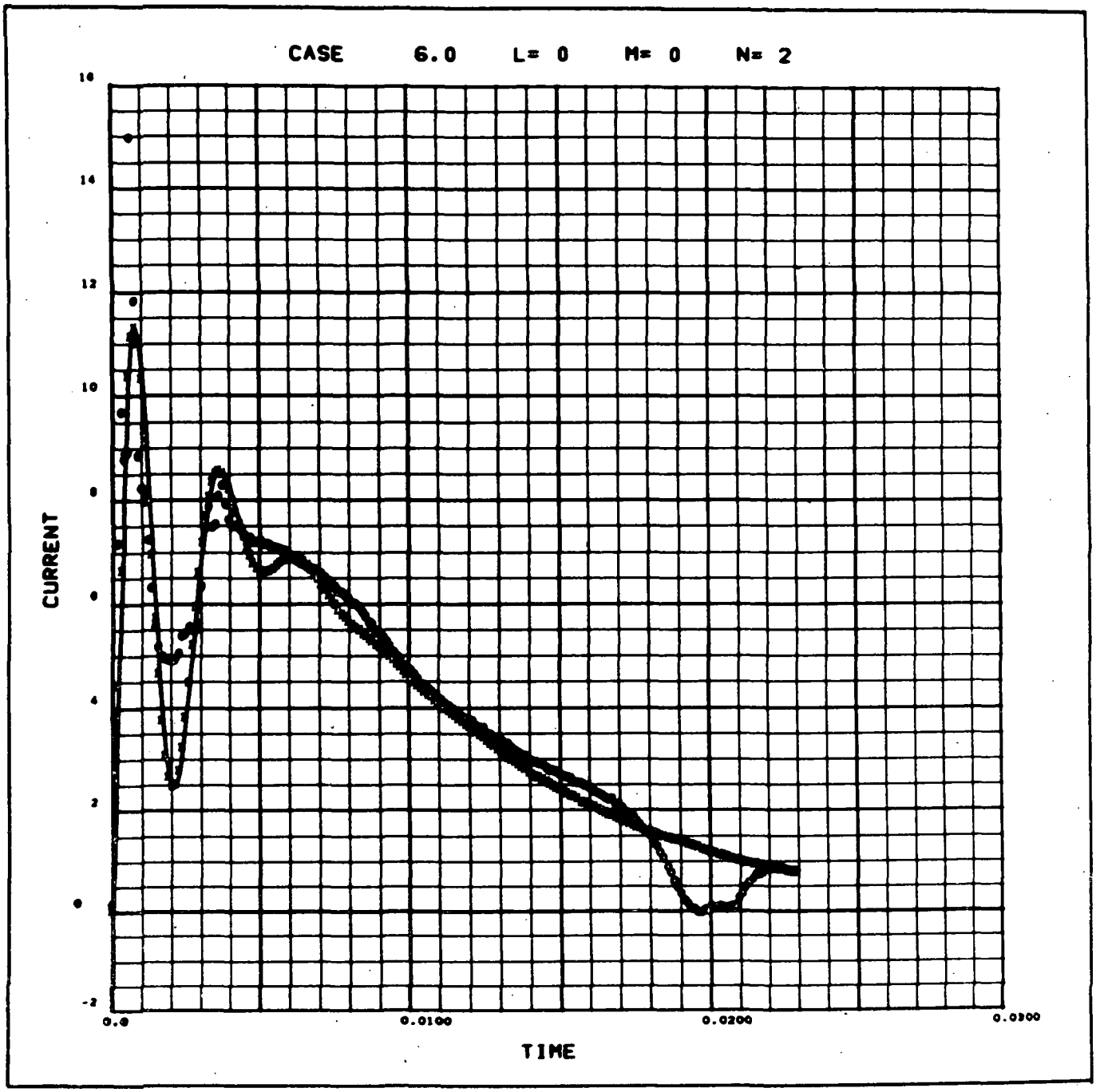

FIGURE 4-65 Simulation of VHF/AM Transceiver, Run 11C, Using Rounded Element Values

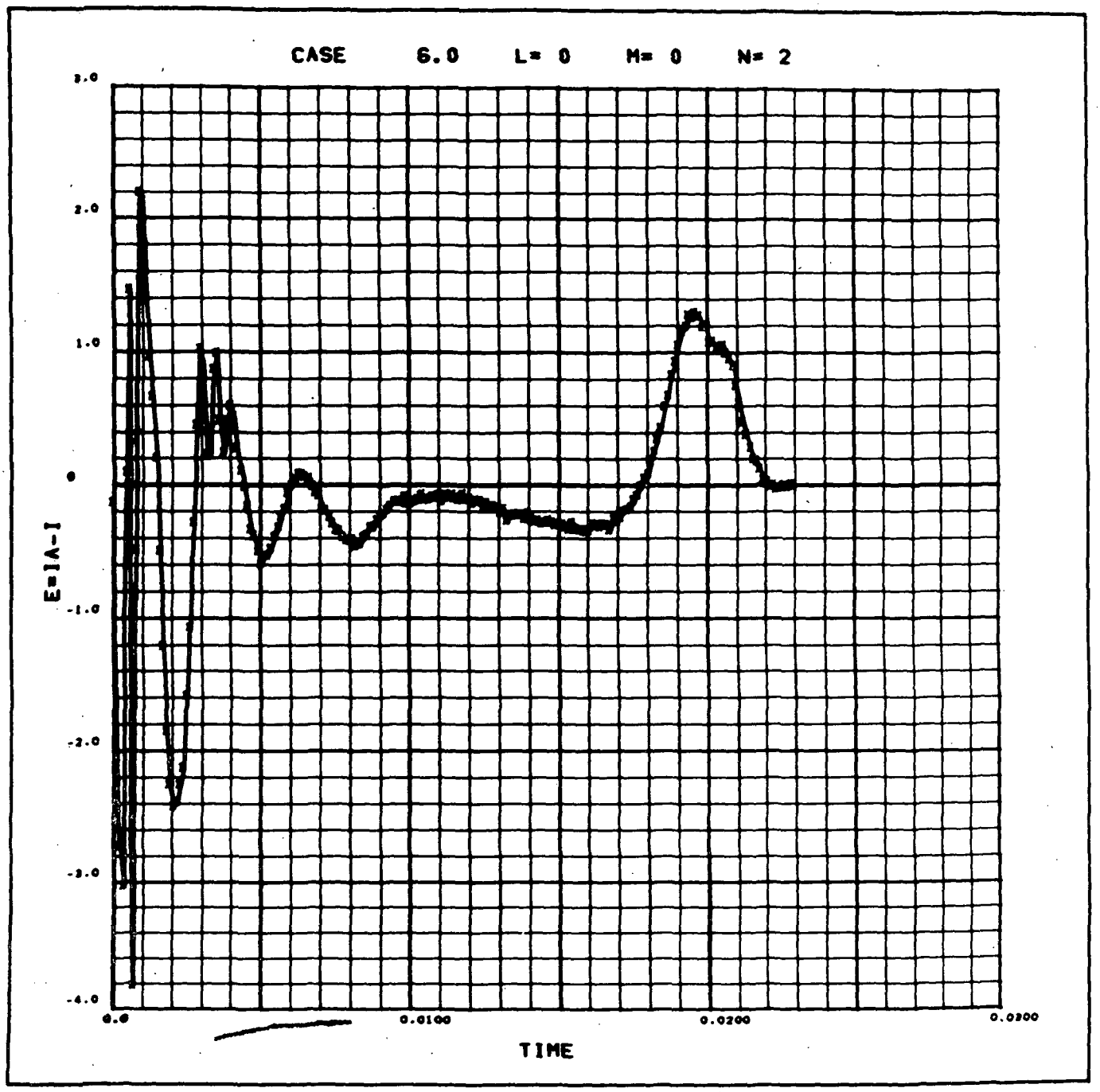

FIGURE 4-66 Current Errors for VHF/AM Transceiver, Run 11C, Using Rounded Element Values

Similar studies were carried out in each case to select the optimum rounded-off values for each response curve. These values are identified in Table 4-IX and the responses are shown in Figures 4-67 through 4-72. During these exercises an additional branch was included in the models for Runs 6B and 9A to provide greater accuracy in these responses. In Figure 4-68 (Run 6B), the response is shown on a different time scale from the corresponding earlier traces. In evaluating the predicted response of each model, subjective judgment was used to select the "best" model. This judgment was biased toward emphasizing those characteristics of the response considered most significant to a power system. Thus, for example, peak current was judged more important than high-frequency ripple. Model selections reflect this bias.

In those cases in which the model response and original equipment response were not identical, the emphasis was placed upon providing worst-case transient behavior. That is, the model should provide a response equal to or slightly more severe than that of the interrogated equipment.

TABLE 4-IX

REFERENCE ELEMENT VALUES

Equipment Type	Branch	Element Values				Switch Time t
		Resistance	Inductance	Capacitance	1/Conductance	
		ohms	henries	farads	ohms	secs
Motor Switch Run 3C	1	5.0	1.5×10^{-3}	1.0×10^{-4}	open	0.0408
	2	short	6.2×10^{-3}	1.5×10^{-6}	open	
	3	4.0	3.0×10^{-3}	8.0×10^{-3}	10.0	
Heat Exchanger Valve Run 6B	1	1500.0	0.20	- -	- -	- -
	2	80.0	8.0×10^{-3}	1.0×10^{-7}	open	
Varo Inverter Run 8A	1	0.4	2.0×10^{-4}	8.0×10^{-3}	15.0	0.585
	2	15.0	1.0	- -	- -	
	3	12.0	0.05	4.0×10^{-4}	open	
Apollo Inverter Run 9A	1	0.4	5.0×10^{-5}	4.0×10^{-3}	12.0	- -
	2	1.0	4.0×10^{-4}	6.2×10^{-5}	800.0	
VHF/AM Transceiver Run 11C	1	1.2	1.0×10^{-3}	1.5×10^{-4}	open	- -
	2	3.0	1.2×10^{-3}	4.0×10^{-3}	open	

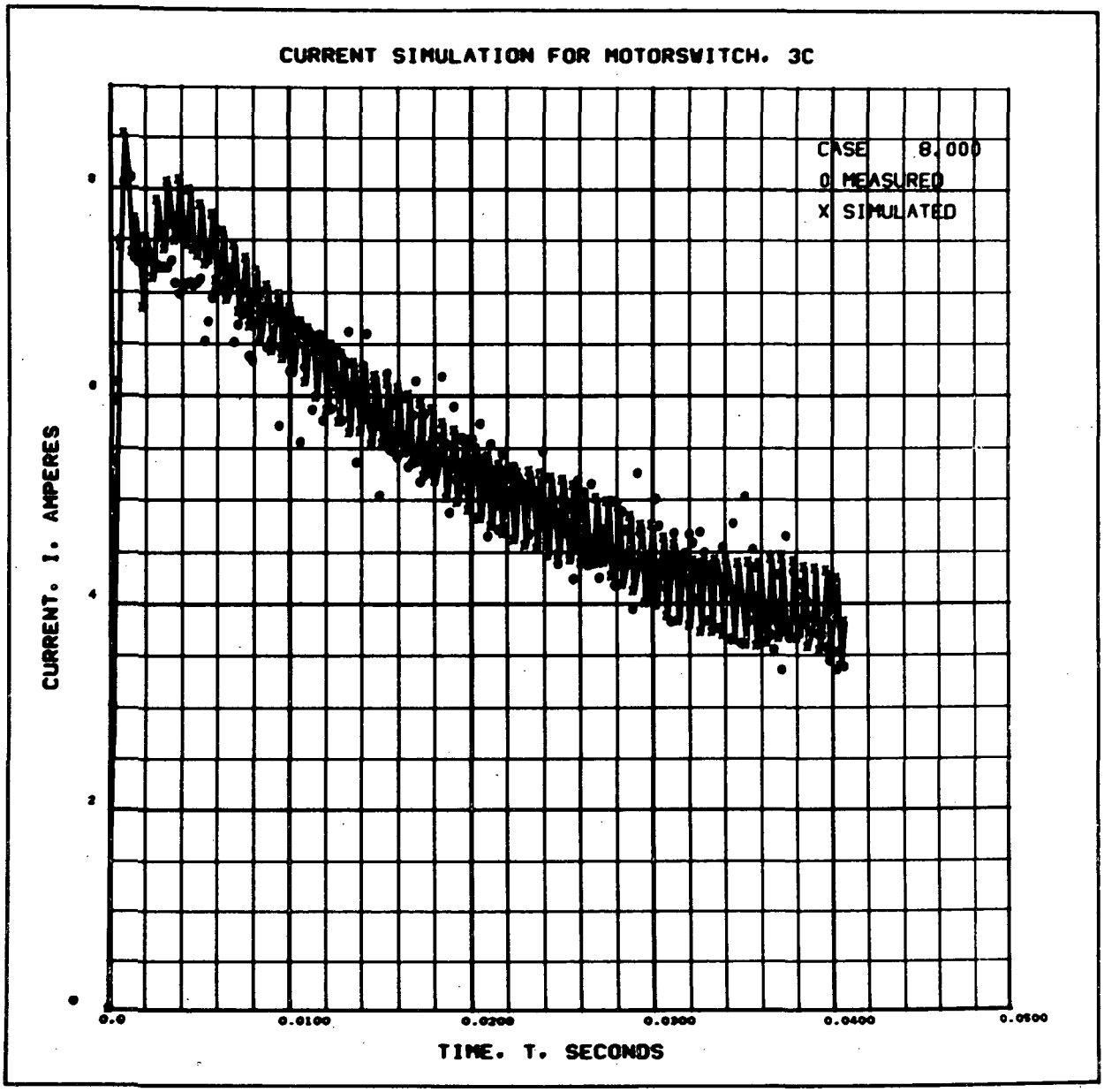

FIGURE 4-67 Current Simulation for Motor Switch, Run 3C

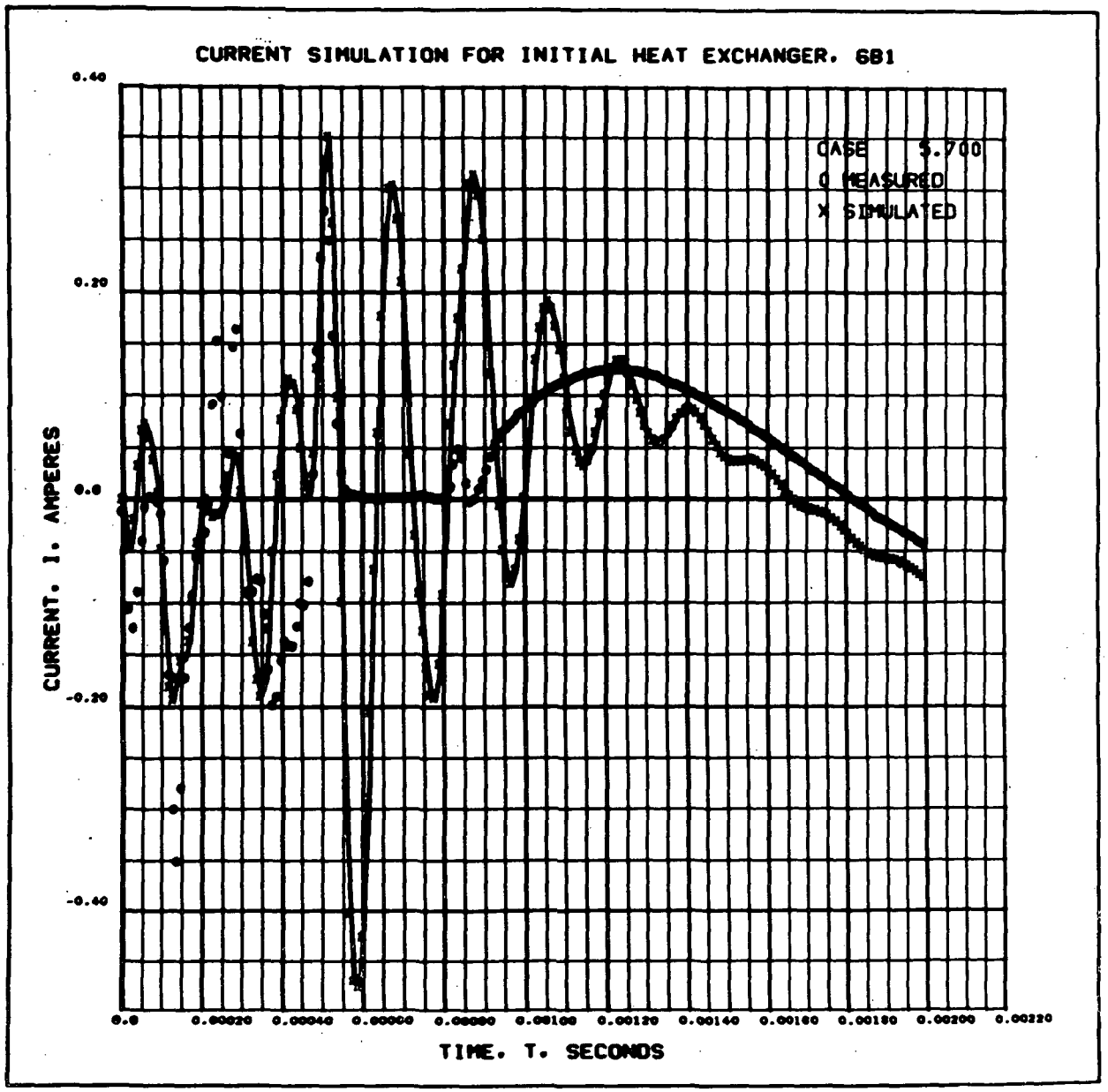

FIGURE 4-68 Current Simulation for Initial Heat Exchanger Valve, Run 6B1

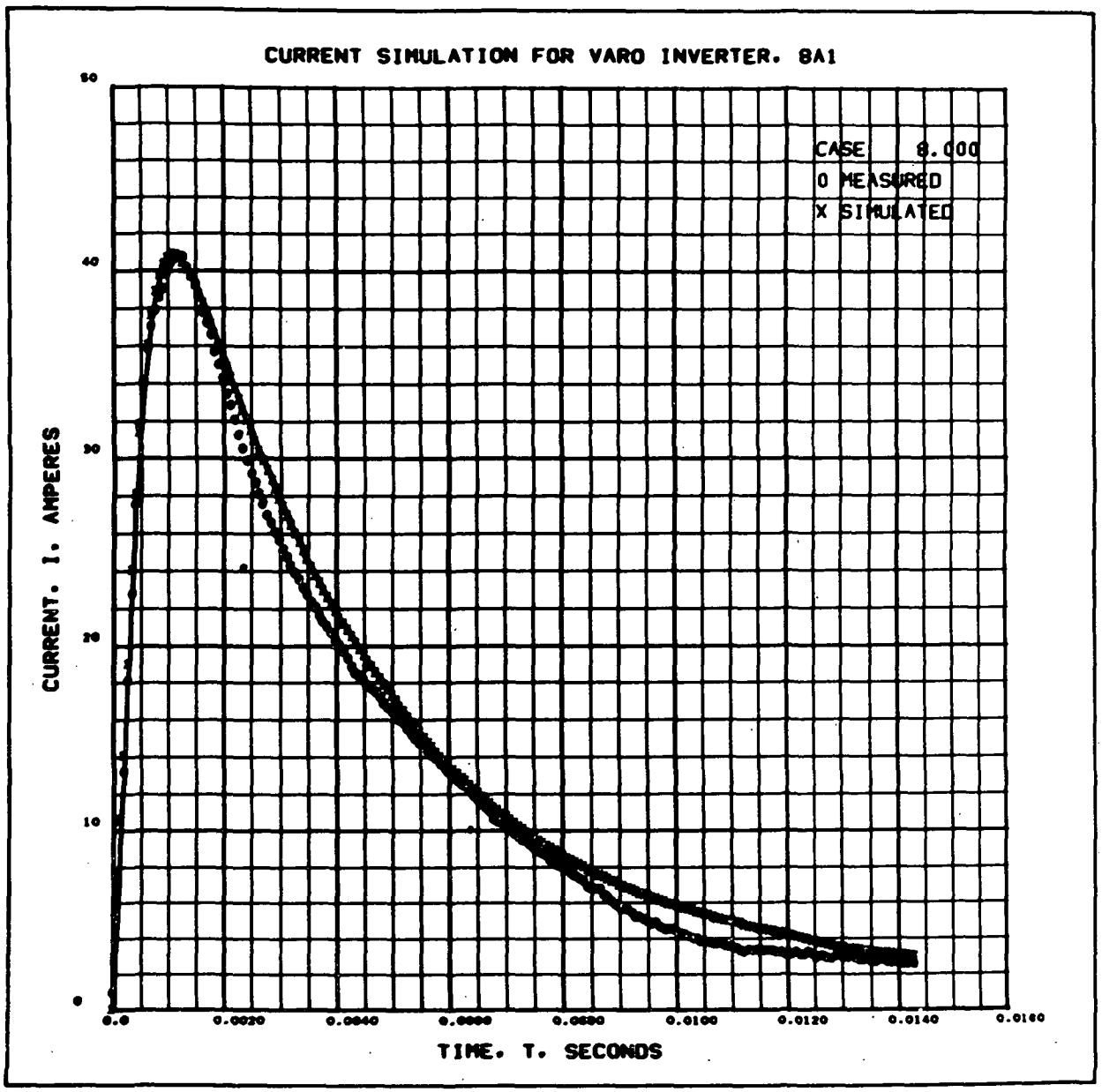

FIGURE 4-69 Current Simulation for Varo Inverter, First Event, Run 8A1

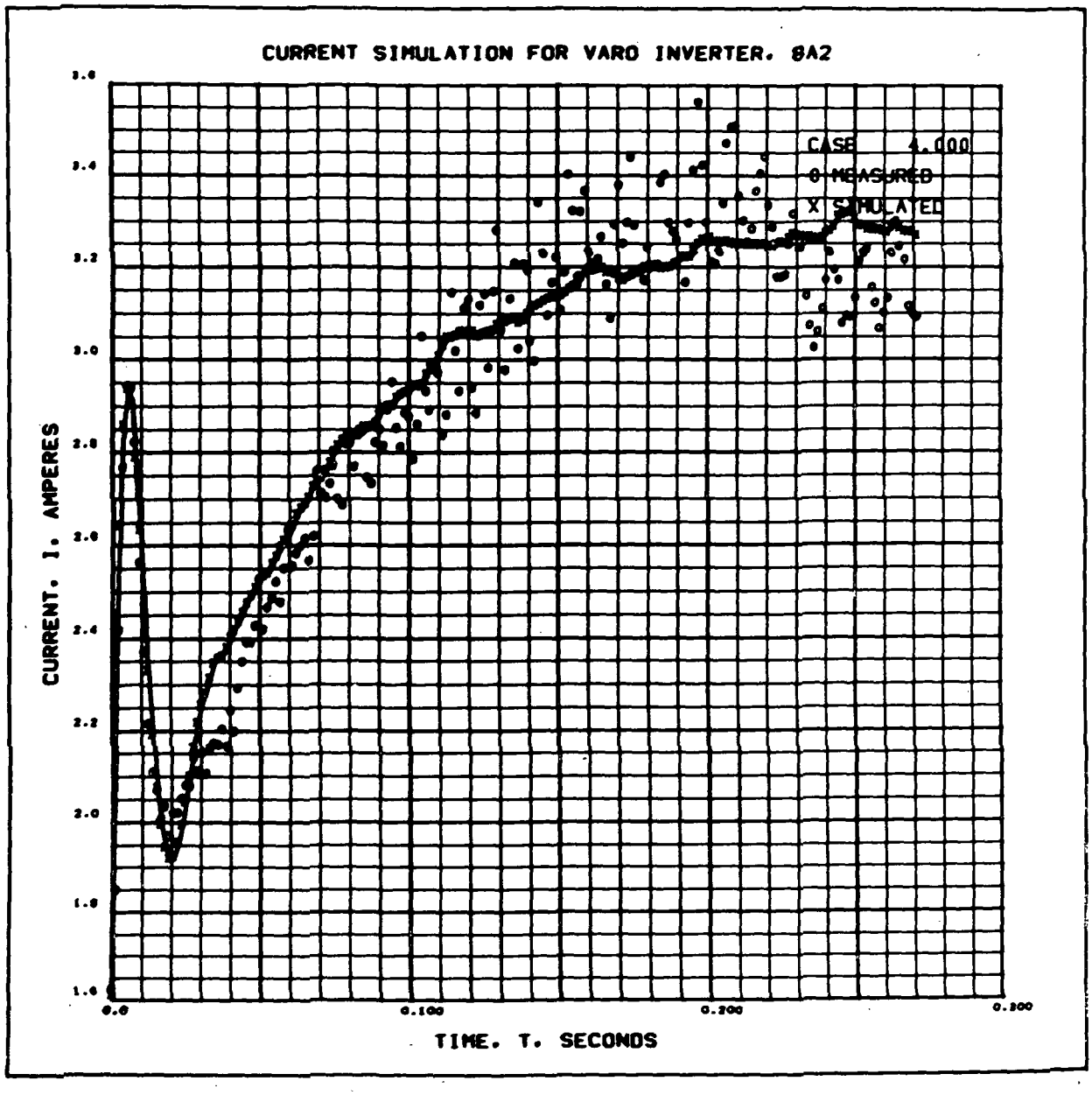

FIGURE 4-70 Current Simulation for Varo Inverter, Second Event, Run 8A2

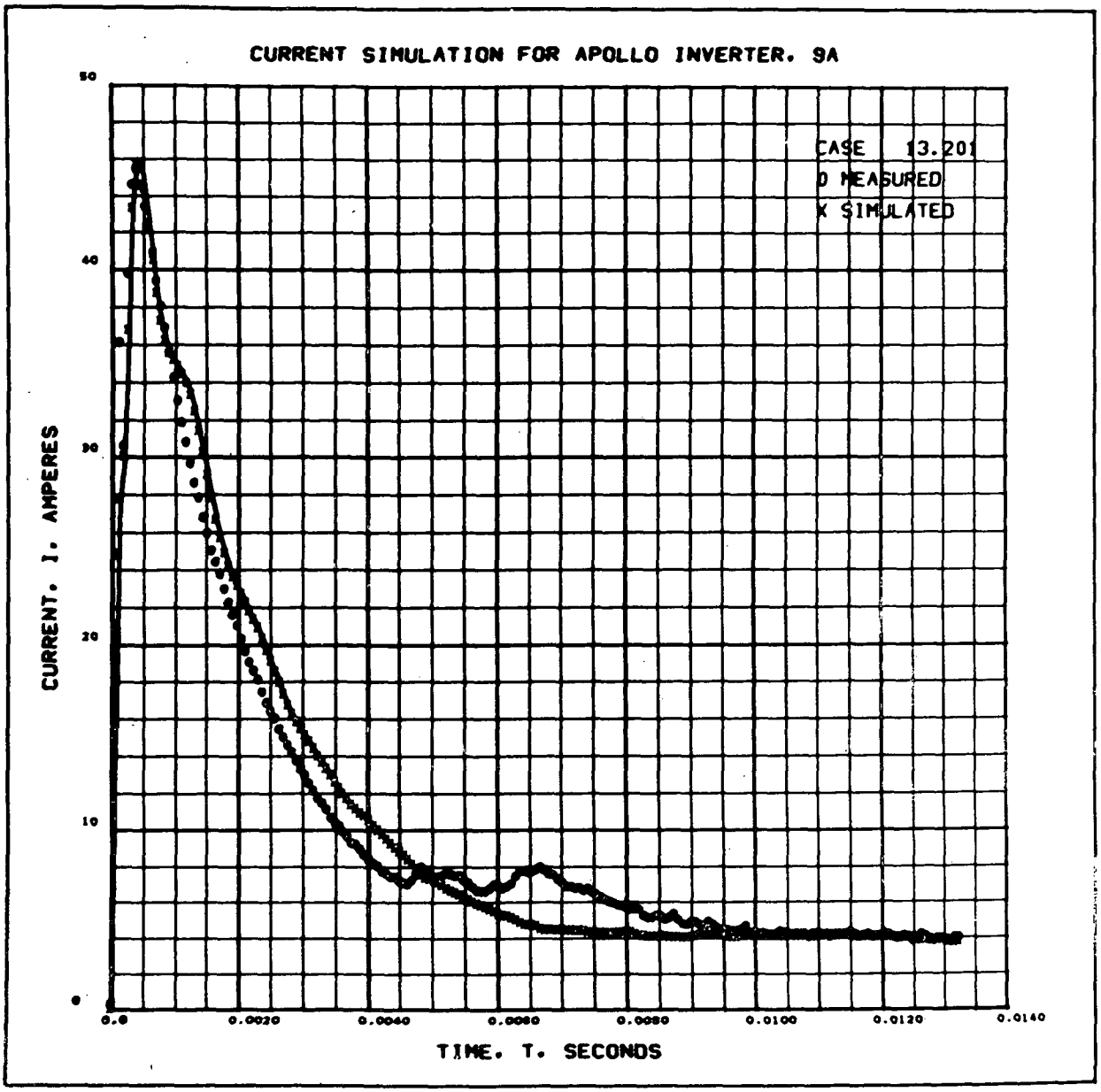

FIGURE 4-71 Current Simulation for Apollo Inverter, Run 9A

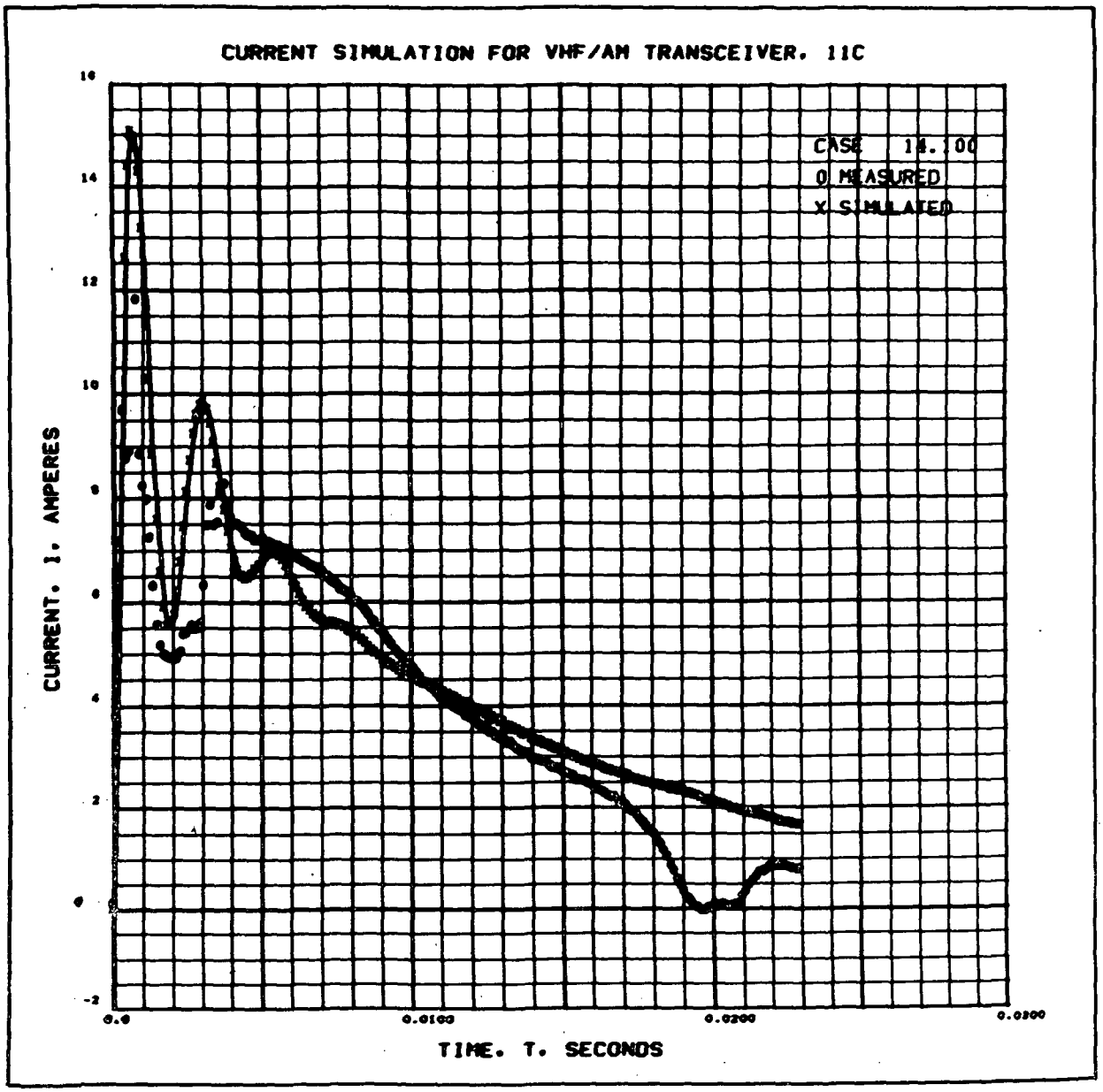

FIGURE 4-72 Current Simulation for VHF/AM Transceiver, Run 11C

5. SIMULATOR DESIGN

The overriding principle in designing and developing the simulation hardware was to provide: (1) an engineering tool for demonstrating the feasibility and usefulness of such devices, and (2) a test bed for evaluating and improving the techniques employed.

5.1 DESIGN REQUIREMENTS

As a first step in the development of the dynamic load simulation hardware, a preliminary set of design requirements was established. These requirements, included in the third monthly progress report, guided design efforts.

5.2 DESCRIPTION

The dynamic load simulator (DLS) developed during this program provides two different and independent means for simulating the dynamic and steady-state response of electrical loads on power lines. These two means are:

1. Model

   A variable topology network consisting of discretely variable resistors, inductors, and capacitors. The network topology and element values are selected to provide the same time-domain response as the original equipment.

2. Variable R

   A two-port electrical network whose input resistance at one port is controlled by a signal applied to the second port. For simulation, the control signal is made an analog of the current/voltage ratio on the power lines of the equipment to be simulated.

Both the model and the variable R are designed for operation at the same voltage and power levels as the equipment they are simulating.

A simplified block diagram of the DLS is shown in Figure 5-1. The model and variable R are discussed in the following sections.

5.2.1 Model

The DLS model is a 3-branch electrical network consisting of resistors, capacitors, and inductors arranged such that the branch topology and element values are discretely variable. A simplified block diagram of the model is shown in Figure 5-2. A front panel view of the model is provided in Figure 5-3.

The model is designed for simulation of equipment with the following input power characteristics:

Voltage - 100 to 130 VRMS, 60 or 400 Hz, 1 phase
20 to 60 VDC

Current - Up to 8 amperes continuous
Up to 50 amperes peak for up to 100 milliseconds duration

Power - Up to 250 watts continuous

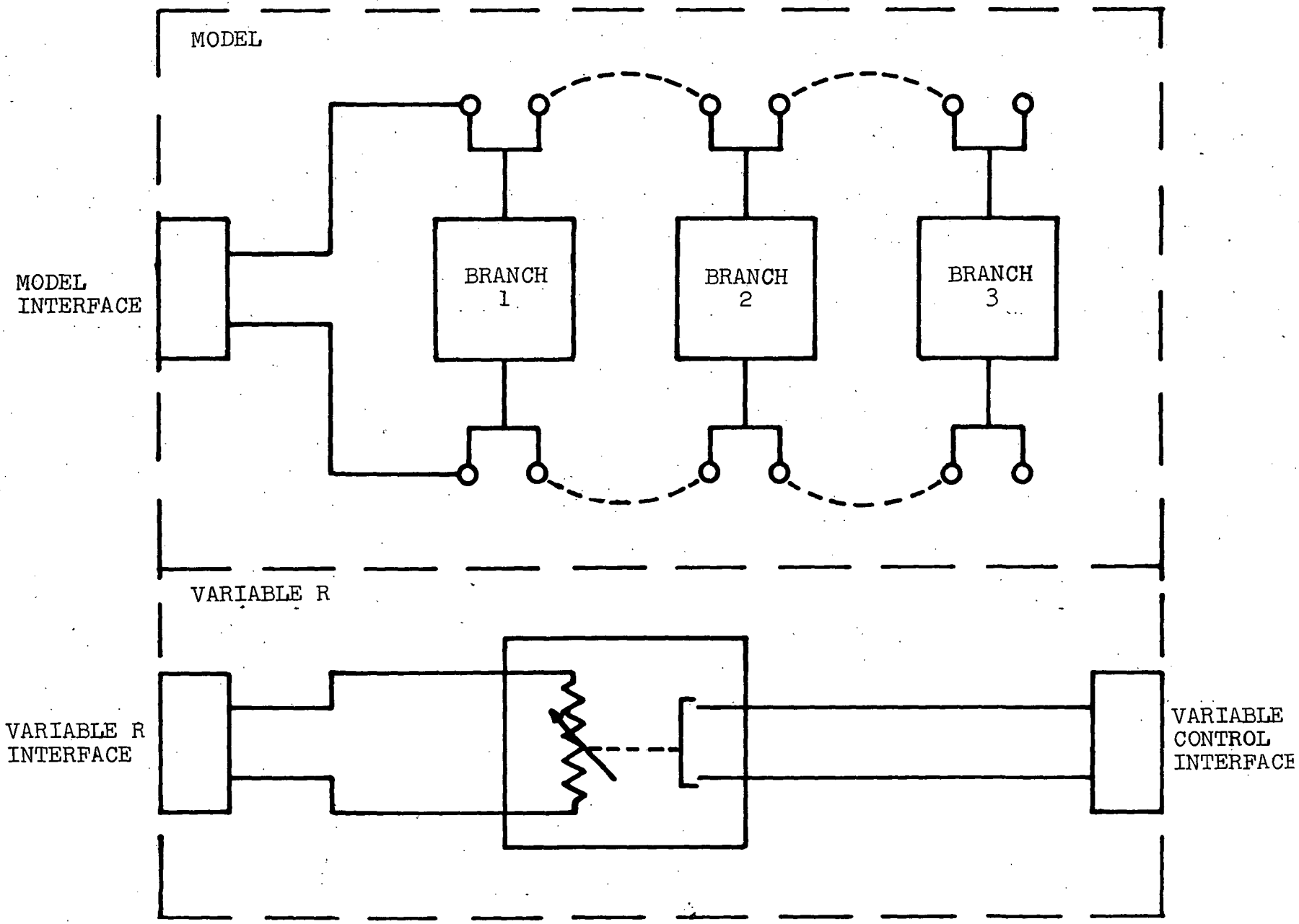

FIGURE 5-1 Dynamic Load Simulator--Simplified Block Diagram

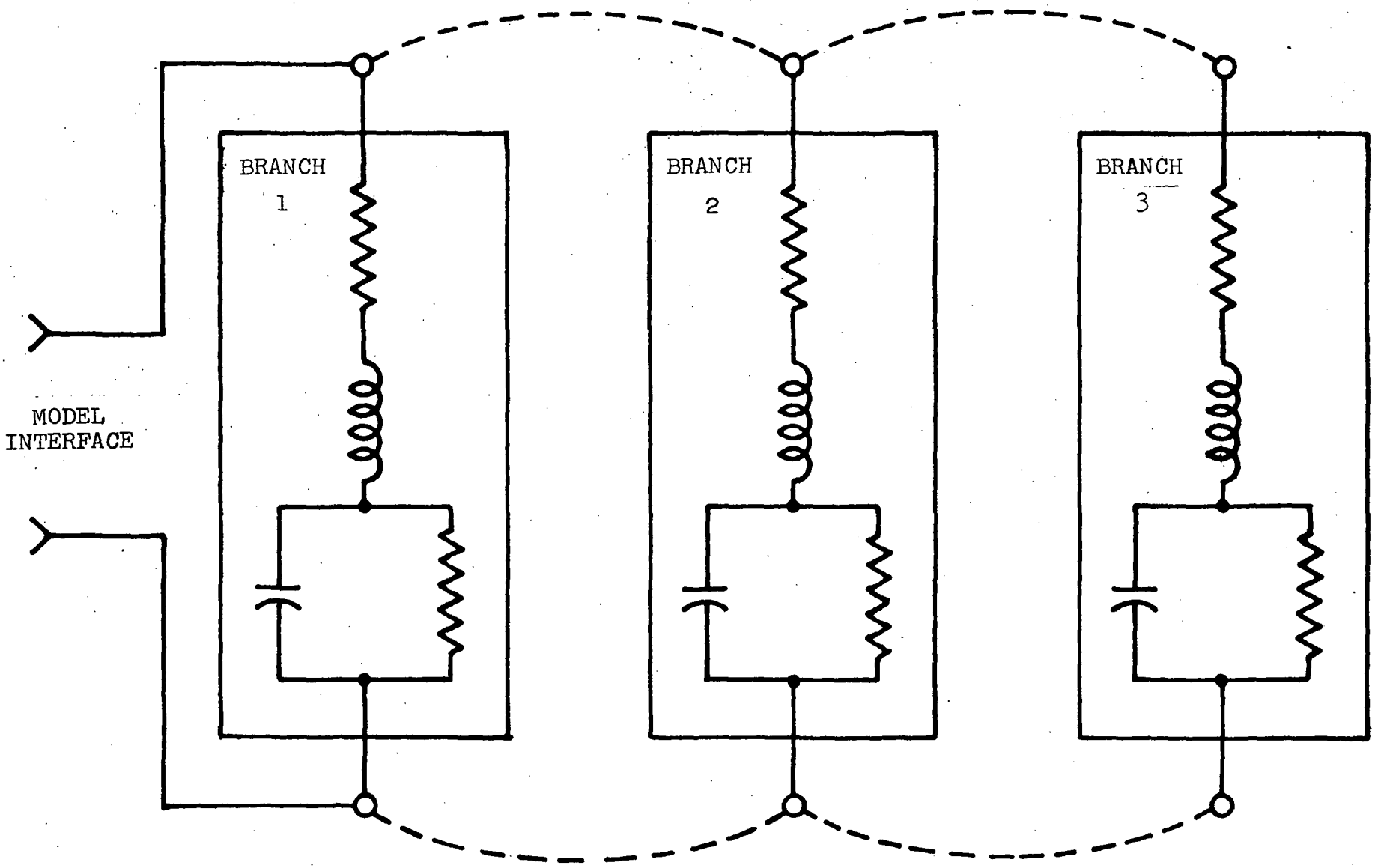

FIGURE 5-2 Model Block Diagram--Simplified

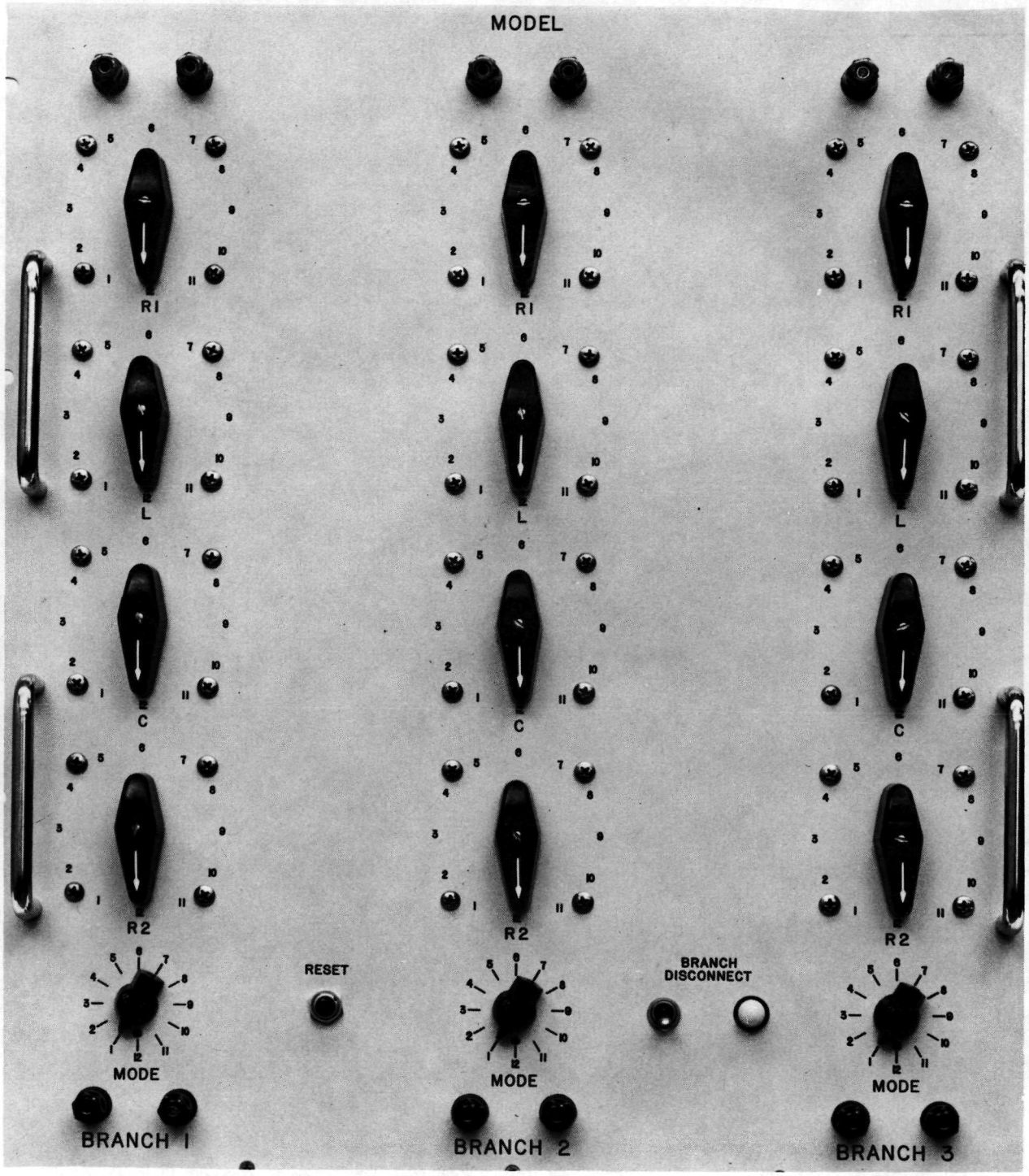

FIGURE 5-3 Front View of Model Panel

5.2.1.1 Branches

Each branch of the model consists of the combination of elements shown in Figure 5-4. By means of switching, each of the elements of the branch may be made open or zero, thus providing one means of altering branch topology. The elements are located remote from the model and are connected into the model by front panel switching.

The branch topology may also be varied by means of mode switches located on the front panel. Table 5-I identifies the available modes and provides a tabulation of their features. In general, there are 3 basic modes of operation, each of which results in a change to the branch topology shown in Figure 5-4. For example, mode 2 shorts out the resistor/capacitor parallel network and provides a series R, L circuit. Mode 3 opens R2 and results in a series R, L, C network. Mode 4 provides all 4 elements in the configuration shown in Figure 5-4.

Modes 5, 6, and 7 are identical to modes 2, 3, and 4, respectively, except the entire branch is open until a preset time when the K1 relay is operated. Modes 8, 9, and 10 are identical to modes 2, 3, and 4, respectively, except the entire branch is closed until a preset time when the K1 relay is released.

In Mode 1, the branch remains open throughout the operation.

Interconnection of the branches with the elements is accomplished by front panel switching. Figure 5-5 is an interconnecting diagram showing the interconnection of the branches with the element decades.

Interconnection of the branches with one another is accomplished by jumpers on the model front panel.

Each branch is equipped with a conventional meter shunt in series with the branch in the return leg. The shunt is a standard 100 millivolt/10 ampere unit. The sense leads for the shunt are brought out to appropriate connectors on the interface panel to provide convenient means for monitoring the branch current.

5.2.1.2 Elements

A total of twenty element decades are provided for connection into the model. These decades are identified in Table 5-II.

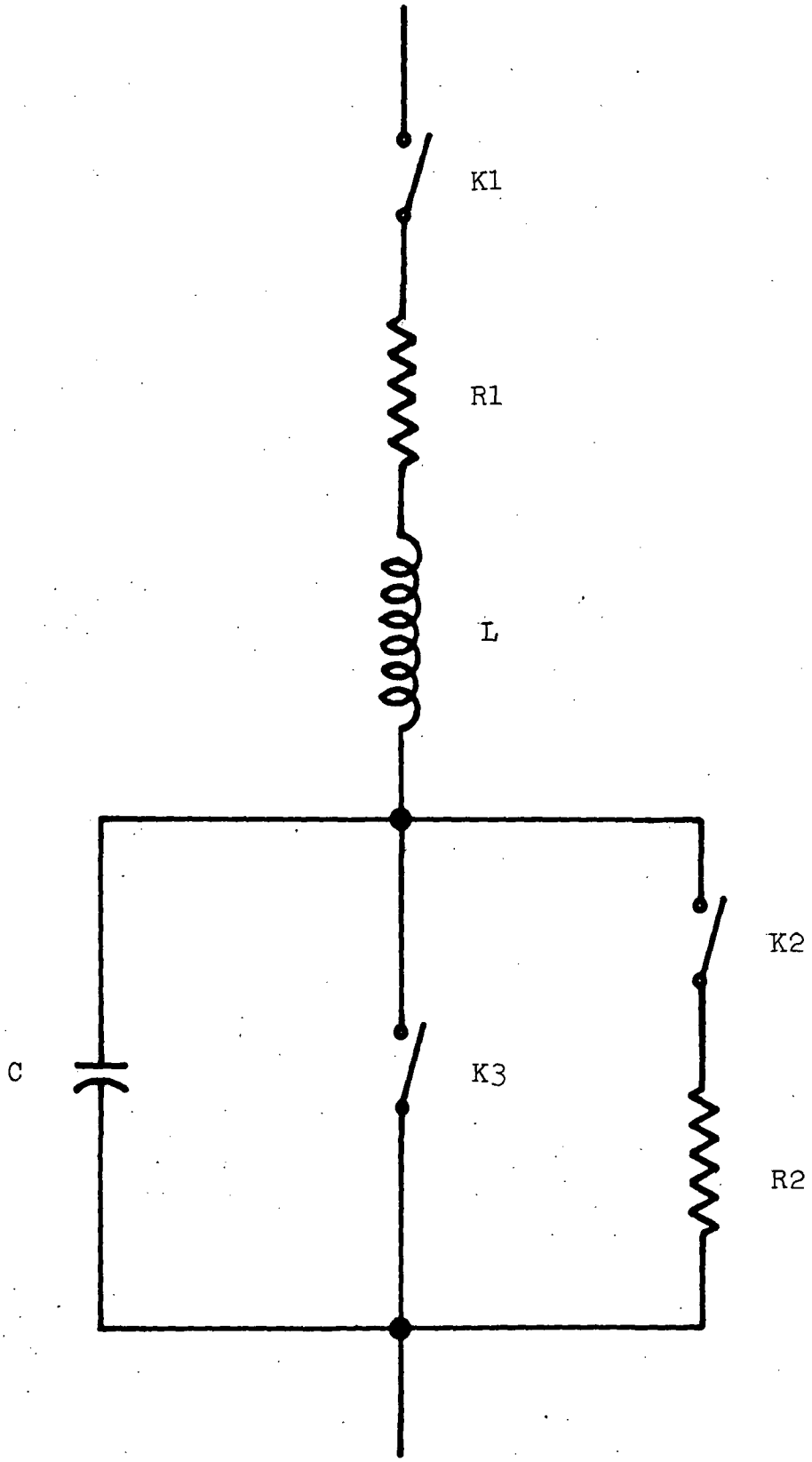

FIGURE 5-4 Model Branch Schematic Showing Mode Switching

TABLE 5-I

MODE SWITCH MATRIX

MODE SWITCH POSITION	K1	K2	K3	BRANCH CONFIGURATION
1	O	-	-	No Branch
2	C	-	C	A Fixed
3	C	O	O	B Fixed
4	C	C	O	C Fixed
5*	C	-	C	A K1 N/O
6*	C	O	O	B K1 N/O
7*	C	C	O	C K1 N/O
8**	C	-	C	A K1 N/C
9**	C	O	O	B K1 N/C
10**	C	C	O	C K1 N/C
11				Not Used
12				Not Used

---

* Same as corresponding fixed configuration except K1 closes at pre-selected time.

** Same as corresponding fixed configuration except K1 opens at pre-selected time.

Configurations:

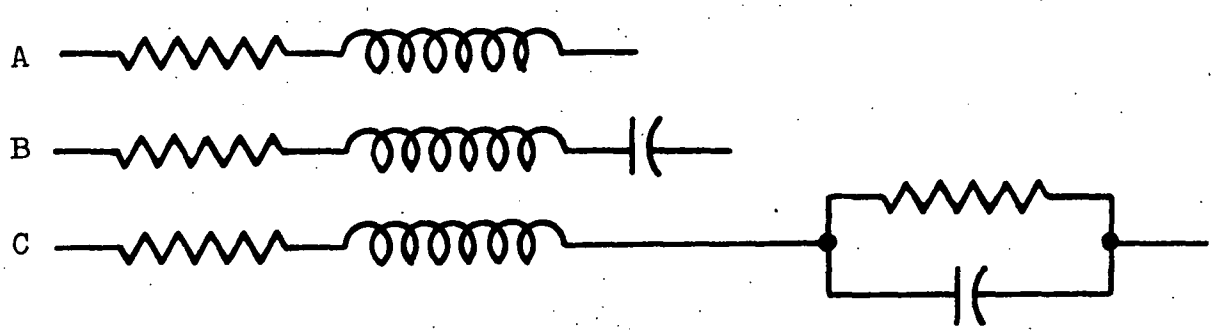

NOTES

(1) SHOWN IN MODE 3

(2) SHOWN SIMPLIFIED FOR CLARITY AND TRACEABILITY

(3) COMPONENTS PHYSICALLY LOCATED IN MODEL CONTROL SUBASSEMBLY

(4) SEE INTERCONNECTING WIRING REF WIRING TABLE

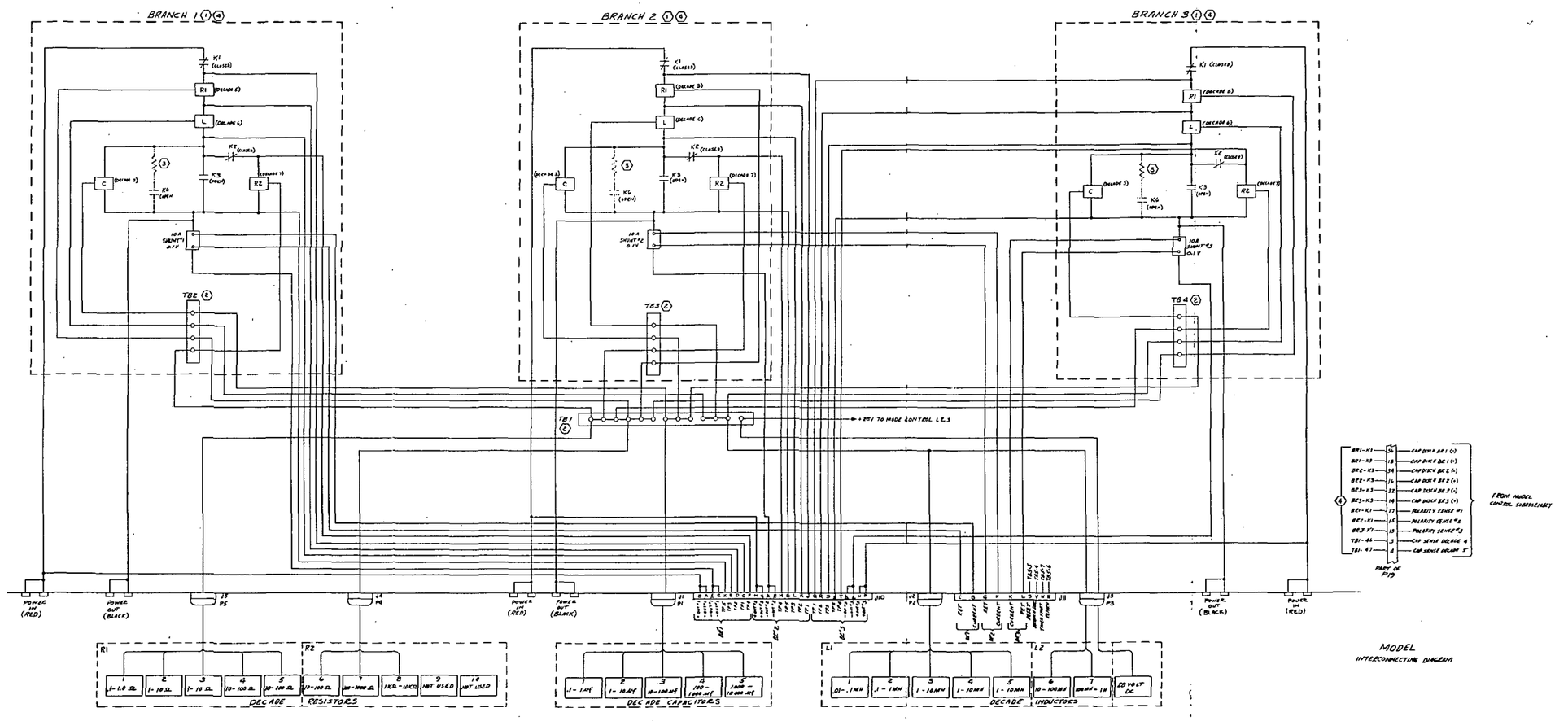

FIGURE 5-5 Model Interconnecting Diagram

TABLE 5-II

MODEL ELEMENT RANGES AND QUANTITIES

Element	Range	Quantity	Chassis
Resistance	0.1 to 1 ohm	1	R1
	1 to 10 ohms	2	R1
	10 to 100 ohms	3	R1/R2
	100 to 1K ohms	1	R2
	1K to 10K ohms	1	R2
Capacitance	0.1 to 1 microfarad	1	C
	1 to 10 microfarads	1	C
	10 to 100 microfarads	1	C
	100 to 1000 microfards*	1	C
	1000 to 10,000 microfarads*	1	C
Inductance	0.01 to 0.1 millihenry	1	L1
	0.1 to 1 millihenry	1	L1
	1 to 10 millihenries	3	L1
	10 to 100 millihenries	1	L2
	100 to 1000 millihenries	1	L2

* For DC application only.

Each decade provides 11 element values in a pseudo-logarithmic scale. Thus, the values available within each decade are 1, 1.2, 1.5, 2, 2.5, 3, 3.5, 4, 6.2, 8, and 10 multiplied by a power of 10.

The elements are located in 5 chassis.

Element stress ratings were selected consistent with the voltage, current, and power operating range of the simulator.

Resistors:--All resistors are provided in the 2 resistor chassis (R1 and R2). A front view of resistor chassis R1 is shown in Figure 5-6 and front view of resistor chassis R2 is shown in Figure 5-7.

A schematic of the two resistor chassis is provided in Figure 5-8.

Power dissipation was calculated on the basis of I^2R or V^2/R with a maximum current of 8 amperes and a maximum power of 250 watts. The power rating for each resistor value is shown in Table 5-III. The calculated ratings are for ambient conditions with no air circulation. The console is equipped with a blower thus providing margin additional to that shown in the derating column of the table.

Capacitors:--All capacitors are provided in the capacitor chassis, a front view of which is provided in Figure 5-9.

A schematic of capacitor decades 1, 2, and 3 is provided in Figure 5-10 and a schematic of decades 4 and 5 is provided in Figure 5-11.

All capacitors are derated at least 100% in voltage. In addition, the capacitors used for AC applications (Decades 1, 2, and 3) were selected on the basis of a maximum current of 3 amperes RMS and a maximum of 20 volt-amperes per square inch of surface area.

Protection against reverse voltage application to the electrolytic capacitors (decades 4 and 5) is provided by two diodes (D1 and D2) located in the model chassis. In addition, the polarity sense circuits will open all branches upon sensing reverse voltage application to these decades.

Inductors:--The inductors are provided in two chassis, L1 and L2. A front view of L1 is shown in Figure 5-12. Chassis L2 also houses

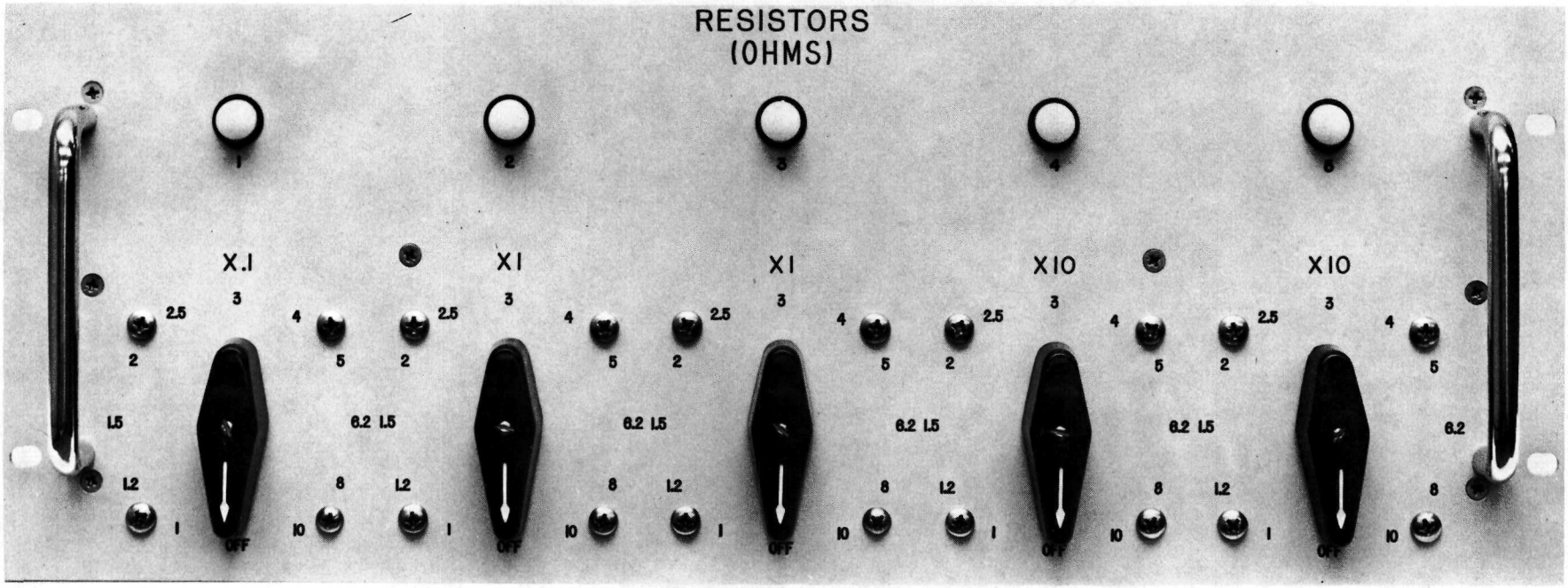

FIGURE 5-6 Front View of Resistor Chassis R1

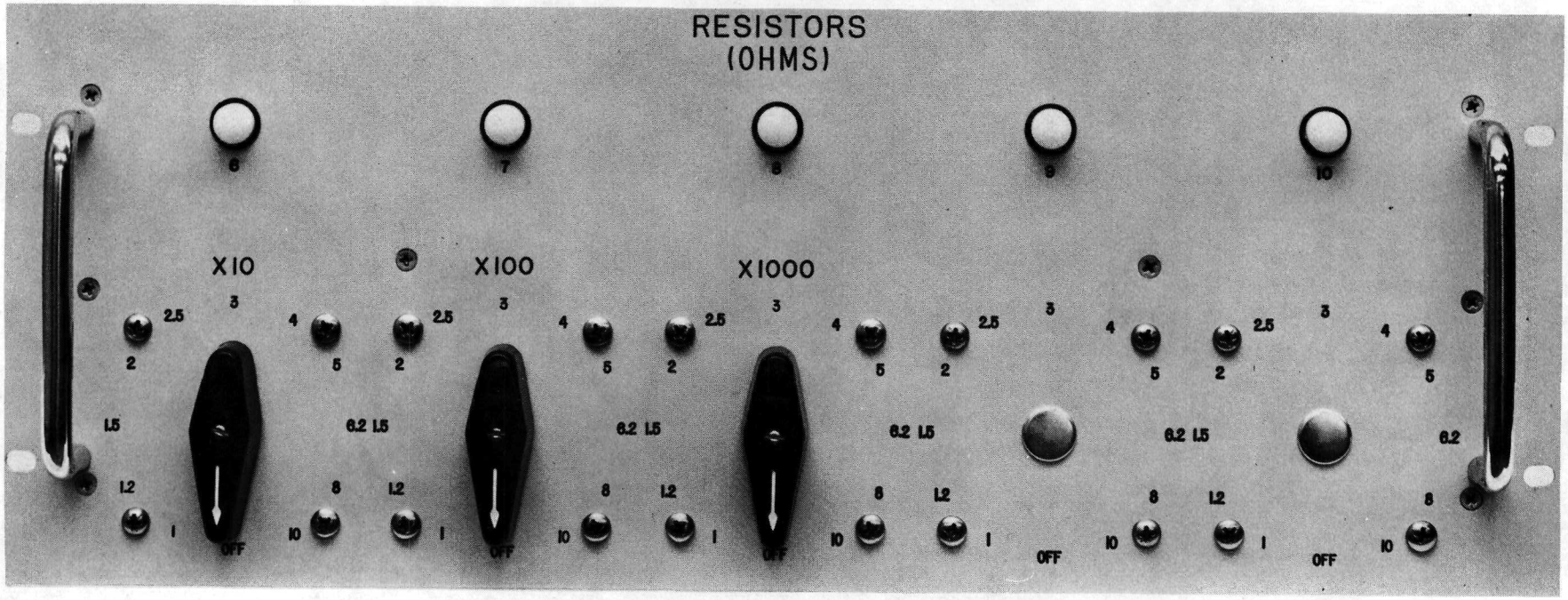

FIGURE 5-7 Front View of Resistor Chassis R2

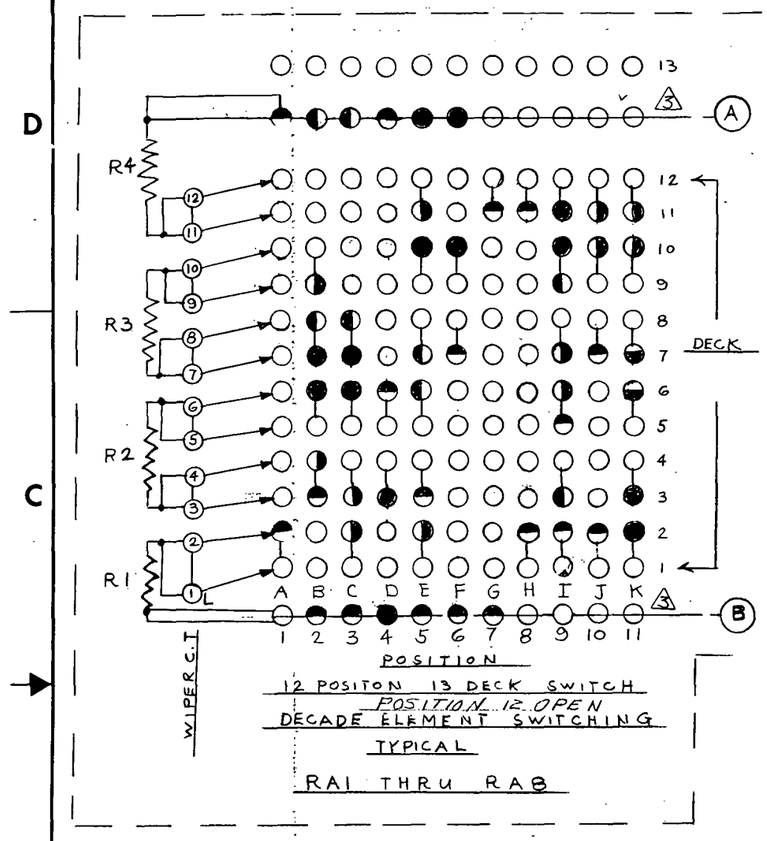

12 POSITON 13 DECK SWITCH
POSITION 12 OPEN
DECADE ELEMENT SWITCHING
TYPICAL
RA1 THRU RA8

NOTES
1 - ●◑●●◑ DENOTES JUMPER IN PARTICULAR COLUMN

2 - DECADES RA-1 THRU RA-5 ON RESISTOR PANEL NO. 1.
DECADES RA-6 THRU RA-8 ON RESISTOR PANEL NO. 2.

3 DENOTES JUMPER ON SWITCH

RESISTOR VALUES

DECADE	SWITCH POSITIONS										
	1	2	3	4	5	6	7	8	9	10	11
RA1	.1	.12	.15	.2	.25	.3	.4	.5	.62	.8	1.0
RA2	1.0	1.2	1.5	2	2.5	3	4	5	6.2	8	10.0
RA3	1	1.2	1.5	2	2.5	3	4	5	6.2	8	10
RA4	10	12	15	20	25	30	40	50	60	80	100
RA5	10	12	15	20	25	30	40	50	62	80	100
RA6	10	12	15	20	25	30	40	50	62	80	100
RA7	100	120	150	200	250	300	400	500	620	800	1000
RA8	1000	1200	1500	2000	2500	3000	4000	5000	6200	8000	10000

ALL RESISTOR VALUES IN OHMS

DECADE ELEMENTS

DECADE	CONNECTOR	gauge WIRE
RA1 - A	P4 - A, B	2 - 16
RA1 - B	P4 - C, D	
RA2 - A	P4 - E, F	
RA2 - B	P4 - G, H	
RA3 - A	P4 - J, K	
RA3 - B	P4 - L, M	
RA4 - A	P4 - N, P	
RA4 - B	P4 - Q, R	
RA5 - A	P4 - S, T	
RA5 - B	P4 - U, V	
RA6 - A	P5 - A, B	
RA6 - B	P5 - C, D	
RA7 - A	P5 - E, F	
RA7 - B	P5 - G, H	
RA8 - A	P5 - J, K	
RA8 - B	P5 - L, M	2 - 16
RA1 - L14-1	P4 - W	1 - 22
RA2 - L15-1	P4 - X	
RA3 - L16-1	P4 - Y	
RA4 - L17-1	P4 - Z	
RA5 - L18-1	P4 - 3	
RA6 - L19-1	P5 - W	
RA7 - L20-1	P5 - X	
RA8 - L21-1	P5 - Y	
L13 - 2	L16 - 2	
L14 - 2	L15 - 2	
L14 - 2	P4 - 4	
L19 - 2	L20 - 2	
L21 - 2	P5 - 6	
L16 - 2	L17 - 2	
L17 - 2	L18 - 2	
L20 - 2	L21 - 2	1 - 22

ENGR CHG	ZONE	LTR	REVISIONS DESCRIPTION	DATE	APPROVED
B			Revised	5-1-72	

LIST OF PARTS

QTY REQD	CODE IDENT	PART OR IDENTIFYING NO.	NOMENCLATURE OR DESCRIPTION	MATERIAL OR NOTE	SPECIFICATION	ZONE	ITEM NO.
	ASSY NO.			R1 / R2 / R3 / R4			
8		101-5030-0937-201	LIGHTS, DIALCO	L14 THRU L21			
8		JM25313A	SWITCH	S14 THRU S21	ELECTRO SWITCH		
2		MS3106A-36-15P	CONNECTOR	P4, P5			
1	RA1	RH50 DALE	RA1 DECADE	.05Ω / 1Ω / 3Ω / (5) 12Ω			
1	RA2	210 OHMITE	RA2 DECADE	210-100 1Ω / 210-225 2Ω / 210-225 1 ± 2Ω (5) / (2) 2Ω (5)			
1	RA3	210 OHMITE	RA3 DECADE	210-100 1Ω / 210-225 2Ω / 210-225 1 ± 2Ω (5) / (2) 2Ω (5)			
1	RA4	210 OHMITE	RA4 DECADE	210-225 20Ω (5) / 210-225 20 10Ω (5) / 210-75 60 5Ω (5) / 210-225 200 25Ω (5)			
1	RA5	210 OHMITE	RA5 DECADE	210-225 20Ω (5) / 210-225 20 10Ω (5) / 210-75 60 5Ω (5) / 210-225 200 25Ω (5)			
1	RA6	210 OHMITE	RA6 DECADE	210-225 20Ω (5) / 210-225 20 10Ω (5) / 210-75 60 5Ω (5) / 210-225 200 25Ω (5)			
1	RA7	210 OHMITE	RA7 DECADE	210-225 100Ω / 210-100 20 100Ω (5) / 210-75 300Ω / 210-50 200 20Ω (5)			
1	RA8	RH50 DALE	RA8 DECADE	1000Ω	2000Ω / 3000Ω / 4000Ω		

UNLESS OTHERWISE SPECIFIED
TOLERANCE AND DRAWING INTERPRETATION PER D143
X ± .08 XX ± .04 XXX ± .020
MACHINED ANGLES ± 0° 30'
SHEET METAL BEND ANGLES ± 2°
P10001
SURFACE ROUGHNESS ✓

CONTR NO. / RELEASE / DWG APPD / CHECKED / DRAWN / DESIGN APPROVAL / MANAGER / SECT CH / DESIGNER

AVCO CORPORATION
AVCO SYSTEMS DIVISION WILMINGTON, MASSACHUSETTS 01887

TITLE: RESISTANCE DECADE ELEMENT SCHEMATIC

SIZE	CODE IDENT NO.	DWG NO.
C	04614	DL 9 REV. B

SCALE | WT | SHEET

PART CLASS:	DWG CLASS:	ASG BY:	DASH NO.	NEXT ASSY	USED ON	QTY PER NHA	END ITEM NUMBER	SERIAL NO.
				APPLICATION			EFFECTIVITY	
					DYNAMIC LOAD SIMULATOR			

DO NOT SCALE DRAWING

FIGURE 5-8 Resistance Decade Element Schematic (DL 9, Rev. B)

TABLE 5-III

RESISTOR POWER RATINGS

Resistance	Calculated Dissipation	Resistor Rating	Derating
ohms	watts	watts	percent
0.1	6.4	50	100
0.2	12.8	50	100
0.3	19.2	50	100
0.4	25.6	100	100
1	64	100	36
2	128	225	42
3	192	325	41
4	250	450	44
10	250	450	44
20	250	450	44
30	250	450	44
40	250	360	31
100	144	225	36
200	80	200	100
300	48	75	36
400	40	100	100
1000	17	50	100
2000	8.5	50	100
3000	6	50	100
4000	4	50	100

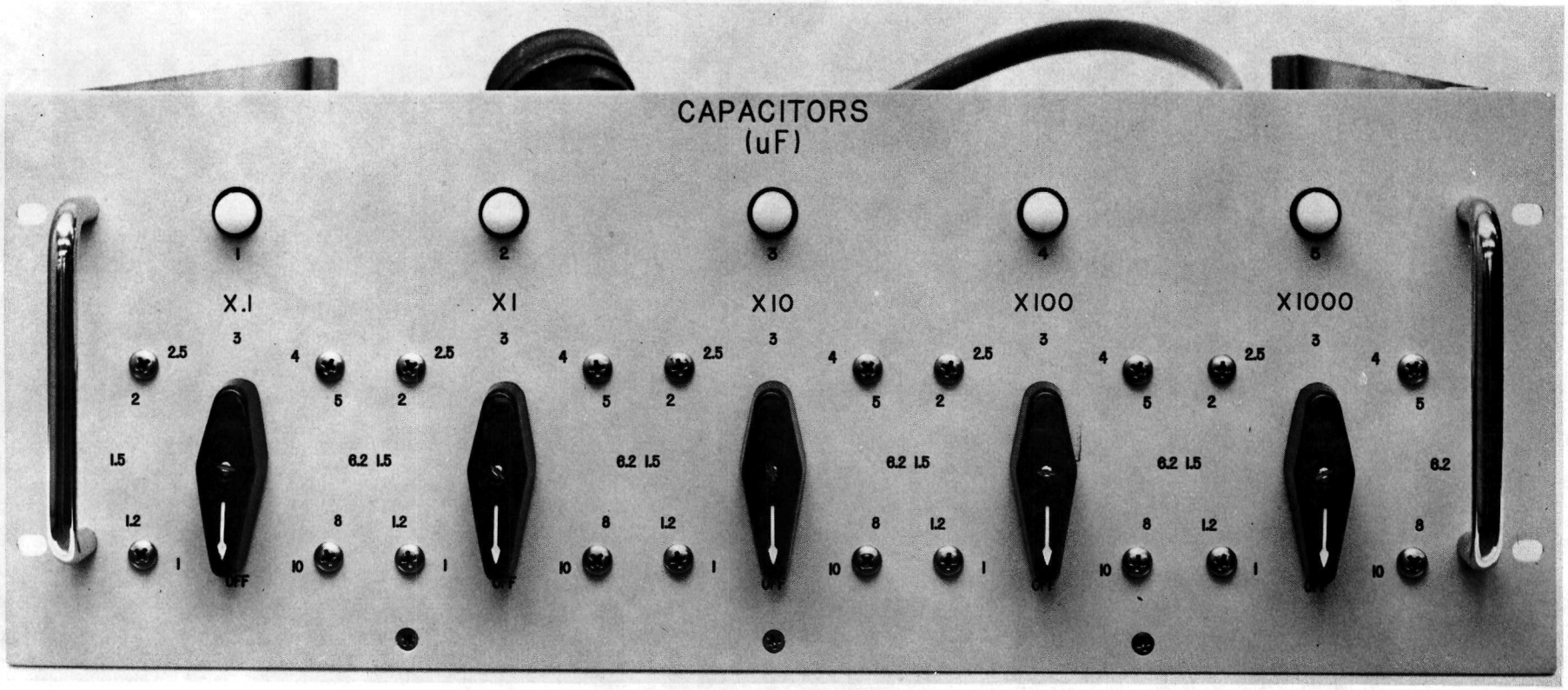

FIGURE 5-9 Front View of Capacitor Chassis

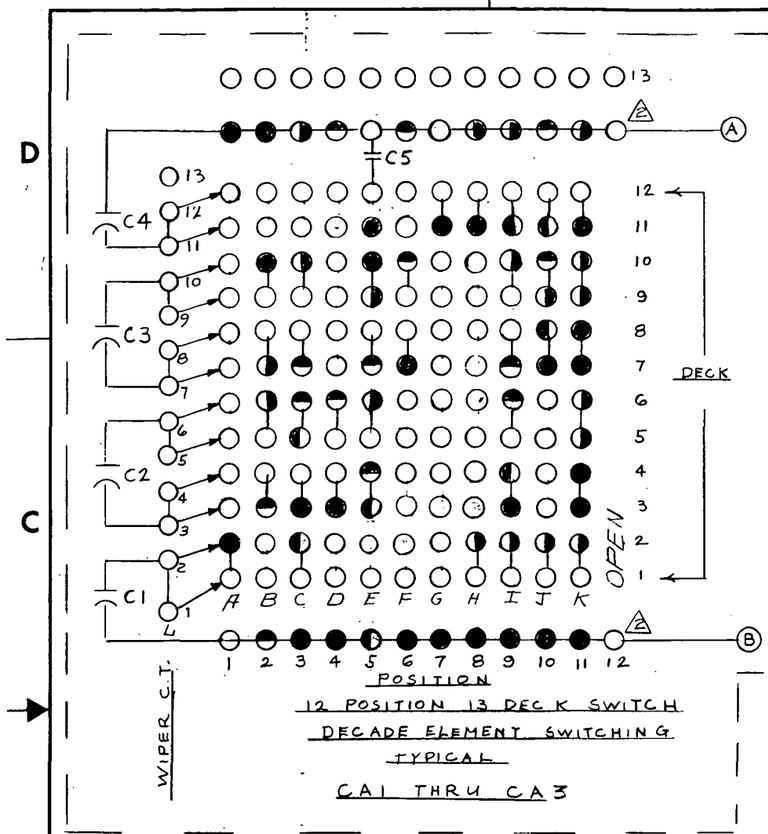

12 POSITION 13 DECK SWITCH
DECADE ELEMENT SWITCHING
TYPICAL
CA1 THRU CA3

NOTES
1- ●●●● DENOTES JUMPER IN PARTICULAR COLUMN

2 DENOTES JUMPERS ON SWITCH

NOMINAL VALUES

DECADE	SWITCH POSITIONS											
	1	2	3	4	5	6	7	8	9	10	11	12
CA2	1	1.2	1.5	2	2.5	3	4	5	6.2	8	10	
CA3	10	12	15	20	25	30	40	50	62	80	100	
CA4	100	120	150	200	250	300	400	500	620	800	1000	
CA5	1000	1200	1500	2000	2500	3000	4000	5000	6200	8000	10000	
CA1	.1	.12	.15	.2	.25	.3	.4	.5	.62	.8	1.0	

ALL CAPACITOR VALUES IN UF

DECADE ELEMENTS

DECADE	CONNECTOR	WIRE GAUGE
CA1 - A	P1 - A,B	2-16
CA1 - B	P1 - C,D	
CA2 - A	P1 - E,F	
CA2 - B	P1 - G,H	
CA3 - A	P1 - J,K	
CA3 - B	P1 - L,M	
CA4 - A	P1 - N,P	
CA4 - B	P1 - Q,R	2-16
CA5 - A	P1 - S,T	1-22
CA5 - B	P1 - U,V	
L1-1	P1-W	
L2-1	P1-X	
L3-1	P1-Y	
L4-1	P1-Z	
L5-1	P1-a	
L1-2	P1-b	
L2-2	L3-2	
L3-2	L4-2	1-22
L4-2	L5-2	

QTY REQD	CODE IDENT	PART OR IDENTIFYING NO.	NOMENCLATURE OR DESCRIPTION	MATERIAL OR NOTE	SPECIFICATION	ZONE	ITEM NO.
5		101-5030-0937-201	LIGHTS	L1 THRU L5	DIALCO		
5		JM25313A	SWITCH	S1 THRU S5	ELECTRO SWITCH		
1		MS3106A-36-15P	CONNECTOR	P1			
				C1	C2	C3	C4	C5	C6		
1	CA2	CORNELL DUBILIER	CAPACITOR DECADE	KRX66P105Q	KRX44P205Q	KRX44P305Q	KRX44P405Q	78TP1uf Sprague			
1	CA3	CORNELL DUBILIER	CAPACITOR DECADE	KRX44P505Q (2) REQ	4 Req KRX44P205Q	KRX66P105(1) KRX44P305Q(3)	KRX44P505(8) KRX44P405Q	KRX44P505Q			
1	CA4	36D SPRAGUE	CAPACITOR	950F350AA	2 Reqd 950F350AA	950F350AA 191F350AB 6 Reqd	191F350AB 2 REQD	KRX44P505(9) KRX66P105(9)	500F450AB		
1	CA5	36D SPRAGUE	CAPACITOR	901F150AC	2/2F150BC	142F150BB	762F150CC	191F350AB	191F350AB(2) 950F350AB(1)		
1	CA1	SPRAGUE	160P/16P	.047uf(2)	.1uf (2)	.25uf (1) .047uf (1)	.25uf (1) .047uf (3)	.1uf (1)			

ASSY NO.

LIST OF PARTS

ENGR CHG	REVISIONS				
	ZONE	LTR	DESCRIPTION	DATE	APPROVED
H				5-10-66	

REV. TT
DRAWING NUMBER B

PART CLASS:	DASH NO.	APPLICATION: NEXT ASSY	APPLICATION: USED ON	EFFECTIVITY: QTY PER NHA	EFFECTIVITY: END ITEM NUMBER	SERIAL NO.
DWG CLASS:			DYNAMIC LOAD SIMULATOR			
ASG BY:						

UNLESS OTHERWISE SPECIFIED
TOLERANCE AND DRAWING INTERPRETATION PER D143
X ± .08 XX ± .04 XXX ± .020
MACHINED ANGLES ± 0° 30'
SHEET METAL BEND ANGLES ± 2°
P10001 _____
SURFACE ROUGHNESS ✓

CONTR NO.	
RELEASE	
DWG APPD	
CHECKED	
DRAWN	S. Mintz 6/20/66
DESIGN APPROVAL	
MANAGER	
SECT CH	
DESIGNER	S. Mintz 6/20/66

AVCO CORPORATION
AVCO SYSTEMS DIVISION WILMINGTON, MASSACHUSETTS 01887

TITLE
CAPACITOR DECADE ELEMENT SCHEMATIC

SIZE	CODE IDENT NO.	DWG NO.
C	04614	DL10 REV. B

SCALE | WT | SHEET 1 of 2

DO NOT SCALE DRAWING

FIGURE 5-10 Capacitor Decade Element Schematic (DL 10, Rev. B, Sheet 1 of 2), Decades 1, 2, and 3

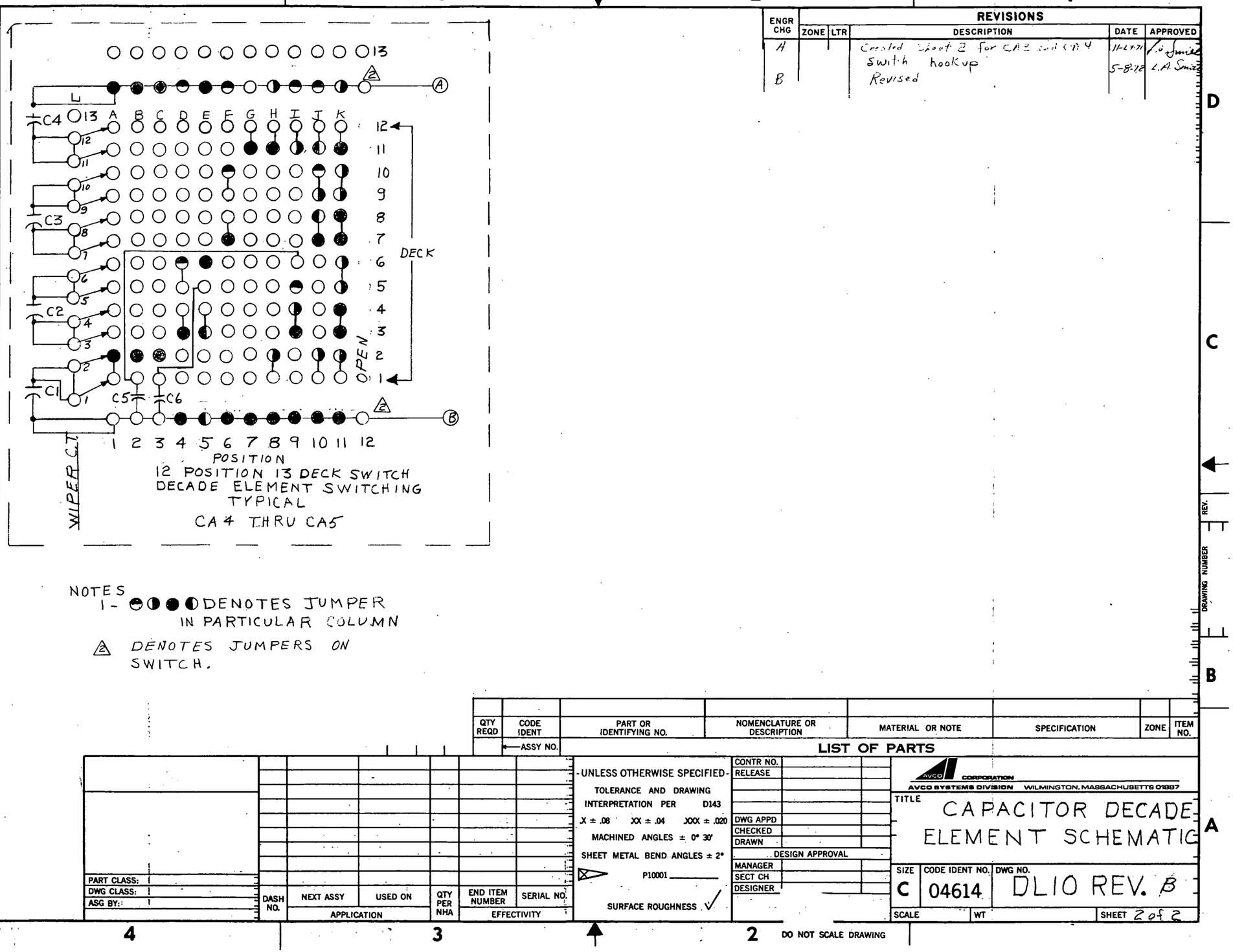

FIGURE 5-11 Capacitor Decade Element Schematic (DL 10, Rev. B, Sheet 2 of 2), Decades 4 and 5

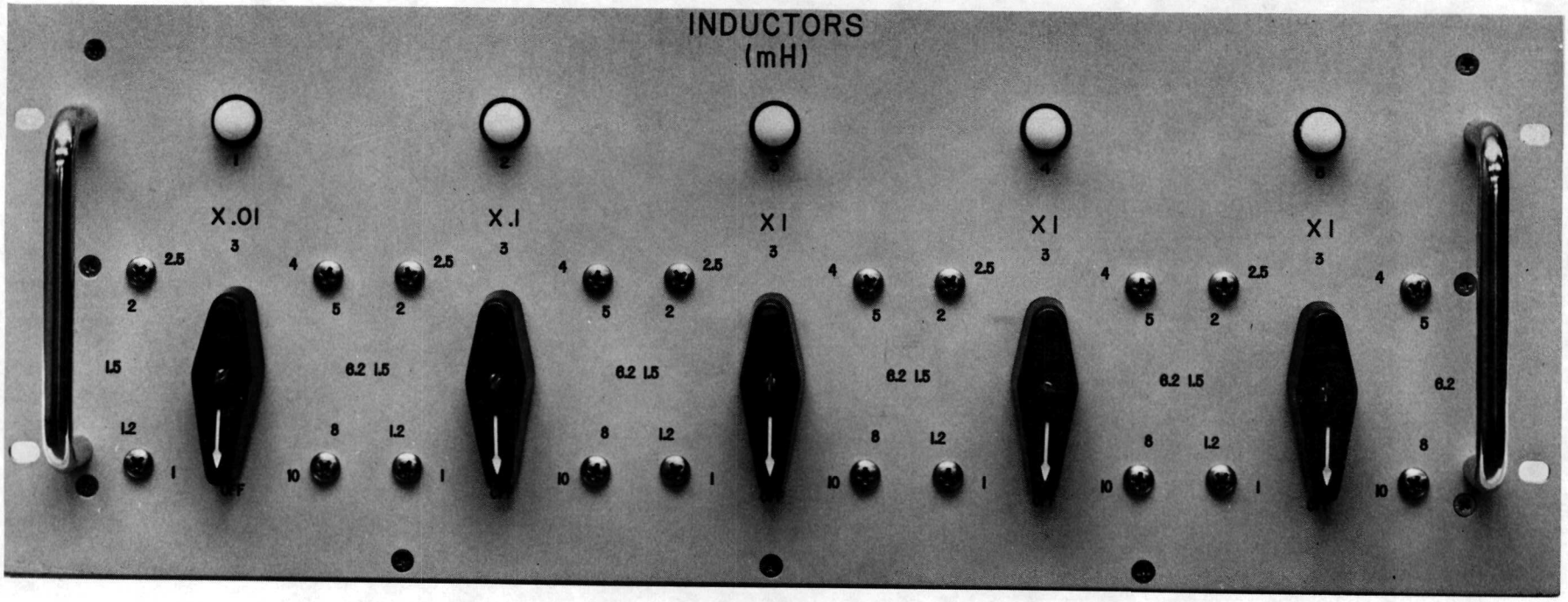

FIGURE 5-12 Front View of Inductor Chassis L1

the 28-volt DC power supply and the console circuit breaker. A front view of this chassis is shown in Figure 5-13. A schematic of the inductor chassis is provided in Figure 5-14.

All inductors are rated at 8 amperes RMS and 130 volts RMS except for the 0.1 to 1 henry inductor which is rated at 4 amperes RMS. In order not to degrade the frequency response of the inductors, no additional safety factor was included in the inductor ratings.

As a means of monitoring the use of the element inventory, each element decade provides a lamp indication when that decade has been connected into a branch. In addition, if an element is connected into more than one branch location, the lamp will light with increased intensity. The lamps are operated by the console 28-volt power supply through dropping resistors. The dropping resistors are mounted on a single board installed on one of the two side supports of the model chassis. A schematic diagram showing the decade lamp wiring for the resistor decades is shown in Figure 5-15. The lamp wiring for the capacitor and inductor chassis is similar.

5.2.1.3 Interface

Except for interconnection of the branches which is accomplished at the model front panel, all access to the model is through the interface panel located at the rear of the console. Figure 5-16 is a front view of the interface panel.

A schematic diagram of the interface panel is provided in Figure 5-17.

5.2.1.4 Controls

The model provided in the model DLS 1000 Dynamic Load Simulator is manually operated. Control of the model is accomplished by appropriate operation of the switches and interconnection with the connectors and binding posts. All switches and connectors are conservatively rated for their application in the model. All manual branch switches and element switches are rated at 10 amperes per contact and two decks are used in parallel in each application. The connectors are either standard MS rated at 20 amperes per pin or 5-way binding posts rated at 30 amperes.

5.2.1.4.1 Timer

In addition to the manual controls, the model also makes use of a preset interval timer for altering the model branch topology dynamically. The timer is a Model 5301 Preset Interval Timer manufactured by Electronic

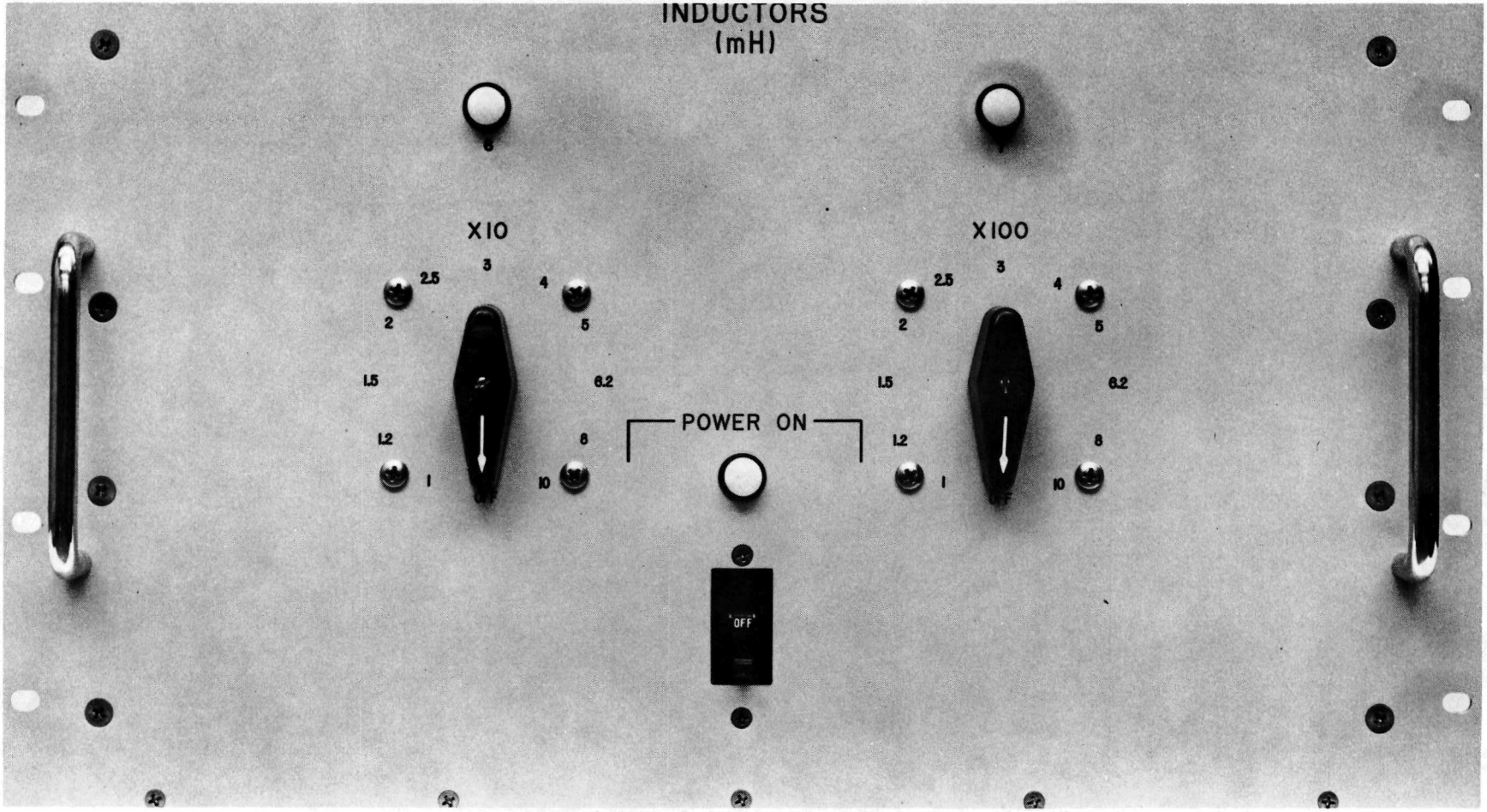

FIGURE 5-13 Front View of Inductor Chassis L2

ENGR CHG	REVISIONS ZONE	LTR	DESCRIPTION	DATE	APPROVED
B			Revised	5-8-72	

NOMINAL VALUES

DECADE	SWITCH POSITION 1	2	3	4	5	6	7	8	9	10	11	12
LA1	.01	.012	.015	.02	.025	.03	.04	.05	.062	.08	.1	
LA2	.1	.12	.15	.2	.25	.3	.4	.5	.62	.8	1.0	
LA3	1	1.2	1.5	2	25	3	4	5	6.2	8	10	
LA4	1	1.2	1.5	2	2.5	3	4	5	6.2	8	10	
LA5	1	1.2	1.5	2	2.5	3	4	5	6.2	8	10	
LA6	10	12	15	20	25	30	40	50	62	80	100	
LA7	100	120	150	200	250	300	400	500	620	800	1000	

ALL INDUCTOR VALUES IN MH

DECADE ELEMENTS

DECADE	CONNECTOR	WIRE GAUGE
LA1-A	P2-A,B	2-16
LA1-B	P2-C,D	
LA2-A	P2-E,F	
LA2-B	P2-G,H	
LA3-A	P2-J,K	
LA3-B	P2-L,M	
LA4-A	P2-N,P	
LA4-B	P2-Q,R	
LA5-A	P2-S,T	
LA5-B	P2-U,V	
LA6-A	P3-A,B	
LA6-B	P3-C,D	
LA7-A	P3-E,F	
LA7-B	P3-G,H	2-16
L6-1	P2-W	1-22
L7-1	P2-X	
L8-1	P2-Y	
L9-1	P2-Z	
L10-1	P2-a	
L11-1	P3-W	
L12-1	P3-X	
L6-2	P2-b	
L6-2	L7-2	
L7-2	L8-2	
L8-2	L9-2	
L9-2	L10-2	
L11-2	P3-b	
L11-2	L12-2	1-22

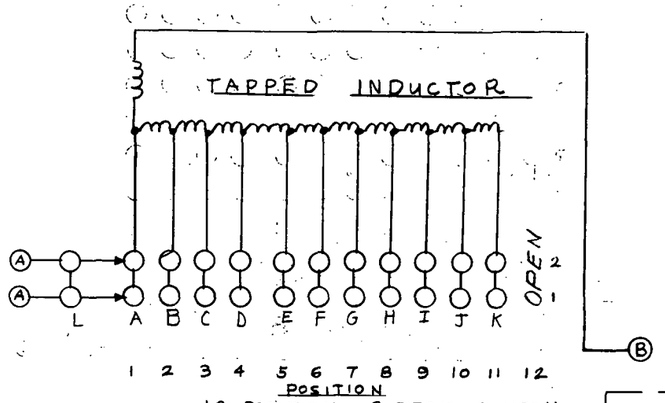

12 POSITION 3 DECK SWITCH
DECADE ELEMENT SWITCHING
TYPICAL
LA1 THRU LA7
S6 THRU S13

QTY REQD	CODE IDENT	PART OR IDENTIFYING NO.	NOMENCLATURE OR DESCRIPTION	MATERIAL OR NOTE	SPECIFICATION	ZONE	ITEM NO.
2		3600 uf-36D-150V	Capacitors		Sprague		
1		MS3102R18-11P		Connector			
1		BX28N10	POWER SUPPLY		AC/DC		
7		101-5030-0937-201	LIGHT, DIALCO		DIALCO		
7		JM25303A	S6 THRU S13	12 POS. 3 DECK	ELECTRO SWITCH		
2		CONNECTOR	P2, P3	MS-3106A-36-15P			
1		Terminal STRIP	12-540				
1		INDUCTOR DECADE	LA1 AE-2867-T	.01mh TO .1 mh	ATLAS ENG.		
1		INDUCTOR DECADE	LA2 AE10330	.1mh TO 1 mh	ATLAS ENG.		
1		INDUCTOR DECADE	LA3 AE10329	1mh TO 10mh	ATLAS ENG.		
1		INDUCTOR DECADE	LA4 AE10329	1mh TO 10mh	ATLAS ENG.		
1		INDUCTOR DECADE	LA5 AE10329	1mh TO 10mh	ATLAS ENG.		
1		INDUCTOR DECADE	LA6 AE10236	10mh TO 100mh	ATLAS ENG.		
1		INDUCTOR DECADE	LA7 AE10328	100mh TO 1000mh	ATLAS ENG.		
1		122-215-101	CIRCUIT BREAKER		WOOD ELECTRIC		

LIST OF PARTS

PART CLASS:	DASH NO.	NEXT ASSY	USED ON	QTY PER NHA	END ITEM NUMBER	SERIAL NO.
DWG CLASS:		APPLICATION			EFFECTIVITY	
ASG BY:			DYNAMIC LOAD SIMULATOR			

UNLESS OTHERWISE SPECIFIED
TOLERANCE AND DRAWING INTERPRETATION PER D143
.X ± .08 .XX ± .04 .XXX ± .020
MACHINED ANGLES ± 0° 30'
SHEET METAL BEND ANGLES ± 2°
P10001
SURFACE ROUGHNESS ✓

CONTR NO.
RELEASE
DWG APPD
CHECKED
DRAWN
DESIGN APPROVAL
MANAGER
SECT CH
DESIGNER

AVCO CORPORATION
AVCO SYSTEMS DIVISION WILMINGTON, MASSACHUSETTS 01887

TITLE: INDUCTOR DECADE ELEMENT SCHEMATIC

SIZE	CODE IDENT NO.	DWG NO.	REV.
C	04614	DL 11	REV.B

SCALE | WT | SHEET

DO NOT SCALE DRAWING

FIGURE 5-14. Inductor Decade Element Schematic
(DL 11, Rev. B)

NOTES

1. [SCHEMATIC IS TYPICAL OF INDUCTOR AND CAPACITOR SCHEMATICS SEE MODEL WIRING TABLE FOR WIRING OF EACH]
2. INDUCTORS USE SWITCHES S25, S26, S27
3. CAPACITORS USE SWITCHES S22, S23, S24

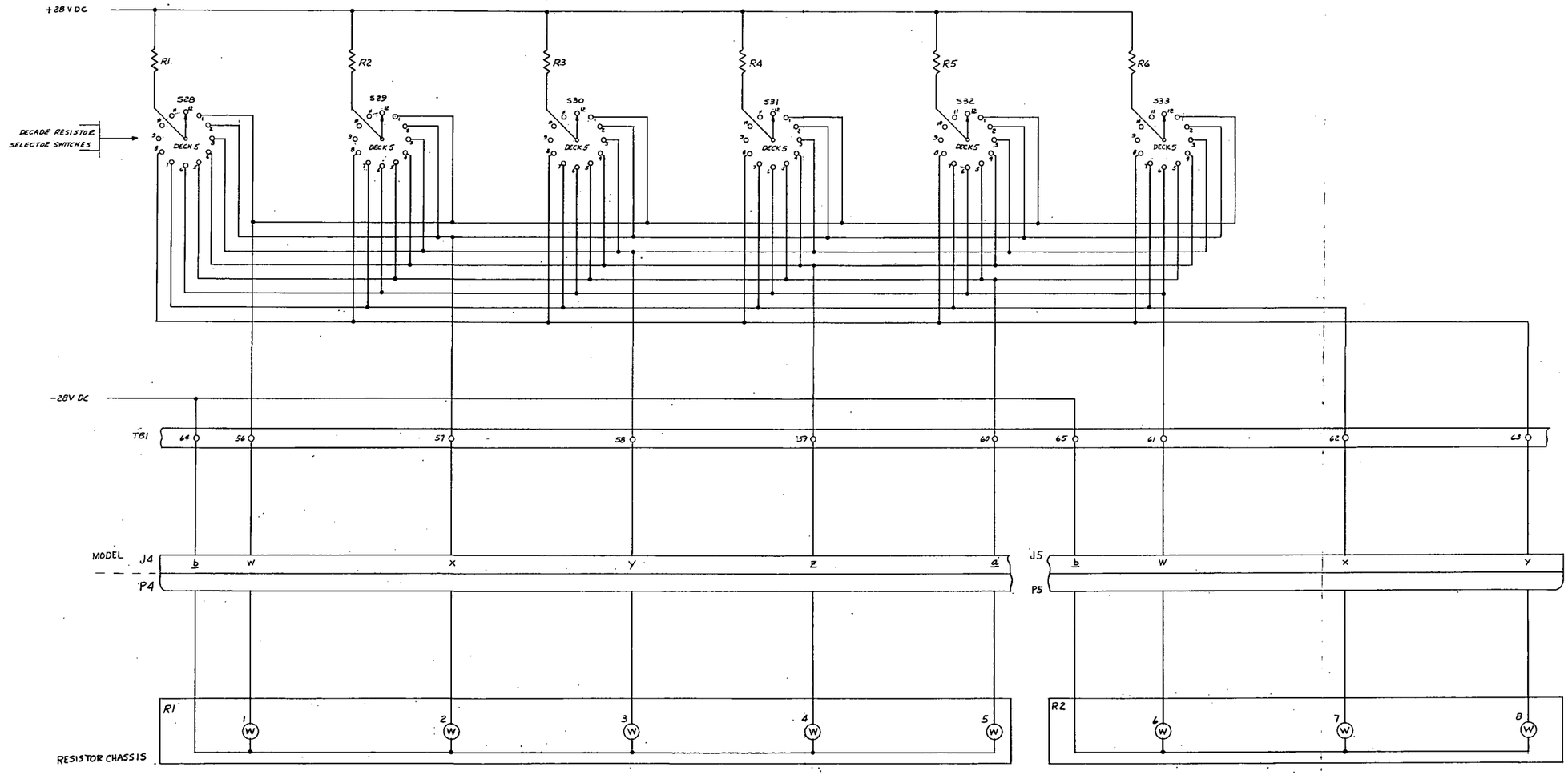

FIGURE 5-15 Resistor Decade Monitor Light Schematic

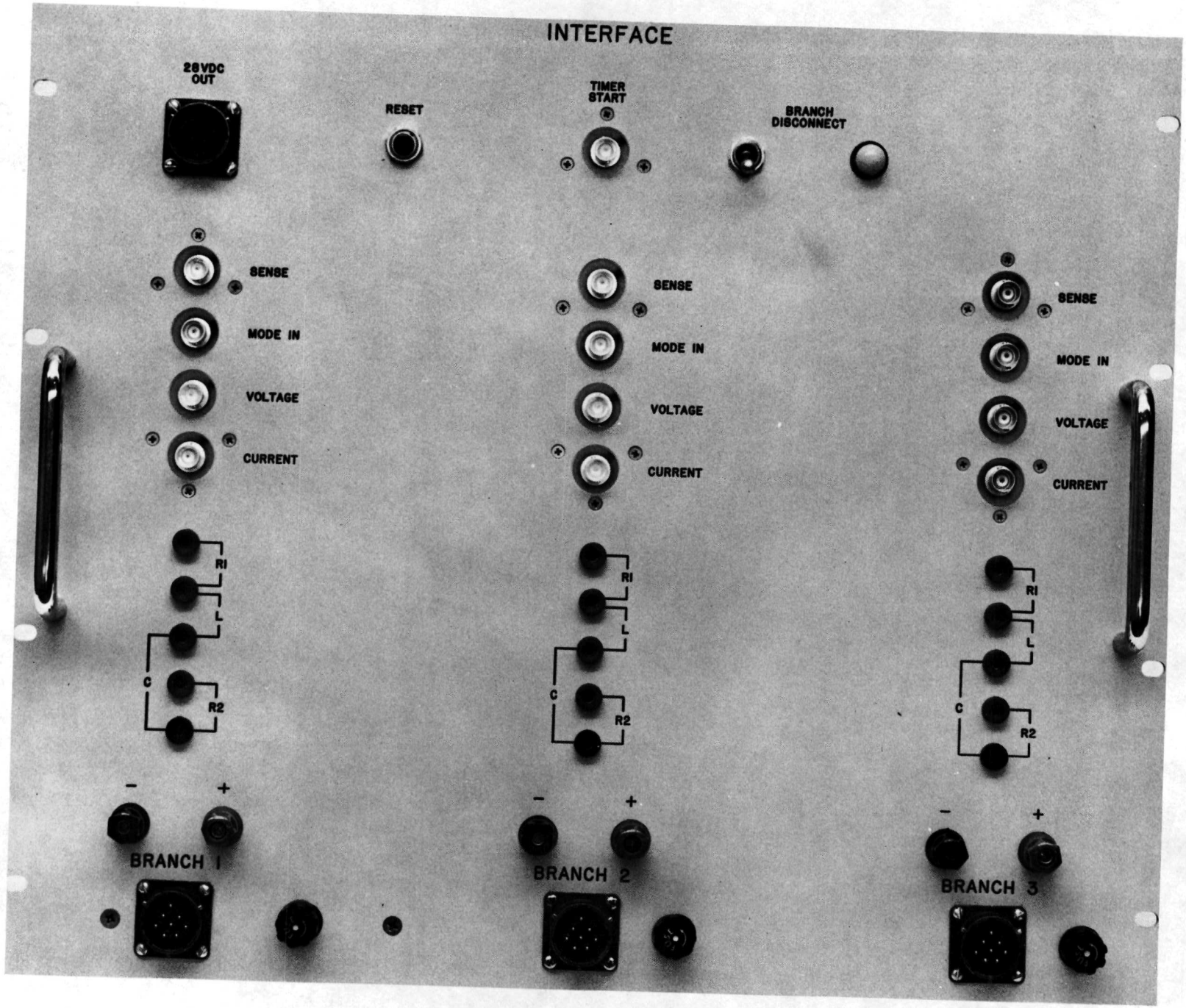

FIGURE 5-16 Front View of Interface Panel

NOTES

1. COAX CABLE SYMBOL REPRESENTS CONNECTOR ONLY. CONNECTOR IS WIRED WITH NO. 22 AWG WIRE

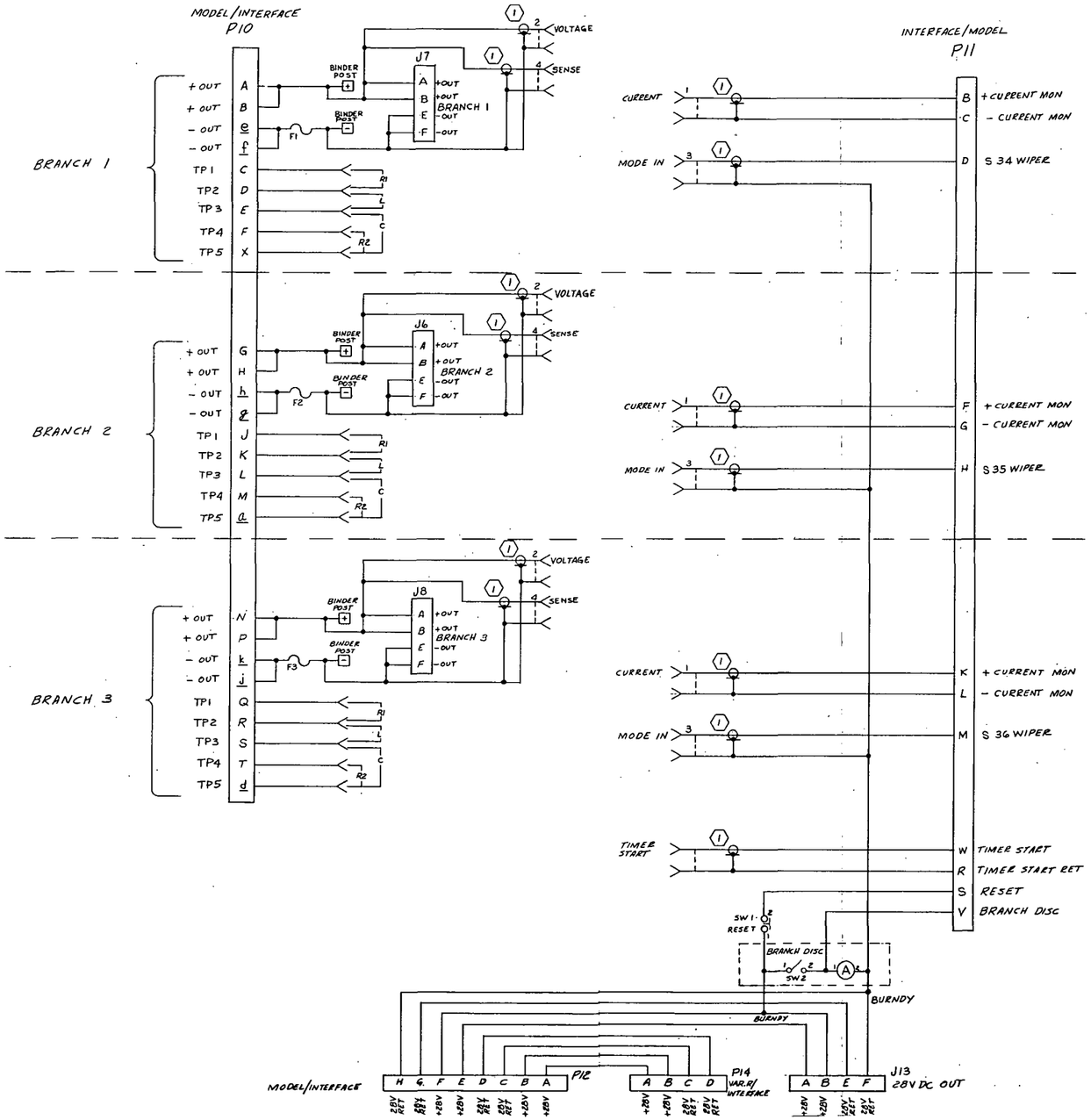

FIGURE 5-17 Interface Panel Schematic

Counters Incorporated. See Figure 5-18 for a front panel view of the timer. The timer provides four independent output channels each of which may be set to operate at 000 to 1.999 seconds (in 1 millisecond increments) following application of a start signal common to all four channels.

5.2.1.4.2 Control Electronics

The control electronics of the model provides various control functions as described below. The control electronics are in several locations in the model chassis. The model control electronics subassembly is located at the rear of the chassis and is connected into the model by P19. The mode control circuit boards are located on both side supports of the model chassis and are hardwired into the model.

5.2.1.4.2.1 Control Electronics Subassembly

The control electronics subassembly provides the following functions. A schematic diagram is provided in Figure 5-19.

START:--The START circuit provides a positive voltage pulse for initiation of the preset timer. The START circuit obtains a sense voltage by connection to the SENSE connector of the branch selected to provide the start signal. Thus, when voltage is applied to the branch, it is detected by the START circuit which generates a start signal for the timer.

Reset:--The RESET circuit provides a positive voltage pulse for resetting the preset timer to zero. The RESET circuit also resets the Polarity Sense circuit and resets the model branch to the topology set by the front panel switches and patching. This feature is necessary following a simulator operation in any one of modes 5, 6, 7, 8, 9, or 10. And, finally, the RESET circuit applies a low resistance across the capacitor (C) switch of each branch to discharge all capacitors connected into the model.

Total reset time is set for approximately four seconds to permit complete discharge of the model capacitors.

The Branch Disconnect lamp will light during the reset operation.

Polarity Sense:--A polarity sense circuit is provided for each branch to protect the electrolytic capacitors (capacitor decades 4 and 5) against reverse voltage application. A monitor is applied to the polarity sense circuit for each branch from the K1 relay

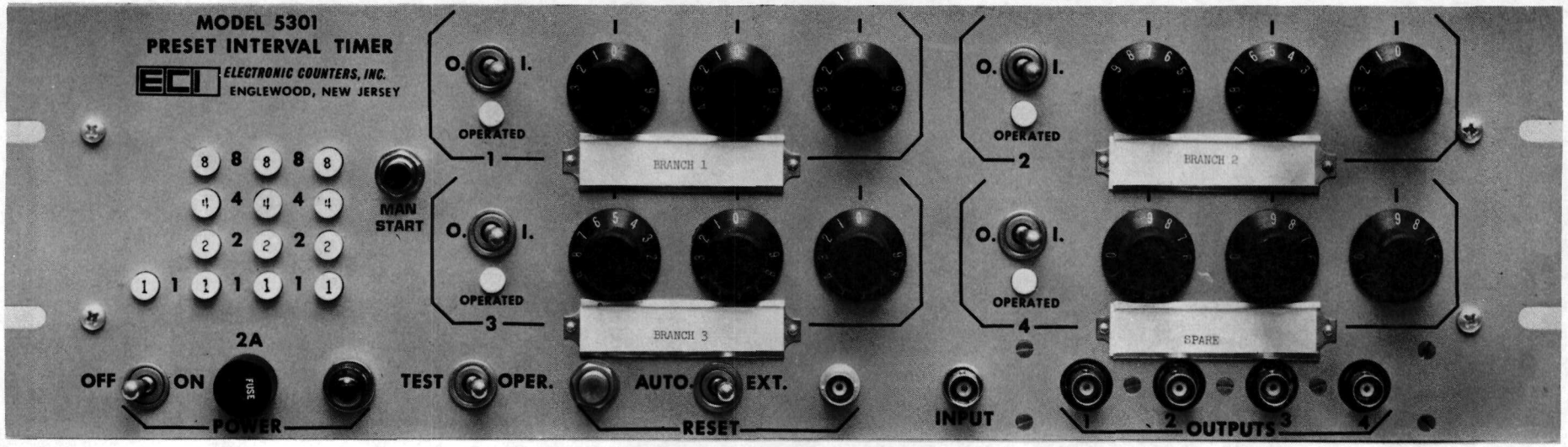

FIGURE 5-18 Front View of Preset Interval Timer

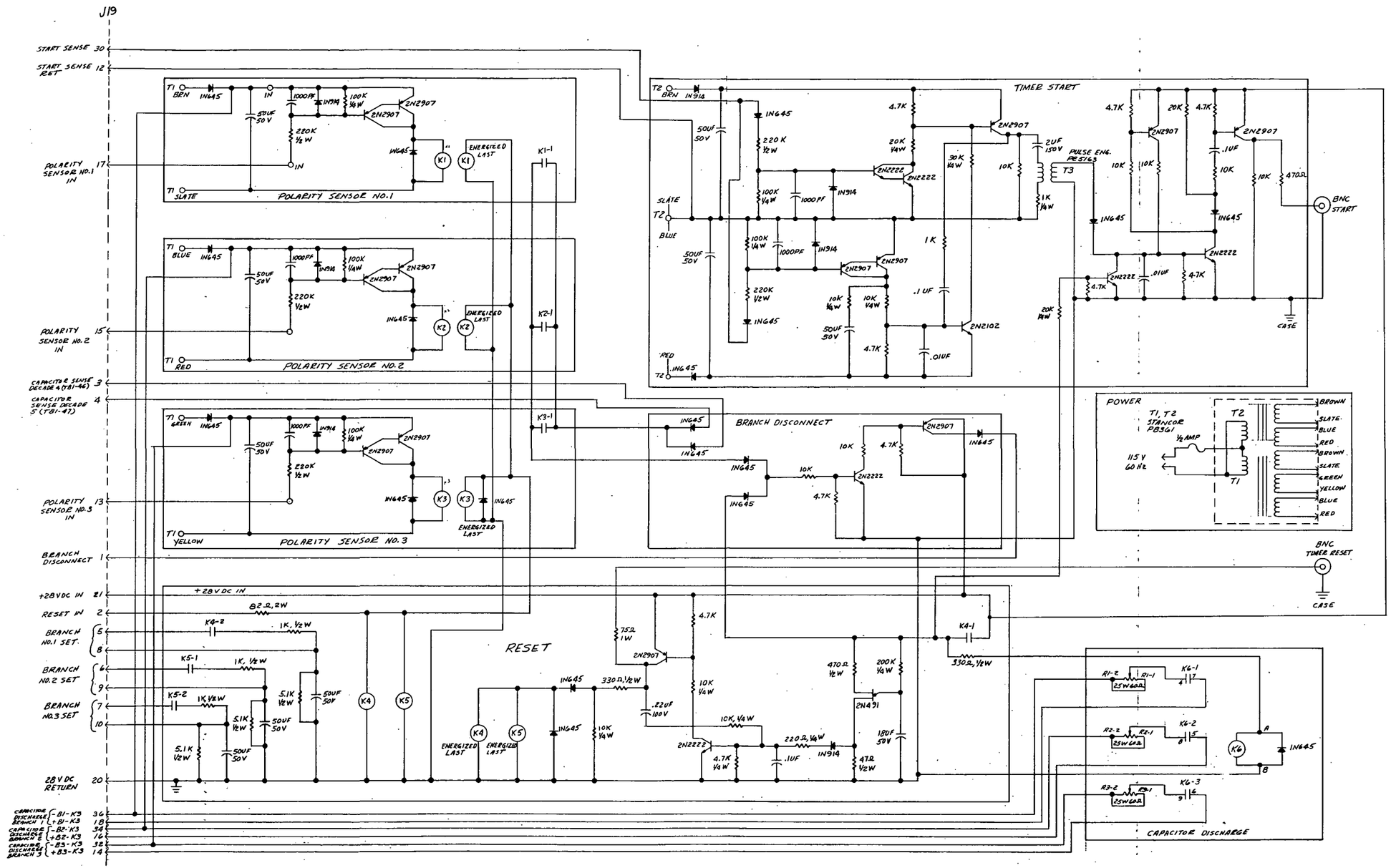

FIGURE 5-19. Model Control Electronics Subassembly Schematic

of the same branch. The return for the sense circuit is to the low side of the capacitor discharge circuit (lower end of branch). Thus, if reverse voltage is applied to the model while either of the electrolytic capacitor decades is being used, the polarity sense circuit will operate and provide an output to the branch disconnect circuit which, in turn, will open the K1 relay of all three branches.

Branch Disconnect:-- The branch disconnect circuit is activated manually by operation of the BRANCH DISCONNECT switch or RESET switch or, automatically, by output from the polarity sense circuit. The branch disconnect circuit opens relay K1 in each branch and illuminates the BRANCH DISCONNECT lamp.

5.2.1.4.2.2 Mode Control

The branch mode relays are a part of and are operated by the mode control circuit in each branch. A schematic diagram of the mode control circuit is provided in Figure 5-20. Three of these circuits are provided--one for each branch.

5.2.2 Variable R

The dynamic load simulator variable R is an electronic circuit whose output resistance can be made to vary as a function of a control voltage, as depicted in the simplified block diagram shown on Figure 5-21.

The variable R can be used to simulate equipment response to application of voltage by first interrogating the equipment and computing the input current/voltage ratio and then using this ratio (conductance analog) as the control signal.

The variable R will respond to control signals over a frequency range of DC to 10 KHz at current levels as high as 8 amperes continuous. The variable R delivered as part of the dynamic load simulator may be operated at positive, non-zero-crossing voltage inputs of 20 to 60 volts. The maximum power dissipation is 250 watts continuous.

Figure 5-22 shows the block diagram of the variable R electronics. The following description is based on this block diagram and the schematic, Figure 5-23. The isolation block in Figure 5-22 is obtained by two operational amplifier stages, A1 and A2 of the schematic. The two inputs are into inverting amplifier stages. A1 inverts the signal on the + input and then the signal is summed

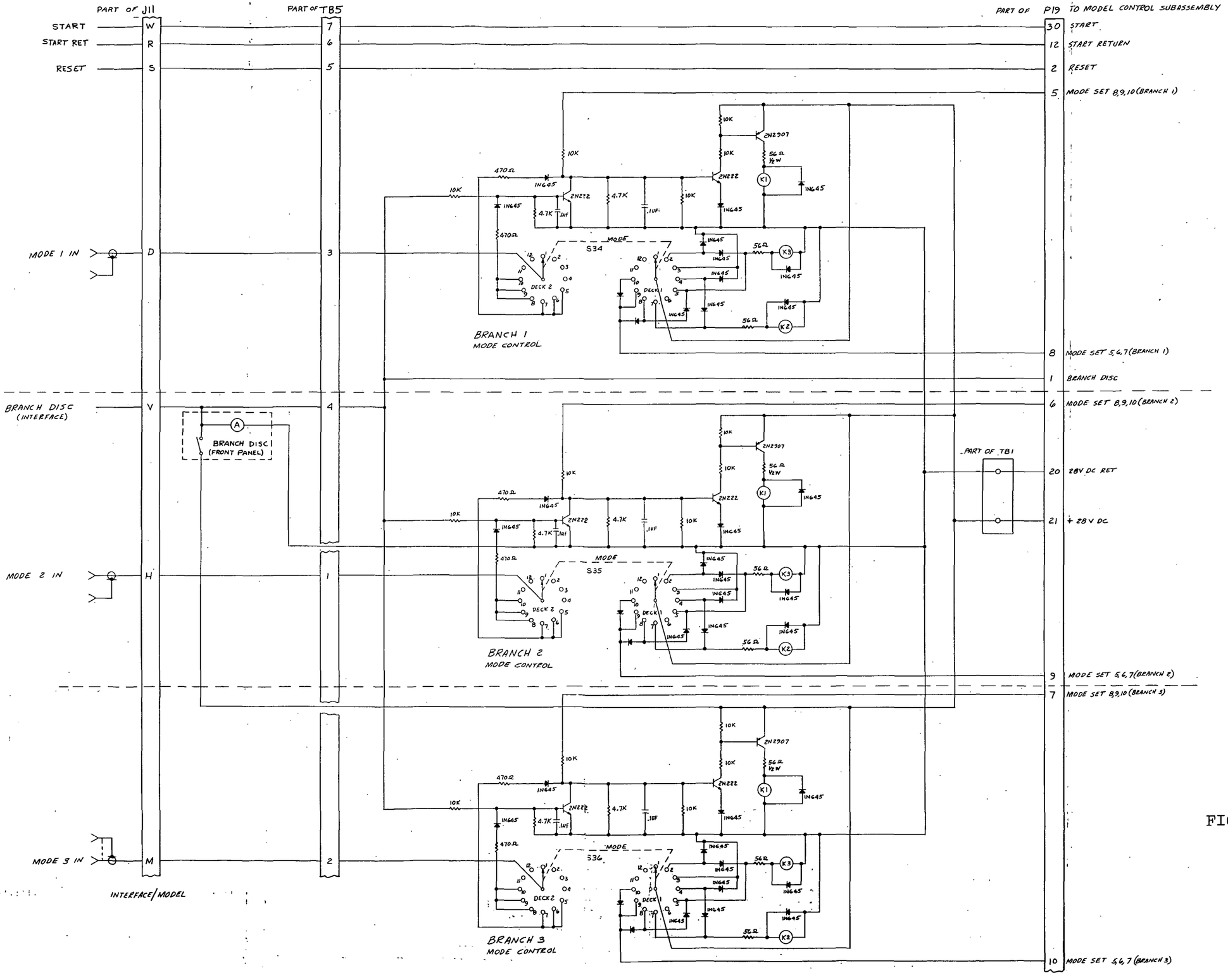

FIGURE 5-20 Mode Control Schematic

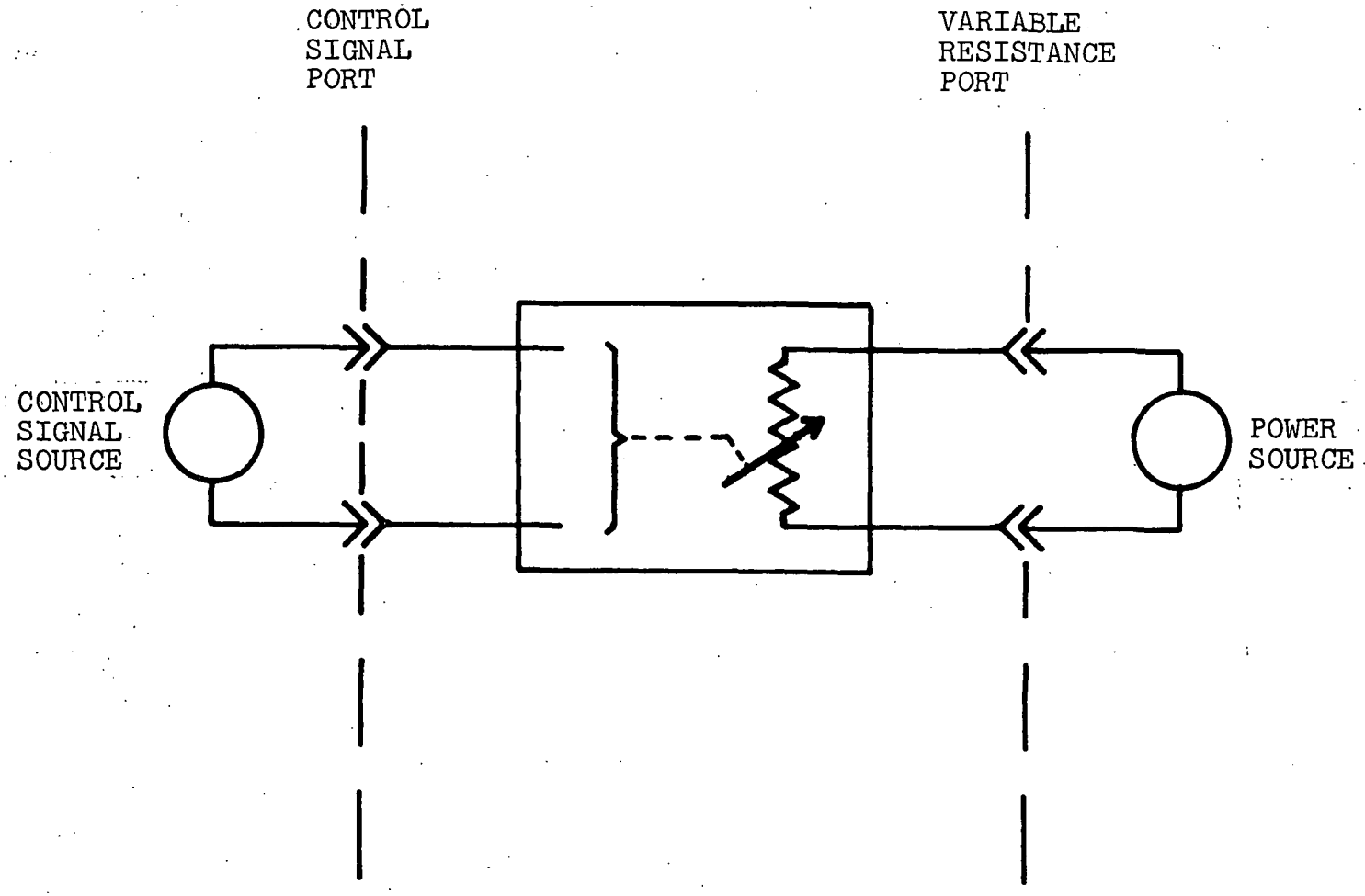

FIGURE 5-21 Variable R Concept--Simplified Diagram

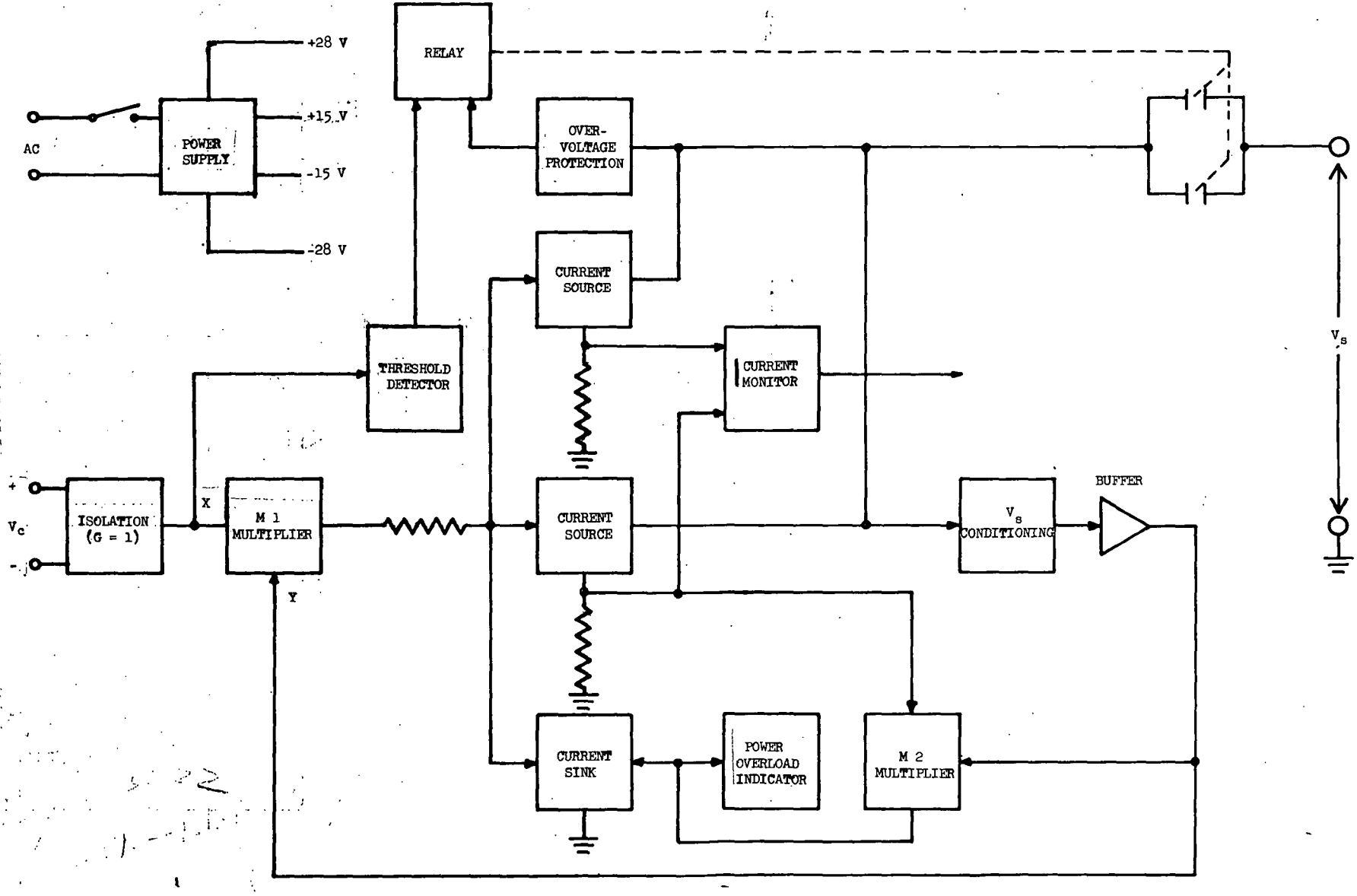

FIGURE 5-22 Variable R--Block Diagram

ENGR CHG	ZONE	LTR	REVISIONS DESCRIPTION	DATE	APPROVED

Relay "ON" Threshold Override by Jumper

Over voltage Protection

Power ON (WHITE) LP1 -28V

LP2 KIC -28V No Control or OVERVOLTAGE (AMBER)

OVER-RIDE

J2 Rear Connector

C1 0.1μf

R39 51K, R38 51K, R37 100Ω, ~15mV

A6 741, R36 1K, R35 2K, R34 2K, D5 1N914

+28V D4 1N914 KNP14D55 K1

Q12 2N4300, Q13 2N2222A, R40 68Ω

D6 IN4978 68V 5W

R41 470Ω

SW2 4PDT ON TEST

D3 1N3891

KIA NO, KIB NO

RB 1Ω

V_s LOAD (OUTPUT) + 20 TO 60V DC

28V Test Input A,B J2 Rear Connector MS3112E-16-8P

+V_s A,B

V_s return C,D

J1 Front Connector MS3112E-16-8P

Test Input 28V Return C,D J2 Rear Connector

V_s return LOAD (OUTPUT)

J1 F, G

V_c + −

R1 50K RN60, R2 50K RN60, R51 20K

R3 5K RN55, R33 5K RN55

A1 2500, A2 2500, A3 2500

R4 5K RNS5, R5 5K RNS5, R6 50K RN60, R53 500K

C2 0.1μf, C3 0.1μf, C8 1000pf

R50 2K, IN962 D7

M1 AD530K Multiplier

R7 20K Y-Fd thru, R8 20K X-Fd thru, R9 20K Offset

R10 5K, XY / 10

Y

Gain R32 5K 6K, R31 75K

Power Overload Limit R54 5K

M2 AD530K

Power Overload (RED) LI3

Q14 2N2222A, Q15 2N2907

R42 6.98K, R43 1K, R30 6.98K, R29 1K

Q11 2N2222A

A4 2500, A5 2500

C4 0.1μf, C5 0.1μf, C6 120pf, C7 120pf

D1 1N914, D2 1N914

R13 100Ω, R14 2K, R12 20K, R11 10K

R21 100Ω, R25 2K, R26 20K, R28 10K

Q1 2N2222A, Q2 2N2222A

Q3 2N4076, Q4 2N3773, Q5 2N4076, Q6 2N3773

Q7 2N4076, Q8 2N3773, Q9 2N4076, Q10 2N3773

R55 100Ω, R56 100Ω, R58 100Ω

R15 0.1Ω, R16 0.1Ω, R17 2Ω, R23 0.1Ω, R22 0.1Ω, R24 2Ω

R19 1Ω, R20 50K, R21 10K, R45 10K, R44 10K

A7 2500, A8 2500

R46 5K, R47 10K, R48 10K, R99 1K

Current Monitor (1V/A)

SW1 DPST

AC LINE

POWER SUPPLY Calif. Elect. Mfg. Co. Model 226

+28V A, +15V C, gnd H, −15V X, −28V B

QTY REQD	CODE IDENT / ASSY NO.	PART OR IDENTIFYING NO.	NOMENCLATURE OR DESCRIPTION	MATERIAL OR NOTE	SPECIFICATION	ZONE	ITEM NO.

LIST OF PARTS

PART CLASS: Unclassified

DWG CLASS:

ASG BY: L.D. Bruce

DASH NO.	NEXT ASSY	USED ON	QTY PER NHA	END ITEM NUMBER	SERIAL NO.
	APPLICATION			EFFECTIVITY	

UNLESS OTHERWISE SPECIFIED

TOLERANCE AND DRAWING INTERPRETATION PER D143

X ± .08 XX ± .04 XXX ± .020

MACHINED ANGLES ± 0° 30'

SHEET METAL BEND ANGLES ± 2°

P10001

SURFACE ROUGHNESS ✓

DO NOT SCALE DRAWING

CONTR NO.	
RELEASE	
DWG APPD	
CHECKED	
DRAWN	L.D. Bruce 3-2-72
DESIGN APPROVAL	
MANAGER	
SECT CH	
DESIGNER	L.D. Bruce 3-2-72

AVCO CORPORATION
AVCO SYSTEMS DIVISION WILMINGTON, MASSACHUSETTS 01887

TITLE VARIABLE-R SCHEMATIC LOAD SIMULATOR

SIZE	CODE IDENT NO.	DWG NO.
C	04614	DL 14

SCALE | WT | SHEET

REV. B

DRAWING NUMBER DL14

FIGURE 5-23 Variable R Schematic Diagram (DL 14)

into the A2 amplifier stage giving unity gain for the differential signal, V_C , and rejection of the common mode signals (signal from circuit ground to the + and to the - inputs) based mainly on the resistor matching.

The V_S conditioning block is a voltage divider the output of which is buffered by the A3 amplifier to drive the Y input of the multiplier. This feature makes the variable R load current (I_S) sensitive to load voltage (V_S) changes, and, therefore, provides a true variable resistance. The multiplier output is proportional to the product of the X and Y inputs and provides the drive to the parallel current sources. The current sources are shown in the schematic with inputs at pin 3 of A4 and A5. One current source consists of the A4 operational amplifier, Q1, Q3, Q4, Q7 and Q8, Diode D1, and Resistors R11 through R18. The other is an identical current source circuit.

The input at pin 3 forces a corresponding signal at pin 2 by operational amplifier action, since the differential input (pin 2 to pin 3) must be zero ideally. The resistive divider R11 and R12 require that the voltage across R17 be (R12 + R11)/R11 times the input signal. This sets the emitter current of the Darlington stage transistors and forces the collector current (approximately equal to the emitter current) to flow, thus forming a voltage-input-controlled current source. The current source is unipolar and diode D1 protects against negative input signals.

The other current source with A5 input and similar circuitry operates similarly. The two current sources are summed providing a current flow proportional to the control voltage, V_C, and the source voltage, V_S .

Transfer Characteristic

The source current, I_S, is given by the following equation in terms of the schematic, Figure 5-23, designations.

$$I_s = \frac{1}{R17}\left(\frac{R12+R11}{R11}\right) k_1 G_1 \left(\frac{R21}{R21+R20}\right) V_s V_c +$$

$$\text{---} + \frac{1}{R24}\left(\frac{R26+R28}{R28}\right) k_1 G_1 \left(\frac{R21}{R21+R20}\right) V_s V_c$$

where k_1 is the multiplier constant = 1/10 and G_1 is the gain of the A1-A2 isolation stage. Substituting unity gain for G_1, 1/10 for k_1 and assuming matching values of R17-R24, R12-R26, and R11-R28, a simplified expression is as follows:

$$I_s = \frac{2}{R17}\left(\frac{R12+R11}{R11}\right)\frac{1}{10}\left(\frac{R21}{R21+R20}\right) V_s V_c$$

substituting values

$$I_s = \frac{2}{2(\Omega)}\left(\frac{20K+10K}{10K}\right)\frac{1}{10}\left(\frac{10K}{10K+50K}\right) V_s V_c$$

$$= \left(\frac{3}{10}\right)\left(\frac{1}{6}\right) V_s V_c$$

gives the general simplified equation:

$$\boxed{I_s = \frac{V_s V_c}{20}}$$

which is the simplified expression of the transfer characteristic. Therefore for a constant V_s of 20 volts the expression is $I_s = V_c$.

Likewise, for V_s = 40 volts, $I_s = 2 V_c$, and for V_s = 60 volts, $I_s = 3 V_c$.

The equation for R_s is, therefore:

$$R_s = \frac{V_s}{I_s} = \frac{V_s}{\frac{V_s V_c}{20}} = \frac{20}{V_c}$$

$$\boxed{R_s = \frac{20}{V_c}}$$

The circuitry is designed for a 0 to 10V range for V_c.

Leakage Current

Operational amplifier A6 is employed as a comparator with pin 2 input set for approximately 15 millivolts. As the control signal at the multiplier input exceeds the 15 mv the amplifier output swings positive turning on transistor Q12 and relay K1, thus closing the contacts K1A and K1B on V_s.

Relay K1 is off for signals below 15 mv and lamp LP2 is ON for this condition, since it is operated by the normally closed contact K1C. This provides a 10 μa maximum leakage at V_s for zero or control signals up to approximately 15 mv.

For those cases where operation of the unit requires a step input starting from a zero-current level, an override feature has been provided to maintain the relay in a closed condition. This may be accomplished by either: (1) operation of the OVERRIDE switch located at the rear of the unit, or (2) jumpering pins E and H of connector J2, also located at the rear of the unit.

Overvoltage Protection

An overvoltage protection is provided by D6 and Q13 which senses the overvoltage and shunts the drive from A6 to the relay driver, Q12. Therefore, for control signals under 15 mv or an overvoltage condition, the amber lamp, LP2, is on as an indicator.

Power Overload Protection

Multiplier M2 performs a product function whereby I_s and V_s are sensed and used to drive M2, giving an output proportional to the output power ($V_s \times I_s$). The M2 output is used to drive a threshold detector to limit the drive to the current sources. Therefore any $V_s \times I_s$ product equal to the threshold value will prevent further drive to the current sources and, therefore, limit power. The power limit is set at approximately 250 watts.

An identical threshold circuit is used to drive lamp LP3 for a power overload indication.

Reverse Polarity Protection for V_s

Diode D3 is placed in the V_s input line to prevent damage for a reversed V_s polarity.

Current Monitor

Amplifiers A7 and A8 form a summing amplifier, and an inverter and buffer amplifier for an output proportional to the I_s current. The scaling is 1 volt/ampere for simplicity of conversion. The output is a direct representation of the current waveform and has sufficient bandwidth and slewing rate to accurately follow the current waveform.

Power Supply

The power supply is a commercially available unit which provides unregulated ± 28V for relay and light supplies and a regulated ± 15 volts at 300 ma capability. Fuzing and short circuit protection are provided.

The supply line and load regulation are specified at 0.05% for 10% line variation, and no load to full load, respectively.

Test Mode

Switch 2 is a 4PDT switch employed for testing the performance of the variable R from a 28V source which is available in the test console. Thus, operation can be checked without applying an external source voltage, V_s . In the ON position the REMOTE connector and the LOAD (OUTPUT) binding posts are connected to the variable R output stage. In the TEST position 28 volts is applied to the variable R output stage through the rear connector.

Figure 5-24 is a front view of the variable R assembly. Figure 5-25 is a top view of the assembly showing the power supply, K1 relay, and electronics subassembly with the housing removed to show the heat sink and the circuit boards.

As shown in Figure 5-25, the unit contains a blower assembly, thus making the variable R self-sufficient.

5.2.3 Dynamic Load Simulator Assembly

As described in 5.1.2.1, the DLS consists of two separate and independent means of providing dynamic simulation, a model and a variable R. Both of these items are housed in a single upright console identified as Dynamic Load Simulator Model DLS 1000.

Figure 5-26 is an interconnecting diagram showing the interconnection of all chassis of the DLS. Figure 5-27 is a front view of the DLS. Figure 5-28 is a rear view of the DLS.

The DLS requires 115 volts rms, 60 Hz, single-phase power for its operation. A three-wire cable is provided with the console for connection to a suitable power source. Console power is controlled by a 15-ampere circuit breaker located on the bottom inductor chassis in series with the 'high' side of the primary power line. The POWER ON indicator lamp, located just above

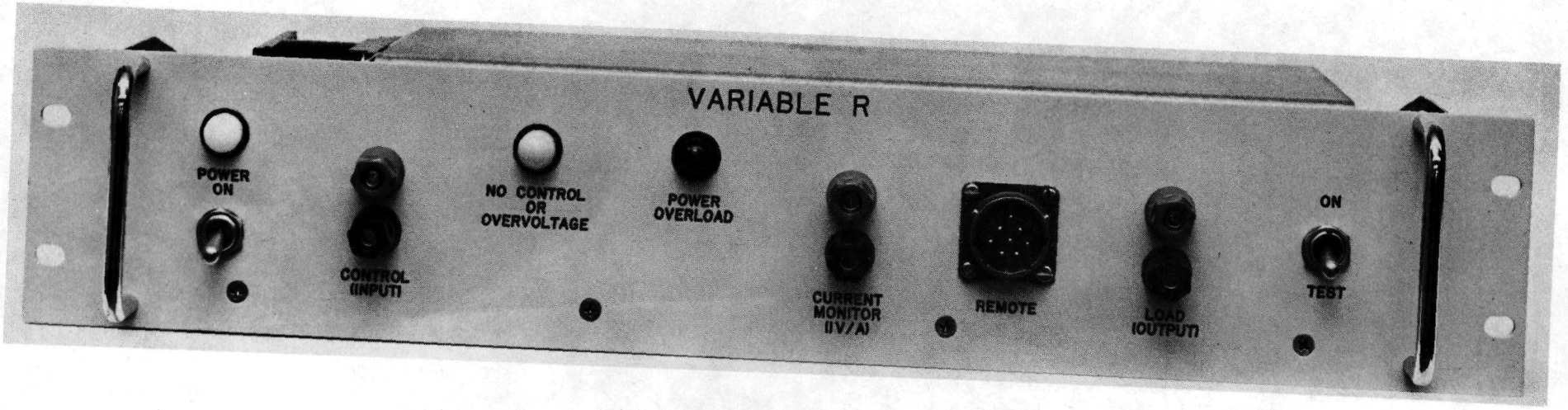

FIGURE 5-24 Front View of Variable R Chassis

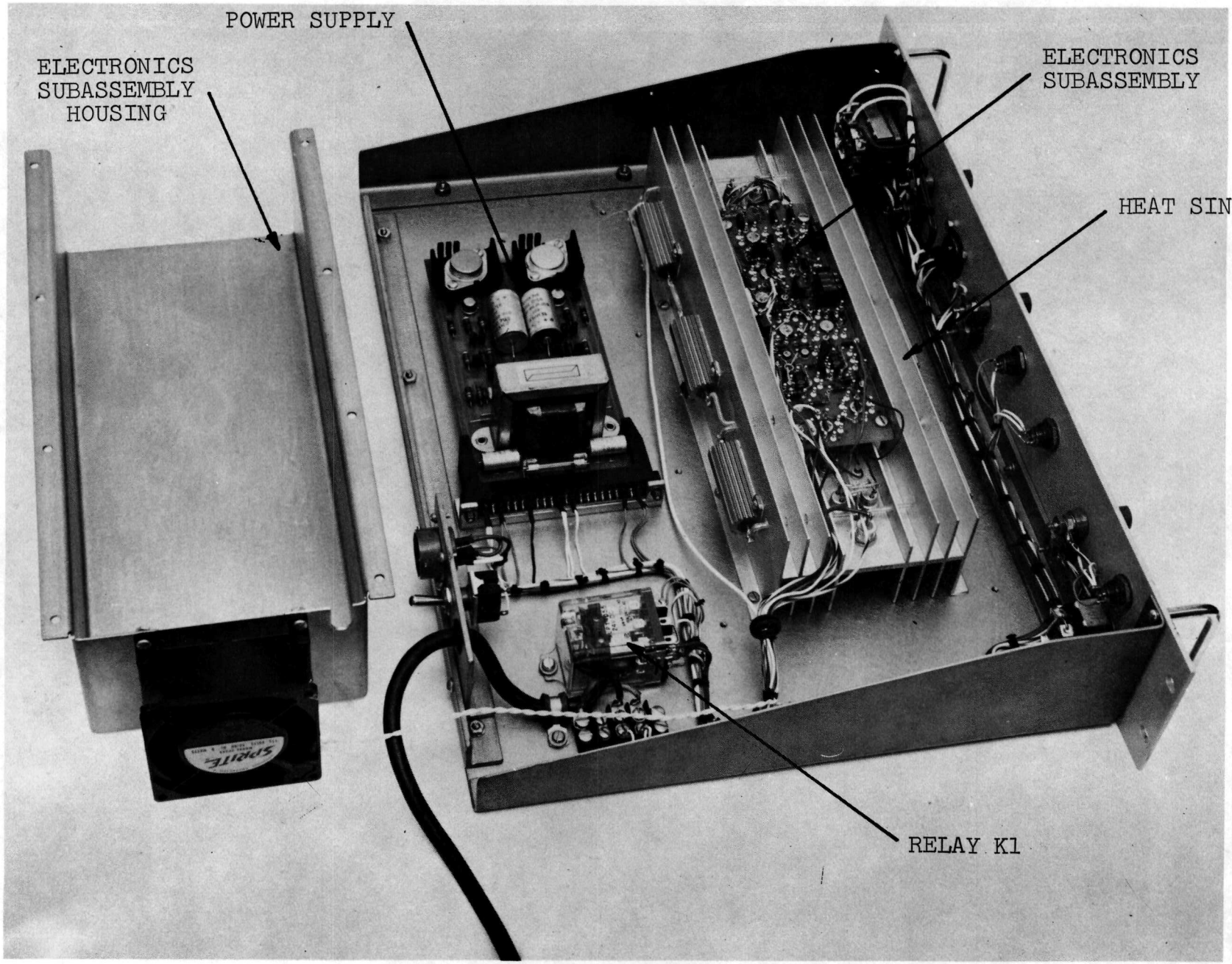

FIGURE 5-25 Top View of Variable R Assembly Showing Major Elements

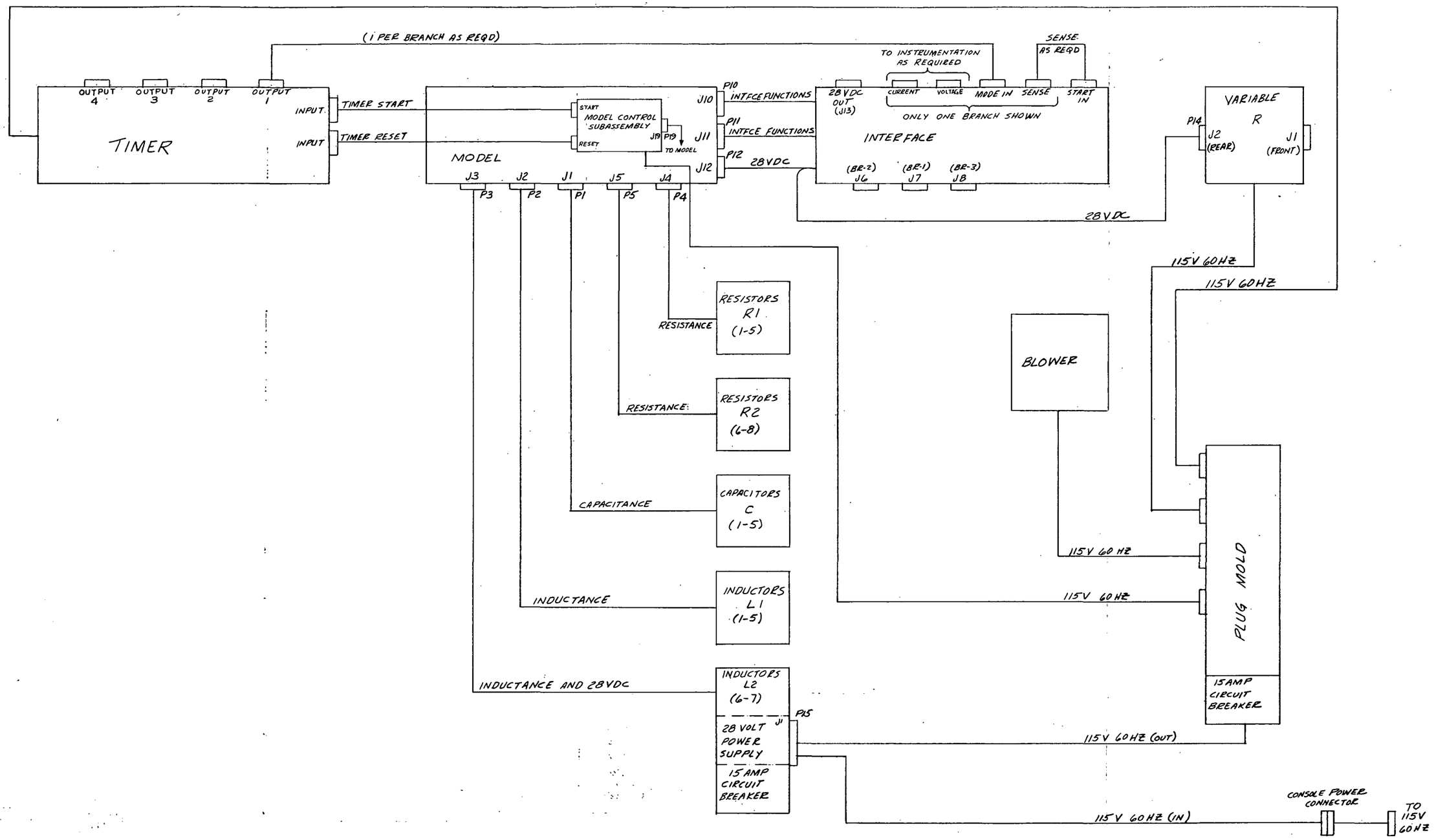

FIGURE 5-26 Dynamic Load Simulator Interconnecting Diagram

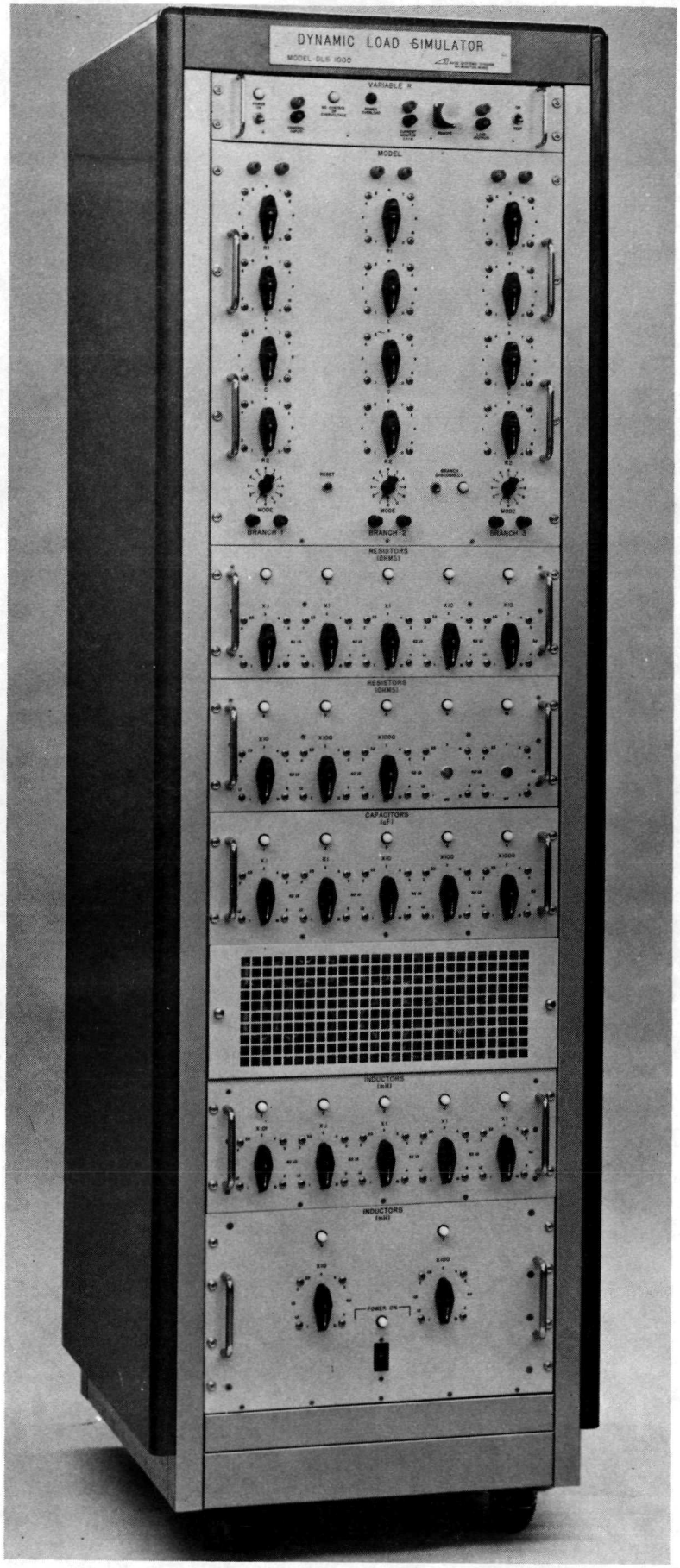

FIGURE 5-27 Dynamic Load Simulator, Model DLS 1000, Front View

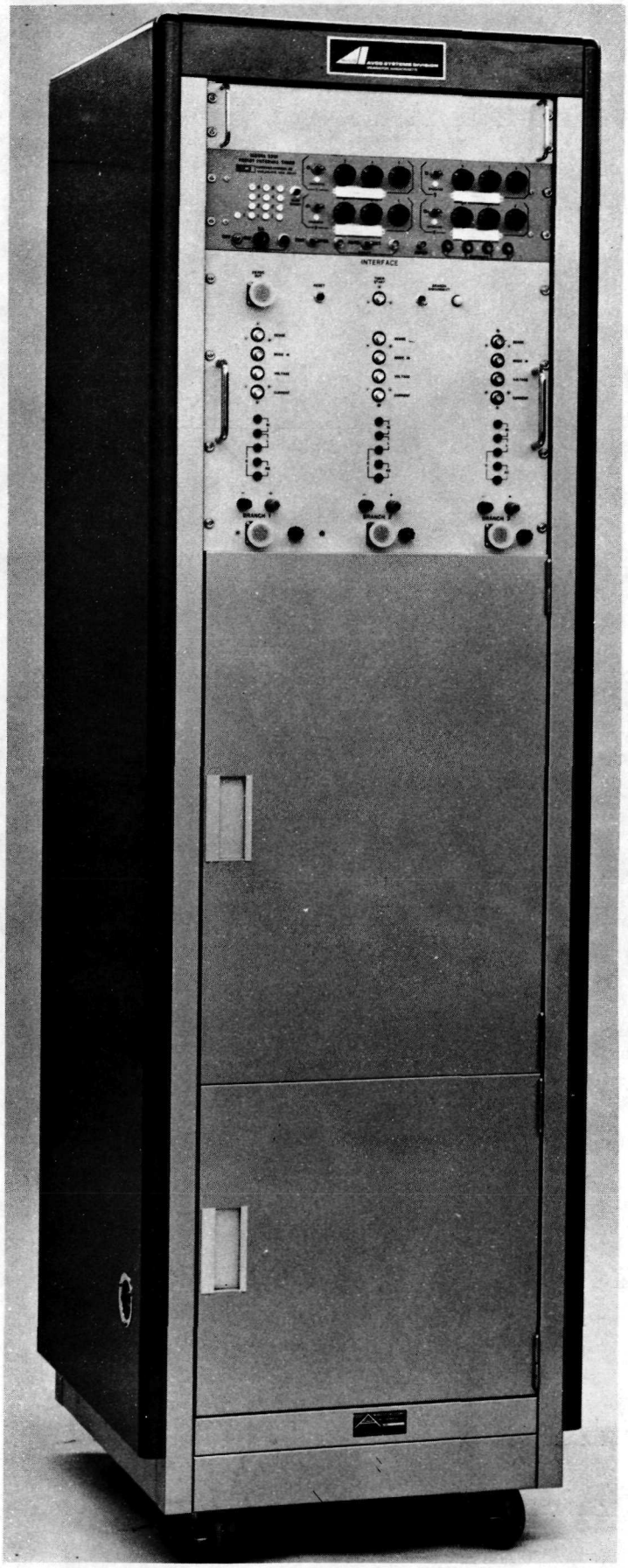

FIGURE 5-28 Dynamic Load Simulator, Model DLS 1000, Rear View

the circuit breaker, is operated by the console 28-volt DC power supply and indicates when primary power is applied. Figure 5-29 provides a schematic diagram of the power distribution.

A blower unit equipped with a removable air filter and located on the front of the console provides cooling for the resistor loads. The air is exhausted through the top of the DLS console.

A grounding stud, located directly below the primary power connector on the side of the console, provides a convenient tie point for connecting the console to instrumentation ground.

5.2.4 Operating and Maintenance Manual

Also provided as part of this program is a Dynamic Load Simulator, Model DLS 1000, Operating and Maintenance Manual. This manual describes the DLS, and provides operating instructions, safety precautions, maintenance instructions, and all necessary diagrams and wire lists.

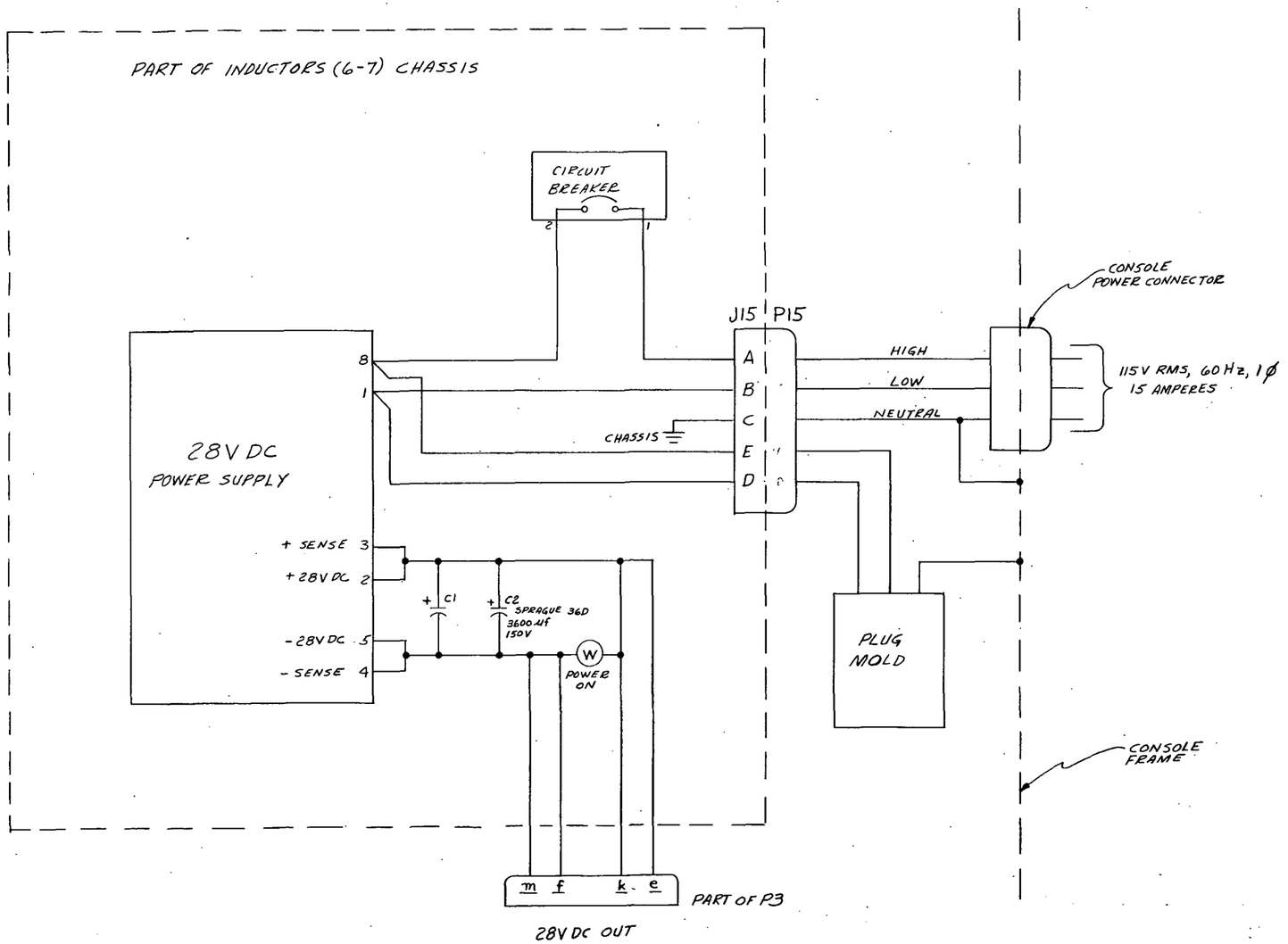

WIRE LIST

FROM	TO	GAUGE
115V POWER	P15-A	14
115V POWER RETURN	P15-B	14
115V POWER NEUTRAL	CASE - GND	14
CASE GND	P15-C	14
PLUG MOLD HIGH	P15-D	-
PLUG MOLD RETURN	P15-E	-
PLUG MOLD NEUTRAL	CASE - GND	-
J15-A	CKT BREAKER #1	14
J15-B	P.S. #1	14
J15-C	CHASSIS	14
CKT BREAKER #2	P.S. #8	14
P.S. #1	J15-D	14
P.S. #8	J15-E	14
P.S. #3 (SENSE)	P.S. #2	16 BUSS
P.S. #4 (SENSE)	P.S. #5	16 BUSS
P.S. #2	C1 (+)	16
P.S. #2	C2 (+)	16
P.S. #5	C1 (-)	16
P.S. #5	C2 (-)	16
C1 (+)	C2 (+)	14
C1 (-)	C2 (-)	14
P.S. #3	LIGHT L3-1	22
P.S. #4	LIGHT L3-2	22
C1 (+)	P3-e	16
C2 (+)	P3-k	16
C1 (-)	P3-f	16
C2 (-)	P3-m	16

FIGURE 5-29 Power Distribution Schematic

6. SIMULATOR EVALUATION

Tests were conducted on the dynamic load simulator (both model and variable R) to evaluate certain operating characteristics and, for selected items, to compare the response of the simulator with that of the original equipment.

It is important to note, in the equipment comparisons, that the equipments interrogated at MSC were operated by different power supplies and were interconnected by different wire sizes and lengths than those used for the simulator tests at Avco. The DC power supply used at Avco, in particular, was "softer" than the supply at MSC. Accordingly, this voltage regulation difference resulted in differences in the response waveforms.

As mentioned in Paragraph 4.2.1, the computer plots of the original data (rather than the oscillograph records) were used in comparing the interrogation data with actual equipment response. To compare simulator response with the original oscillograph records of the interrogation data, refer to Figure 4-1 through 4-17.

6.1 MODEL EVALUATION

Testing of the model consisted of verification of control operation and wiring integrity; measurements of all element decade values to establish the actual values available; and measurement of the resistance inherent in the wiring, switches, connectors, etc. in each branch. In addition, the model's ability to simulate equipment response was demonstrated for five items of spacecraft equipment.

6.1.1 Basic Operation Evaluation

The actual value of each element decade setting was measured to determine the element values available in the simulator. These measurements were made at the cable connector on each chassis, therefore they are low by the value of resistance, capacitance, and inductance inherent in the wiring within the model chassis between the connectors and the branch element locations. The resistance of this wiring is approximately 0.050 ohm. The inductance and capacitance values are too low to have an effect on the element values recorded. In the case of the low resistance decade (0.1 to 1 ohm), this additional 0.050 ohm should be added to the values tabulated to arrive at the actual values available at the branch location.

Table 6-I provides a tabulation of the resistance values of the two resistor chassis as measured at the P4 and P5 connectors.

Table 6-II provides a tabulation of the capacitance values of the capacitor chassis as measured at the P1 connector.

Table 6-III provides a tabulation of the inductance values of the two inductor chassis as measured at the P2 and P3 connectors.

A tabulation of the series resistance of the inductor elements is provided in Table 6-IV for each inductance value setting.

The inherent resistance of each branch between (+) and (-) interface terminals (with all branch switches in the shorted position, Position 11, and all mode switches in Position 2) is as follows. These values include the shunt resistance of 0.01 ohms, nominal.

Branch	Resistance (in ohms)
1	0.10
2	0.11
3	0.11

TABLE 6-I

RESISTANCE OF RESISTOR DECADES MEASURED AT PINS OF CONNECTORS P4 AND P5*

SWITCH POSITION	DECADE							
	R1 (X.1)	R2 (X1)	R3 (X1)	R4 (X10)	R5 (X10)	R6 (X10)	R7 (X100)	R8 (X1000)
	ohms	ohms	ohms	ohms	ohms	ohms	ohms	Kohms
1	0.094	0.97	1.01	9.8	9.8	9.9	97.2	1
1.2	0.124	1.21	1.27	11.8	11.9	11.9	116	1.2
1.5	0.134	1.49	1.56	14.8	14.8	14.9	145	1.49
2	0.150	1.94	2.05	19.6	19.5	19.8	198	2.0
2.5	0.209	2.48	2.55	24.7	24.8	24.8	242	2.5
3	0.249	3.0	3.09	29.8	30.1	29.9	285	2.99
4	0.314	4.02	4.04	39.9	39.9	39.9	390	4.0
5	0.374	4.92	5.00	49.7	49.6	49.7	488	5.0
6.2	0.464	6.07	6.19	61.4	61.3	61.6	603	6.2
8	0.614	7.88	8.02	79.5	79.7	79.6	773	8.0
10	0.684	9.75	10.0	99.0	99.1	99.3	971	10.0

* Add 0.050 ohms to each value for total resistance at branch location.

TABLE 6-II

CAPACITANCE OF CAPACITOR DECADES MEASURED AT PINS OF CONNECTOR P1*

SWITCH POSITION	DECADE C1 (X.1)	C2 (X1)	C3 (X10)	C4 (X100)	C5 (X1000)
	μf	μf	μf	μf	μf
1	0.103	0.99	9.8	108	1120
1.2	0.121	1.18	11.8	128	1330
1.5	0.152	1.48	14.8	164	1640
2	0.204	1.97	19.4	199	2080
2.5	0.254	2.48	24.6	254	2570
3	0.301	2.96	29.9	313	2990
4	0.408	4.01	29.9	401	4050
5	0.511	5.00	49.8	509	5190
6.2	0.633	6.19	61.5	621	6360
8	0.812	7.97	79.8	821	8200
10	0.102	9.94	99.2	1040	10260

* All measurements made at a frequency of 1 kHz.

TABLE 6-III

INDUCTANCE OF INDUCTOR DECADES MEASURED AT PINS OF CONNECTORS P2 AND P3*

SWITCH POSITION	DECADE L1 (X.01)	L2 (X.1)	L3 (X1)	L4 (X1)	L5 (X1)	L6 (X10)	L7 (X100)
	mH	mH	mH	mH	mH	mH	mH
1	0.01	0.08	1.08	1.08	1.0	8.0	95
1.2	0.013	0.10	1.35	1.32	1.3	10.	110
1.5	0.016	0.14	1.73	1.70	1.7	13	140
2	0.021	0.198	2.35	2.25	2.2	17	180
2.5	0.026	0.25	2.65	2.63	2.55	21	230
3	0.0306	0.30	3.10	3.08	3.0	25	270
4	0.0406	0.36	4.30	4.30	4.2	34	360
5	0.0516	0.46	5.5	5.5	5.5	42	450
6.2	0.0626	0.60	6.90	6.8	6.6	52	550
8	0.0800	0.79	8.3	8.3	8.1	73	720
10	0.100	0.98	10.5	10.6	10.3	90	900

* All measurements made at a frequency of 1 kHz.

TABLE 6-IV

RESISTANCE OF INDUCTOR CIRCUITS MEASURED AT PINS OF CONNECTORS P2 AND P3

SWITCH POSITION	DECADE						
	L1 (X.01)	L2 (X.1)	L3 (X1)	L4 (X1)	L5 (X1)	L6 (X10)	L7 (X100)
	ohms	ohms	ohms	ohms	ohms	ohms	ohms
1	0.06	0.09	0.12	0.12	0.12	0.17	0.75
1.2	0.06	0.09	0.12	0.12	0.12	0.17	0.81
1.5	0.06	0.09	0.12	0.12	0.13	0.18	0.91
2	0.06	0.09	0.13	0.13	0.13	0.19	1.07
2.5	0.06	0.09	0.14	0.14	0.14	0.20	1.22
3	0.06	0.09	0.15	0.15	0.15	0.22	1.36
4	0.06	0.09	0.16	0.16	0.16	0.24	1.62
5	0.06	0.10	0.17	0.17	0.17	0.27	1.87
6.2	0.06	0.11	0.18	0.18	0.19	0.29	2.13
8	0.07	0.12	0.20	0.20	0.20	0.38	2.54
10	0.07	0.13	0.22	0.22	0.22	0.37	2.96
OFF	Open	Open	Open	Open	Open	Open	Open

The response time of the branch K1 relays was measured to permit suitable correction to be made when operating in any dynamic mode (Modes 5 through 10). The response times were determined to be:

K1 Closure Time	0.010 seconds
K1 Opening Time	0.030 seconds

The response time is defined in this case as the time from initial application of load voltage to the interface to the time the K1 operating contacts open or close.

6.1.2 Demonstration of Model Simulation Capability

As described in Paragraph 4.3, five items of spacecraft equipment that were interrogated at MSC were selected for simulation by the model. The interrogation data was processed as described in Paragraph 4.5 and the resultant data used as input to the model. This data identifies the model topology and element values necessary for achieving the desired time-domain response for each item of equipment to be simulated. Using this data, the model was then set up, by suitable patching and switching, for each of the five items in turn. Table 6-V tabulates the model set-up data for each equipment. The Branch 3 inductance value for Run 8 was inadvertently transcribed as 0.050 millihenries instead of 50 millihenries from Table 4-IX. This incorrect value was used throughout the evaluation.

The power source in each case was adjusted to provide the voltage level corresponding to that used during interrogation.

The DC voltage source used at Avco did not exhibit the same regulation characteristics as that used at MSC. Also, the interconnecting wire size, length, and routing were not identical. These differences resulted in some difference in the observed current amplitudes.

In the case of the AC load (heat exchanger valve, Run 6B) the responses are difficult to compare since the transient current depends upon the line voltage at the instant the switch is closed. No attempt was made to sense the AC line voltage and close the switch at the same point on this waveform for each simulation. Therefore, although it can be seen that the transient interval and frequency of the simulator response is similar to those observed in the original interrogation, a direct point-by-point comparison is not made with the same facility as those made in the cases of the DC-operated equipments.

TABLE 6-V

NOMINAL MODEL CONTROL SETTINGS FOR SIMULATION OF FIVE SELECTED EQUIPMENTS

Equipment	Run	Branch	R1 ohms	L mH	C f	R2 ohms	Input Voltage	Mode	Timing secs
Motor Switch	3C	1	5	1.5	100	∞	35 DC	9	0.010[a]
		2	0	6.2	1.5	∞		9	0.010
		3	4	3	8000	10		10	0.010
VHF/AM Transceiver	11C	1	1.2	1	150	∞	30 DC	3	N/A
		2	3	1.2	4000	∞		3	N/A
Varo Inverter	8A	1	0.4	0.2	8000	15	26 DC	4	N/A
		2	15	1000[c]	0	0		5	0.575[b]
		3	12	0.05	400	∞		6	0.575
Apollo Inverter	9A	1	0.4	0.05	4000	12	26 DC	4	N/A
		2	1	0.4	62	800		4	N/A
Heat Exchanger Valve	6B	1	1500	200	0	0	114 rms, 400 Hz	2	N/A
		2	80	8	0.1	∞		3	N/A

a This value has been changed from that shown in Table 4-IX to correct for K1 relay opening response time of 0.030 second.

b This value has been changed from that shown in Table 4-IX to correct for K1 relay closure response time of 0.010 second.

c Incorrectly transcribed from Table 4-IX (value should have been 50 millihenries).

In order to account for the effects of the supply voltage regulation differences and the differences between the nominal and actual element values, three different evaluations were made.

1. Comparison of model response with interrogation data.

2. Comparison of model response with computer-predicted response using nominal element values and Avco voltage history*.

3. Comparison of model response with computer-predicted response using measured element values** and Avco voltage history.

6.1.2.1 First Comparison

The first comparison shows the effect of the different power sources used in obtaining the two sets of data. These comparisons are shown graphically in Figures 6-1 through 6-12. The figure following each current response comparison is a comparison of the NASA (interrogation) voltage and Avco voltage histories.

6.1.2.2 Second Comparison

The second comparison shows the computer-predicted response of the model using nominal element values and the Avco voltage history versus the model responses measured at Avco. This comparison eliminates the effects of the different voltage sources in that it substitutes the Avco voltage history for the NASA voltage history in the computer-predicted response of the model. These comparisons are shown in Figures 6-13 through 6-18.

6.1.2.3 Third Comparison

The third comparison was made to reduce the effects of using nominal element values in the computer calculation. In this comparison, the element values actually measured in the simulator were used in the computer along with the Avco voltage histories. Table 6-VI is a tabulation of the measured element values for each model. These predicted responses were then compared with the measured model responses. These comparisons are shown in Figures 6-19 through 6-24.

---

* Voltage history for each trace measured during model evaluation tests at Avco.

** Actual element values measured in the model.

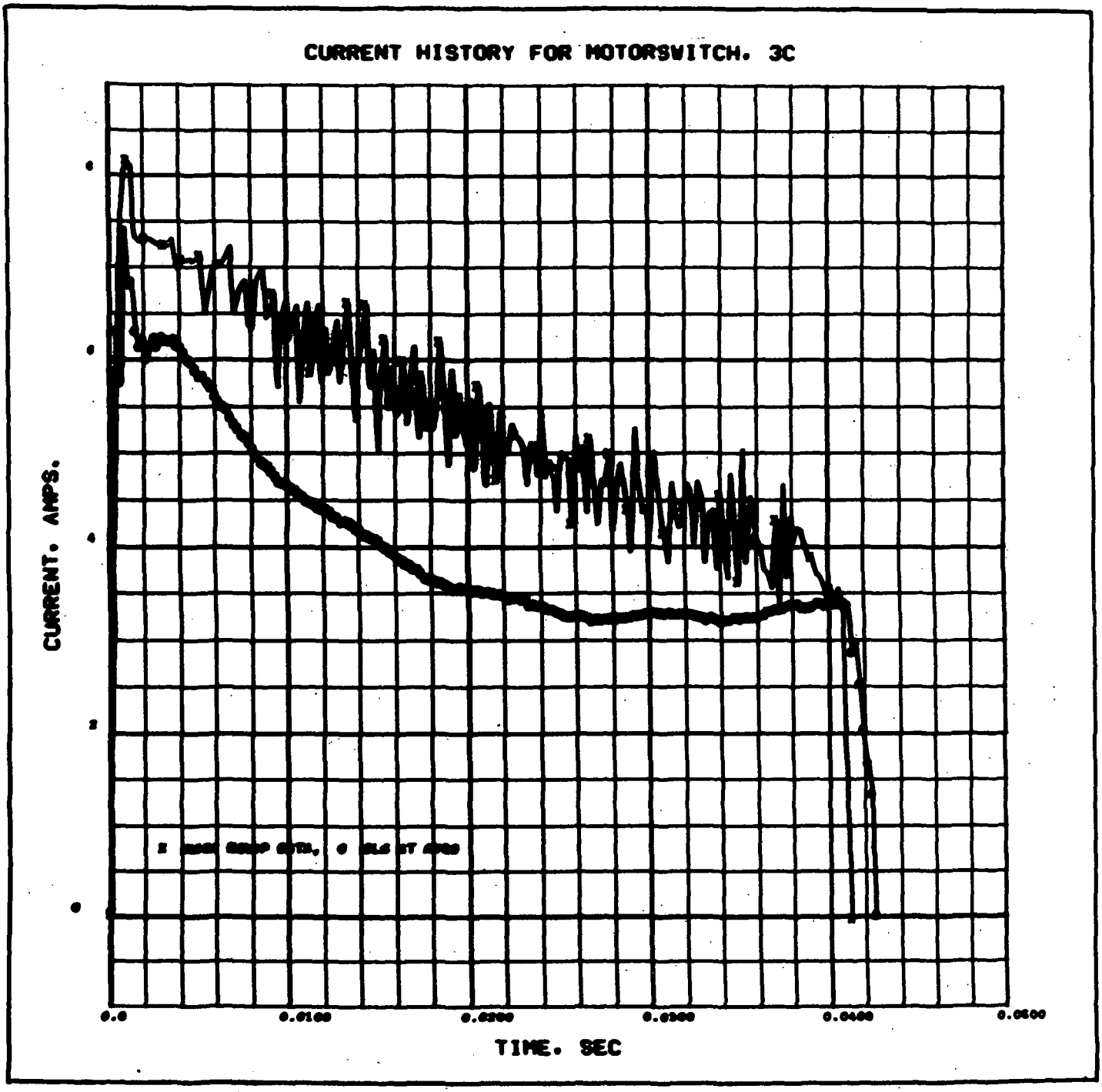

FIGURE 6-1 Comparison of Interrogation Data with Model Response for Motor Switch, Run 3C

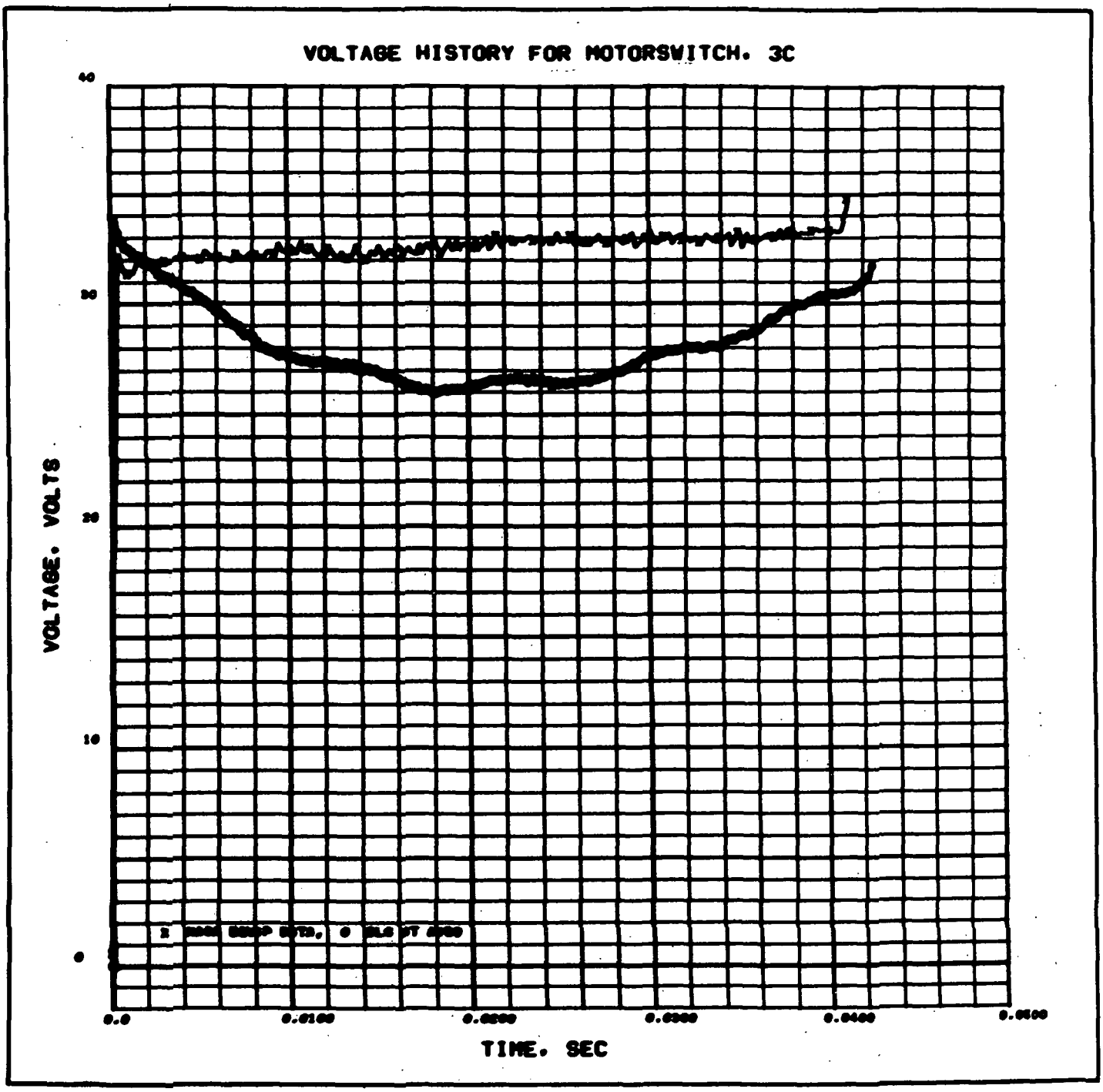

FIGURE 6-2 Comparison of NASA Voltage History (Interrogation Data) with Avco Voltage History for Motor Switch, Run 3C

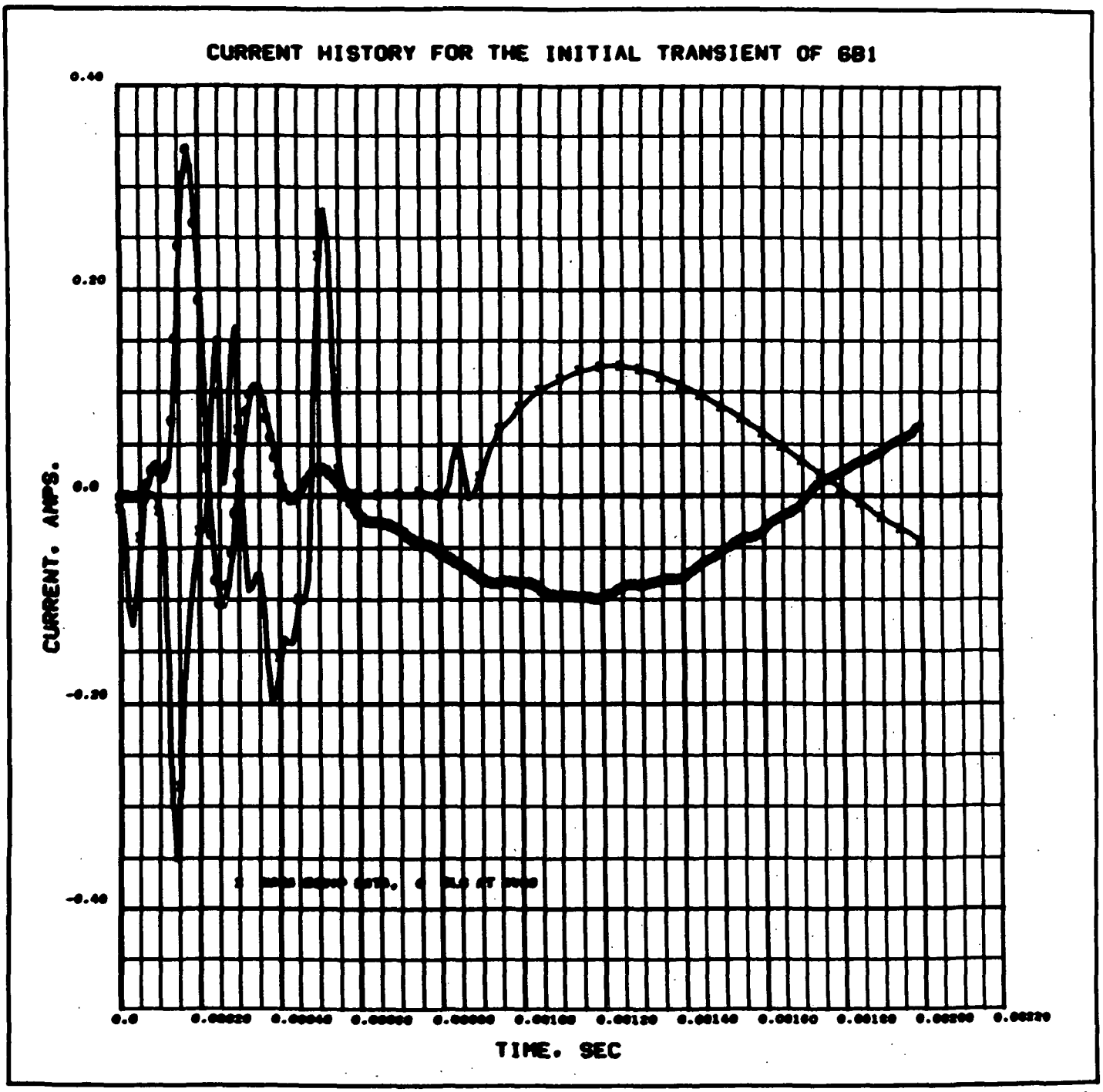

FIGURE 6-3 Comparison of Interrogation Data with Model Response for Heat Exchanger Valve, Run 6B

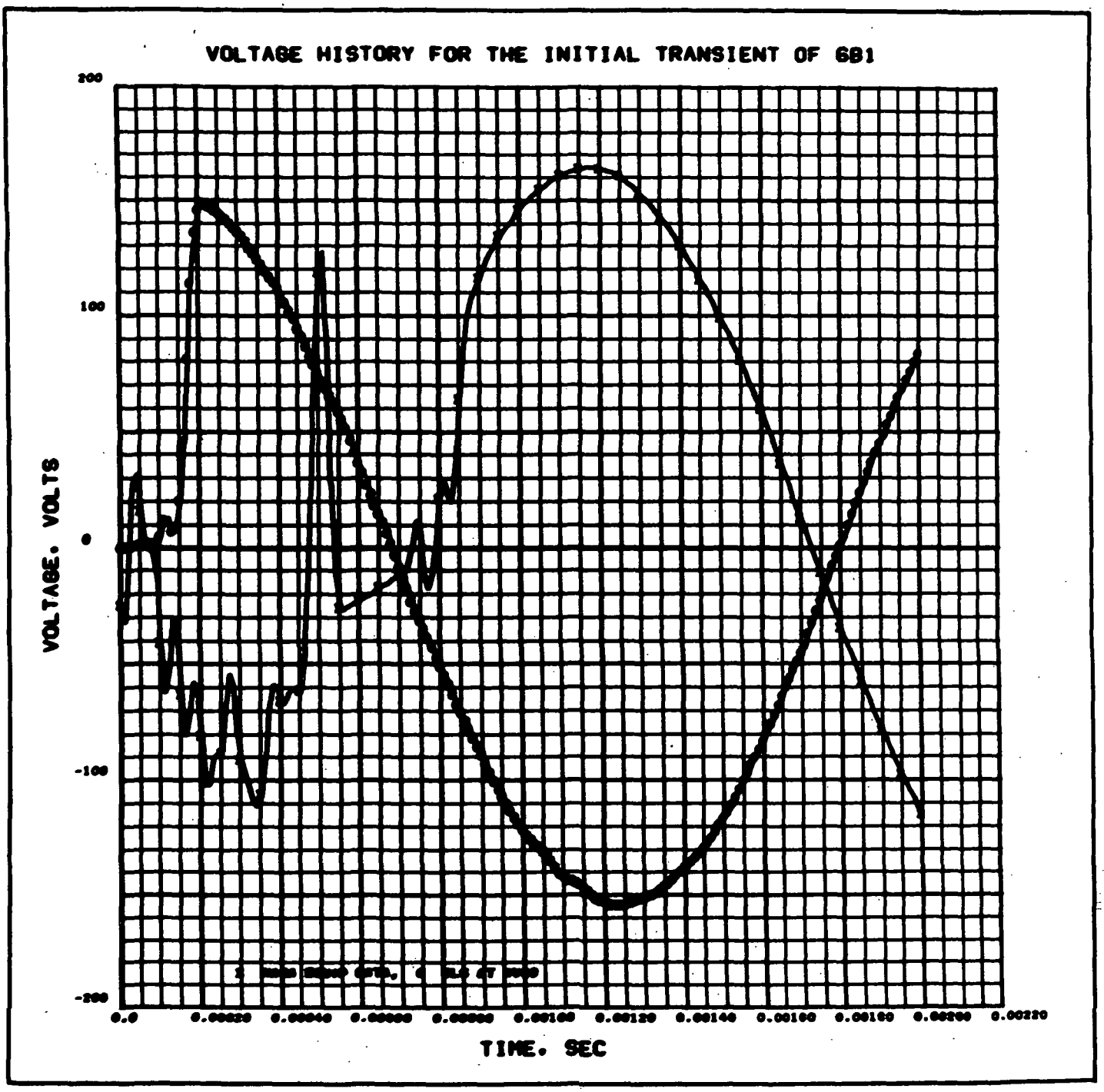

FIGURE 6-4 Comparison of NASA Voltage History (Interrogation Data) with Avco Voltage History for Heat Exchanger Valve, Run 6B

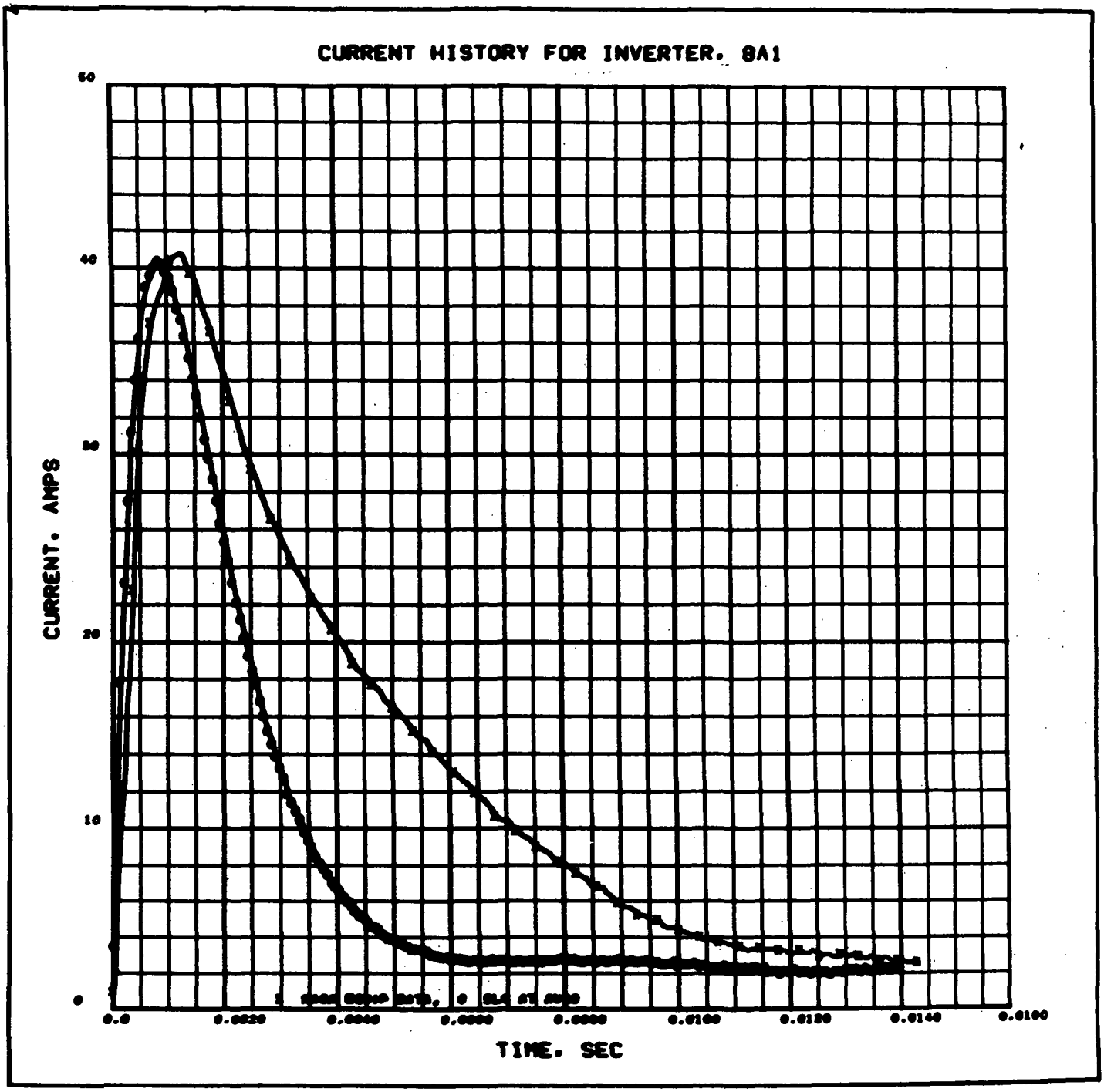

FIGURE 6-5 Comparison of Interrogation Data with Model Response for Varo Inverter, First Event, Run 8A1

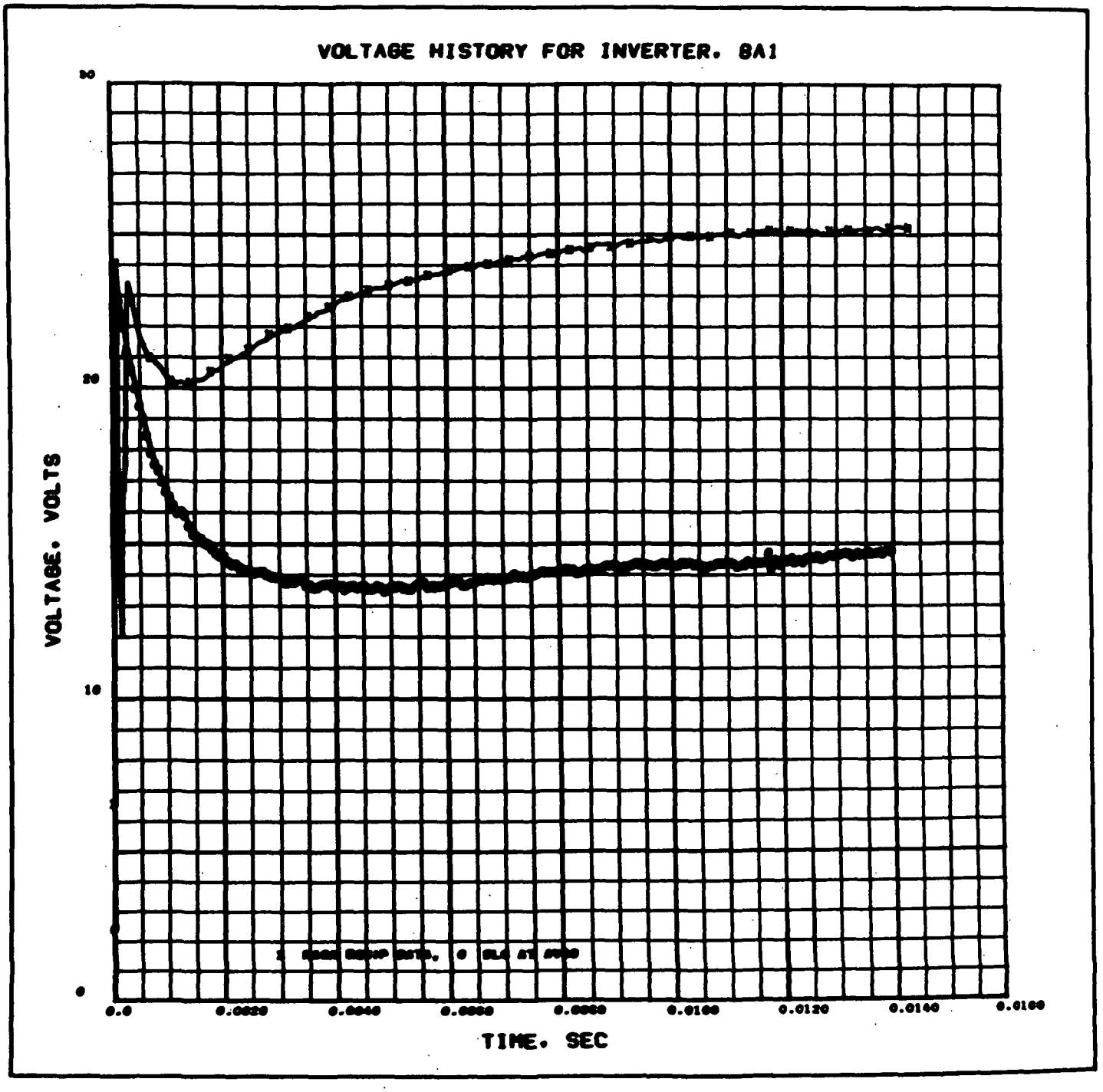

FIGURE 6-6 Comparison of NASA Voltage History (Interrogation Data) with Avco Voltage History for Varo Inverter, First Event, Run 8A1

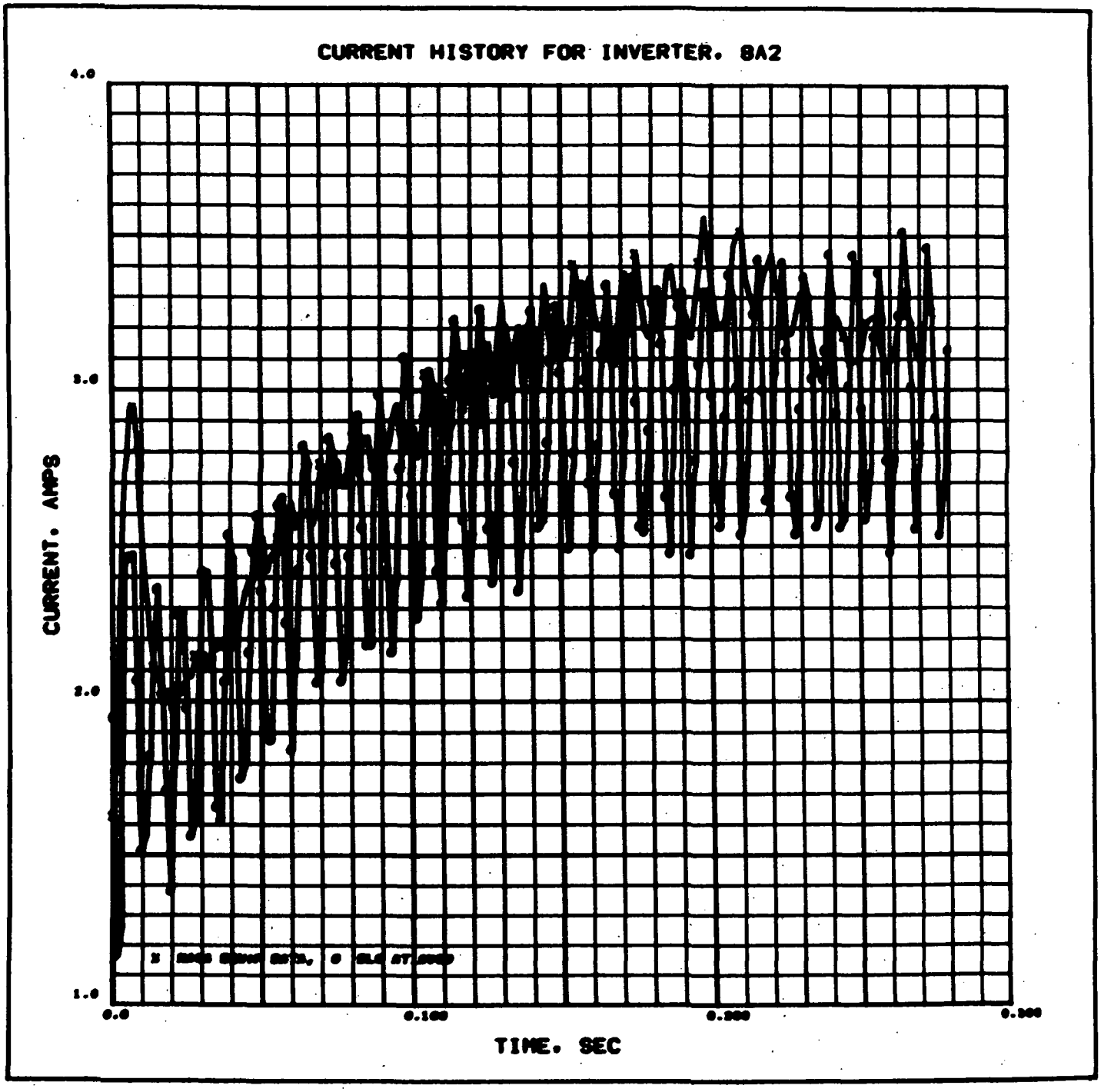

FIGURE 6-7 Comparison of Interrogation Data with Model Response for Varo Inverter, Second Event, Run 8A2

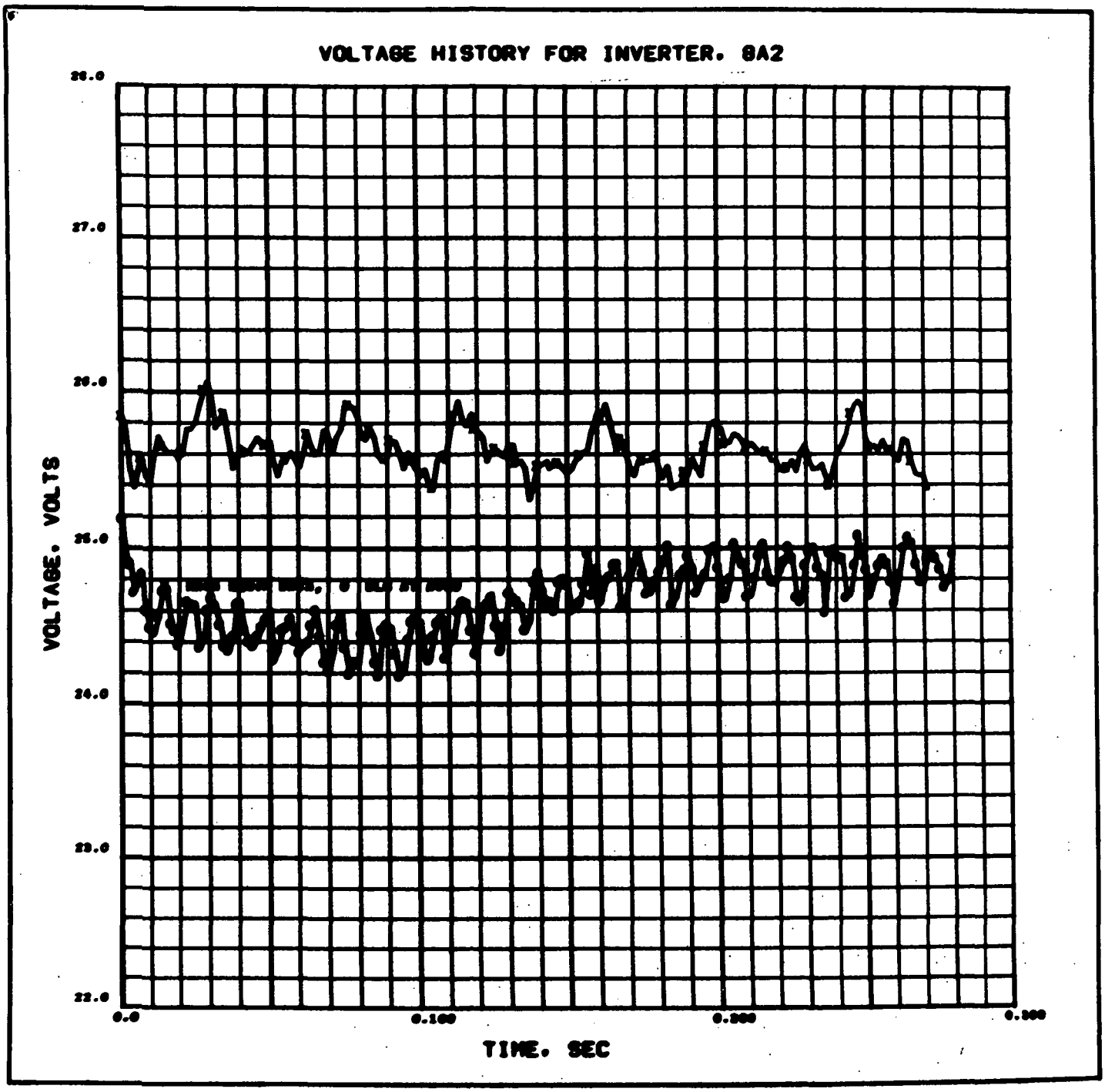

FIGURE 6-8 Comparison of NASA Voltage History (Interrogation Data) with Avco Voltage History for Varo Inverter, Second Event, Run 8A2

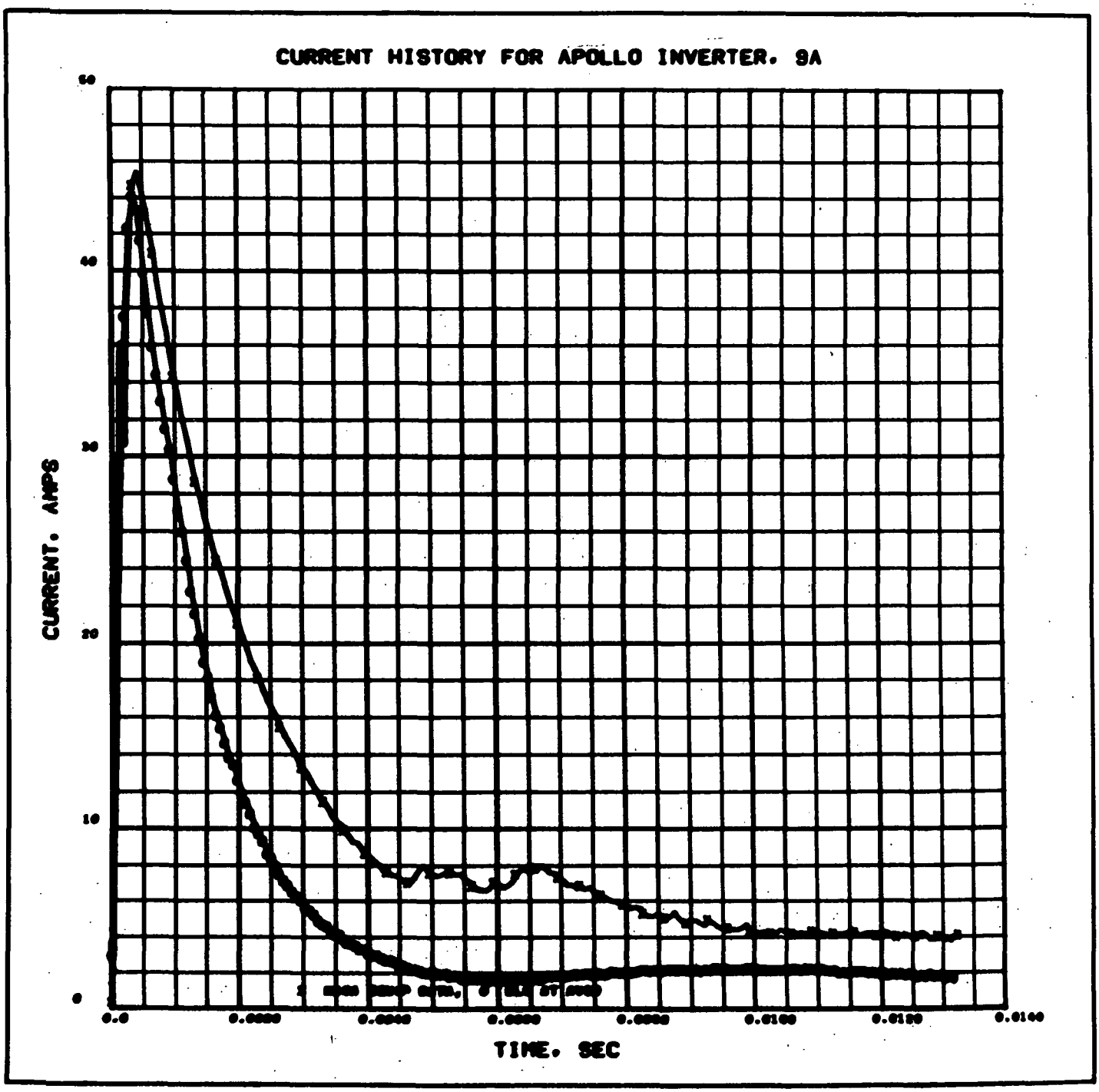

FIGURE 6-9 Comparison of Interrogation Data with Model Response for Apollo Inverter, Run 9A

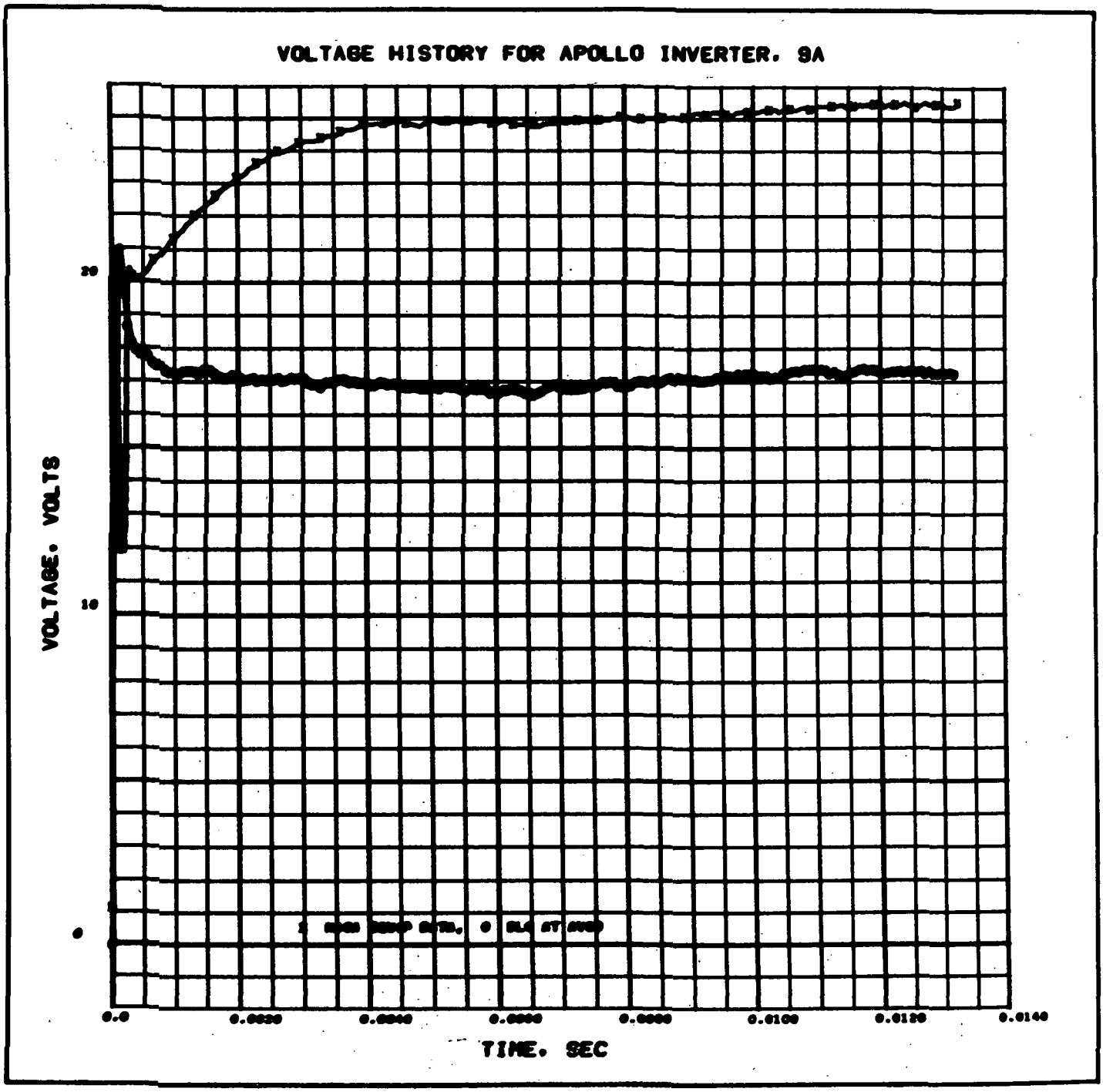

FIGURE 6-10 Comparison of NASA Voltage History (Interrogation Data) with Avco Voltage History for Apollo Inverter, Run 9A

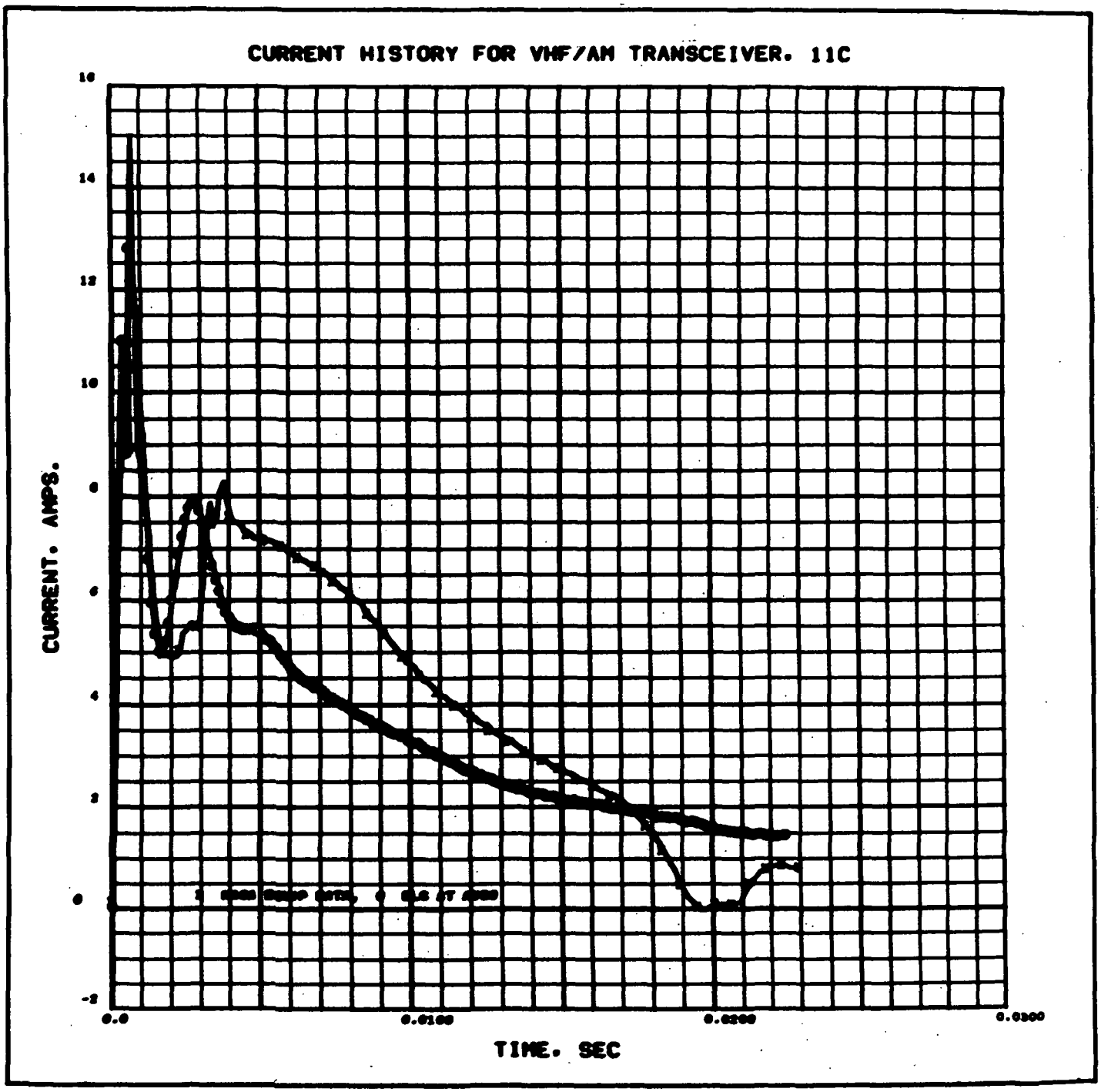

FIGURE 6-11 Comparison of Interrogation Data with Model Response for VHF/AM Transceiver, Run 11C

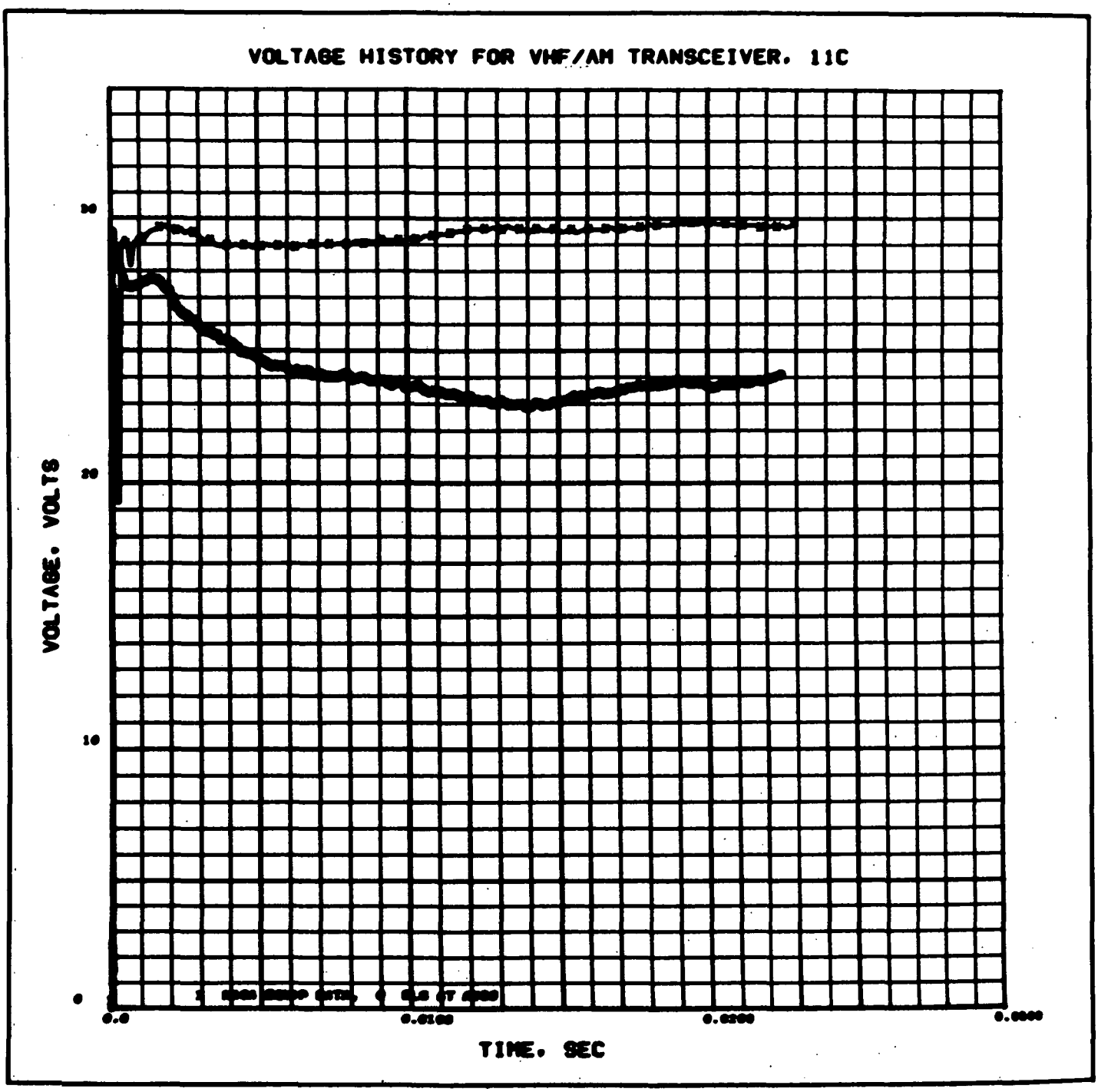

FIGURE 6-12 Comparison of NASA Voltage History (Interrogation Data) with Avco Voltage History for VHF /AM Transceiver, Run 11C

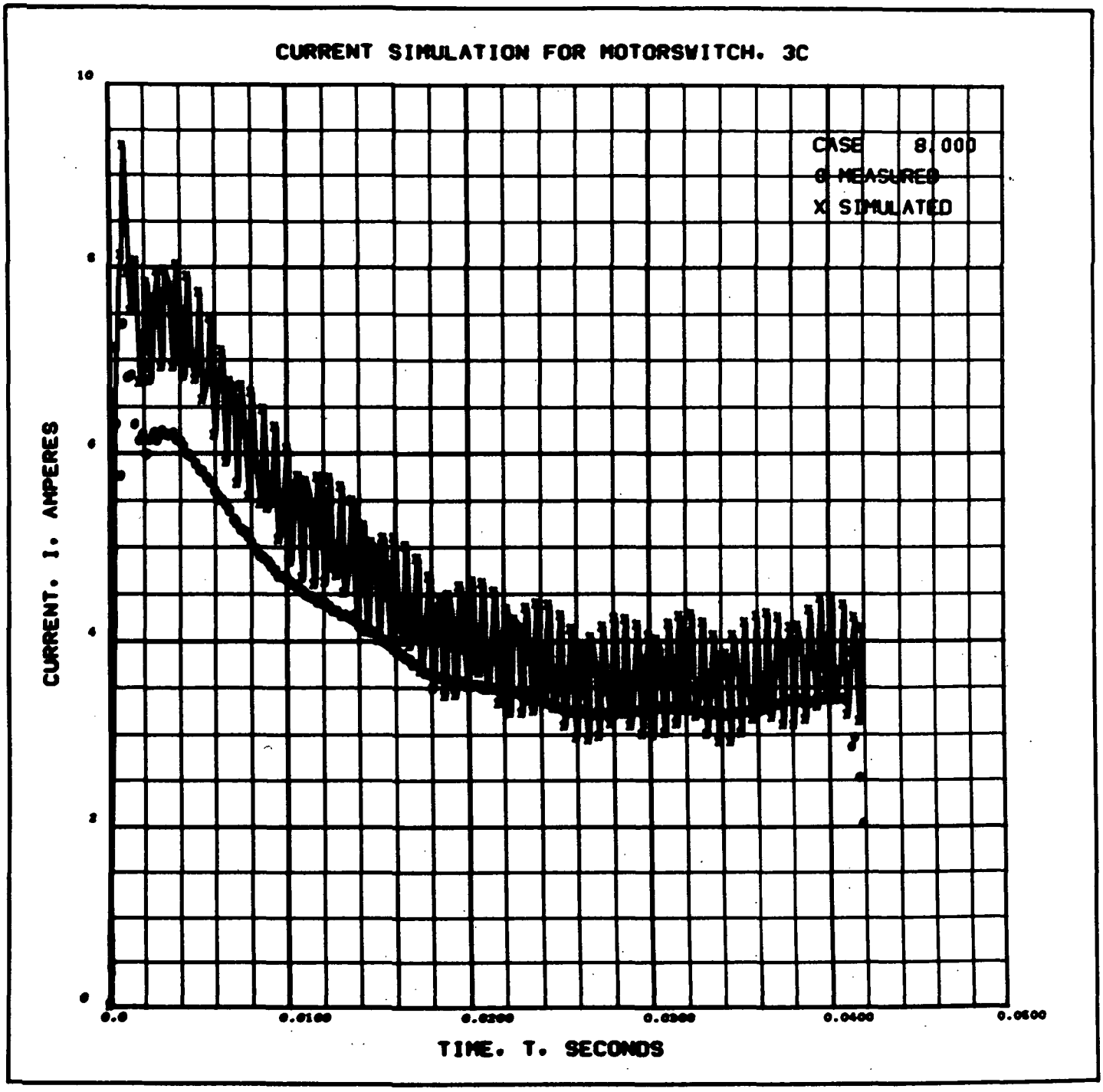

FIGURE 6-13 Comparison of Model Response with Computer-Predicted Response Using Nominal Element Values and Avco Voltage History for Motor Switch, Run 3C

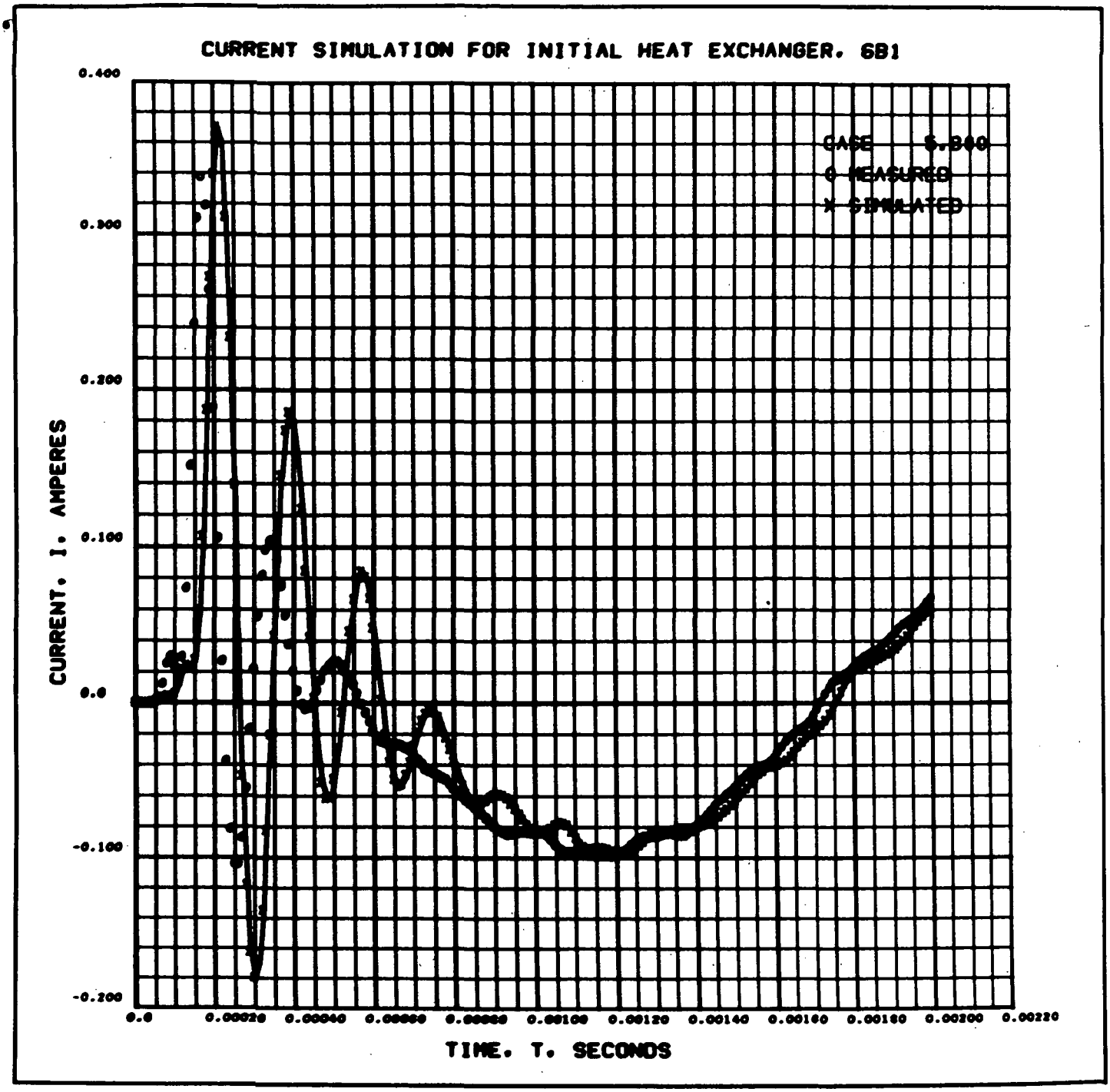

FIGURE 6-14 Comparison of Model Response with Computer-Predicted Response Using Nominal Element Values and Avco Voltage History for Heat Exchanger Valve, Run 6B

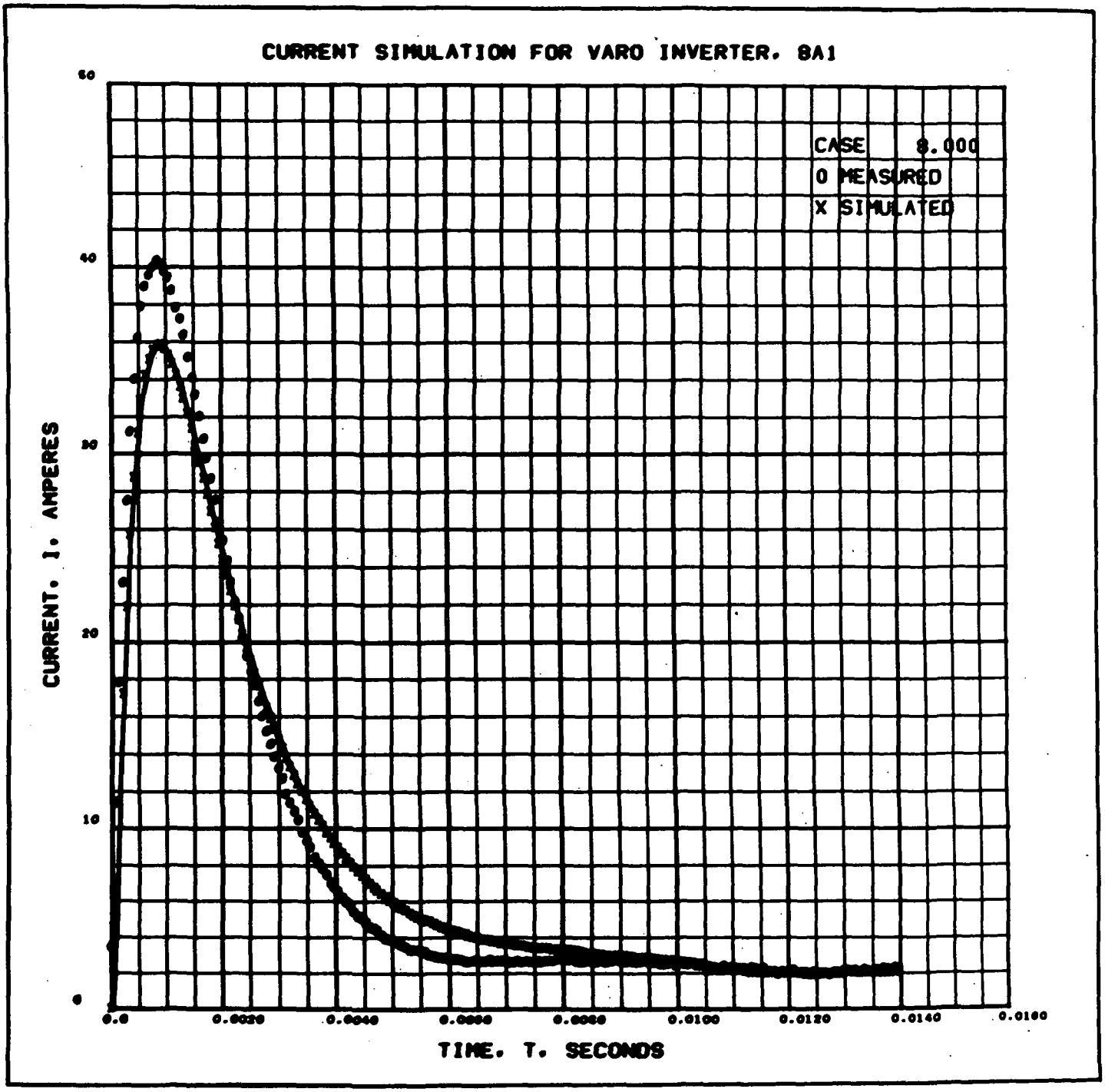

FIGURE 6-15 Comparison of Model Response with Computer-Predicted Response Using Nominal Element Values and Avco Voltage History for Varo Inverter, First Event, Run 8A1

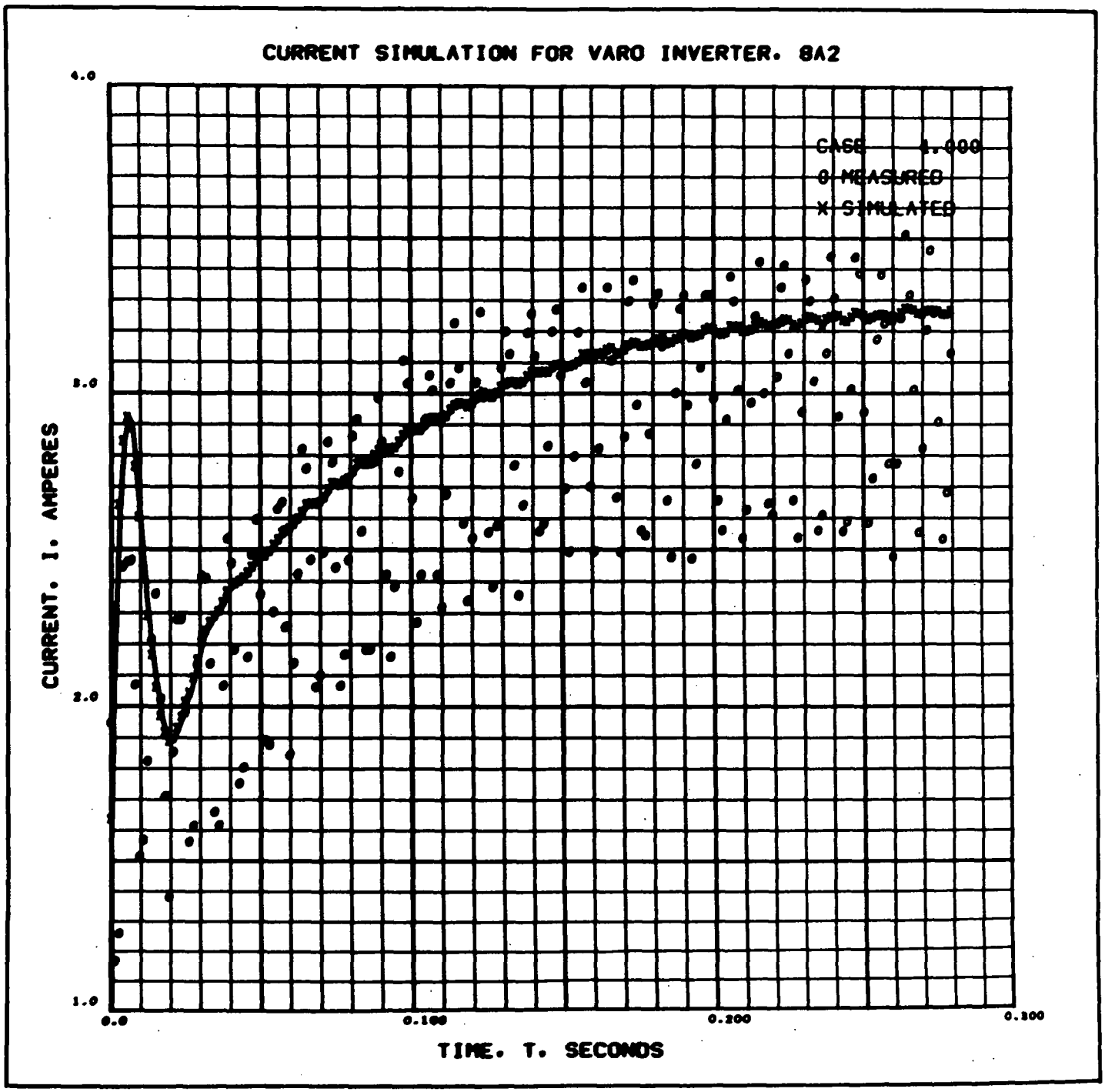

FIGURE 6-16 Comparison of Model Response with Computer-Predicted Response Using Nominal Element Values and Avco Voltage History for Varo Inverter, Second Event, Run 8A2

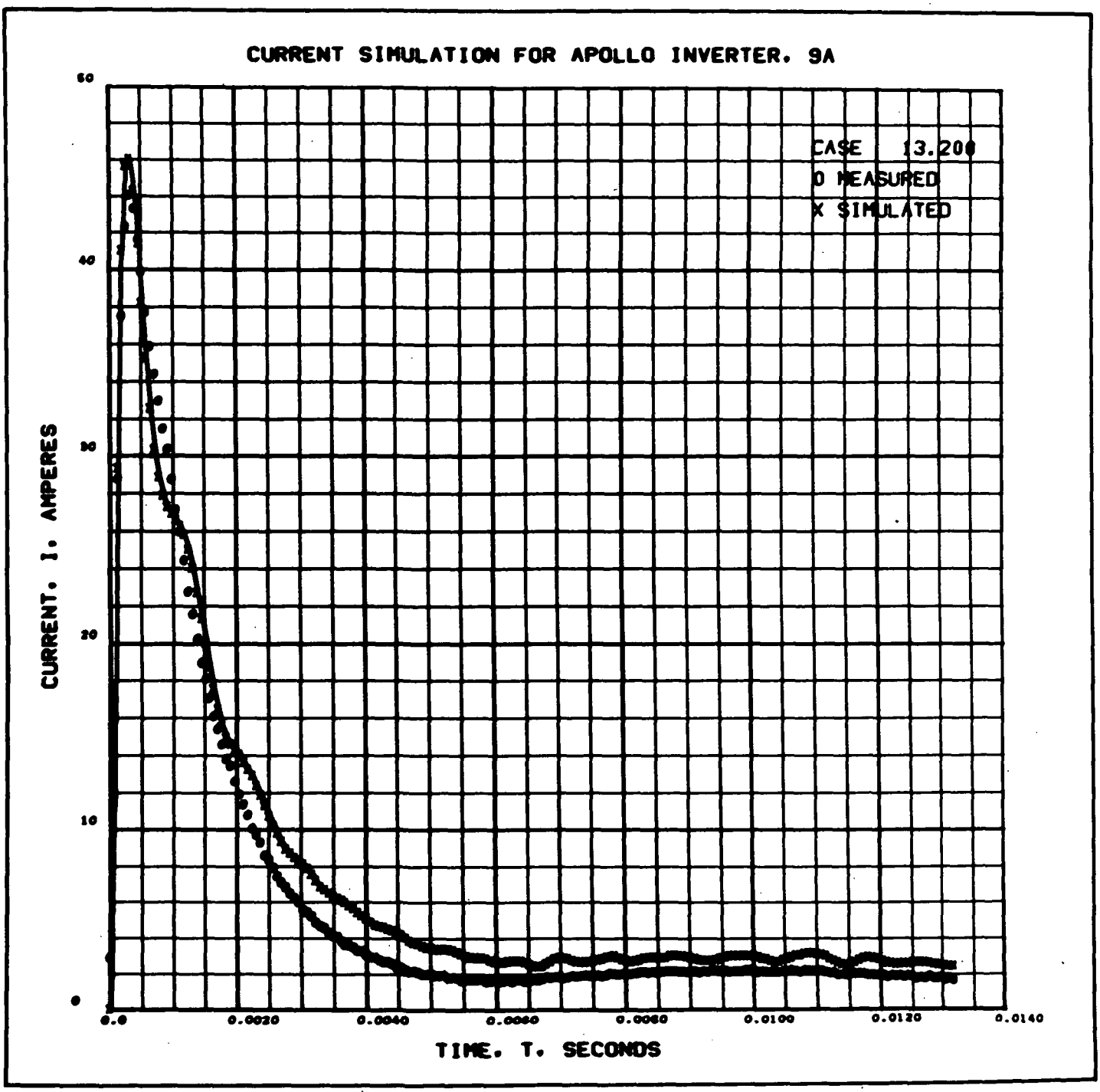

FIGURE 6-17 Comparison of Model Response with Computer-Predicted Response Using Nominal Element Values and Avco Voltage History for Apollo Inverter, Run 9A

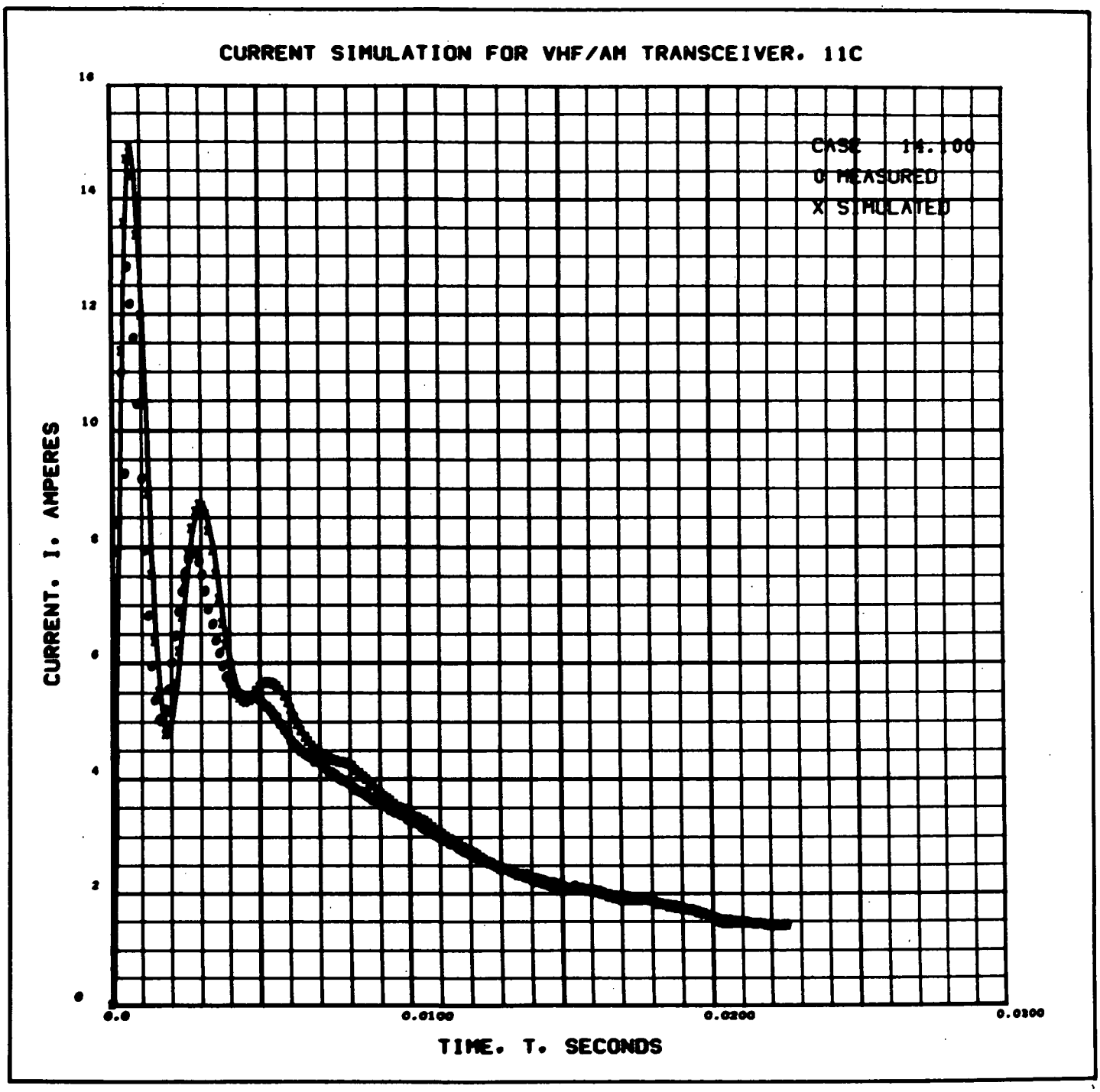

FIGURE 6-18 Comparison of Model Response with Computer-Predicted Response Using Nominal Element Values and Avco Voltage History for VHF/AM Transceiver, Run 11C

TABLE 6-VI

ACTUAL MODEL VALUES FOR SIMULATION OF FIVE SELECTED EQUIPMENTS

Run	Branch	R1	L	L_R	C	1/G	R_s
		ohms	mH	ohms	μf	ohms	ohms
3C	1	4.92	1.73	0.14	108	Open	0.10
	2	0.01	6.8	0.15	1.48	Open	0.10
	3	4.04	3.0	0.14	8200	9.8	0.10
6B	1	1490	180	1.09	0	0.01	0.10
	2	79.5	8.3	0.22	0.103	Open	0.10
8A	1	0.209	0.198	0.11	8200	14.9	0.10
	2	14.8	900	2.98	0	0.01	0.10
	3	11.9	0.052	0.08	401	Open	0.10
9A	1	0.209	0.052	0.08	4050	11.8	0.10
	2	0.97	0.36	0.11	61.5	773	0.10
11C	1	1.21	1.08	0.14	164	Open	0.10
	2	3.09	1.32	0.14	4050	Open	0.10

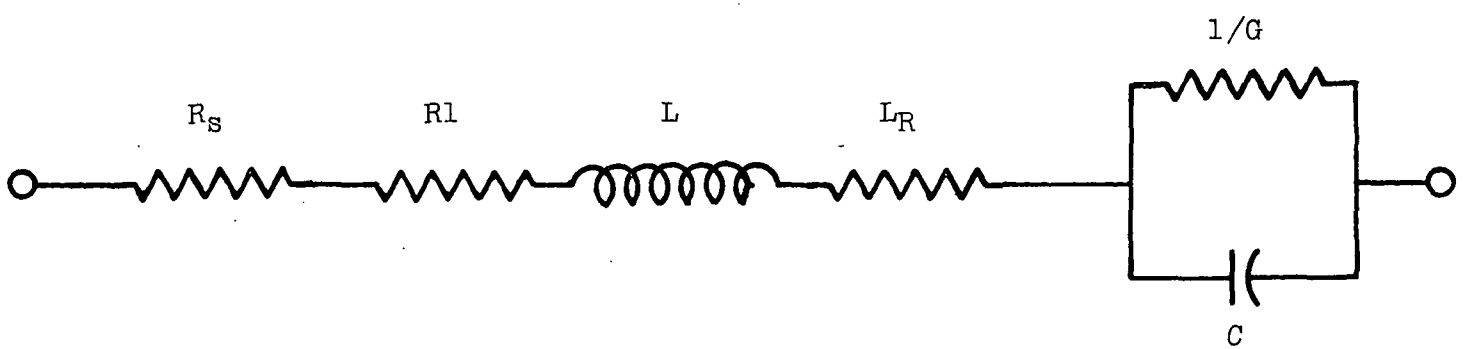

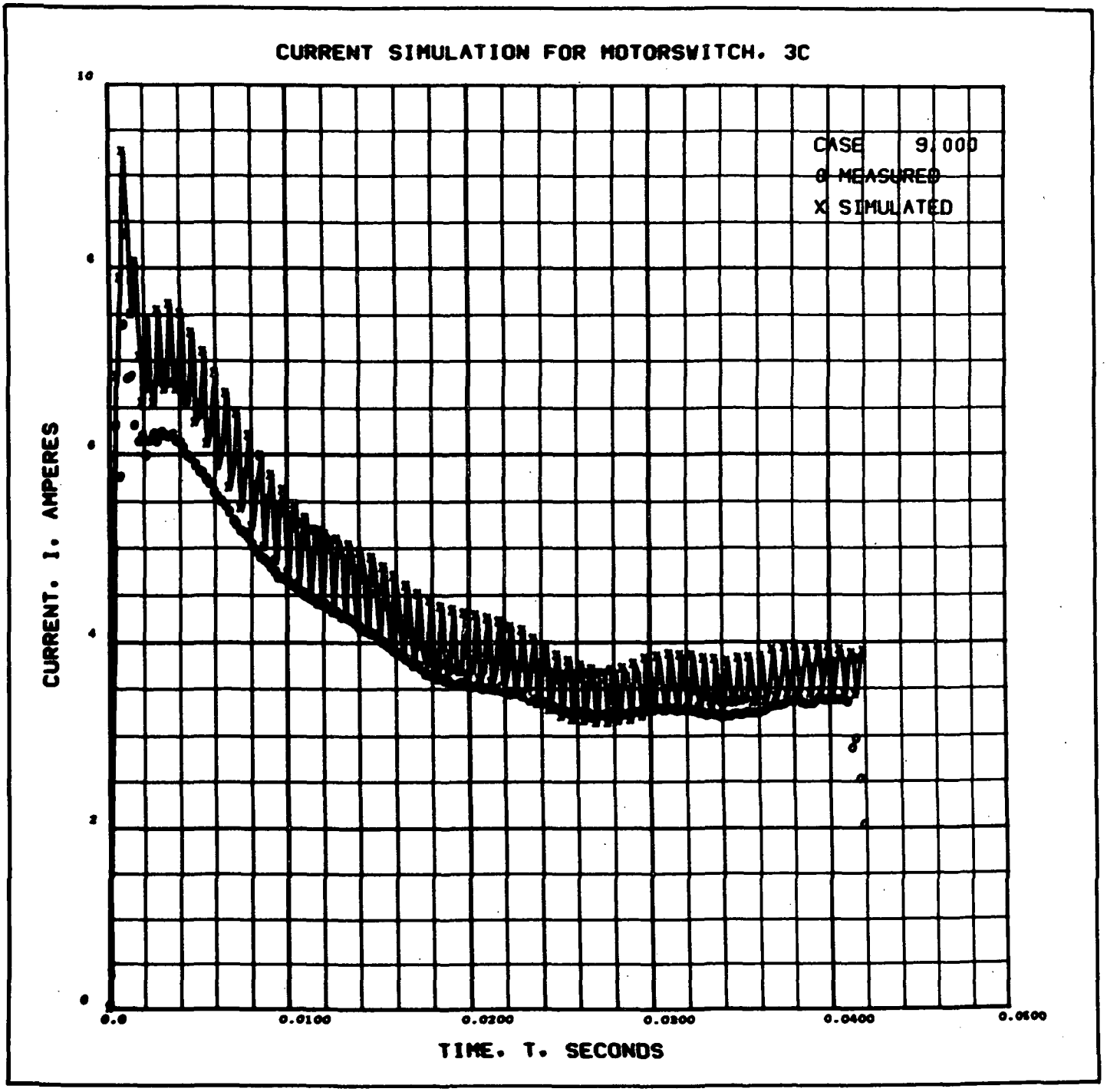

FIGURE 6-19 Comparison of Model Response with Computer-Predicted Response Using Actual Element Values and Avco Voltage History for Motor Switch, Run 3C

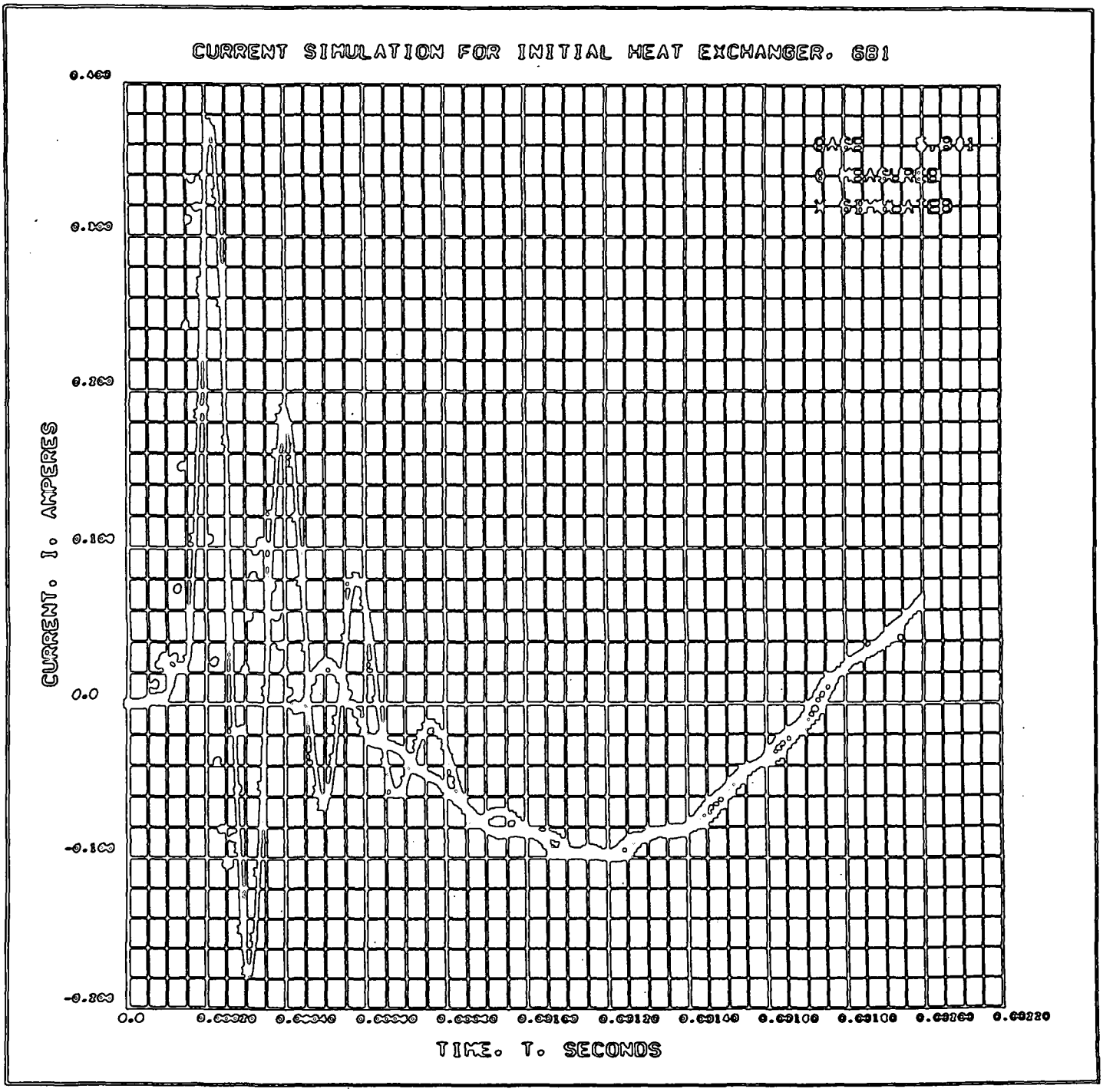

FIGURE 6-20 Comparison of Model Response with Computer-Predicted Response Using Actual Element Values and Avco Voltage History for Heat Exchanger Valve, Run 6B

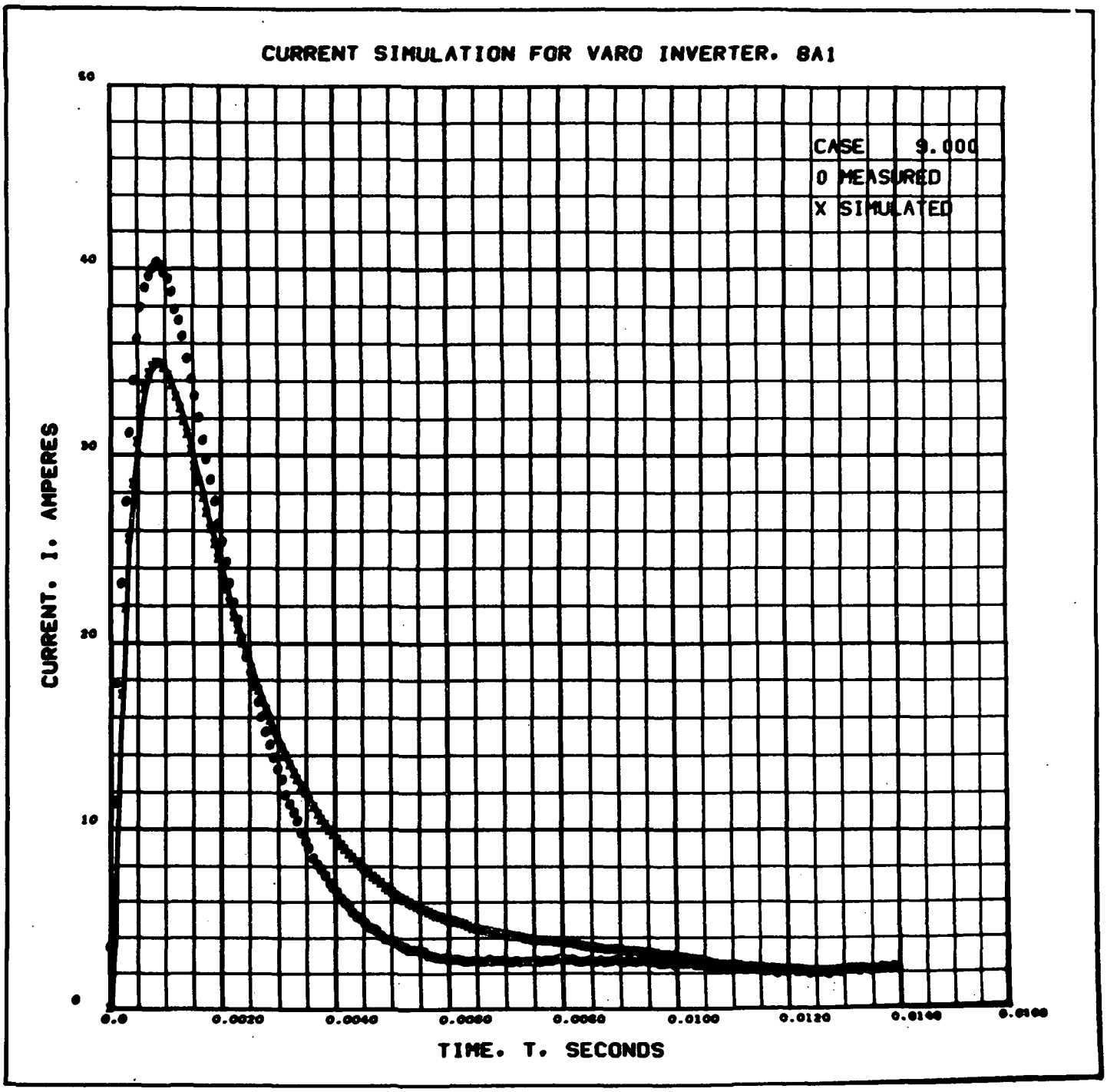

FIGURE 6-21 Comparison of Model Response with Computer-Predicted Response Using Actual Element Values and Avco Voltage History for Varo Inverter, First Event, Run 8A1

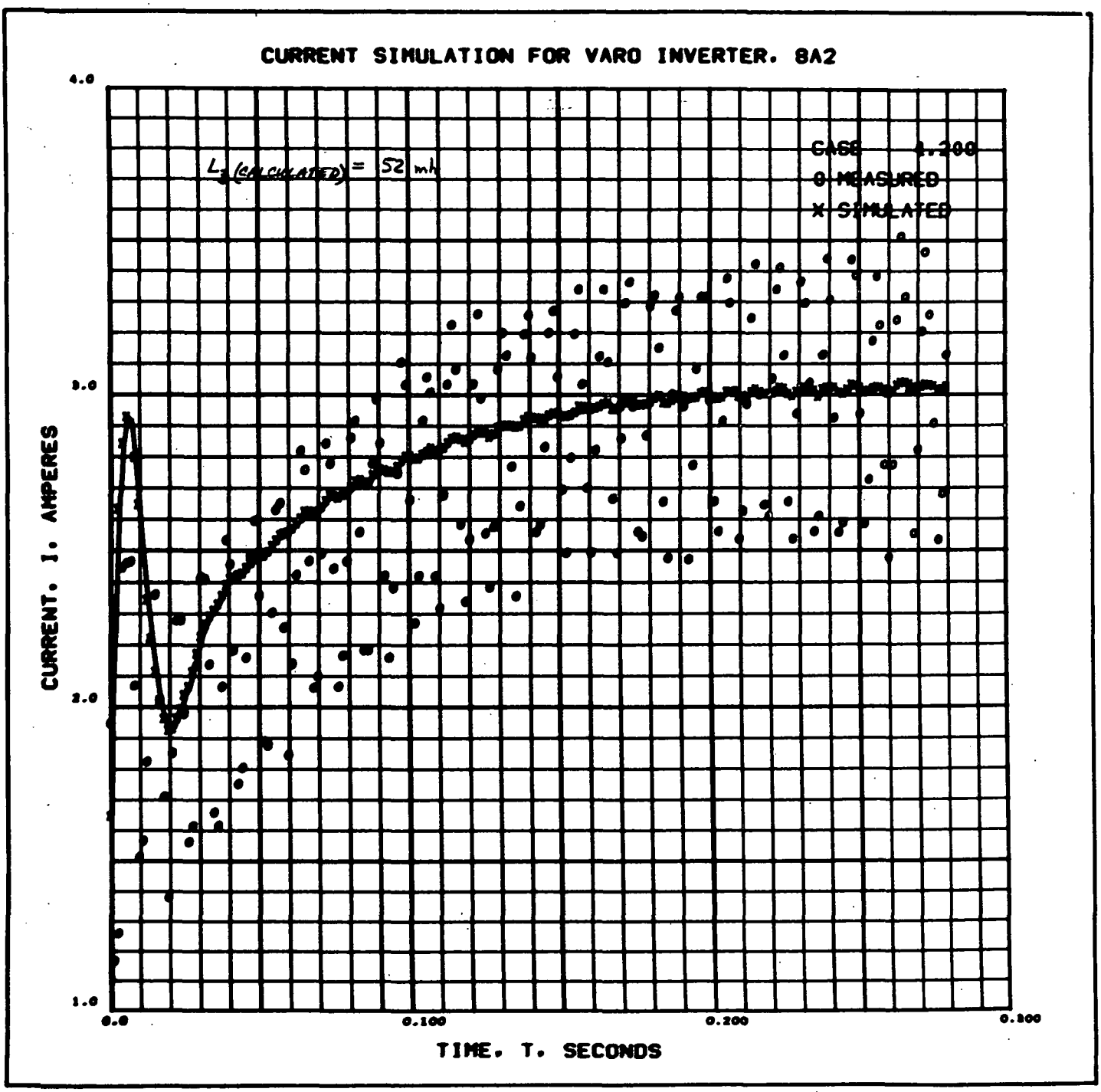

FIGURE 6-22 Comparison of Model Response with Computer-Predicted Response Using Actual Element Values and Avco Voltage History for Varo Inverter, Second Event, Run 8A2

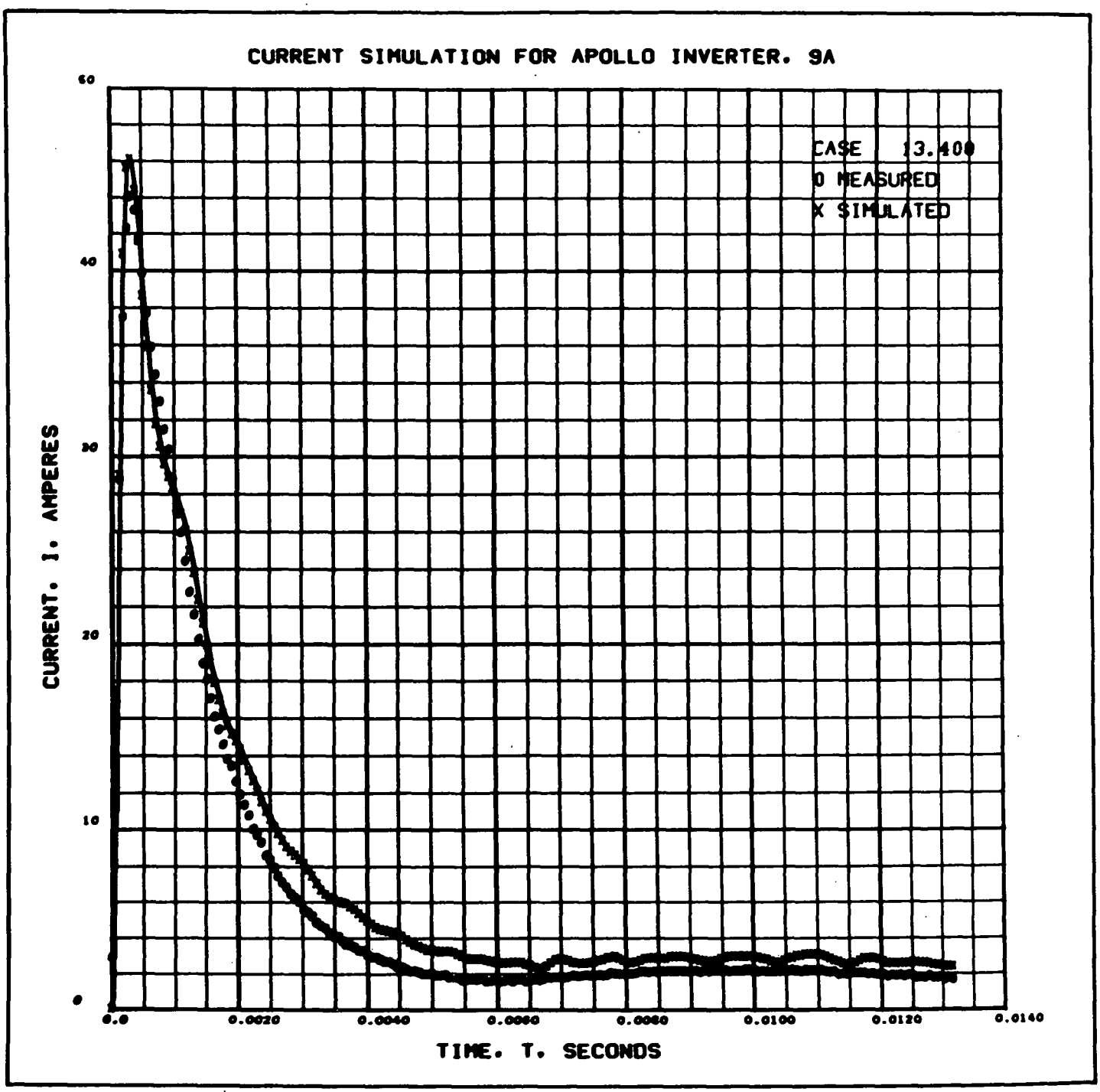

FIGURE 6-23 Comparison of Model Response with Computer-Predicted Response Using Actual Element Values and Avco Voltage History for Apollo Inverter, Run 9A

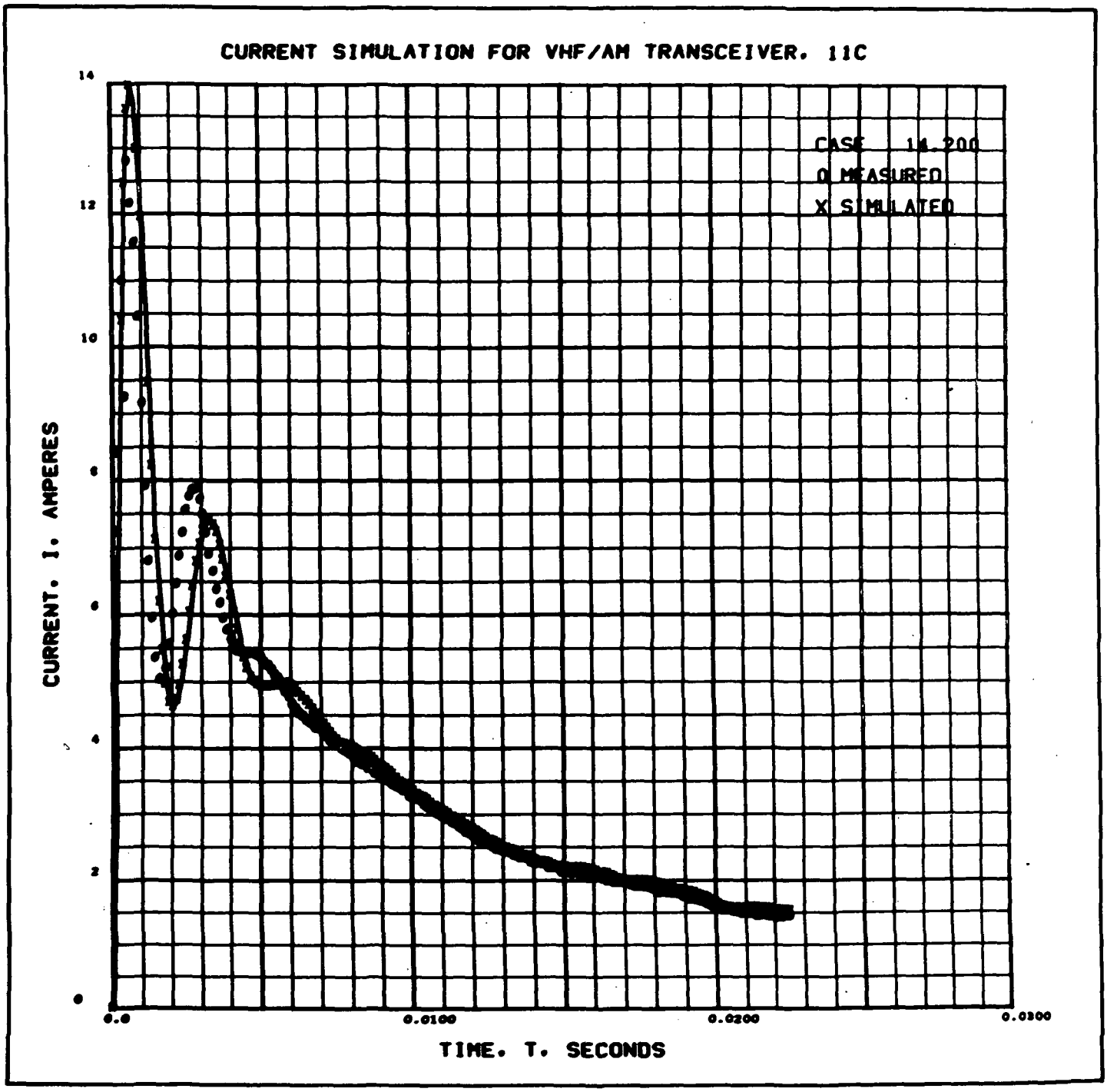

FIGURE 6-24 Comparison of Model Response with Computer-Predicted Response Using Actual Element Values and Avco Voltage History for VHF/AM Transceiver, Run 11C

Having eliminated the effects of the differences in voltage sources and having taken into account the actual element values used, the computer-predicted responses and the model responses show good correspondence. Thus, it is reasonable to conclude that had the model simulation performance been tested using the NASA voltage source and the optimizations done with the actual element inventory instead of the nominal values, the model response/actual equipment response comparisons would have shown more improved correspondence than that shown in Figures 6-1 through 6-12.

Figures 6-25 through 6-29 are oscilloscope traces of each of the five equipments simulated by the model during acceptance tests at NASA MSC. During these tests, the voltage source used was the same as that used during the original interrogations.

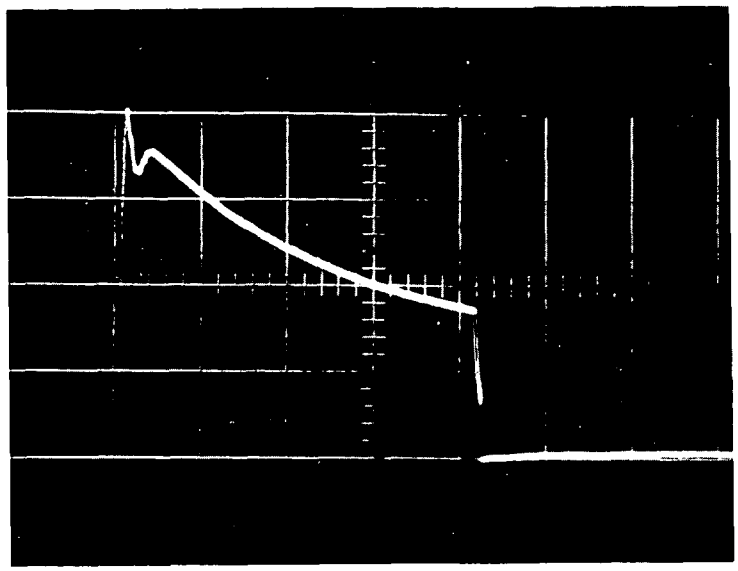

2 amp/cm

10 msec/cm

FIGURE 6-25 Model Response at MSC, Motor Switch, Run 3C (Load Voltage = 35 VDC)

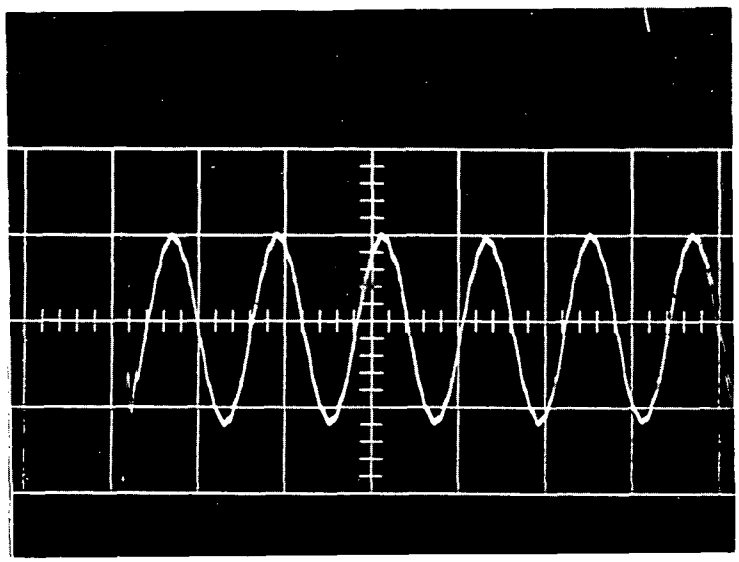

0.1 amp/cm

2 msec/cm

FIGURE 6-26 Model Response at MSC, Heat Exchanger Valve, Run 6B (Load Voltage = 114 VRMS, 400 Hz)

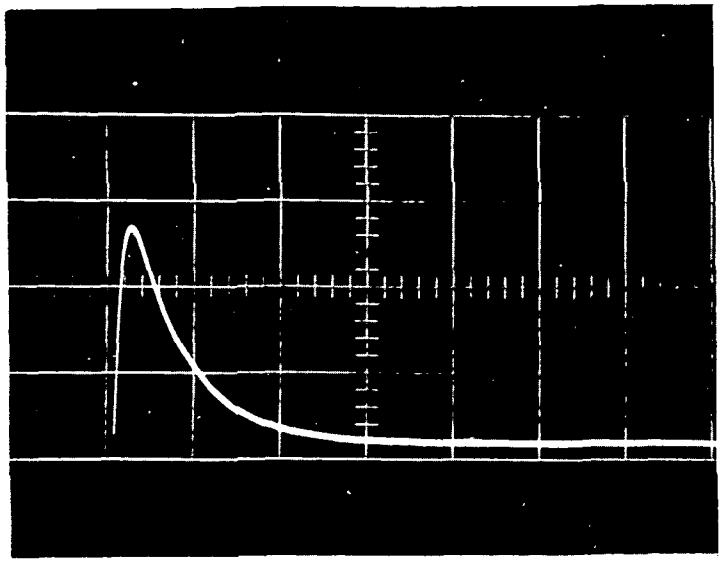

15 amp/cm

5 msec/cm

RUN 8A1

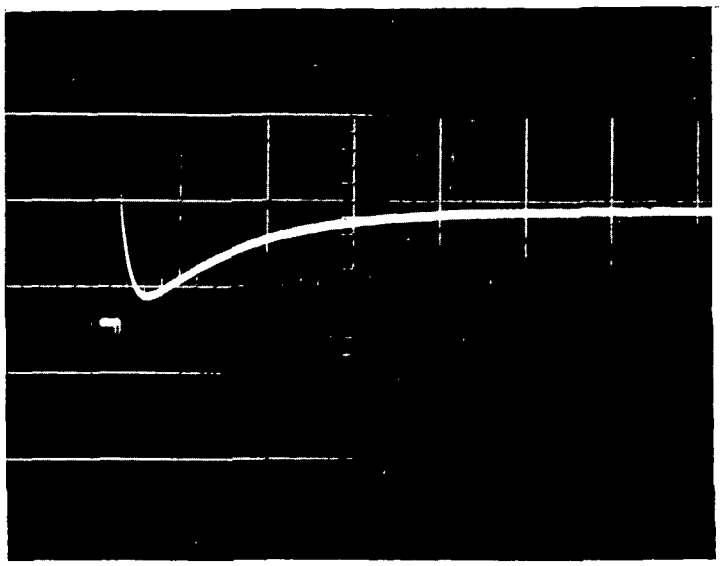

1 amp/cm

50 msec/cm

RUN 8A2

FIGURE 6-27 Model Response at MSC, Varo Inverter, Run 8A1, First Event, and Run 8A2, Second Event (Branch 1 R1 = 0.2 ohm, Load Voltage = 26 VDC)

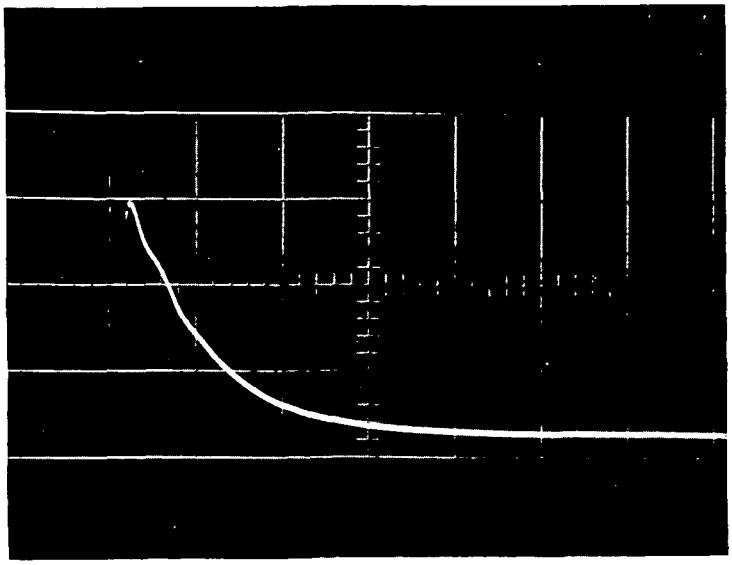

15 amp/cm

2 msec/cm

FIGURE 6-28 Model Response at MSC, Apollo Inverter, Run 9A (Branch 1 R1 = 0.2 ohm, Load Voltage = 26 VDC)

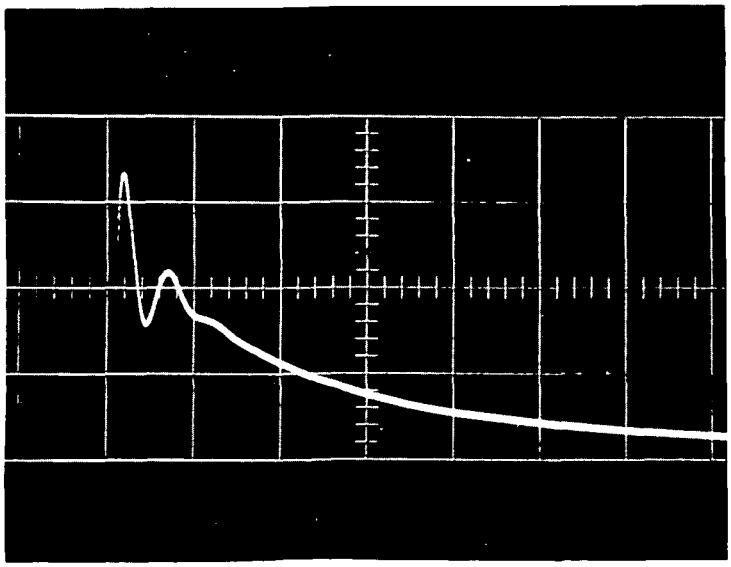

4 amp/cm

5 msec/cm

FIGURE 6-29 Model Response at MSC, VHF/AM Transceiver, Run 11C (Branch 1 R1 = 1 ohm, Branch 2 R1 = 2.5 ohms, Load Voltage = 30 VDC)

6.2 VARIABLE R EVALUATION

Development testing of the variable R consisted of an evaluation of the unit's performance capabilities and safety features. In addition, the ability of the variable R to simulate actual spacecraft hardware was demonstrated for seven items of equipment. The results of this testing are presented in the following paragraphs.

6.2.1 Basic Performance

6.2.1.1 Safety Features

The variable R provides four basic safety features for protection of its circuitry against improper operation. These features are identified in Table 6-VII along with the measured performance level of each.

6.2.1.2 Frequency Response

The frequency response of the variable R was determined by measuring the current response to a square wave control signal at a pulse repetition frequency (PRF) of 10 kHz. The response was judged to be flat over the range of DC to 10 kHz.

The transient response of the variable R was evaluated on its ability to respond to pulse control signal inputs. Pulses obtained from a function generator were provided as control signals while the variable R output was connected to a 20-volt DC source. The pulse inputs were essentially square (zero rise and fall times) and flat. Table 6-VIII lists the output current rise and fall times for a 1-amp, 5-amp, and 10-amp pulse.

6.2.1.3 Variable R Transfer Characteristic

As discussed in Paragraph 5.2.2, the basic variable R equation is

$$I_s = (V_s \ V_c)/20$$

where

I_s = Source current

V_s = Source voltage

V_c = Control voltage

TABLE 6-VII

VARIABLE R SAFETY CIRCUIT OPERATING LEVELS

Function	Measured Level	Indication
No control signal	$\leq$ 0.015 volts, peak	Amber Light
Load over-voltage	$\geq$ 77 volts, peak	Amber Light
Power overload	$\geq$ 250 watts, peak	Red Light
Reverse voltage	Not applicable	No Indication

TABLE 6-VIII

VARIABLE R PULSE RESPONSE TEST RESULTS

CONTROL SIGNAL AMPLITUDE	OUTPUT CURRENT*				
	AMPLITUDE	10% to 90%		0% to 100%	
		RISE TIME	FALL TIME	RISE TIME	FALL TIME
volts	amperes	microsecs	microsecs	microsecs	microsecs
1	1	8	7	20	20
5	5	6	13	14	25
10	10	7	18	15	30

* Load voltage = 20 volts

The variable R was evaluated for its ability to conform to this equation. The measured static transfer characteristics of the variable R are provided in Figure 6-30. These curves shown linear performance from the maximum current level of approximately 8 amperes to as low as 30 milliamperes, depending on the applied source voltage. The characteristic curves show varying degrees of non-linearity at the low current levels (less than 100 ma). The curves also show the limiting action of the power over-load circuit at the high current levels where the dissipation is automatically limited to 250 watts.

6.2.1.4 Current Monitor Transfer Characteristic

The variable R provides a convenient circuit for monitoring source current. This circuit provides a transfer function of 1 volt per ampere at any control or source voltage within the variable R's operating range. Thus, for a source current of 5 amperes, the current monitor circuit will provide 5 volts. The measured transfer characteristic for this circuit is provided in Figure 6-31.

6.2.2 Demonstration of Simulation Capability

The basic application of the variable R is the simulation of equipment response on the power lines. As a means of demonstrating this application, certain of the equipments that had been interrogated were selected for simulation and the interrogation data obtained at NASA MSC was used to generate an analog control signal to the variable R.

As described in Paragraph 4.2.2, the variable R control signal is an analog of the conductance-time curve of the equipment to be simulated. This signal is generally obtained by interrogating the equipment to be simulated and computing the input current/voltage ratio versus time, $G(t) = I(t)/E(t)$ and then scaling this function to correspond with the transfer characteristic. Thus, $V_c(t) = KG(t) = KI(t)/E(t)$.

For purposes of demonstrating the variable R device, the interrogation data obtained for the seven selected equipments (see Paragraph 4.3) was processed in a slightly different way than that depicted in Figure 4-32. For convenience, the input voltage was assumed constant, and the current data was simply scaled to obtain the $V_c(t)$ control signal. That is,

$$V_c(t) = K'I(t)$$

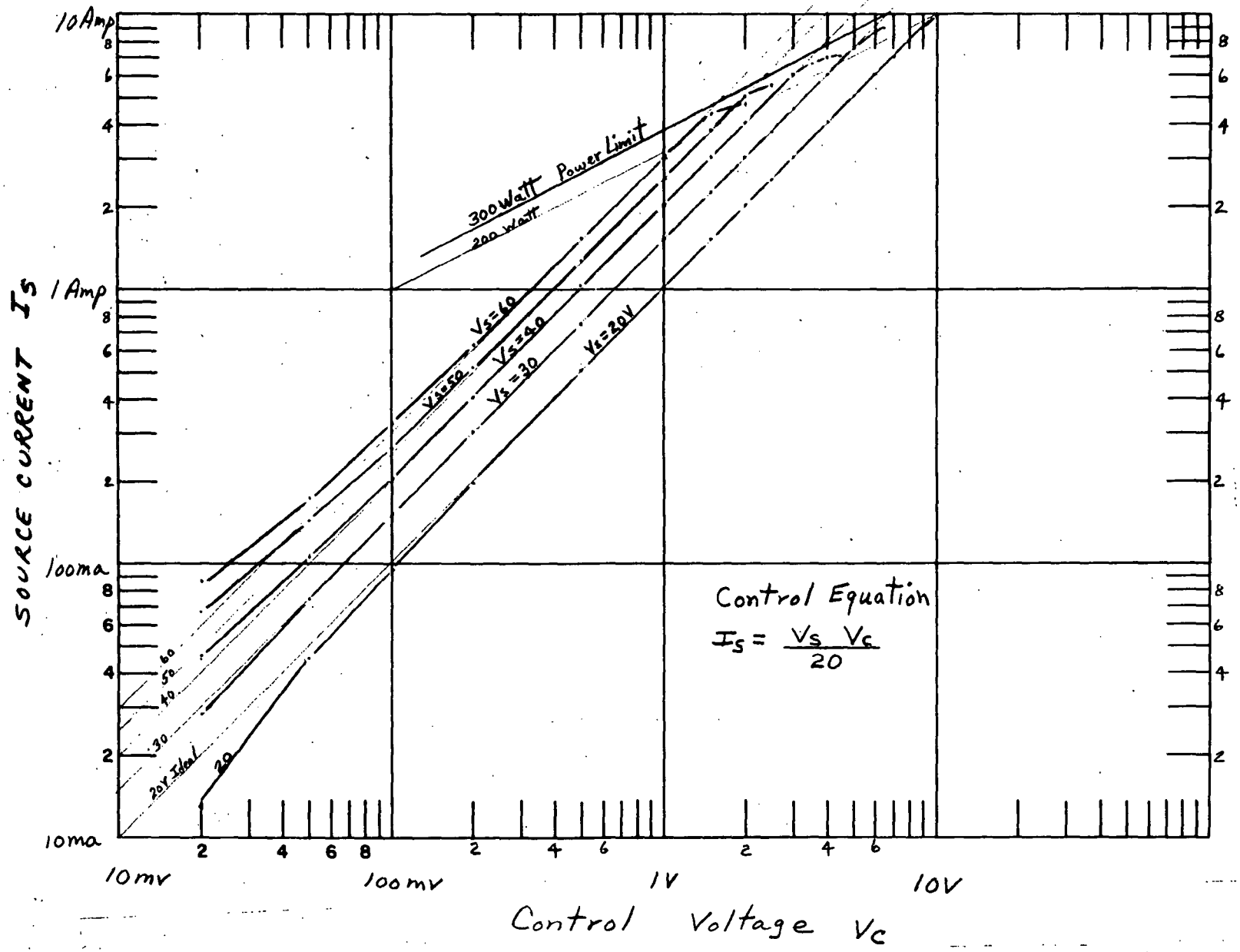

FIGURE 6-30 Variable R Static Transfer Characteristics

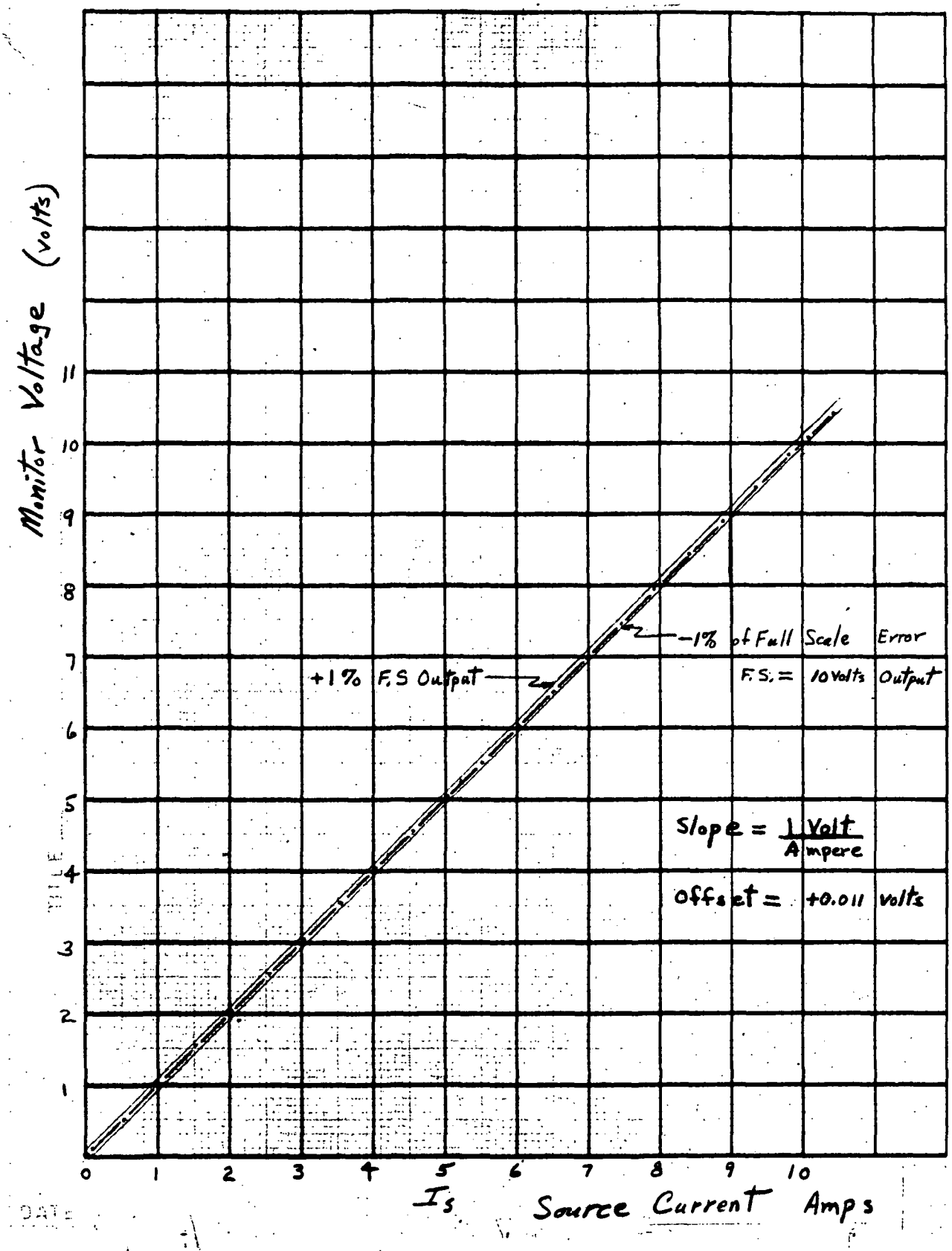

FIGURE 6-31 Variable R Current Monitor Transfer Characteristics

The variable R delivered as part of the Model DLS 1000 simulator is a 250-watt, peak, device. Several of the equipments selected for demonstration on the variable R have peak loads of up to approximately 1500 watts, therefore, in order to limit dissipation to 250 watts, the control voltages for these equipments were scaled. That is, the control voltage was reduced in amplitude such that the highest resultant peak current was 8 amperes.

In practice, of course, a variable R of higher power dissipation capabilities would be used for these equipments. However, for purposes of demonstrating the capabilities of a variable R device to faithfully reproduce even complex current waveforms, the scaling technique was justified.

The control tape used for demonstration of the variable R was generated in the following manner:

a. The calibration and current histories on the data acquisition tapes were FM demodulated and the levels measured.

b. A scaling factor was computed for reducing the calibration levels to fall within the variable R limits.

c. The playback demodulator was then calibrated such that the center frequency = 0 volts, and +40% deviation = +8 volts.

d. The demodulated signal was input to a 108 kHz VCO which was calibrated such that 0 volts = center frequency, and +8 volts = 40% deviation.

e. Approximately 20 seconds of both the 0-level and +8 volt level of calibration were then recorded on the control tape at a record speed of 60 ips. These calibrations are used for adjusting the playback demodulator on the control tape recorder each time the tape is used with the variable R.

f. Each original data run was then played back from the original tape and recorded on the control tape.

g. In addition, a voice annotation on track 1 of the control tape identifies the tape and data tracks, identifies the start and stop of each interval of data, and describes user tasks for calibrating the playback demodulator and adjusting the load power source.

h. This control tape was then played back on a tape reproducer and applied to the control input of the variable R. The load terminals of the variable R were connected to a suitable source of DC voltage.

The results of this testing are shown in the traces of Figures 6-32 through 6-38. In each case the control voltage input is shown on the lower trace, and the output (load) current is shown in the upper trace. The load voltage was adjusted for each equipment simulation to correspond to the level used during interrogation of the original equipment at MSC. These levels are identified on each figure. The control and current traces show excellent correspondence.

In addition to this data which was recorded at Avco, Figures 6-39 through 6-43 show oscilloscope traces of several of the simulations accomplished at NASA MSC during equipment acceptance. The control signals used in this instance were obtained from a magnetic tape generated from the master just described, and reproduced on an MSC-provided FR-600 tape recorder.

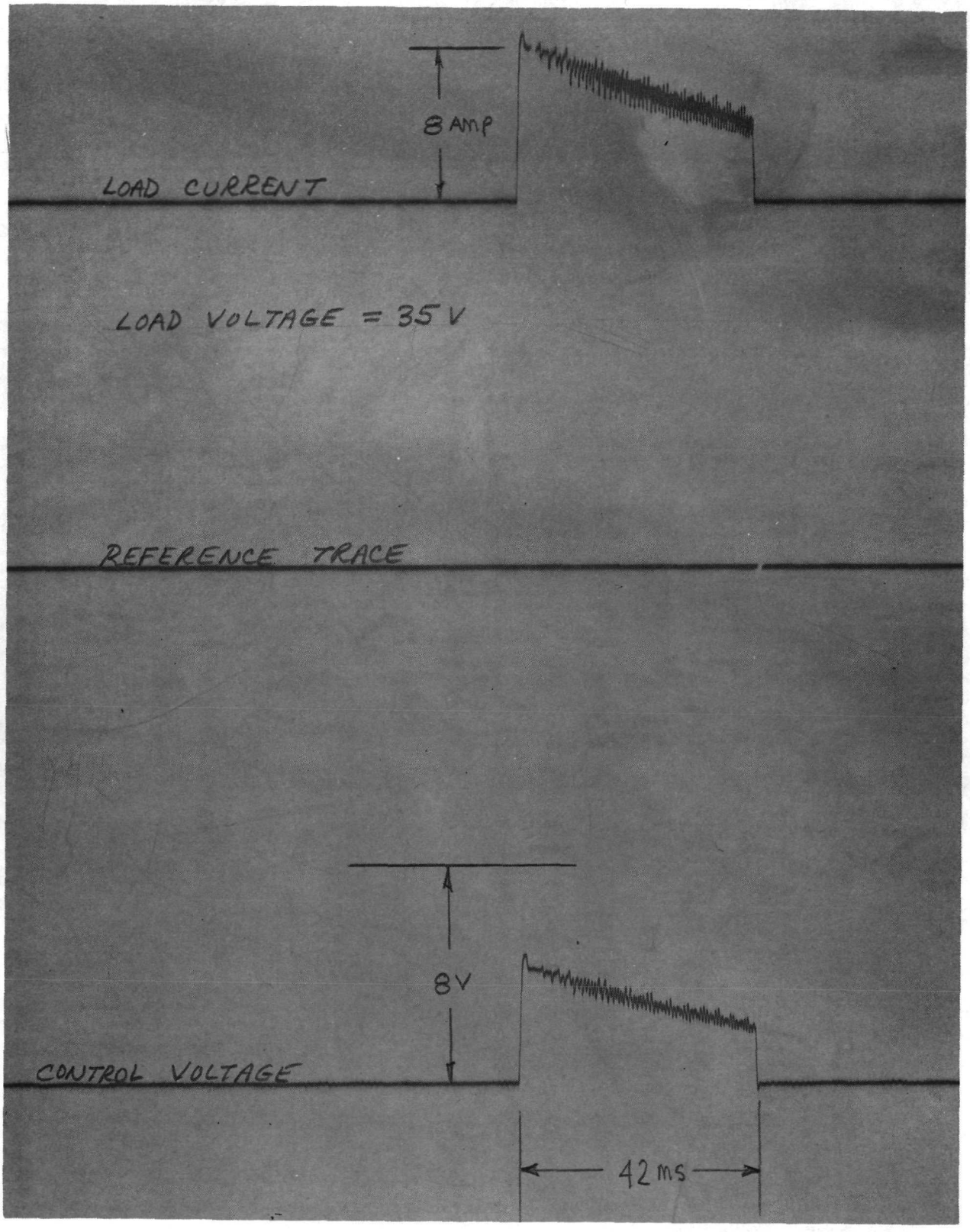

FIGURE 6-32 Oscillograph Record--Variable R Simulation of Motor Switch, Run 3C

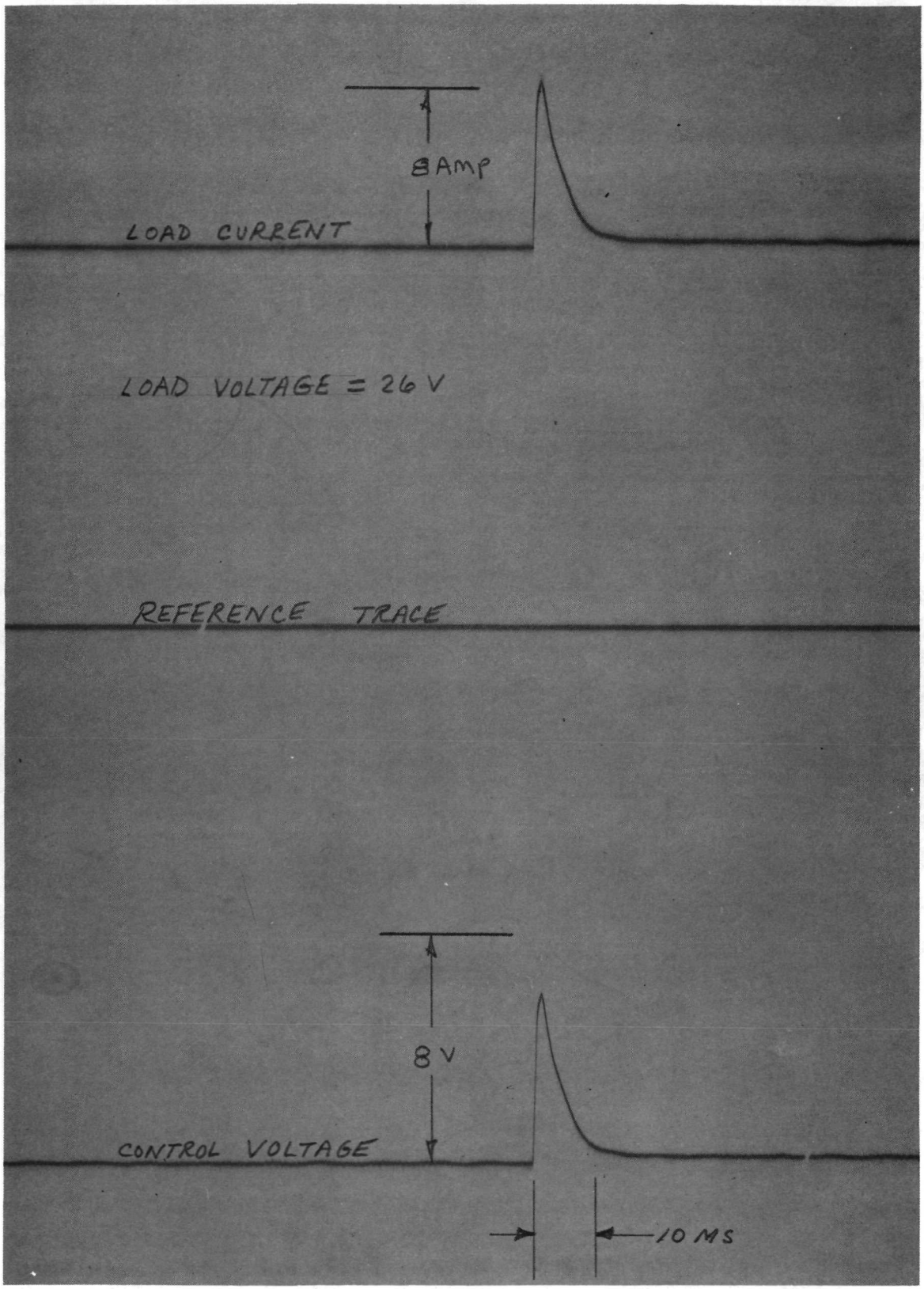

FIGURE 6-33 Oscillograph Record--Variable R Simulation of Varo Inverter (First Event), Run 8A1

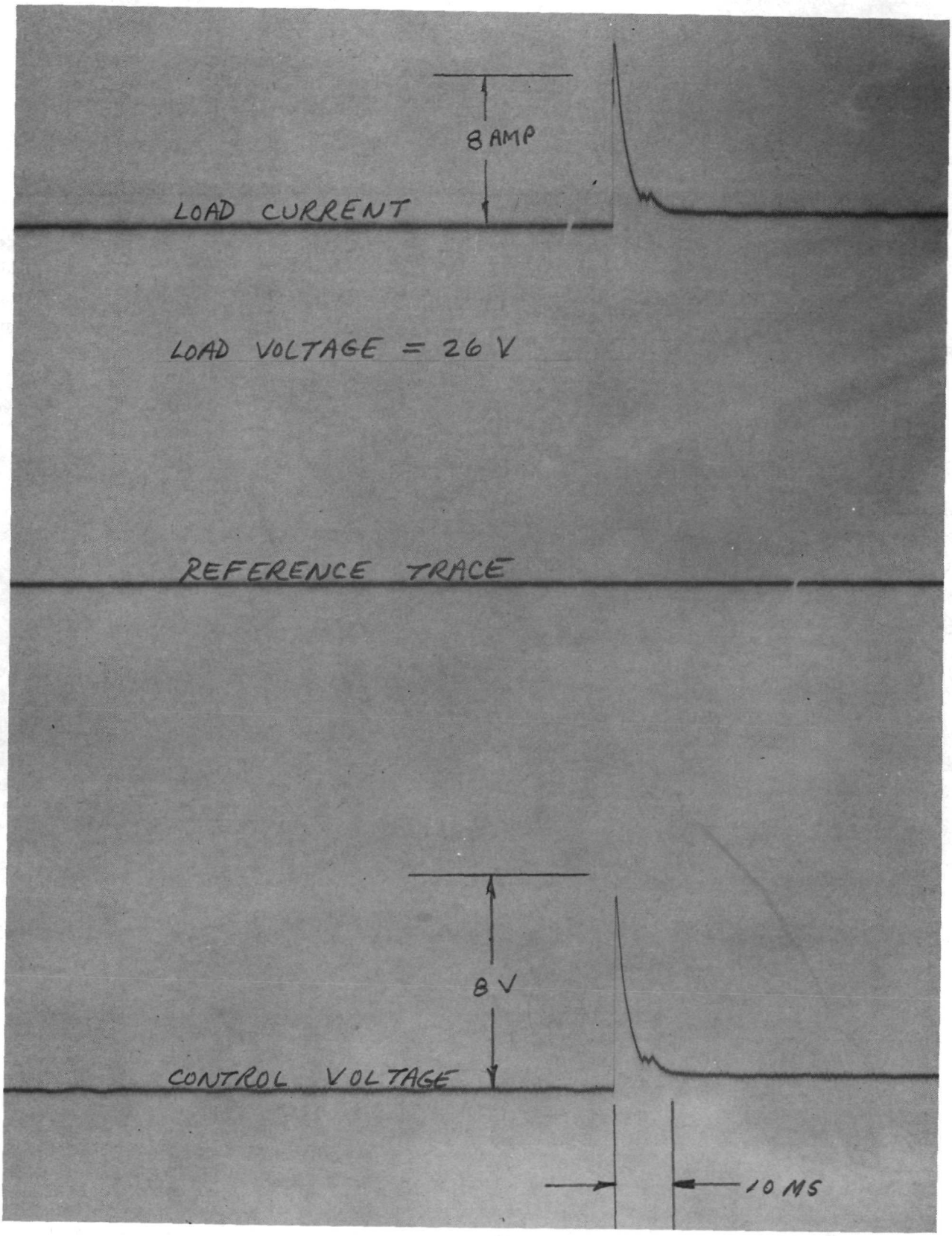

FIGURE 6-34 Oscillograph Record--Variable R Simulation of Apollo Inverter, Run 9A

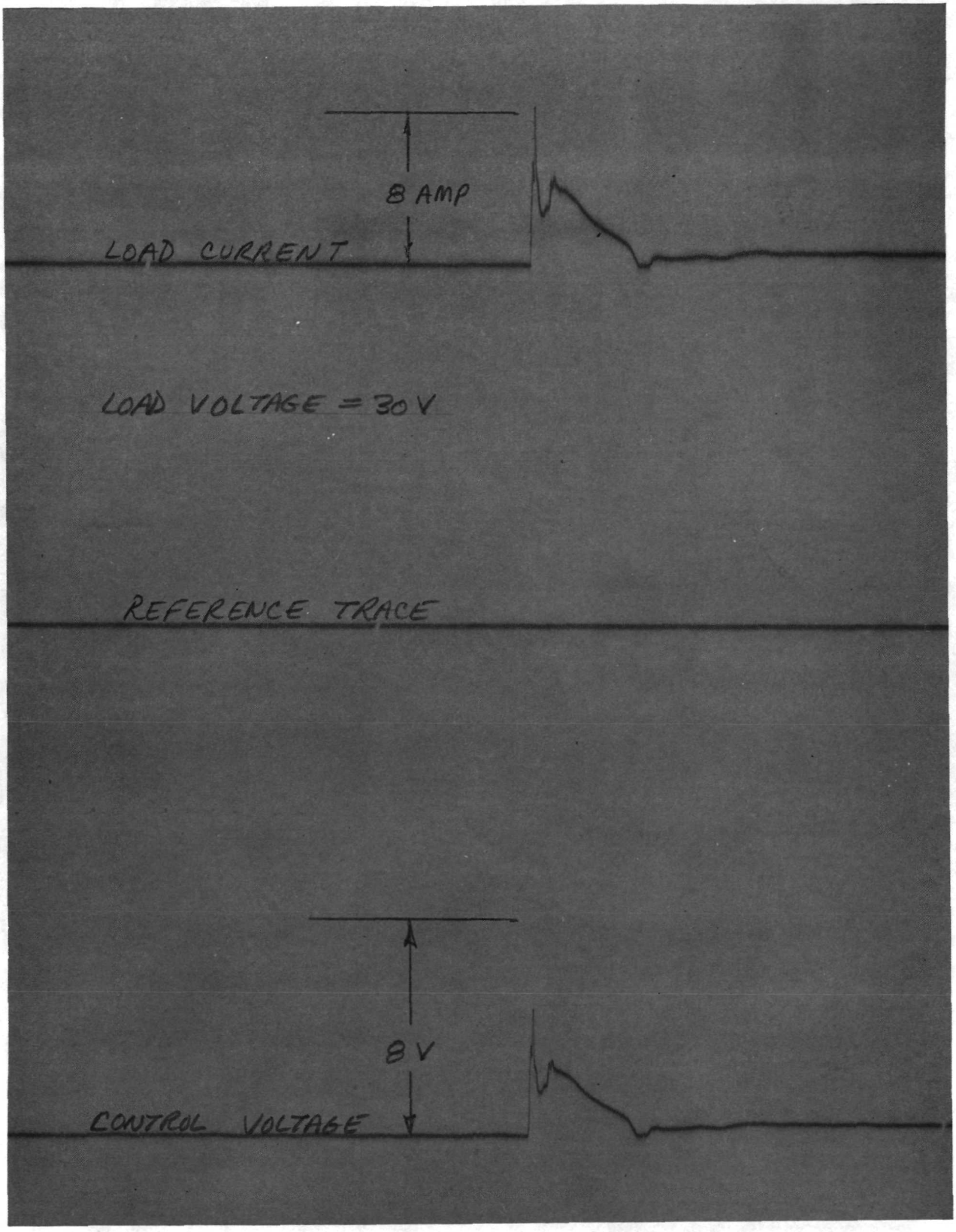

FIGURE 6-35 Oscillograph Record--Variable R Simulation of VHF/AM Transceiver, Run 11C

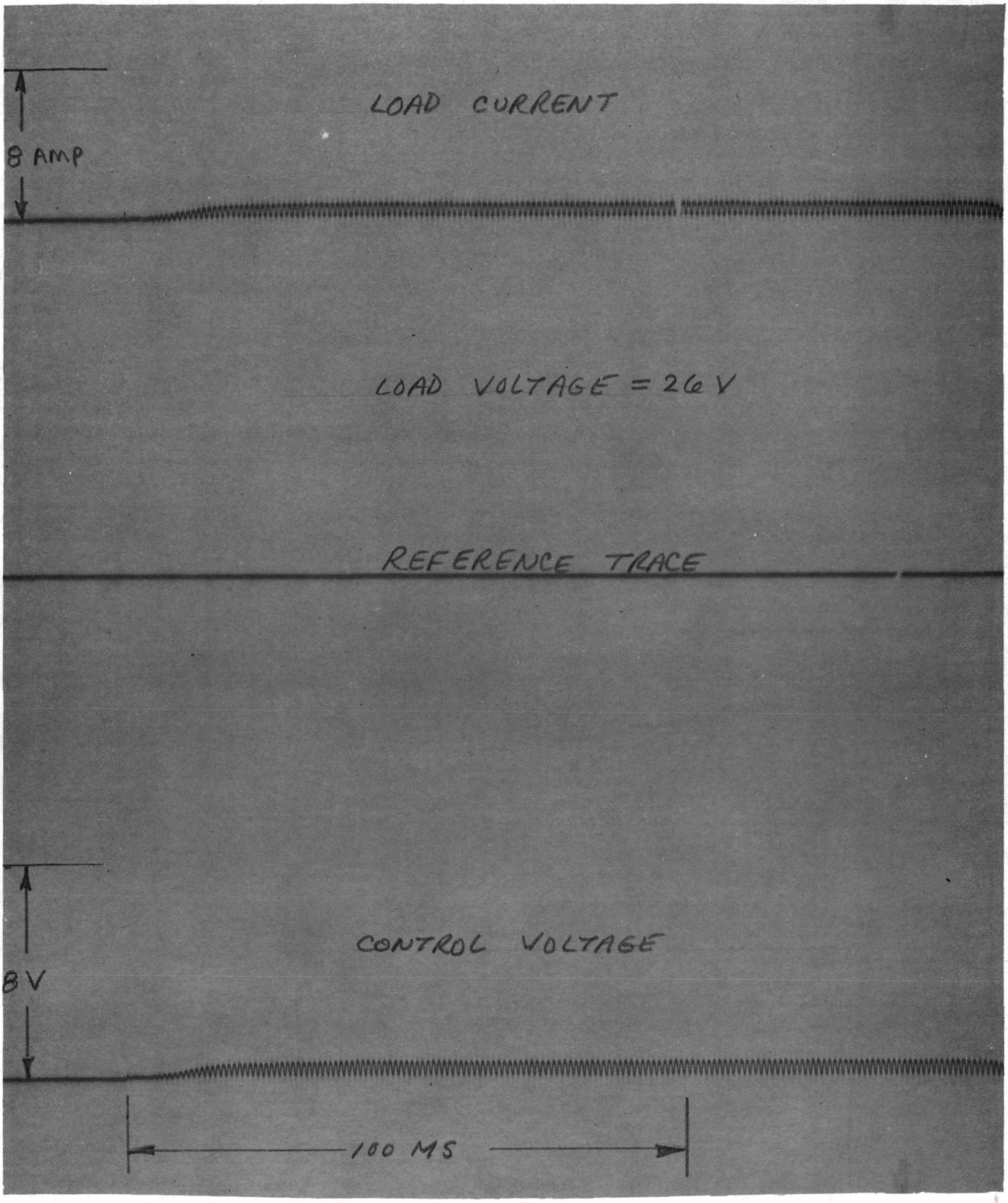

FIGURE 6-36 Oscillograph Record--Variable R Simulation of Recovery Beacon, Run 12A

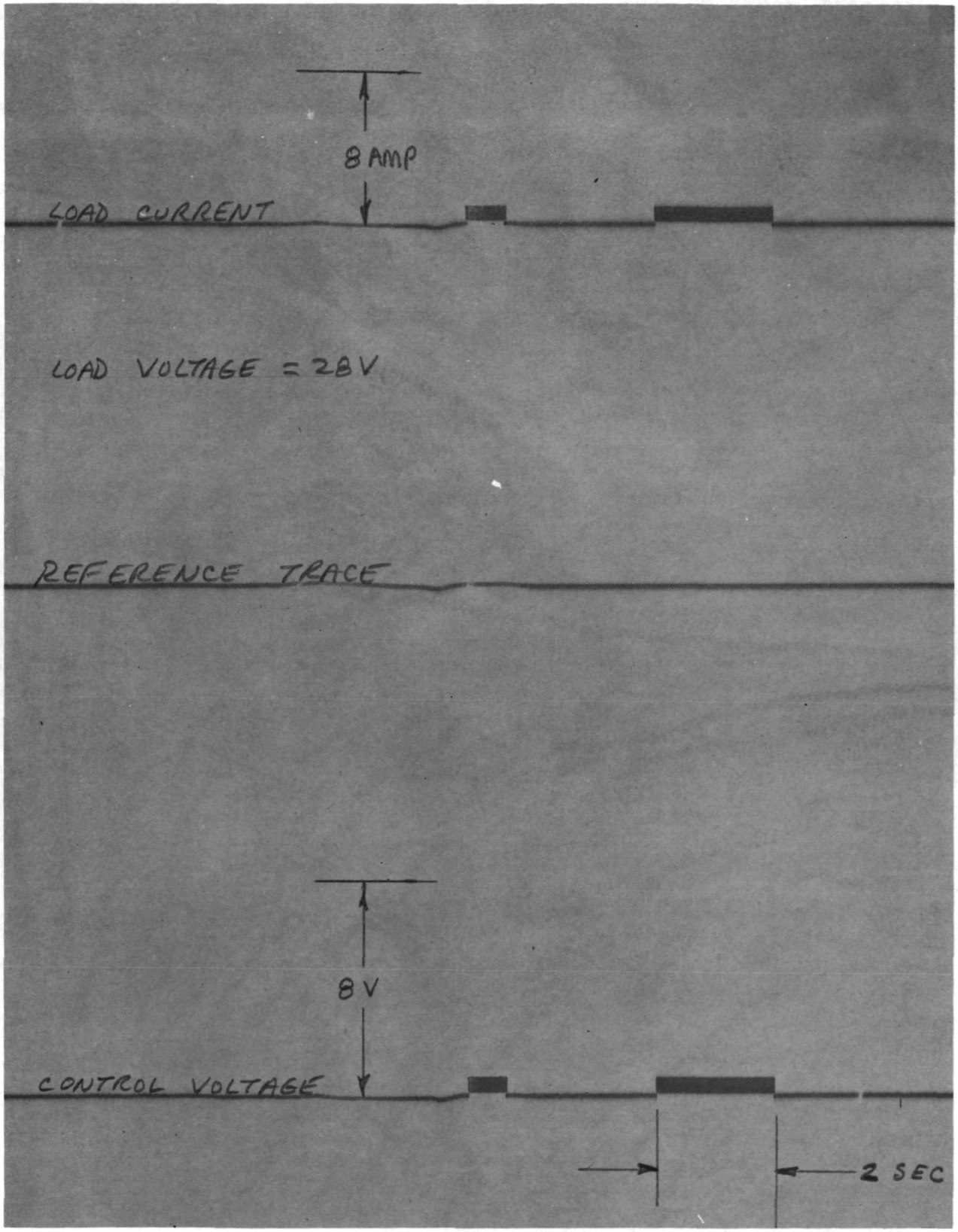

FIGURE 6-37 Oscillograph Record--Variable R Simulation of UHF/FM Transmitter, Run 13B

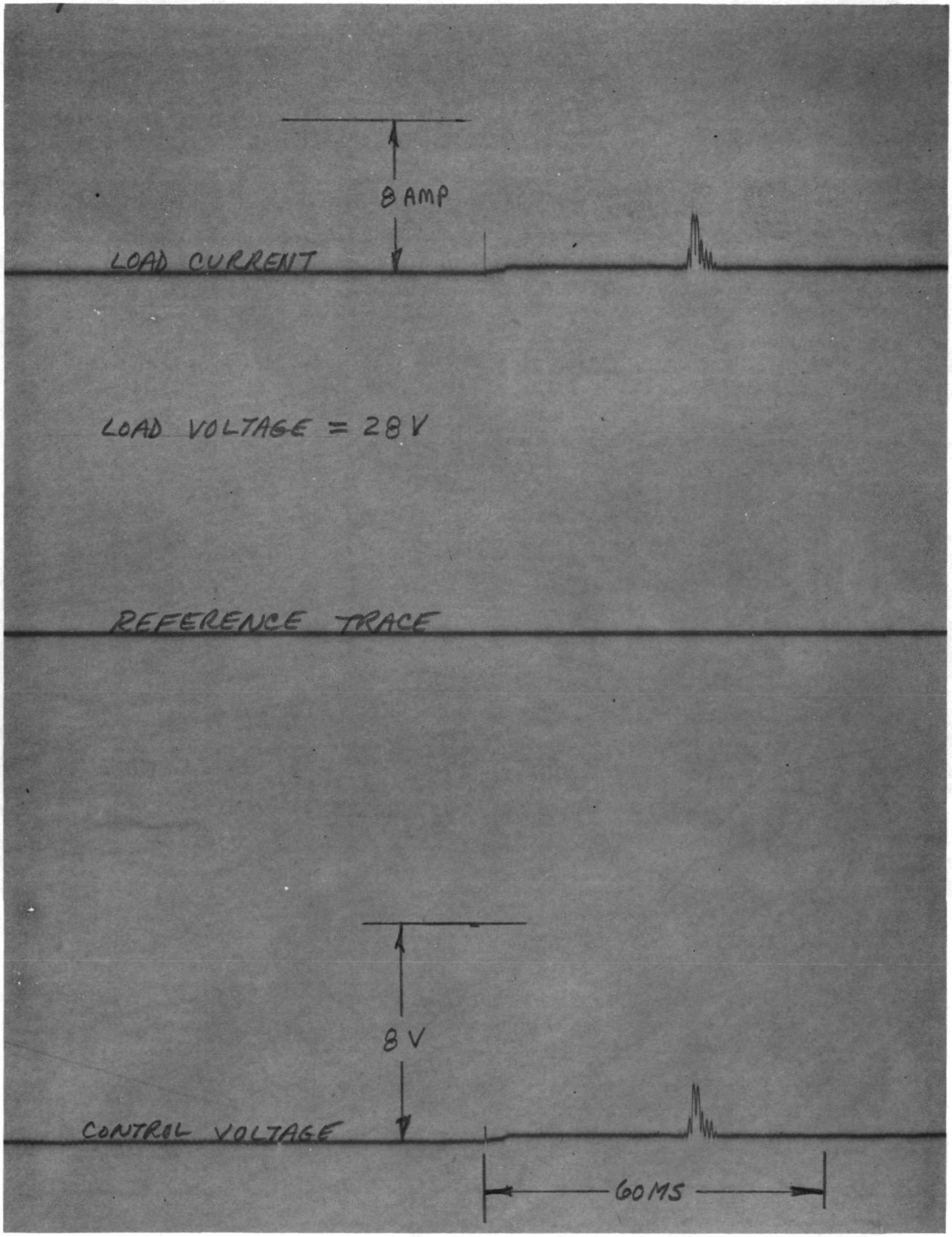

FIGURE 6-38 Oscillograph Record--Variable R Simulation of HF Transceiver, Run 16A

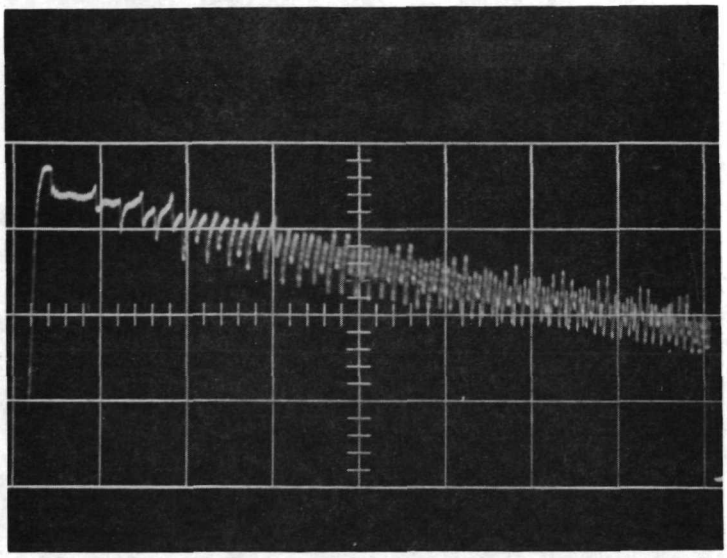

5 amp/cm

5 msec/cm

FIGURE 6-39 Variable R Response at MSC, Motor Switch, Run 3C (Load Voltage = 33 VDC)

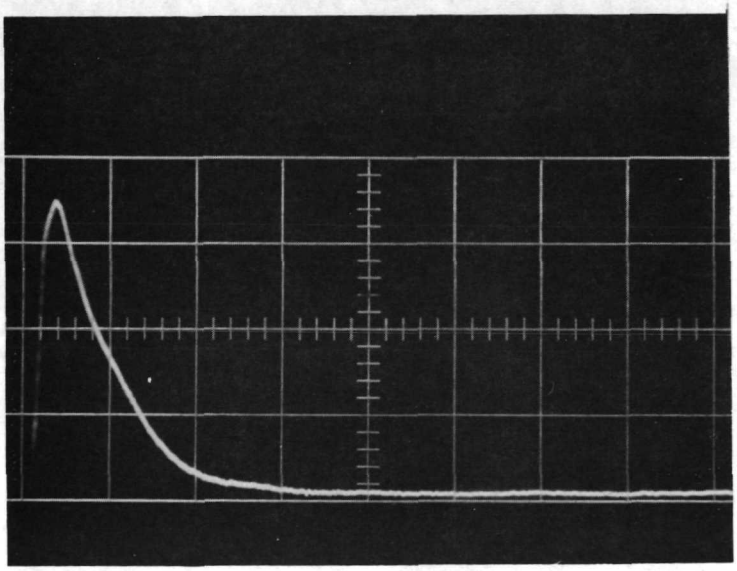

2 amp/cm

5 msec/cm

FIGURE 6-40 Variable R Response at MSC, Varo Inverter, First Event, Run 8A1 (Load Voltage = 26 VDC)

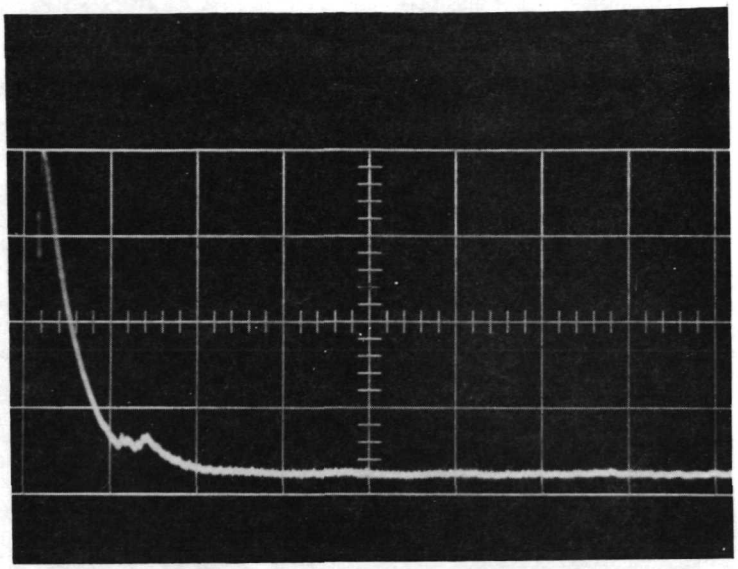

2 amp/cm

5 msec/cm

FIGURE 6-41 Variable R Response at MSC, Apollo Inverter, Run 9A (Load Voltage = 26 VDC)

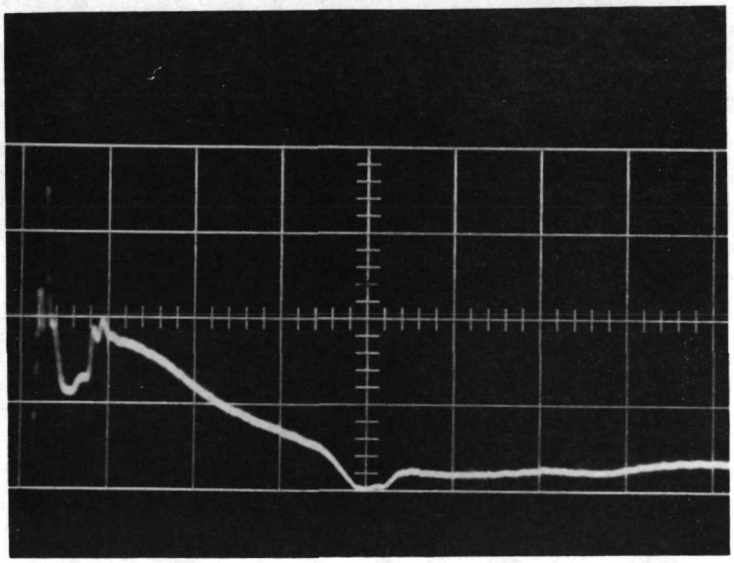

2 amp/cm

5 msec/cm

FIGURE 6-42 Variable R Response at MSC, VHF/AM Transceiver, Run 11C (Load Voltage = 30 VDC)

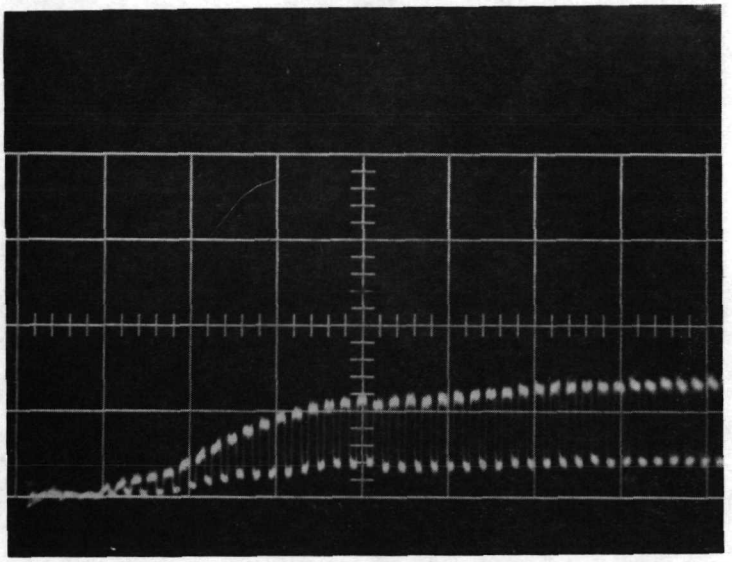

0.5 amp/cm

5 msec/cm

FIGURE 6-43 Variable R Response at MSC, Recovery Beacon Run 12A (Load Voltage = 26 VDC)

APPENDIX A

SUMMARY - PROGRESS REPORTS

This appendix summarizes the eight monthly progress reports published by Avco Systems Division under the Dynamic Load Simulator program, NASA Contract Number NAS-9-12016.

APPENDIX A

1. First Monthly Progress Report, for the Period 24 June 1971 to 31 July 1971, Avco Document No. AVSD-0365-71-CR, dated 5 August 1971.

   SUMMARY

   Describes Avco's efforts in the following three areas of concentration:

   1. Selecting the spacecraft loads to be interrogated.
   2. Preparing an interrogation test plan.
   3. Assembling the interrogation equipment and shipping it to NASA MSC.

2. Second Monthly Progress Report, for the Period 1 August 1971 to 31 August 1971, Avco Document No. AVSD-0404-71-CR, dated 7 September 1971.

   SUMMARY

   Covers efforts in the following-listed areas:

   1. Interrogation of selected spacecraft loads at NASA MSC.
   2. Preliminary review of interrogation data.
   3. Optimization program checkout.

3. Third Monthly Progress Report, for the Period 1 September 1971 to 30 September 1971, Avco Document No. AVSD-0443-71-CR, dated 6 October 1971.

   SUMMARY

   Describes efforts in the area of:

   1. Processing the interrogation data.
   2. Synthesizing a preliminary model.
   3. Initiating simulator design.

4. Fourth Monthly Progress Report, for the Period 1 October 1971 to 5 November 1971, Avco Document No. AVSD-0491-71-CR, dated 9 November 1971.

SUMMARY

Describes efforts in the areas of:

1. Completion of model synthesis.
2. Preliminary design of the simulator.
3. Conduct of a preliminary design review (PDR).

5. Fifth Monthly Progress Report, for the Period 6 November 1971 to 30 November 1971, Avco Document No. AVSD-0518-71-CR, dated 8 December 1971.

SUMMARY

Describes Avco's efforts in the following three areas:

1. Completion of preliminary deisgn of the variable R element.
2. Initiation of detailed design of the simulator.
3. Initiation of hardware procurement.

6. Sixth Monthly Progress Report, for the Period 1 December 1971 to 31 December 1971, Avco Document No. AVSD-0004-72-CR, dated 5 January 1972.

SUMMARY

Covers efforts in the following-listed two areas of concentration:

1. Detailed design of the simulator.
2. Additional optimization activities.

7. Seventh Monthly Progress Report, for the Period 1 January 1972 to 31 January 1972, Avco Document No. AVSD-0046-72-CR, dated 9 February 1972.

SUMMARY

Describes efforts in the following-listed areas:

1. Conduct of the final design review (FDR).
2. Hardware fabrication.
3. Mode relay control.

8. Eighth Monthly Progress Report, for the Period 1 February 1972 to 29 February 1972, Avco Document No. AVSD-0092-72-CR, dated 6 March 1972.

SUMMARY

Describes activities in the area of simulator fabrication.